THE UNIVERSITY
of EDINBURGH

This thesis has been submitted in fulfilment of the requirements for a postgraduate degree (e.g. PhD, MPhil, DClinPsychol) at the University of Edinburgh. Please note the following terms and conditions of use:

This work is protected by copyright and other intellectual property rights, which are retained by the thesis author, unless otherwise stated.
A copy can be downloaded for personal non-commercial research or study, without prior permission or charge.
This thesis cannot be reproduced or quoted extensively from without first obtaining permission in writing from the author.
The content must not be changed in any way or sold commercially in any format or medium without the formal permission of the author.
When referring to this work, full bibliographic details including the author, title, awarding institution and date of the thesis must be given.

Regulation and function of *Rootletin* - a gene differentially expressed in *Drosophila* sensory neurons.

15th April 2015

Katarzyna Styczynska-Soczka

A thesis presented for degree of Ph.D.

University of Edinburgh

2015

Abstract

Drosophila melanogaster is a widely used and efficient genetic model to study nervous system development. The conservation of many genes from *Drosophila* to vertebrates and a short reproduction cycle makes the fruitfly a great tool for providing insight into crucial events in nervous system formation. In studying the development of the sensory nervous system, *Drosophila* also provides a model for understanding the formation and function of structurally diverse cilia. Cilia are hairlike organelles present throughout our bodies and responsible for many processes such as chemo, mechano, and thermosensation, fluid movement, hearing and fertility. In *Drosophila* the only somatic ciliated cells are the Type I sensory neurons in which a cilium forms the sensory dendrite. There are more than two diverse subtypes of the ciliated sensory neurons and the mechanism by which this diversity is achieved remains unclear.

The mechanism of ciliated sensory neuron differentiation was hereby studied on an example of a differentially expressed ciliary gene - *CG6129* - a *Drosophila* orthologue of human *Rootletin*, a main protein components of ciliary rootlets. *CG6129* expression is specific to the ciliated cells and exhibits so called chordotonal-enriched pattern - a strong and permanent expression in the chordotonal subtype of type I neurons and weaker and transient expression in the external sensory subtype. I have shown that *CG6129* knock-down causes severe disruption of the chordotonal organs function without any obvious change in the structure of the cilium, other than the lack of ciliary rootlet. The function of the external sensory subtype was only slightly affected which further highlights the difference between the two types of ciliated sensory organs.

The fact that *CG6129* is differentially expressed in the two subtypes of the *Drosophila*

ciliated sensory neurons suggests that the genes involved in the formation of various cilia are differentially regulated. I have shown that *CG6129* is regulated by the two well known ciliary transcription factors - RFX and fd3F (distant homologue of Foxj1). Of the two enhancers found the early-to-late enhancer is almost entirely dependent on RFX and not on fd3F while the late enhancer is dependent on both fd3F and RFX. The fact that there is some residual *CG6129* expression in the absence of both RFX and fd3F suggests involvement of another regulator that may contribute to the cilia diversity.

Zmynd10 is a recently characterised ciliary gene that is involved in the axonemal dynein arms assembly. Mutations in human *Zmynd10* cause primary ciliary dyskinesia (PCD) and *Drosophila Zmynd10* mutants have immotile cilia that lack dynein arms. Due to the presence of specific protein domains Zmynd10 has been suggested to act as a transcriptional regulator. I have shown that the transcript levels of *CG6129* and other ciliary genes are reduced in the *Zmynd10* mutant. This implies that *Zmynd10* may regulate ciliary genes on a transcriptional or post transcriptional level and may contribute to the regulatory network governing ciliogenesis.

Lay summary

Despite obvious differences in appearance *Drosophila melanogaster* - the fruitfly - is in many ways very similar to humans. For example the way humans perceive the environment - hear, taste and smell - is almost the same in the fruitfly. In human, fruitflies and many other organisms hearing, taste and smell is possible thanks to cilia. Cilia are small hair-like structures present on almost every cell in our body. The fruitfly is a very useful model to study cilia because it has a limited number of ciliated cells. The only ciliated cells in *Drosophila* are nerve cells that perceive stretch and allow for movement coordination. Any disruptions in these cells can be specifically examined and determined in an easy way.

Cilia can be divided into two groups - motile and immotile. Motile cilia are responsible for moving fluid (like removing mucus from the airways) or moving in fluid (like sperm cells). Immotile cilia are responsible for communication between the cells in our body. The vast variety of functions that cilia have is underlain by the fact that they can differ greatly in terms of structure. Although cilia in general have been studied extensively the mechanism by which the ciliary diversity is achieved is largely unknown.

In this thesis I examine the function of a *Drosophila* gene - *CG6129* - that is very similar to human *Rootletin* gene. In *Drosophila* the product of the *CG6129* gene is only expressed in ciliated cells and its activity differs in structurally different types of cilia. I have shown that when the *CG6129* gene expression is reduced, one type of ciliated nerve cells loses its function. In the same conditions a structurally different type of ciliated nerve cell does not lose its function. This shows that the different levels of genes expression in various ciliated cell types underlie the differences in which these cells function.

Having shown that *CG6129* is a good example of a gene that is expressed on different levels in different ciliated cell types I have turned to the regulation of this gene. The expression of every gene is regulated by specialised proteins called the transcription factors. In *Drosophila* there are two transcription factors that are known to specifically regulate genes involved in cilia - RFX and fd3F. I have shown that CG6129 is regulated by both RFX and fd3F but in a different manner in different ciliated cell types. In addition to this I have also shown that another protein - Zmynd10 - may also be involved in regulation of some ciliary genes.

Declaration

I declare that this thesis is my own work unless otherwise stated in the text, and that this work has not been submitted for any other degree or qualification.

Katarzyna Styczynska-Soczka

January 2015

Acknowledgments

I would like to thank my supervisor Andrew Jarman for his continued support and guidance during my PhD. I am immensely grateful for his help and encouragement to pursue my research interests.

I would like to thank the members of the Jarman lab. Petra zur Lage for introducing me to all lab procedures, protocols and and for helpful advice in the tricky experiments. Lynn Powell for day to day help in the lab and advice on Western blotting. Giusy Pennetta, my second supervisor for advice and lending me fly stocks and antibodies. My fellow PhD students Daniel Moore, Fay Newton, Giuseppe Gallone, Lina Ma, Thomas Suslak, Iain Hunter and Ibtisam Abokhrais and members of the Armstrong lab - Lysimachos Zografos, Manuela Marescotti, Valentina Ferlito for advice and great atmosphere. Last but not least thanks to Carol Wollaston for letting me use her colour printer to print the figures.

I feel I have been very lucky to work in the Jarman Lab. I wish every student had as great and helpful supervisor and such amazing colleagues that ensure a professional yet relaxed atmosphere during their studies.

Finally I would like to thank my parents Maciej and Ewa, my husband Maciej and my son Antoś, for their support.

Abbreviations

AS-C - Achaete-Scute complex

ChIP - chromatin immunoprecipitation

Cho - chordotonal

CNS - central nervous system

CROCC - ciliary rootlet coiled-coil

DBD - DNA binding domain

DNA - deoxyribonucleic acid

DNAAF - dynein arm assembly factor

ES - external sensory

GGT - G1-G2 tether

HH - Hedgehog

IDA - inner dynein arm

IFT - intraflagellar transport

ISH - RNA *in situ* hybridisation

JO - Johnston's organ

KD - knock-down

KLC - kinesin light chain

lch - lateral chordotonal

md - multidendritic neuron

MTOC - microtubule organising centre

ODA - outer dynein arm

PCD - primary ciliary dyskinesia

PCMC - periciliary membrane compartment

PI - propidium iodide

PNC - proneural cluster

PNS - peripheral nervous system

RFX - regulatory factor X

RNA - ribonucleic acid

RNAi - RNA interference

RPKM - Reads Per Kilobase of transcript per Million mapped reads

RT-PCR - reverse transcription followed by a PCR

SML - S-M linker

SOP - sensory organ precursor

TEM - transmission electron microscopy

TF - transcription factor

vch - ventral chordotonal

VDRC - Vienna *Drosophila* Resource Centre

WT - wild type

Contents

Part I

General Introduction

1 Sensory neuron diversity and cilia diversity

All living organisms can respond to the surrounding environment. Plants can turn towards the light source and modulate the water loss via opening/closing their stomata. Unicellular organisms sense changes in the environment humidity or the nutrient concentration. Multicellular or higher organisms can respond to the environmental stimuli thanks to their complex nervous systems.

In general, nervous system can be divided into the central nervous system (CNS) and the peripheral nervous system (PNS). The role of the peripheral nervous system is to directly receive the very wide variety of external stimuli like smell and taste (chemosensation), touch, sound and movement (mechanosensation), temperature, pressure or light (photosensation). The PNS then passes the gathered information to the CNS which in turn is responsible for integrating the stimuli and governing a response to the environment (like hand withdrawal from fire). Many of the PNS cells use cilia as the direct stimuli receivers. The examples of ciliated sensory neurons in human are the photoreceptors (retinal rods connecting cilia), olfactory receptors, chemoreceptors in taste buds, and the hair cells in the inner ear (sound/mechanoreceptors). Considering the wide array of stimuli that cilia can detect it is only natural that they are very diverse in structure and therefore function. It remains poorly understood as to how this structural and functional diversity is achieved during the development. The whole PNS is derived from a fairly homogenous ectoderm and a very intricate and complex network of proneural factors and

differential transcriptional regulation leads to development of many vastly different tissues.

In *Drosophila* the PNS consists of internal sensory organs - chordotonal organs, and external sensory organs (ES). While the division is mostly based on the position of organs within the body, chordotonal organs are fairly homogenous set of organs, but the external sensory organs vary greatly in terms of development, function and structure. Some ES are mechanosensory receptors armed with bristles, and other ES are chemoreceptors and touch receptors. In contrast to the vertebrate models, *Drosophila* has a limited number of somatic ciliated cells and those are the type I sensory neurons (chordotonal and a subset of ES organs). The small number and the ease of examining the ciliated cells makes *Drosophila* a great model to study cilia. The types, function, and structure of *Drosophila* ciliated cells will be discussed in more detail in the following sections.

2 Roles and functions of cilia

Cilia are small membranous cellular protrusions that occur widely in eucaryota from animals to some species of plants. In human cilia are found on virtually every cell type except the cells derived from the bone marrow (blood cells) (Praetorius and Spring, 2005). Another name for some types of cilia that can be found in literature is flagellum. Although flagella have slightly different characteristics cilia and flagella are both treated as functionally different types of the same organelle. They are both very much conserved both functionally and structurally. Both cilia and flagella structures are based on a radially symmetric array of microtubules axoneme (Haimo and Rosenbaum, 1981). The microtubules are organised into a circle of 9 doublets with another pair localised in the center. Those arrays are called 9+2 or 9+0 if the

central microtubule pair is absent. In general there are many types of cilia that vary in structure and function but two main types can be distinguished: motile cilia, and immotile cilia.

2.1 Motile cilia

Motile cilia, as the name indicates, are characterised by the ability to move. The movements of cilia are achieved due to the dynein complexes localised along the axoneme. The dynein proteins 'move' along the microtubules creating a bend of the cilium (Haimo and Rosenbaum, 1981). These bends are synchronised and create a wave-like movement or a spiral movement of the whole cilium (see Fig. 1.1). Motile cilia can be found in single-cell organisms like algae *Chlamydomonas* or a planarian *Schmidtea mediterranea*. The cilia of these species are locomotory and enable them to move within their environment. Motile cilia are also abundant in higher organisms like animals. In human, motile cilia line the respiratory tract and coordinated movement of these cilia ensure the mucus clearance (Mall, 2008). Motile cilia are also found in the ependyma of brain and spinal chord where their function is to provide the cerebrospinal fluid flow (Worthington and Cathcart, 1963). Both male and female fertility depends on cilia motility. In females the fallopian tubes are lined with ciliated epithelium which helps the movement of the ovum to the uterus. In males the sperm cells have a specialised motile cilium - flagellum. Another type of motile cilia - nodal cilia - can be found in mouse embryo. These cilia are responsible for establishing the left-right body symmetry in some vertebrates like human and mice (Nonaka et al., 1998). Motile cilia most commonly exhibit the 9+2 microtubule arrangement but in some cases (like the nodal cilia in mice) the 9+0 arrangement can be found.

The structures that are characteristic of motile cilia and indeed are necessary for the

motility are the dynein arms. These are visible on the cilia TEM images as electron dense arms protruding from each of the microtubule doublets towards the center or outwards. Based on the localisation they are subdivided into the inner dynein arms and the outer dynein arms. A study by Ritsu Kamiya (Kamiya, 1995) describes that inner and outer dynein arms are responsible for different components of the ciliary movement. Apparently the inner dynein arms are are necessary to achieve the optimal bending angle of the axoneme while the outer dynein arms are involved in establishing the beating frequency. Other structures necessary for cilia motility are the radial spokes and the central apparatus (Smith and Yang, 2004).

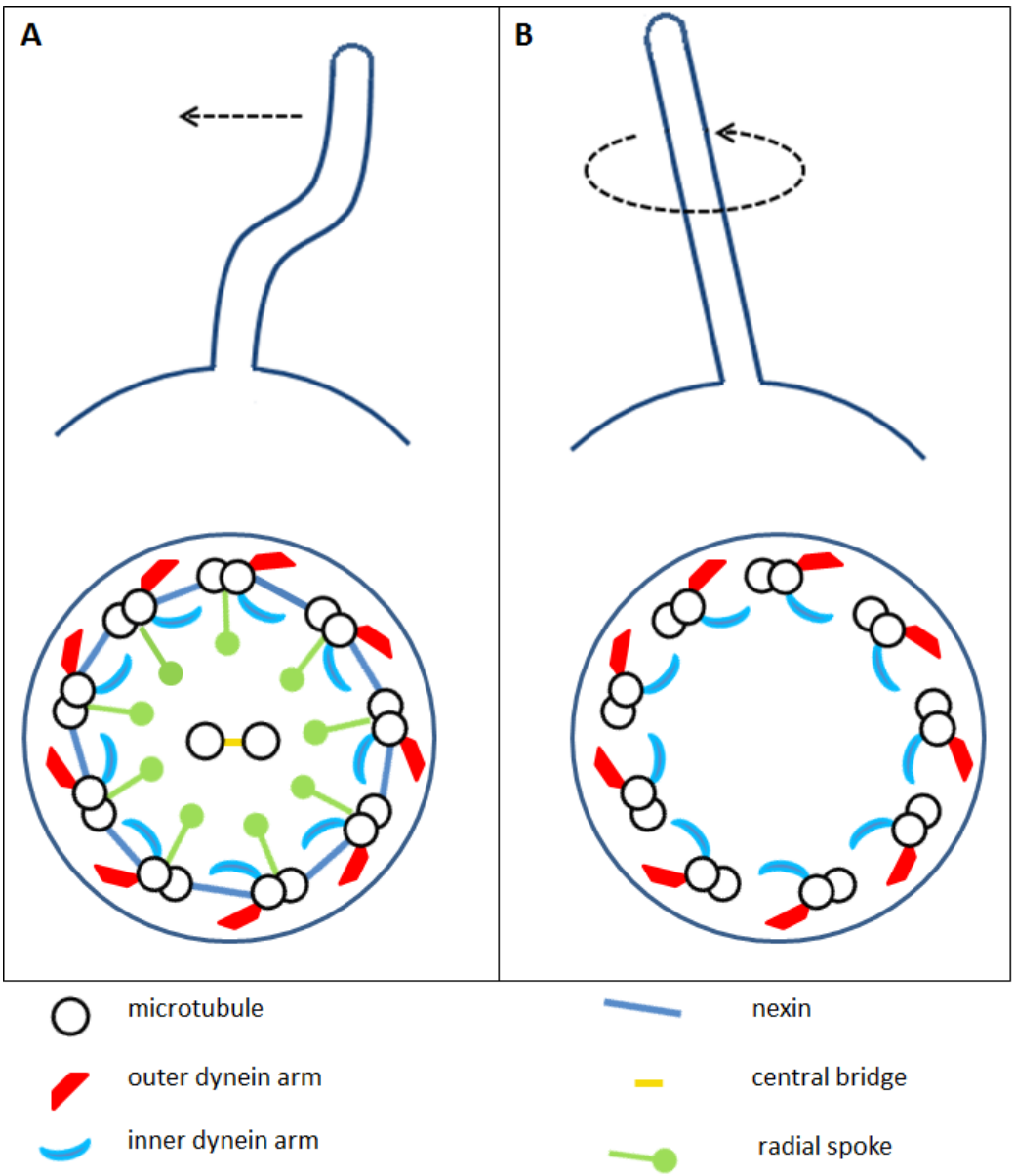

Figure 1.1 Motile cilia. **A** - motile cilium that has a beating motion, can be found in cilia lined epithelia (airway epithelia, ependyma) where each cell has multiple cilia. Their beating is synchronised and allows the movement of fluid. Those cilia have the 9+2 array. **B** - single motile cilium that has a rotary motion. Example of such cilium is a nodal cilium that produces the left-right symmetry in the mouse embryo. Those cilia have the 9+0 array and miss the central apparatus together with nexin and radial spokes.

2.2 Immotile cilia

Immotile cilia, also called primary cilia, do not have the dynein arms and therefore are unable to produce movement. Their function is generally linked to signal transduction. In human a single immotile cilium can be found on almost every cell. Primary cilia present in human kidneys act as mechanosensors of the fluid movement. When those cilia are absent the cells cannot properly control the water resorption which leads to formation of liquid filled cysts on kidneys - a condition called the Polycystic Kidney Disease (PKD) (Yoder and Yoder, 2007). Immotile cilia also play a role in chemosensation, namely they act as olfactory receptors. Mammalian photoreceptors also contain a short connecting cilium which is immotile. Its outer segment role is solely to transduce the light signals through the intraflagellar transport. An unfortunately named immotile cilium - the kinocilium - is a single cilium on a hair cell which forms the center of the mechanosensory apparatus in the mammalian inner ear. In humans, the kinocilium disappears after the haircell maturation and the stereocilia are the mechanosensory organelles. The sound vibrations cause the ion channels localised on the ciliary membrane to open which in turn leads to membrane depolarisation. This depolarisation effect is mediated further by neurotransmitters release. The immotile cilia generally lack the central pair and exhibit the 9+0 microtubules layout but some primary cilia have the 9+2 array such as rats olfactory cilia (Menco, 1984).

2.3 Ciliopathies

Because of the numerous functions that cilia can have any ciliary formation/function disruption may cause serious diseases with a wide range of symptoms. Such diseases are called ciliopathies. There are many known ciliopathies that can affect a single

organ/system like the nephronophthitis (Hurd and Hildebrandt, 2010), polycystic kidney disease (Wilson, 2004), polycystic liver disease (Everson et al., 2004), or retinitis pigmentosa (Hartong et al., 2006). Those disorders are caused by defects in the immotile cilia. Other ciliopathies are classified as syndromes and are systematic diseases affecting many organs. Examples are Bardet-Biedl syndrome or primary ciliary dyskinesia (PCD). PCD is a systematic disorder caused by disruptions in the ciliary motility apparatus. The symptoms include chronic respiratory infections leading to bronchiectasis caused by impaired mucus clearance. PCD patients often exhibit various forms of situs inversus (situs ambiguus, situs inversus totalis) due to loss of motility of the nodal cilia. PCD is also characterised by male and female sub/infertility, otitis media, and hearing loss.

3 Ciliary structure

3.1 Basal body

Basal bodies are short microtubule based cylindrical structures which are necessary for the ciliary axoneme nucleation. They have a characteristic 9-fold symmetry of nine microtubule triplets (each microtubule in a triplet is called A, B, and C). This symmetry origins from and relies on the cartwheel structure - the centriole/basal body precursor. The cartwheel is built of the Sas6, Sas4 and Cep135/Bld10 proteins and the Sas5 protein seems also to have a role in this structure (Carvalho-Santos et al., 2011). Ciliary basal bodies are modified centrioles that are docked to the cell membrane. It is thought that the transition from the centriole to the ciliary basal body is dependent on the antagonistic actions of two proteins - CP110 and Cep290 (Kobayashi and Dynlacht, 2011). When a cell exits the cell cycle with two

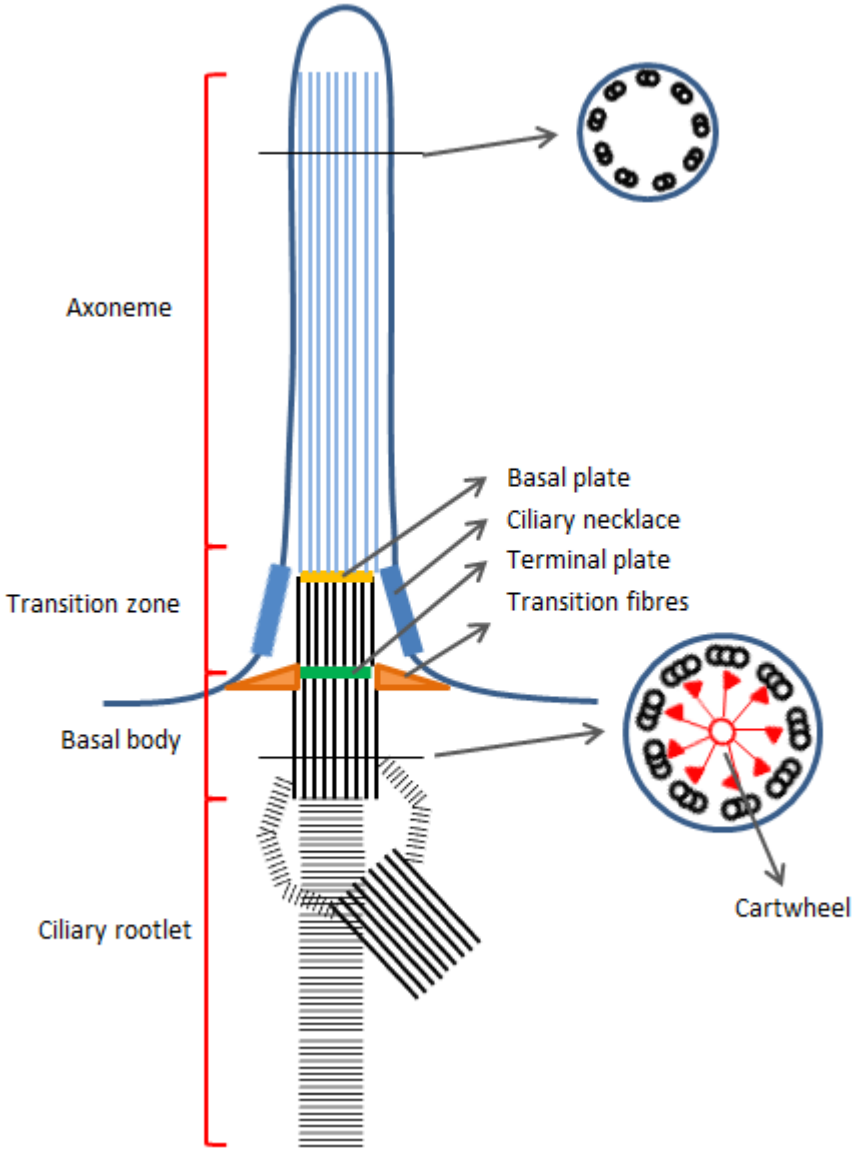

Figure 1.2. Structure of the cilium with 9+0 microtubule doublet arrangement. Transverse section accross the axoneme shows the 9+0 arrangement. The transition zone at the base of the cilium reveals substructures like the basal plate (yellow), ciliary necklace (blue), terminal plate (green), and the transition fibers (orange). Transverse section at the basal body level shows the 9 microtubule triplet arrangement together with the cartwheel structure. Proximally to the basal body is the ciliary rootlet structure that connects the ciliary basal body with the proximal ciliary centriole and extends to the cell body.

centrioles tethered, they both migrate to the cell membrane. It is usually the mother centriole that docks to the membrane because the distal appendages present on it are necessary for this process (Schmidt et al., 2012). Proteins necessary for the migration and docking include *Paramecium* orthologue of human Centrin 3 (PtCen3p), FOR20 (Aubusson-Fleury et al., 2012), and Talpid3 (Yin et al., 2009). Actin cytoskeleton enrichment at the apical membrane seem also to have a role in axoneme nucleation (Pan et al., 2007). There are two ways basal bodies dock at the membrane - they can either approach the apical membrane directly or dock at a subapical membranous vesicle which will subsequently fuse with the cell membrane (Sorokin, 1962, 1968). Once the basal bodies dock at the membrane a ciliary rootlet structure starts to form. The transition from a centriole to the basal body and the membrane docking process are the first steps of ciliogenesis.

3.2 Transition zone

The most proximal part of the newly forming axoneme is called the ciliary gate and it can be subdivided into the transition fibers and the transition zone (Williams et al., 2011). The ciliary gate is the first axonemal structure to be formed during ciliogenesis and it is thought to appear before the axoneme elongation is established (Szymanska and Johnson, 2012). The basal body terminates with the C-tubule termination and the transition zone starts slightly proximally to that (Szymanska and Johnson, 2012). The boundary between the basal body and the transition zone is called the transition plate in the motile cilia and is thought to be involved in the central microtubule pair nucleation (Gilula and Satir, 1972). The transition fibers are formed from the mature centriolar appendages (Sorokin, 1968) and protrude from the B-tubules. The protein components of these fibers are not known but some reports suggest that they may have a role in docking the axoneme to the membrane

via CEP164 (Graser et al., 2007), and cenexin (Ishikawa et al., 2005). Proteins known to be defective in ciliopathies - MKS (Meckel-Grueber Syndrome), and NPHP (nephronophtitis) have been shown to localise to the TZ in *C. elegans* ciliated sensory neurons (Williams et al., 2011). Although single MKS/NPHP mutants do not exhibit any cilia phenotype both proteins have been shown to be collectively needed for basal body/transition zone attachment to the membrane (Williams et al., 2011). Another report localises a protein involved in the axoneme elongation - IFT52 - at the transition fibers and suggests their role in organising the intraflagellar transport (Deane et al., 2001). Other structural components of the transition zone are the Y-shaped linkers and the ciliary necklace. In general the detailed molecular structure of the transition zone is not well known but based on some proteins found in the area it is considered to function in docking and selective trafficking of the proteins destined to the distal part of the axoneme.

3.3 Axoneme

The axoneme is the main and largest structural component of cilium. As explained before the axoneme consists of microtubules that are arranged into a so called 9+0 or 9+2 array. As the microtubules are the main structure within the cilium various forms of tubulin are the most abundant proteins in cilia. However in the motile cilia a wide array of proteins builds the dynein arms, the radial spokes and the central apparatus. The dynein arms consist of many conserved components including the heavy chains, light chains, intermediate chains, and light intermediate chains (Pazour et al., 2006). All these protein building the axoneme are transported to their final destination in the cilium via the intraflagellar transport - IFT.

4 Formation of the cilium - intraflagellar transport (IFT)

This phenomenon has first been reported by Kozminsky et al (Kozminski et al., 1993) in *Chlamydomonas* where movement of particles along the ciliary microtubules and the ciliary membrane was seen. The transport was observed to be taking place in both directions and later the IFT has been divided into two separate categories - the anterograde and retrograde IFT.

4.1 Anterograde transport and IFT-B

The anterograde transport carries the particles towards the tip of the cilium. The motor protein responsible for the anterograde IFT - kinesin part FLA10 - has first been reported to have a role in *Chlamydomonas* cilia in 1995 by Kozminsky (Kozminski et al., 1995). The IFT kinesin II has later been found to be a complex trimer consisting of two kinesin like proteins (*Drosophila* KLP64D and KLP68D) and a kinesin associated protein (Sarpal et al., 2003). The *klp64D Drosophila* mutant is characterised by a complete lack of cilia (Sarpal et al., 2003) and accumulation of cilia structural components (tubulins) at the basal body (Avidor-Reiss et al., 2004). In general truncated cilia or complete lack of cilia is a phenotype characteristic of disrupted anterograde IFT.

The kinesin motors are not however the only proteins responsible for the anterograde IFT. The group of proteins cooperating in the anterograde IFT is called the IFT-B complex. So far 17 protein components of the IFT-B have been identified - IFT172, 88, 81, 80, 74/72, 57/55, 52, 46, 27, 20, Qilin/Dyf-3, IFTA-2, Dyf-11, Dyf-1, Dyf-13 (Follit et al., 2009). IFT-81 and IFT-74 have been shown to have a role in tubulin

transport towards the ciliary tip which allows the elongation of the microtubules in a forming cilium (Bhogaraju et al., 2013). IFT-46 for example has a role in radial spokes assembly (Hou et al., 2007) and the IFT-20 has been found to localise in the cytoplasm and the Golgi apparatus. This suggests that some IFT-B components might also be involved in transport of proteins from Golgi to the cilium (Follit et al., 2006).

4.2 Retrograde transport and IFT-A

The retrograde transport is a means of transport from the ciliary tip towards the base of the cilium. The motor proteins responsible for the retrograde transport are cytoplasmic dyneins (Pazour et al., 1998). The *Chlamydomonas* IFT-A complex consists of the dynein heavy chain DHC1B together with other smaller components like D1bLIC, FAP133, and LC8 (Engel et al., 2012). Mutations in dynein motor proteins have been shown to cause cilia shortening together with a characteristic swelling of the ciliary tip (in human, Merrill et al., 2009, in *C. elegans*, Signor et al., 1999, and in mouse, May et al., 2005). The swelling at the ciliary tip represents the accumulation of ITF-B proteins together with other axonemal turnover proteins. It has however remained unclear whether the shortening of the cilia is a primary IFT-A disruption effect or rather a secondary effect caused by the fact that the IFT-B machinery accumulates at the ciliary tip unable to perform the anterograde transport. In the study by Engel et al (2012) the use of a conditional *Chlamydomonas* dhc1b-3 mutant enabled the uncoupling of the antero- and retrograde transport. This allowed to conclude that IFT-A indeed has a role in both ciliary length maintenance and axoneme assembly.

4.3 Dynein arm assembly

The axonemal motility apparatus - the dynein arms, are large protein complexes that need to be pre-assembled before being mounted as cargoes for the IFT. The dynein arm assembly machinery, among other proteins, consists of chaperones that assist in folding of the dynein chains. Next step is mounting the appropriate dynein chains on each other in thecorrect order and spatian orientation. Such pre-assembled dynein arm is then transferred to the axoneme along the cytoskeleton. A number of factors are known to be necessary to assemble the dynein arms in the cytoplasm and to transfer them to the axoneme (Fowkes and Mitchell, 1998). Those factors are called dynein assembly factors (DNAAFs). Many recent publications report new proteins falling into this category (Freshour et al., 2007; Mitchison et al., 2012Omran et al., 2008).

5 Cilia in *Drosophila*

Drosophila provides a great model to study cilia function and formation due to a high degree of ciliary genes conservation, easy and quick genetic manipulations, and a relatively small number and variety of ciliated cells. One of the ciliated cell types in *Drosophila* is the sperm cell. The other *Drosophila* ciliated cells and the only somatic cell type that possess cilia are some of the peripheral nervous system neurons.

5.1 Sperm cells

Drosophila sperm cells contain a very long motile flagellum allowing them to move in fluid environment. The sperm cells in the fruit fly possess the 9+2 microtubule arrangement characteristic of motile cilia and also bear the cilium motility machinery

(the axonemal dyneins). In addition to the 9+2 microtubules the *Drosophila* sperm cells also have a ring of 9 outer accessory microtubules (Raff, 1997). In contrast to other ciliated cells in *Drosophila* the sperm flagella biogenesis is independent of IFT because the axoneme elongation takes place within the cells body and only after the axoneme is assembled it is docked to the outer cell membrane (Han et al., 2003).

5.2 PNS

Drosophila peripheral nervous system can be divided into two types of sensory organs based on their localisation - the external and the internal organs (see Figure 1.3). The external sensory organs are positioned externally and are connected to epidermal structures that assist in receiving the chemical (olfactory and gustatory) and mechanical environmental stimuli. The ES organs include the mechanoreceptors (with external structure being the bristle) (Hartenstein and Posakony, 1989) and chemoreceptors (the external structure being the cuticle sockets and domes), which due to different function and structure will not discussed in detail (Cole and Palka, 1982). The internal sensory organs are localised under the epidermis and can be divided into two subcategories - the chordotonal organs and the multidendritic neurons.

The *Drosophila* PNS neurons can also be divided into two categories based on their structure. The type I neurons are monodendritic neurons that innervate sensory organs built of several cells of the same lineage - the neuron and several support cells. Each of the type I sensory organs is thought to arise from a single precursor cell - the sensory organ precursor (SOP). All type I neurons have a modified cilium at the tip of the single dendrite. Those cilia can be either quite long and highly specialised (like the chordotonal cilium) or quite short and rudimentary (like the external mechanosensory cilium or the campaniform sensillum cilium). The type II

sensory neurons possess multiple dendrites and in general unlike the type I neuron they do not seem to be associated with any support cells (Brewster and Bodmer, 1995). The multidendritic neurons can be further subdivided into the md-da neurons (dendritic arborisations), md-bd neurons (bipolar dendrites) and the md-td (dendrites localised along the tracheal tracts) (Bodmer and Jan, 1987).

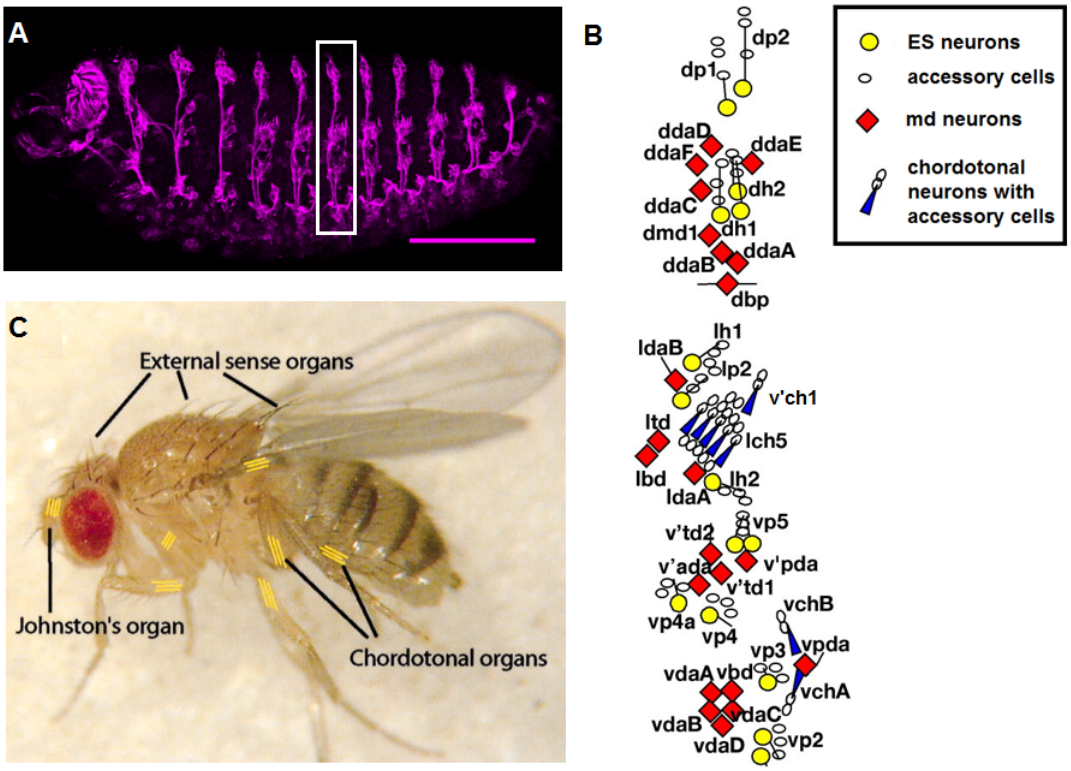

Figure 1.3. PNS in *Drosophila*. A - embryonic PNS stained with neuronal marker (22C10). White rectangle shows one abdominal hemisegment which is shown in detail in B, **B -** schematic representation of all PNS neurons present in an abdominal hemisegment, **C** - type I sensory organs in an adult fly, ES neurons innervate the bristles, cho neurons innervate the antennal Johnston's organs and wing and femoral cho clusters (yellow lines). B diagram adapted from Orgogozo and Grueber (2005), C image taken from Jarman (2002).

5.2.1 Chordotonal organs

Chordotonal organs are internal stretch receptors that are responsible for hearing, balance and coordination (Eberl et al., 2000; Kernan et al., 1994). In embryos/larvae

there are 8 chordotonal organs per each of the seven abdominal hemisegments. Five of them are localised laterally in a cluster (lch5) and a single chordotonal organ is positioned dorsally to the lch5 (v'ch1). A pair of chordotonal organs is localised ventrally pointing in the opposite directions (vchA and vchB). In an adult fly large clusters of chordotonal organs are present at the base of each wing, in the femora and in the antenna (Johnston's organ).

Chordotonal organs consist of four cells - neuron, cap cell, scolopale cell, and the ligament cell. These cells are formed from a single precursor cell - the sensory organ precursor (SOP) in a series of asymmetric cell divisions (see Figure 1.4). According to Inbal et al (2004) some chordotonal organs also possess a cap attachment cell. This cell appears to be derived from the chordotonal lineage and only two of them are present at the lch5 cluster. It remains unclear which organs exactly of the lch5 cluster associated with the cap attachment cells. The central cell of the chordotonal organs is the neuron. Its modified dendrite terminates with a specialised cilium. The tip of the cilium is attached to extracellular cap which is either directly or indirectly (via the cap attachment cell) connected to the cuticle. Chordotonal cilia have a highly organised axoneme with a protein dense structure called the ciliary dilation localised at about half of the ciliary length. The general function and molecular composition of the ciliary dilation is not clearly known but it has been suggested to have a role in maintaining the compartmentalisation of the chordotonal cilia. Each chordotonal cilium is enclosed in a K^+rich endolymph filled scolopidium which is formed by the scolopale cell (Eberl, 1999). The scolopidium is a rigid structure that apart from encapsulating the cilium in an cation rich environment has a role in supporting it when the external mechanical stimuli pull on the ciliary tip (Eberl, 1999). The ciliary tip is attached to the cap cell which in turn is positioned directly beneath the epithelium. The current working model says that when the external stimulus pulls

on the cilium the mechanically gated ion channels present in the ciliary membrane open causing the K^+ influx and subsequent neuron depolarisation. It has been shown that a cytoskeletal protein DmEB1 provides structural tension to chordotonal organs and is necessary for their proper formation and maintaining their integrity (Elliott et al., 2005).

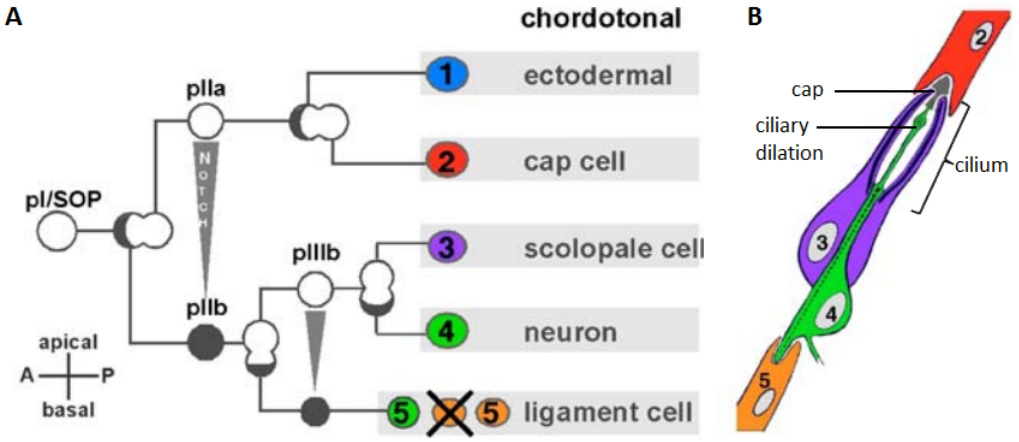

Figure 1.4. Chordotonal organs in *Drosophila*. **A**- diagram showing the SOP divisions leading to the chordotonal organ lineage formation. **B** - chordotonal organ structure, showing the four cell types, 2-cap cell, 3-scolopale cell, 4-neuron, 5-ligaments cell, and the sub/extracellular structures like the extracellular cap, and the cilium with the ciliary dilation. Adapted from Kernan (2007).

5.2.1.1 Chordotonal cilia compartmentalisation

Drosophila chordotonal cilia exhibit a distinct feature - they are compartmentalised in two structurally and functionally different regions. The cilium is divided by the ciliary dilation into the proximal and the distal zone (see Figure 1.5). The two zones differ in terms of the protein composition. The proximal zone houses proteins that are linked to the ciliary motility - axonemal dyneins (Lee et al., 2008). In fact chordotonal cilium is unique in that being a sensory cilium with 9+0 microtubule array it bears the hallmarks of motility crucial for its function. Interestingly the ciliary motility specific components are only localised in the proximal ciliary region. The function of this motility

is to actively mechanically augment the minute sound/mechanical stimuli. As suggested by Gopfert and Robert (2003) some axonemal dyneins are indeed necessary for the mechanical signal amplification and therefore are regarded to be involved in the chordotonal cilium motility. Other proteins present exclusively in the proximal ciliary zone are TRPV channels - Inactive (iav) and Nanchung (nan) (Kim et al., 2003; Gong et al., 2004)

The distal zone of the cho cilium houses the TRPN channel NompC (Lee et al., 2010). NompC mutant flies lack the mechanoreceptor potentials in the ES organs (Kernan et al., 1994) and the sound-evoked potentials in the antennal chordotonal organs ((Eberl et al., 2000).

The two ciliary zones are divided by the ciliary dilation. It is a crystalline structure localised at about half the length of the cilium. The protein composition of the ciliary dilation is largely unknown. One protein shown to localise to the ciliary dilation is RempA (Lee et al., 2008). It has been shown to delimit the ciliary zones.

It is interesting that apart from the compartment specific localisation of motility proteins the TRPN and TRPV channels seem to be localised to a specific ciliary zone. The TRPV (iav and nan) channels are only present on the proximal cilium while the TRPN NompC channel is specifically found distally to the ciliary dilation. It has been proposed that the TRPN and TRPV channels might have opposing functions ((Göpfert et al., 2006; Lee et al., 2008)). The proposed model assumes that the distally localised TRPN triggers the motility response that allows for the stimulus augmentation. The proximally localised TRPN channels are then activated upon the ciliary movement (membrane tension gated - open when the tension along the ciliary membrane increases) and reduce the ciliary motility leading to the neuronal repolarisation and restoration of the resting potential.

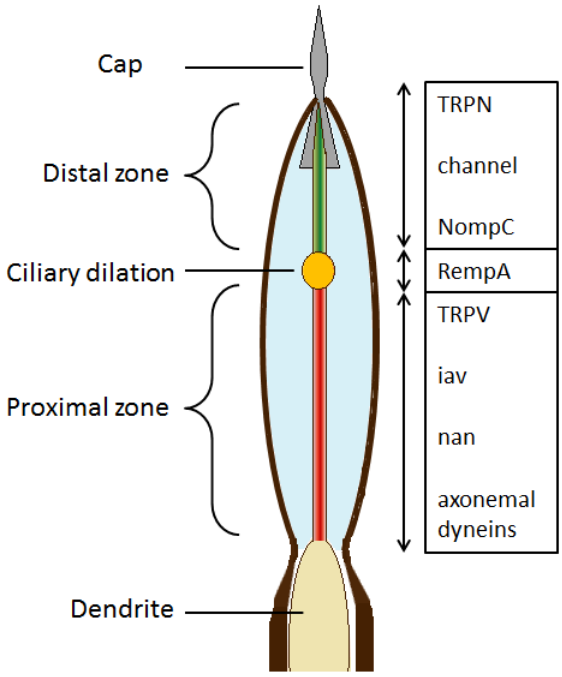

Figure 1.5. Chordotonal cilia compartmentalisation. Chordotonal organ neuron enclosed within a scolopale (brown). The cilium in depicted as a compartmentalised organelle in red (proximal zone), yellow (ciliary dilation), and green (distal zone). Each ciliary compartment houses specifically localised proteins as listed in the boxes on the right side of the figure.

5.2.1.2 Embryonic/larval Each embryonic abdominal hemisegment bears eight chordotonal organs - one v'ch1, a cluster of five - lch5, and a small cluster of two cho - vchA/B. The number and position of the larval chordotonal organs reflects exactly that of the embryos. The function of larval chordotonal organs is hearing (Zhang et al., 2013) and proprioception (Field and Matheson, 1998). The lack of a larval retraction reaction in response to a sound stimulus in *atonal* mutant larvae (lacking cho) demonstrates clearly that larval cho are necessary for hearing (Hope, Jarman unpublished data). *Drosophila* larva lacking the chordotonal organs are also unresponsive to touch (Caldwell et al., 2003) and their crawl path is severely shortened in comparison to the control larvae. This is due to lack of the coordination in peristaltic muscle movements and also due to more frequent decision-making bouts.

5.2.1.3 Johnston's organ Johnston's organ is a large cluster of chordotonal organs positioned in the second segment of the adult fly antenna. JO consists of over 200 chordotonal organs each of which houses two to three neurons. The JO is responsible for the adult fly hearing as well as sensation of wind direction, balance and gravitaxis. The hearing is mediated by sympathetical vibrations of the arista and the third antennal segment (a3) in response to sound (see Figure 1.6). The vibrations are picked up by the large array of ciliated cho neurons localised in the a2, processed into membrane depolarisation, and transmitted to the brain. It has been shown that the JO neurons can be subdivided into five groups that are different genetically and that transfer the input into different brain areas (Kamikouchi et al., 2006). Two of the subgroups respond preferentially to the sound evoked vibrations while another two subgroups seem to specialise in the gravity evoked response (Kamikouchi et al., 2009).

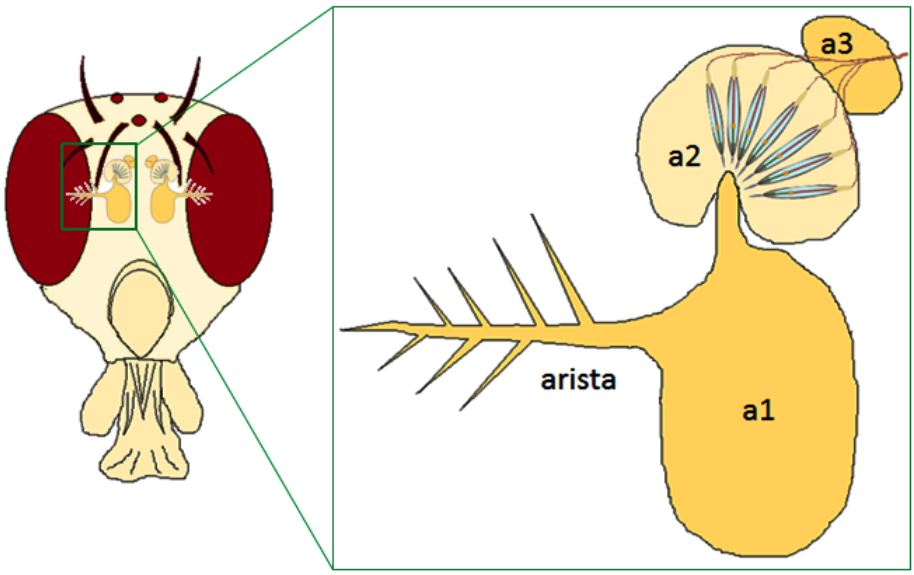

Figure 1.6. *Drosophila* antennal Johnston's organ. *Drosophila* antennae (in the green box) consist of three segments (a1, a2 and a3), the JO containing over 300 single chordotonal organs, is localised in the second segment (a2).

5.2.1.4 Femoral cho Adult fly femoral chordotonal organs are arranged into three groups. One large group of 32 cho is localised at the distal epicuticular surface of the femur. Two other central groups consist of about 42 cho together and ale localised slightly deeper and they are connected to femoral muscles (Shanbhag et al., 1992). Together with the cho localised at the wing base the femoral chordotonal organs are responsible for body balance and the body position feedback.

5.2.2 ES organs

Drosophila external sensory (ES) organs are scattered on the whole body surface. They can be subdivided into two subcategories - the trichoid sensilla (bristles) and the campaniform sensilla. The ES organs are mainly touch receptors, that transform the campaniform dome deformation or the bristle deflection into the mechanosensory signal. The bristles are further divided into macroachaetae and microachaetae. The macroachaetae are localised on the head, thorax and limbs while the microachaetae do not follow any pattern in terms of localisation. Instead they are regularly scattered on the whole body. Each bristle is an independent sensory organ innervated by a single ciliated neuron (with some exceptions, Hartenstein, 1988). The ES organ cilium differs greatly from the cho cilium. It is a lot shorter and it terminates with a microtubule rich tubular body (Hartenstein, 1988; Bechstedt et al., 2010). The short connecting cilium has the 9+0 microtubule arrangement but the tubular body is a lot wider and is composed of a dense pack of microtubules. The ES neuron in enclosed in the sheath cell (see Fig. 1.7). The shaft cell and the socket cell form a cavity which is filled with the receptor lymph. The mechanism of the ES organ mechanotransduction is that the cuticle compresses from the bristle movement and this deformation is sensed by the dendrite tubular body and converted into neuronal potential (Eberl et al., 2000).

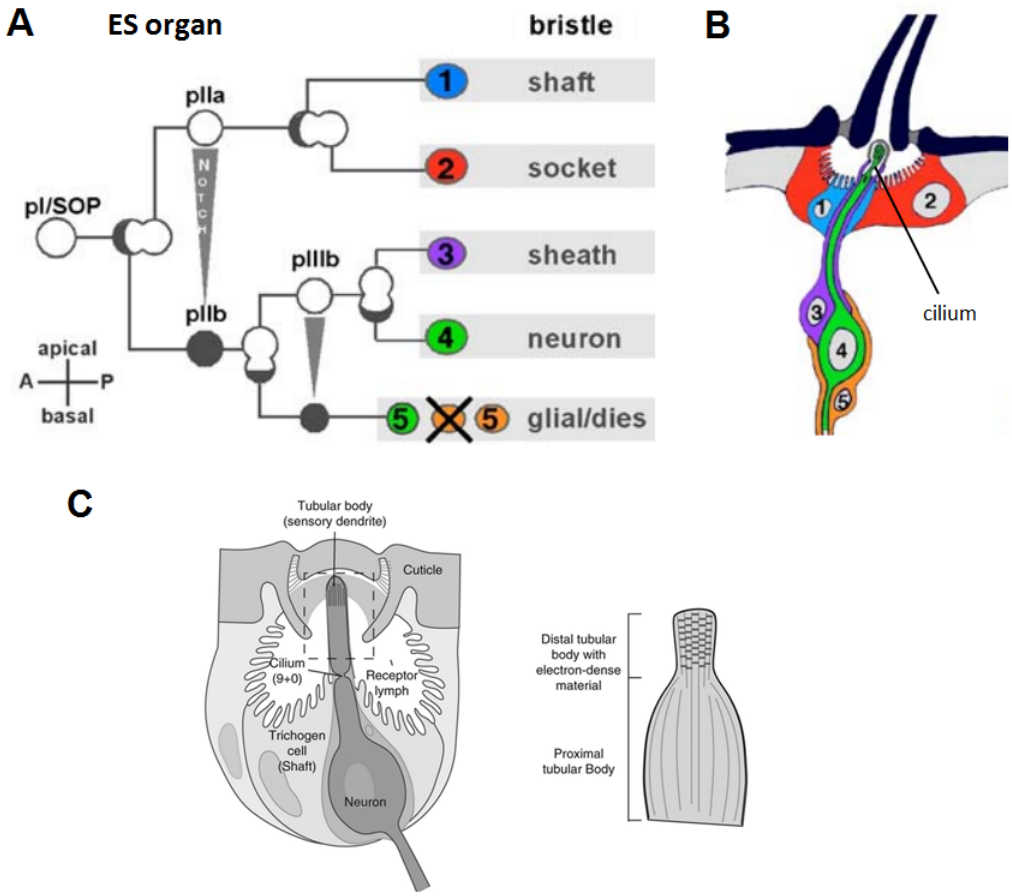

Figure 1.7. ES organs in *Drosophila*. **A**- diagram showing the SOP divisions leading to the external sensory organ lineage formation. **B** - ES organ structure, showing the five cell types, 1-shaft cell, 2-socket cell, 3-sheath cell, 4-neuron, 5-glial cell, and the subcellular structures of the cilium. Adapted from Kernan (2007). **C** - structure of the ES organ cilium and the tubular body. Taken from Bechstedt et al (2010).

6 *Drosophila* PNS development and specialisation

Drosophila PNS formation starts at stage 9 of embryonic development and is completed in late stage 16. The PNS development begins when the endo- and ectoderm layers are established and the embryonic segments are formed.

6.1 Proneural genes and SOP formation

Every *Drosophila* sensory organ is derived from a single precursor cell - sensory organ precursor (SOP). The process by which the SOP is singled out from the surrounding ectoderm starts with expression of proneural factors/genes in small patches of cells called the proneural clusters (Skeath and Carroll, 1994). The first phase of the proneural genes expression is managed by the *emc* and *sc* genes. The complement expression of the *sc* (in a small patch of cells) and the *emc* (in the surrounding cells) defines the proneural cluster - a patch of cells with neural potential (Ghysen et al., 1993). The cells with a high enough level of the scute protein begin the lateral inhibition process which is mediated by the Delta-Notch signaling (reviewed by Artavanis-Tsakonas, 1999). The Delta-Notch lateral inhibition promotes the proneural genes expression in one cell and in turn inhibits the proneural genes expression in the surrounding cells (see Figure 1.8). In the final stage the singled out SOP express high levels of *scute* and other proneural genes while the surrounding cells have the strongest level of activated Notch and Enhancer-of-split (Ghysen et al., 1993).

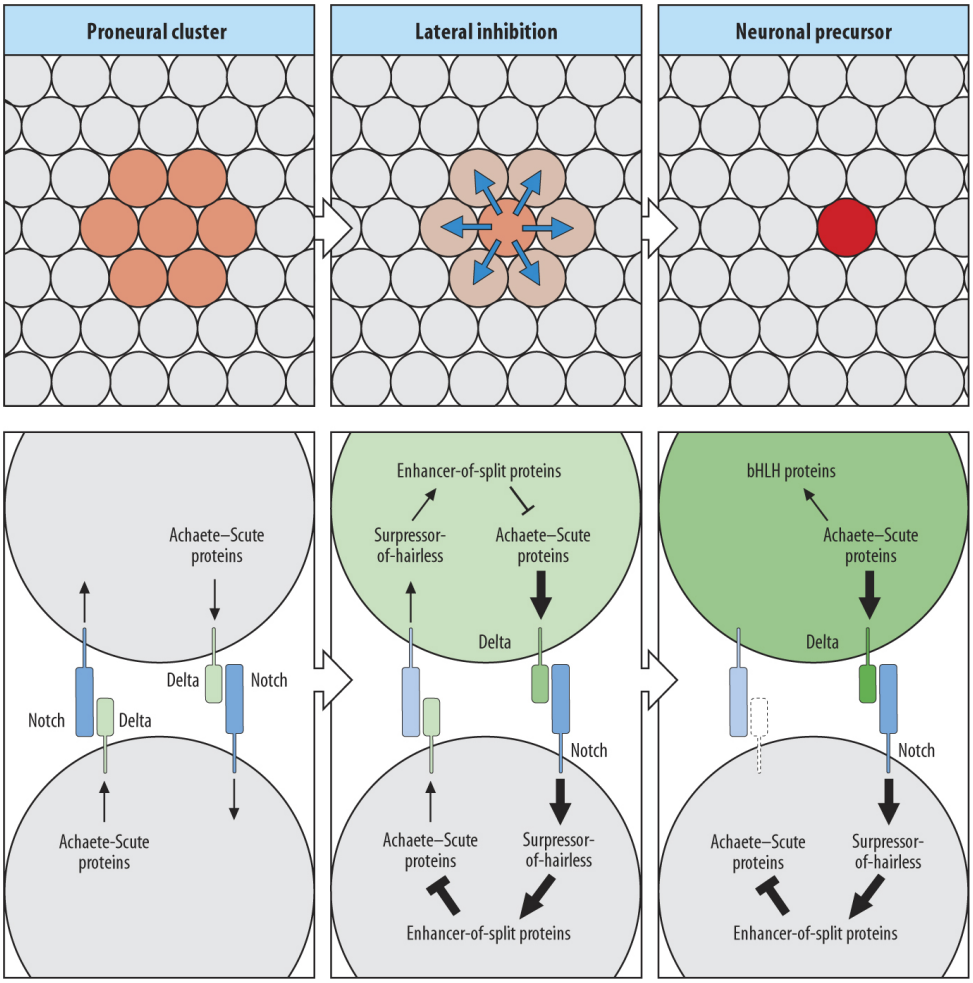

Figure 1.8. Delta-Notch signaling based lateral inhibition leading to designation of a single SOP cell from a proneural cluster. The intensity of red colour represents levels of the proneural gene expression. First the proneural cluster expressing an intermediate levels of a proneural gene emerges. Next, the lateral inhibition takes place between a cell expressing higher levels of the proneural factor and the surrrounding cells. Through this the SOP is singled out and the surrounding cells loose the proneural factor expression completely. Taken from Wolper et al, Principles of Development, Second Edition, 2002, Oxford University Press.

Another transcription factor is involved in proneural gene inhibition in non-SOP cells of proneural clusters. Senseless is a zinc-finger transcription factor required for the selection of SOPs. It is thought that when expressed at low levels Senseless acts as an active repressor of the proneural genes expression by binding to their regulatory regions (Jafar-Nejad et al., 2003). On the other hand high levels of the Senseless

factor can enhance the proneural factors expression which in turn further enhance the expression of Senseless itself (Jafar-Nejad et al., 2003; Acar et al., 2006). This positive feedback loop ensures that only one cell is singled out to commit to the SOP fate.

The SOP specialisation is the first step in which the different sensory organs gain their structural and functional specificity. In *Drosophila* there are five proneural genes which all encode basic Helix-Loop-Helix (bHLH) transcription factors: *atonal, amos, achaete, scute* and *lethal of scute* (Bertrand et al., 2002). The SOPs giving rise to ES lineage are dependent on the Achaete-Scute complex genes (AS-C) (Jiménez and Campos-Ortega, 1990) while the chordotonal SOPs require the atonal gene (Jarman et al., 1993, 1995). The SOP fate choice towards the ES and cho is dependent on the differential expression of the homeobox gene - *cut* (Blochlinger et al., 1990). The expression of *cut* is driven by the AS-C genes and actively repressed by *atonal* (Jarman and Ahmed, 1998). In the *cut* mutants the ES organs SOPs are transformed into chordotonal organs (Bodmer et al., 1987) and when *cut* is misexpressed in Cho SOPs they are transformed into ES organs (Blochlinger et al., 1991). Another proneural factor - *amos* (absent MD neurons and olfactory sensilla) - is necessary for the formation of some subsets of olfactory sense organs and MD neurons (Goulding et al., 2000; zur Lage et al., 2003).

The number and specificity of the proneural factors underlie the diversity of the sensory organs in *Drosophila*. It is the proneural genes that direct the differentiation of various types and subtypes of the sensory neurons. But the expression of some proneural genes overlaps in different sensory lineages. It is therefore important to understand the genetic regulation standing behind the later stages of the PNS organs specialisation and differentiation.

6.2 Transcriptional regulation of the ciliated sensory organs formation

The more intricate second phase of the sensory organ differentiation is modulated by the direct or indirect targets of the proneural genes. Many of these targets are transcriptional factors and expression of some of them is specific only to certain types of sensory organs and not the others. The differential expression of these transcription factors is a means of achieving the sensory organs structural and functional variety.

There have now been several studies aimed at finding the proneural factors downstream target genes. In the study by Reeves and Posakony (2005) a E(spl)m4-Gfp fusion protein has been used to separate the PNC cells. A comparative transcriptome analysis was then carried out that identified 207 genes predicted to be AS-C targets. Those genes included transcription factors, microtubule associated proteins, signaling molecules and receptors. Although the study has only examined the PNC transcriptome (not the SOPs transcriptome) it is conceivable that some of the genes identified can be involved in ES organs specification. Another study by Aerts et al (2010) identified 451 potential Atonal target genes by a R8 photoreceptor microarray. Together with the results of another method - a computational binding motif search (ato specific E-box) (Aerts et al., 2010) this study provides an insight into the transcriptional regulatory network leading to *Drosophila* eye differentiation.

A most recent study by Cachero et al, (2011) has performed *atonal* expressing cells transcriptome analysis in order to identify potential Atonal target genes in the ciliated chordotonal cells. In contrast to other microarray studies looking for proneural genes targets, this one performed the microarray at three different time points. This allowed to differentiate between the genes that are expressed earlier or later during the chordotonal sensory neurogenesis (ciliogenesis). Strikingly some ciliogenesis

specific genes (*Rootletin* orthologue - *CG6129*, IFT-A and IFT-B complex proteins homologues - *IFT46* and *IFT122*, and *unc*) seem to be expressed in the earliest time point tested (namely early stage 11). At this stage the SOP cells still undergo asymmetric divisions and have not yet started to differentiate. Conversely some terminal ciliary differentiation genes like the TRP channels *iav* and *nan*, are not expressed until the latest timepoint examined (late stage 12). This suggests that a specific gene expression temporal program has to be followed for the chordotonal organ neuronal differentiation and ciliogenesis. In fact the differences in the ciliogenesis genes temporal expression pattern suggest existence of a differential transcriptional control.

The RNA *in situ* hybridisation of some *atonal* correlated genes revealed three main expression patterns - pan-neuronal (expression in both CNS and PNS), pan-sensory (expression in PNS only), and chordotonal specific (expression in a subset of PNS neurons - chordotonal neurons). Interestingly a distinct intermediate expression pattern was also seen in a group of potential atonal target genes (for example *CG6129* gene). This pattern was called chordotonal-enriched and was characterised by a strong persisting expression in the Cho cells and weak and often transient expression in the ES cells. Based on this result Cachero et al suggested that the cilia structural differences between the ES and the Cho organs may arise from the modulation of time and level of some ciliogenesis genes expression. The suggested Atonal downstream transcription factors that might confer this differential specification are RFX (Regulatory Factor X), cato and fd3F (Cachero et al., 2011). Examining in detail the transcriptional regulation of an example gene showing the chordotonal-enriched expression pattern would help characterise the interdependancies between RFX, fd3F and possibly other transcription factors.

The *Drosophila RFX* homologue has first been found and characterised by Dubruille et al (2002). By *RFX* mutant analysis it has been shown that RFX is absolutely

necessary for the ciliated sensory organs differentiation and formation. The study by Laurencon et al (2007) identified RFX target genes by a comparative genomic screen for the conserved RFX binding motif - the X-box. The RFX target genes include many IFT genes, homologues of Bardet-Biedl and Meckel-Grueber syndrome (known ciliopathies) causative genes, components of the ciliary axoneme and supporting structures (rootlets). RFX is regarded as a transcriptional regulator of the core ciliary genes. In *Drosophila RFX* is expressed in all ciliated cells - both chordotonal and ES. *Drosophila RFX* itself has the chordotonal-enriched expression pattern (Cachero et al., 2011) which means that its at various timepoints its levels are different in chordotonal cells and in ES cells. This indicates that *RFX* on its own might be responsible for the differential expression of some ciliary genes in the ES and Cho organs.

Another ciliary specific transcription factor in *Drosophila* is fd3F. It is a divergent member of the Forkhead transcription factors and a distant homologue of human cilia motility transcription factor FoxJ1 (Newton et al., 2012). *Fd3F* expression pattern is chordotonal specific (Cachero et al., 2011). In *Drosophila* its target genes include the axonemal dyneins homologues - *Dhc62B, Dhc93AB, Dhc16F,* axonemal dynein light chains *CG8800* (*DNAL1*) and *CG34192* (*DNALRB2*), light-intermediate chain *CG6971* (*DNALI1*), and intermediate chain *CG13930* (*IC138*, *WDR78*). *Drosophila* fd3F also regulates expression of some dynein assembly factors (*tilB*), retrograde IFT proteins necessary for the cilia compartmentalisation into motile and sensory zones (*rempA*), and two TRPV channels (*iav* and *nan*) that are possibly involved in the ciliary motility modulation (Newton et al., 2012). In general the fd3F is not considered to directly regulate core ciliogenesis but it has been shown to drive the aspects of ciliary function that are specific to chordotonal organs.

Although many suggestions have been formulated regarding what might regulate the

ciliary diversity there is no direct evidence of a complete regulatory network standing behind it.

7 Aims of the thesis

Drosophila has two distinct types of ciliated sensory neurons - the external sensory neurons and the chordotonal neurons. Both cell types are derived from one mother cell but vary greatly in terms of both structure and function. This study attempts to clarify the existing knowledge on how this functional and structural difference is achieved. Some genes exhibit a differential expression pattern in ES and Cho cells (the chordotonal-enriched expression pattern) which suggests there might be some differences in the way those genes are transcriptionally regulated in both cell types. Cachero et al (2011) have shown this expression pattern is followed by many genes that fall into the ciliary motility genes category. One of the genes pointed out in the Cachero et al research was *CG6129*. It is presumed *CG6129* is an orthologue of human *Rootletin* and as such was not thought to have a direct link to ciliary motility. I have therefore chosen this gene, as an example of differentially expressed ciliary gene, to examine the the regulatory mechanisms underlying the differences in chordotonal organs and ES organs expression.

This study aims to confirm the orthology between the human *Rootletin* gene and the *Drosophila CG6129* gene. *CG6129* gene is differentially expressed in chordotonal organs and external sensory organs. It may therefore play a role in establishing the structural and functional differences between those two ciliated organ types. I aim to to study the function and regulation of the *CG6129* gene in two different *Drosophila* ciliated cell types. Seeing how a differentially expressed ciliary gene is regulated will potentially help to understand the mechanisms regulating the differential ciliogenesis.

Part II

CG6129 as a potential orthologue of Rootletin

8 Introduction

8.1 Ciliary rootlets

Ciliary rootlets are organelles tightly connected to the presence of cilia. Large striated structures of rootlets are found in various ciliated tissues (airway epithelia, retina, oviduct epithelia) regardless of the function of the cilia and their ability to produce movement.

8.1.1 Ciliary rootlets structure

Ciliary rootlets have first been described over a century ago (Engelmann, 1880) and have since been studied extensively. A fine structure of the ciliary rootlets was described in detail with the advent of the electron microscopy. In the *Anodonta* intestine preparation the rootlets are seen as large striated conical structures localised at the base of the cilium and connected to the ciliary basal corpuscule but not continuous with it. The wide conical shape of the rootlet gradually thins out and the finer fibril goes down as far as the nucleus and is approximately 25um long (Worley et al., 1953). Typical ciliary rootlets are 80-100nm in diameter and span from the base of the cilium through the cell to end near the nucleus. The cross-striation of rootlets is regularly interspaced (70nm) (Fawcett and Porter, 1954). The

apical portion of ciliary rootlets is extensively interconnected with other cytoskeletal structures (actin and intermediate filaments) (Lemullois et al., 1987).

8.1.2 A major protein component of ciliary rootlets.

The rootlets are the largest cytoskeleton structures but the main protein component of this organelle has only been described and isolated over a century later (Klotz et al., 1986; Hagiwara et al., 2000; Yang et al., 2002). First protein component of rootlets was isolated from quail oviduct preparation. The protein was enriched in the cortical region of ciliated cells but also exhibited some centrosomal localisation. In the year 2000 Hagiwara et al described a protein of 195kDa that has been isolated from a semi-purified apical cortex preparation of the human oviduct epithelium. Two years later Yang et al (Yang et al., 2002) have described the main protein component of murine rootlets. Rootletin - a 220kDa large coil-coiled protein has been isolated from murine retinal homogenate. Murine Rootletin has an extensive coiled-coil domain in the COOH-terminus and a globular head domain at the NH_2-terminus. The head domain has been shown to interact with kinesin light chain and thus it may have a role in the vesicular transport within the cell (Yang and Li, 2005). The tail domain mediates multimerization which presumably enables the protein to form a large striated fibrous structure of the rootlet. Rootletin can be found in abundance in apical region of all ciliated tissues. In non ciliated cells mouse Rootletin localizes to the centrosomes and the appearance of the Rootletin here changes cyclically in coordination with the cell cycle.

8.2 Ciliary rootlets proposed functions

Ciliary rootlets vary across species and also across tissues within the same species. The variety can be seen in the rootlets length, width or the number of rootlets protruding from a single ciliary basal body. This could possibly be caused by slightly different roles the cilia play in different tissues. Below are the ciliary rootlet functions as proposed and/or described in various studies.

8.2.1 cilia anchoring

An obvious and first proposed function of the ciliary rootlet is anchoring the cilium (Worley et al., 1953; Sleigh and Silvester, 1983). Especially large ciliary rootlets are seen in the mammalian photoreceptors (Spira and Milman, 1979). It can be explained by the fact that a relatively small connecting cilium is responsible for holding a very large organelle. This means the cilium is under obvious mechanical stress and needs extensive anchoring in order to maintain its integrity. This was supported by the finding that in an organism lacking the ciliary rootlets the photoreceptors degenerate as the specimen ages (Yang and Li, 2005).

8.2.2 Rootletin role in contraction

The cross striation of the ciliary rootlets resembled some researchers of the striated skeletal muscle (Salisbury and Floyd, 1978). This likeness caused some to propose a contractile role of the ciliary rootlets (Salisbury et al., 1984). Other studies also suggested that ciliary rootlets might function through contraction. Anti-actinin and anti-centrin antibodies have been shown to bind the ciliary rootlets of insect scolopidia (Wolfrum, 1992). Centrin has been shown to play a role in Calcium-mediated contraction (Wolfrum, 1995) and actinin is a known marker of the Z-disk of a skeletal

muscle (Sjöblom et al., 2008). Taking those two together Wolfrum suggested that by contraction and relaxation ciliary rootlets might have a role in the sensory transduction in insect mechanoreceptors. He also hypothesised that through contracting the rootlets help position the basal bodies to their original localisation after the mechanical stimulus (Wolfrum, 1992).

8.2.3 signal transduction

Apart form suggestions that ciliary rootlets might have an indirect role in the signal transduction by contractions (previous paragraph) it has also been suggested that rootlets are directly involved in conducting the signal (Sjostrand, 1953). As seen on the electron micrographs of guinea pig retina the ciliary rootlets are very closely associated with mitochondria. Sjostrand implied that the light stimulus is received by the outer segment of the photoreceptor rod and is then passed on through the connecting fibril (connecting cilium) to the ciliary rootlets which then pass the signal on to the mitochondria. From there the signal would be transduced in a manner similar to the non-myelinated nerve fibers signal transduction.

8.2.4 Rootletin role in transport (IFT)

Rootletin was also suggested to be involved in vesicular transport and protein targeting to the cilium. Rootletin interacts with kinesin light chain (Yang and Li, 2005) and other proteins facilitating or directly involved in vesicular transport (Lanzetti, 2007; Bauer et al., 2011). In *C. elegans* Che-10, an orthologue of human Rootletin, is shown to indirectly influence the IFT by modulating the preassembly/localisation of various intraflagellar transport proteins to the periciliary membrane compartment (Mohan et al., 2013). Che-10 protein localises to the ciliary rootlets and also to the transition zone and the basal bodies of cilia. In Che-10 mutant cilia are formed nor-

mally but start to degenerate in late larvae. In Che-10 mutants the transition zone, the basal bodies and the PCMC are also affected (judging by localisation of various markers). PCMC is crucial for IFT machinery assembly and protein docking to the transition zone. By enabling normal assembly of the IFT machinery to the base of the cilium Che-10 is responsible for stable and efficient IFT and thus for maintaining the ciliary structure and functionality.

8.2.5 Rooltetin role in centriolar cohesion - mitosis

All the previous proposed functions of ciliary rootlets were suggested on the basis of its close connection with cilia. However, apart from the localisation at the ciliary base the murine Rootletin can also be found at the centrosomes (Yang et al., 2002). The anti-Rootletin antibody reveals two to four 0.5um long fibers protruding from the proximal end of each of the centrioles found in the U2OS cells. The Rootletin staining is strong throughout the interphase but disappears at the onset of mitosis (prophase).

Its role at this localisation is very specialised. As shown in human cell lines, Rootletin acts as a physical linker between the centrioles during the interphase (Bahe et al., 2005). This linker formation is responsible for centriolar cohesion during the interphase. The importance of the centriolar cohesion is exhibited in the fact that when centrosomes split prematurely (in the interphase) extra-centrosomal structures are formed and the mitotic microtubule array becomes unfocused (Prigent et al., 2005) which can lead to chromosomal aberrations (Lee and Gollahon, 2013; Neal et al., 2014). On the other hand if the centrosomes do not separate before the mitosis the cell division cannot take place (Faragher and Fry, 2003).

8.2.6 Ciliary rootlets in *Drosophila*

There is one proposed Rootletin orthologue gene in *Drosophila* - CG6129 (Laurençon et al., 2007). CG6129 expression is confined to the type I sensory neurons which are the only somatic ciliated cells (apart from the neurons innervating the external sensory organs) in *Drosophila*. The CG6129-GFP fusion protein localises to the dendritic processes of the chordotonal organs just proximally to the base of the cilium. Such pattern is in agreement with the possible function of CG6129 (Rootletin orthologue) as a main protein component of ciliary rootlets. No CG6129 protein is seen in non ciliated cells or the external sensory neurons. As suggested by the FlyBase high-throughput expression data CG6129 transcript is abundant in *Drosophila* testes. Interestingly no publication reports CG6129 expression in *Drosophila* testes.

8.3 Centrosome cycle

As mentioned before Rootletin protein localises to the centrosomes in most organisms. In order to understand the possible function of Rootletin at this localisation it is important to know the correlations between the cell cycle and the centrosome cycle .

Centrosomes and centrioles are formed and function in a very specific manner with coordination with the cell cycle. The mechanisms governing the centrosome/cell cycle have been well studied. The protein control machinery consists of many opposing phosphorylating/dephosphorylating elements and a fine well balanced equilibrium is necessary for the cell to go through the division or to enter the quiescent state (Meraldi and Nigg, 2001). The cell cycle starts when a new cell is formed and it enters the G1 phase (gap 1 phase after mitosis). In this phase the cell grows and proteins necessary for the DNA synthesis are synthesized. In the S (synthesis) phase

the genetic information is replicated in preparation for the cell division. During the G2 (gap 2) phase the cell continues to grow and the G2 checkpoint is executed in order to prepare for the mitosis (Vermeulen et al., 2003). The cytoskeleton plays a key role during the mitotic cell division. A functional mitotic spindle is crucial for normal chromosome segregation and therefore for a successful mitosis and viability of the newly formed cells. The mitotic spindle is build of microtubules and its formation is governed by the microtubule organizing centre (MTOC) - the centrosome. In mammals each centrosome consists of two centrioles which are surrounded by an amorphous structure of the pericentriolar material (Schnackenberg and Palazzo, 1999). The pericentriolar material contains proteins responsible for the anchoring and formation of the microtubules (Andersen, 1999). The centrosomes undergo a cycle of duplication/separation in tight correlation with the cell cycle.

8.3.1 Cell cycle and centrosome cycle

When a new cell is formed in the course of mitotic division it is equipped with one centrosome containing two loosely attached centrioles. Proteins forming the structure of this loose attachment are Rootletin (Bahe et al., 2005; Yang et al., 2006) and C-Nap (Mayor et al., 2000). This tether is also called a G1-G2 tether (GGT) because it occurs during the whole interphase between the mother centrioles (Nigg and Stearns, 2011). When a cell enters the S phase of the cell cycle the centrosomes undergo duplication (see Fig. 2.1). A procentriole is formed at the proximal end of each mother centriole. The mother centrioles are very tightly linked to the procentrioles and this connection is called a S-M linker (SML) as it lasts through the S-M phases of the cell cycle. The procentrioles elongate through the S phase and early G2 phase. When they reach the final length the procentioles undergo maturation. During this process the newly formed centrioles acquire distal and subsidial appendages which

enable microtubule anchoring. Upon the entry into mitosis the loose G1-G2 tether is broken and two centrosomes (each now containing two mature centrioles) can locate on the opposite poles of the dividing cell and nucleate the formation of the mitotic spindle. In late cell division when the sister chromatids are separated each centrosome undergoes disengagement (the S-M linker break). It is worth noting that in human cells the same proteins - separase (Tsou et al., 2009) and cohesin (Schöckel et al., 2011) - are involved in the chromatid separation as well as in the centrioles disengagement. This is a mechanism by which a formation of multipolar mitotic spindles is prevented (Nigg, 2007). The disengagement of the centrioles is crucial for the cell to enter another centrosome cycle. Under various conditions cells can go into a quiescent state (also called a G0 phase of the cell cycle). In G0 centrioles act as a basal body for the cilium (Kobayashi and Dynlacht, 2011).

8.3.2 Ciliary assembly/disassembly in the cell cycle

Cilia undergo a cycle of assembly and disassembly during the cell cycle. This is comprehensible seeing that the centrioles play a dual role in both cell division (as a MTOC-microtubule organising centre) and nucleation of the ciliary axoneme (basal body). After the division cell can either enter the G0 quiescent state and produce a cilium (Tucker et al., 1979) (example of such would be a ciliated type I sensory neuron in *Drosophila*) or continue with the cell cycle and enter the G1 phase.

Interestingly regardless of the phase the cell enters (G0 or G1) many cell types produce a primary cilium. As explained by Seeley and Nachury (2010) a primary cilium assembly in the G1 phase is a characteristic feature of proliferating cells. After the division the centrosome migrates to the cell surface and docks at the plasma membrane (Sorokin, 1962). Typical ciliary basal body has three types of appendages - a ciliary rootlet, basal foot and transition fibers. The last two are structurally very

similar to the distal and subsidial appendages of a newly formed centriole and are responsible for docking to the membrane and the microtubule nucleation (Kobayashi and Dynlacht, 2011). Of the two centrioles present in a cell only the mother centriole is capable of transformation into a ciliary basal body (Piel et al., 2000). When the centrosome transforms into the basal body the cilium is formed through the intraflagellar transport and persists through the interphase. Upon the entry into mitotic cell division the cilia are almost always disassembled (Archer and Wheatley, 1971). If the cell cycle is to progress into mitosis the cilium must be resorbed to free the centrosome. It has been shown that the trigger for the ciliary disassembly is a centrosomal kinase Aurora A. This kinase is also responsible for cell cycle regulation in the S-G2 phase. By phosphorylating (activating) the histone deacetylase 6 (HDAC6) Aurora A promotes entry into mitosis. It has been proposed that HDAC6 can localise in the cilia and when activated deacetylates tubulin and causes a rapid resorption of the cilium. Proteins like katanin (in *C. renhardtii*) (Parker et al., 2010) and Pitchfork (in mouse cells) (Kinzel et al., 2010) are responsible for releasing the basal body from the flagellum. When the basal body is released it assumes its role as a microtubule-organizing centre (MTOC) and takes part in mitosis.

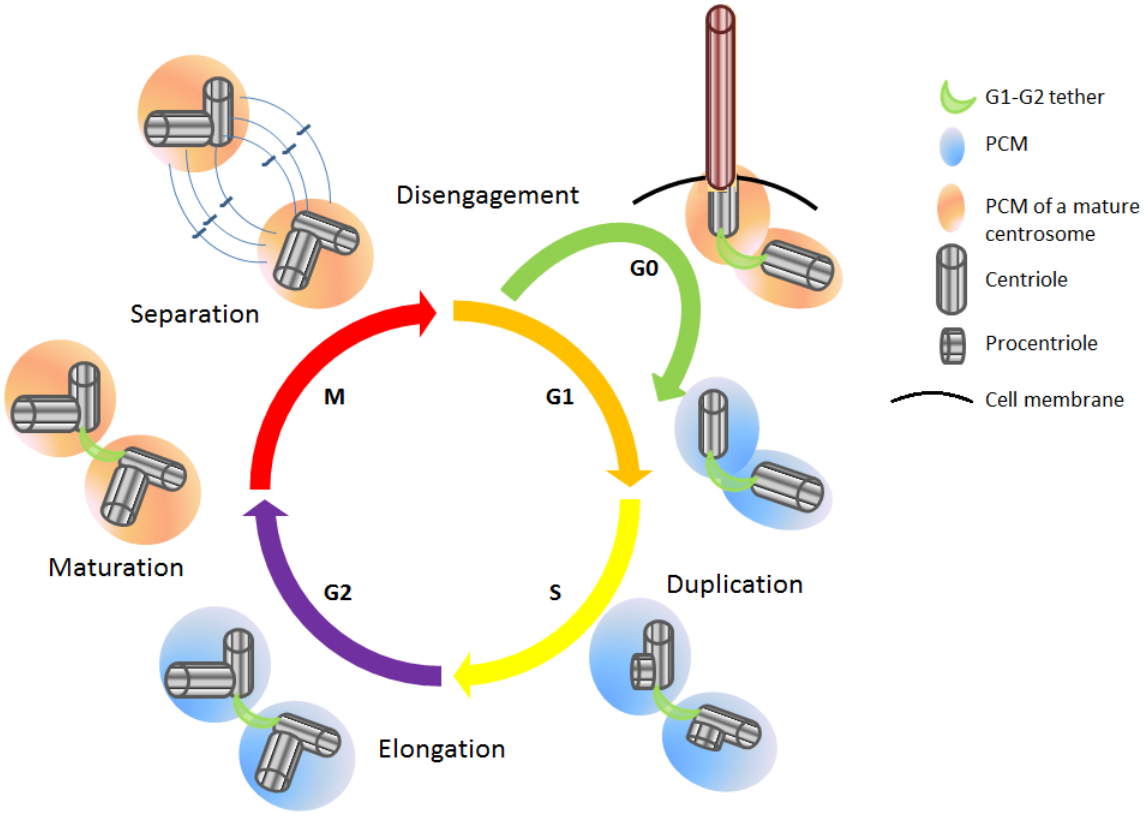

Figure 2.1. Diagram showing the vertebrate centrosome cycle in the context of the cell cycle. Centrosome duplication starts in the S-phase. Procentrioles elongate through the G2-phase and then become a mature centriole on the verge of mitosis. Before the spindle formation centrosomes separate. At the end of mitosis the mother and daughter centrioles disengage. Based on a figure from Bettencourt-Dias M, Carvalho-Santos Z. (2008). Double life of centrioles: CP110 in the spotlight. Trends Cell Biol. 18(1):8-1.

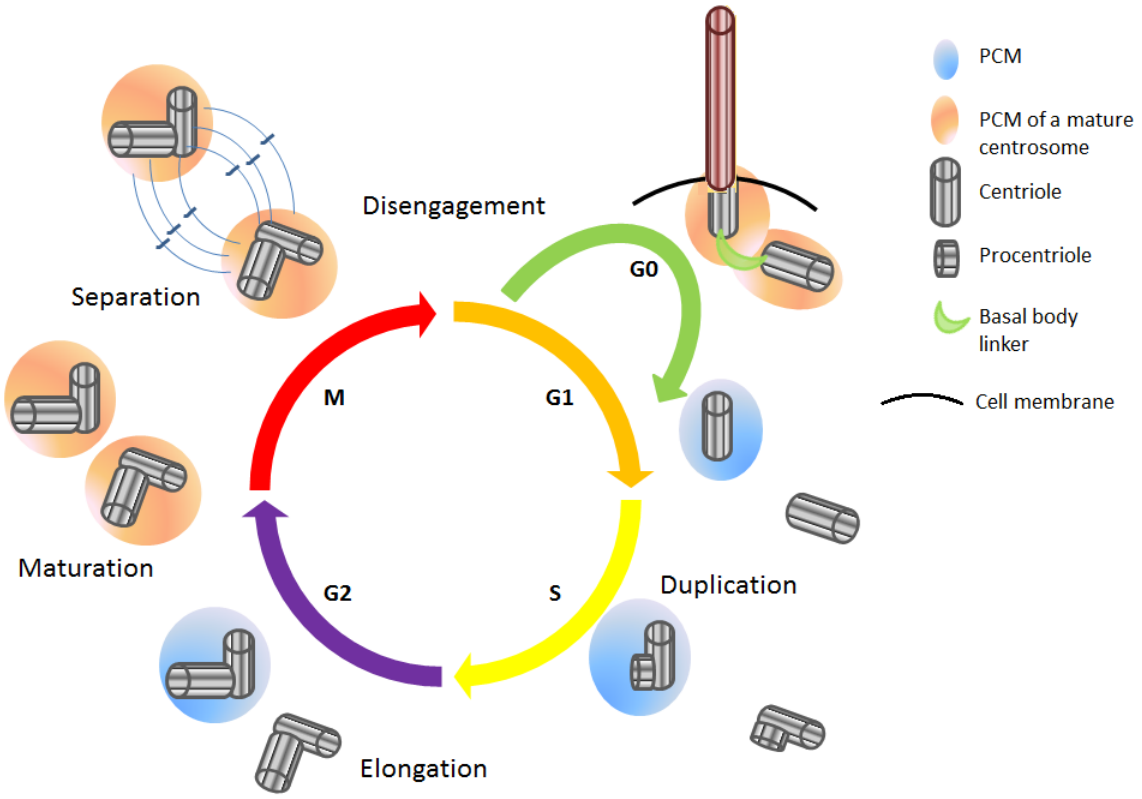

Figure 2.2. Diagram showing the centrosome cycle in *Drosophila*. Note the numerous variations from the vertebrate centrosome cycle - the centrioles are not connected by the GGT-tether theoughout the interphase. The daughter centriole is not surrounded by the pericentriolar material untill the verge of mitosis when its procentriole matures. Based on a figure from Bettencourt-Dias M, Carvalho-Santos Z. (2008). Double life of centrioles: CP110 in the spotlight. Trends Cell Biol. 18(1):8-1.

8.4 Centrosome cycle in *Drosophila*

Centrosome cycle in *Drosophila* is somewhat different than described earlier. The key difference is the lack of the G1-G2 tether (see Fig. 2.2). In early *Drosophila* embryo (Debec et al., 1999) as well as in the dividing larval neuroblasts (Basto et al., 2006) centrosomes separate straight after the cell division. As shown by Callani and Riparbelli (1990) the centrosomes split in the late telophase when the nuclear envelope of a new cell is formed. It is very interesting that the younger (daughter centriole) sheds all the pericentriolar material in the early interphase (Rusan and

Peifer, 2007). This means that the newly formed cell possesses only one microtubule organising centre (MTOC). The centriole that retains the PCM remains stable and the daughter centriole migrates away from the MTOC. At the onset of mitosis (prophase) the daughter centriole matures and becomes a fully functional MTOC which enables the entry into the cell division. In general it appears that in *Drosophila* the centrosomes are largely dispensable for the cell divisions (Basto et al., 2006; Badano and Katsanis, 2006). Flies that do not express some important components of the PCM develop grossly normally which means that cells in developing *Drosophila* embryo/larva can divide without various centriolar (Basto et al., 2006; Mottier-Pavie and Megraw, 2009) or centrosomal (Martinez-Campos et al., 2004; Bettencourt-Dias et al., 2005) proteins.

8.5 Cilia assembly/disassembly in *Drosophila*

The cilia assembly/disassembly cycle does as such not exist in *Drosophila*. The reason for this is that fruitflies posses a very limited number of ciliated cells (sperm cells and type I sensory neurons). Those cells produce cilia upon maturation and once ciliated they do not divide and do not lose cilia. However *Drosophila* dividing spermatocytes follow a very interesting pattern showing that in some cases cilia do not disassemble during the cell division. Judging by the localisation of the basal body protein Unc (Baker et al., 2004) the spermatocytes produce four cilia, one per each membrane docked centriole (Riparbelli et al., 2012). In addition to that the centrioles remain functional as basal bodies when still elongating in the G2 phase. The most striking behaviour takes place in the meiotic division of the spermatocyte. The short cilia are invaginated within a small pocked of the cell membrane and such ciliated centrosomes assemble the bipolar microtubule spindle. After the first meiotic division the centrioles separate to form two centrosomes for the meiotic division II.

After the meiosis is finished each of the four spermatids possesses one centriole still bearing the function of a basal body to a short cilium. As the spermatid matures the short cilium is transiently disassembled, the centriole anchors at the nucleus and a new axoneme is formed (Riparbelli et al., 2012).

8.6 Rootletin and known interactors across species

As said before Rootletin is one of the molecules that serves as a protein link between the centrosomes in the interphase. The breaking of the centrosomal tether is a crucial step that is necessary for the mitosis to occur. On the other hand in some species (i e mouse) the occurrence of centrosomal cohesion during the interphase is quite crucial for normal cell divisions (Yang et al., 2006). It is therefore conceivable that formation and disassembly of the centrosomal linker must be controlled by some protein-protein interactions. Below are known interactors of Rootletin.

8.6.1 C-Nap

Human C-Nap is a 250kDa coiled coil protein which localises to the proximal end of centrioles in the centrosomes (Fry et al., 1998a). C-Nap has been shown to be a structural component of centrosomal linker during the interphase. The ablation of this centrosomal linker component causes centrosome splitting in the interphase (Mayor et al., 2000). Interestingly Mayor and colleagues have shown that the C-Nap protein does not span the entire distance between the centrioles which suggests that another protein might be involved in the tether. It has later been presented that C-Nap interacts with Rootletin (Yang et al., 2006). The two proteins colocalise at the proximal ends of centrioles (both in the ciliary basal bodies and the centrosomes), however the Rootletin spans the whole distance between the centrioles. At the onset

of mitosis C-Nap dissociates from the centrioles which in turn leads to dissociation of Rootletin as well. In a proposed model C-Nap is directly connected to the centrioles and serves as an anchor for Rootletin which is a major component of the centriolar linker.

8.6.2 Nek2

Nek2 is a mammalian homologue of a NIMA kinase first found in *Aspergillus nidulans* (Shultz et al, 1994). The NIMA related kinases are a family of serine-threonine kinases that modulate many aspects of mitotic progression such as chromatin condensation, cytokinesis, spindle formation and the timing of mitotic entry. In human cells Nek2 localises to the centrosomes throughout the cell cycle but its activity peaks in S and G2 cell cycle phases (Fry and Nigg, 1995). It has been shown that Nek2 interacts with both C-Nap (Fry et al., 1998a) and Rootletin (Bahe et al., 2005) and by phosphorylating both components of the centrosome linker causes centrosome splitting. This is a crucial step that is necessary for the mitosis entry. Nek2 activity during the cell cycle is controlled by opposing activity of protein phosphatase 1 (PP1) (Helps et al., 2000). Other substrates of Nek2 are casein, myelin basic protein, and PP1. Nek2 is also capable of autophosphorylation (Helps et al., 2000). Overexpression of active Nek2 protein in human cells causes centrosome splitting and centrosome dispersal.

8.6.3 Kinesin light chains

Kinesin light chains (KLCs) are members of kinesin protein family (Hirokawa et al, 2010). Kinesins are motor proteins responsible for carrying various cargo (proteins, organelles) along the microtubules in the process called intracellular transport. Rootletin has been shown to bind KLC1, KLC2, and KLC3 in mouse cells and tis-

sues (Yang and Li, 2005). This would suggest that rootlets might serve as a tract for kinesin mediated intracelullar transport but apparently the kinesins do not move along the Rootletin fibers. Instead the rootlets have been proposed to act as scaffold for kinesin-1 mediated vesicular transport (Yang and Li, 2005).

8.7 Aims of this chapter

Drosophila CG6129 gene is a proposed Rootletin orthologue. In this chapter the structural and functional similarities between Rootletin and CG6129 will be examined in order to confirm the orthology.

A function of the CG6129 protein in *Drosophila* at various stages of development will be thoroughly examined in order to find out what role the gene/protein has in *Drosophila* ciliogenesis, ciliary function and possibly cell/centrosome cycle in relevant tissues.

9 Results

9.1 CG6129 encodes a large coiled-coil protein

Murine Rootletin has a tail domain consisting of long coiled-coil structures, and a globular head domain (Yang et al., 2002). The head domain is suggested to bind to a kinesin light chain and thus it may be required for targeting the protein to its location at the ciliary basal body. The tail domain mediates multimerization. *CG6129* gene is localised on position 95E1 on the third chromosome and encodes a 232.73kDa protein. As suggested by Laurencon et al *CG6129* is the closest *Drosophila* gene to CROCC and therefore might be an orthologue of human Rootletin gene *CROCC*. There is approximately 20% identity of amino acid sequence between *CG6129* and CROCC and the secondary structure predicted by ModBase show that both have a globular head domain and extensive coiled-coil structure tail domain (see Fig. 2.3 B). Ensembl reveals multiple functional domains - SMC_prok type B - in the tail segment of both CG6129 (see Fig. 2.3 A) and CROCC. These are common bacterial type chromosome segregation domains consisting of large coiled-coil segment and small globular 'hinge' segment (Jessberger, 2002). SMC proteins are characteristic of forming hetero- and/or homo-dimers and the presence of those domains in *CG6129* may confirm its ability to homomultimerize (and form a large striated fibrous structure).

A Second orthology for CG6129 suggested by Ensembl is the human CEP250 gene. CEP250 protein has large coiled-coil domain and is involved in centrosome tethering (Mayor et al., 2000). It is proposed that mouse C-Nap1 (=CEP250) and Rootletin both take part centrosome cohesion by forming a transient filament network dependent on phosphorylation by Nek2 (Bahe et al., 2005). In *Drosophila* there is no *CEP250/C- Nap1* gene orthologue however the FlyBase annotates the *CG6129* as

CEP250 as well as the *CROCC*. Both C-Nap1 and Nek2 are involved in centrosome cycle (in human, Bahe et al., 2005).

Ensembl also implies a distant paralogy between CG6129 and two other *Drosophila* proteins: Gmap and CG3493. Both proteins are suspected to be involved in Golgi targeting based on the presence of the GRIP domain (Gmap and CG3493). The GRIP domain is crucial in targeting proteins to the Golgi apparatus and is present in several coiled-coil proteins. The GRIP domain has a very highly conserved tyrosine residue (Human, *C. elegans*, Yeast) that is necessary for its function (Munro and Nichols, 1999). CG6129 has a domain similar to the GRIP amino acid sequence suggesting a role in protein targeting. However the tyrosine residue is not conserved in CG6129 rendering the domain likely to be non-functional and lowering the possibility of its involvement in protein transport through the predicted GRIP domain.

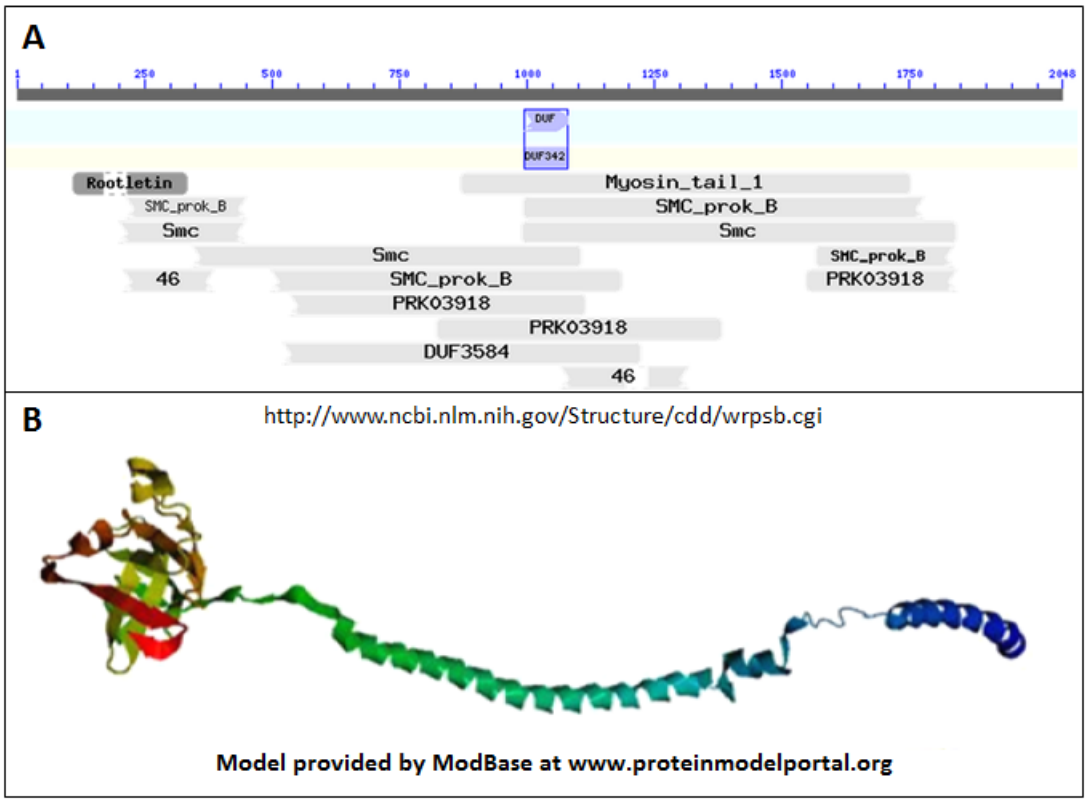

Figure 2.3. CG6129 domains and a spatial protein model. A - The length of the CG6129 protein is represented as a grey bar at the top. Underneath are the predicted domains. **B** - predicted spatial structure of the CG6129 protein.

9.2 CG6129 spatial and temporal expression

The *Drosophila* developing chordotonal neurons transcriptome analysis shows that *CG6129* gene expression is highly enriched in ciliated cells (18.64 times more transcript than in non-ciliated cells (Cachero et al., 2011)). This suggests its expression is specific to ciliated cells which in *Drosophila* are PNS type I neurons. I have carried out a RNA *in situ* hybridisation in order to visualise the *CG6129* expression pattern during *Drosophila* neurogenesis. A DIG-labeled probe hybridising to the 1112bp fragment of the 7th exon was used. As characterised by this technique *CG6129* presents a so-called chordotonal enriched expression pattern. It means that the gene is expressed in all type I sensory neurons but the expression levels are higher in

the chordotonal type neurons than in other types (external sensory neurons - ES) Its expression starts in developmental stage 12 in a cluster of cells most probably representing SOPs of both chordotonal organs and external sensory organs (see Fig. 2.4 A). In addition to evident chordotonal neuron expression in developmental stage 14 *CG6129* is also transiently expressed in all ES neurons (see Fig. 2.4 B). This clear ES cell expression is in contrast with what was reported by Laurencon et al in 2007. In this study a Rootletin-GFP fusion protein was expressed under the control of 1484bp upstream region. The expression of the fusion protein was limited to chordotonal organs only. It is possible that this was due to the fact that some important regulatory elements are missing form this context. In the latest stages (16-17) of embryonic development *CG6129* expression is the strongest and it is highly specific to the chordotonal neurons, clearly showing the lateral lch5 and lch1 and the ventral vcha and vchb neurons (see Fig. 2.4 C). Apart from type I sensory neuron expression CG6129 does not appear to be expressed elsewhere in the embryos.

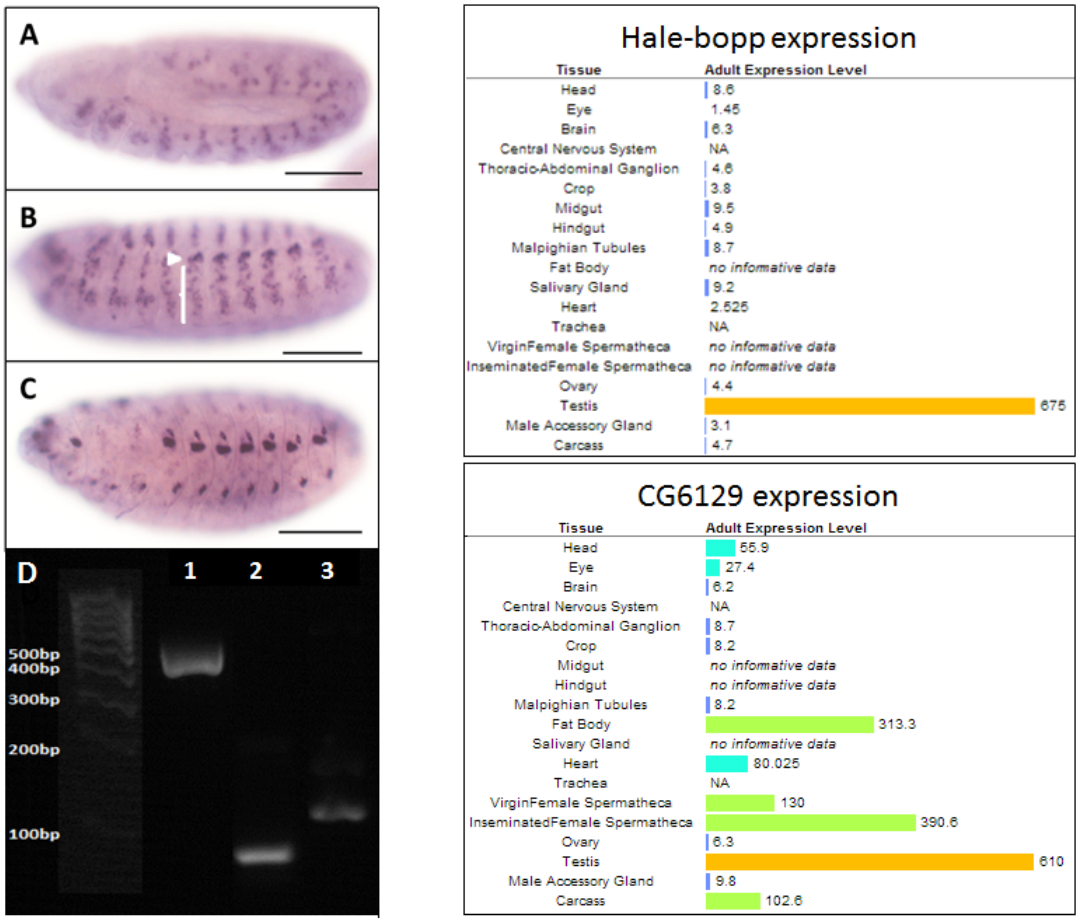

Figure 2.4. CG6129 expression in *Drosophila* embryos (A-C) and testes (D). A – developmental stage 12, transcript expressed in all PNS precursor cells, B – stage 14, transcript expressed in both chordotonal organs (white arrowhead) and external sensory organs (white bracket), C – stage 17, ES expression lost, transcript expression specific to CHO, D – adult testis RT-PCR, lane 1 - Hale-bopp band, 20ul of PCR product, band intensity 255 (average from 3 repetitions); lane 2 - CG6129 band, 45ul of the PCR product, band intensity 135 (average from 3 repetitions); lane 3 - tbp band, 45ul of the PCR product, band intensity 82 (average from 3 repetitions). Right panel shows Hale-bopp expression in various tissues and CG6129 expression in various tissues as shown on FlyBase (scores represent the microarray RPKM - reads per kilobase per million), FlyAtlas Anatomical Expression Data. Scale bars 100um (A-D).

According FlyBase high-throughput expression data *CG6129* is highly expressed in testes (610 RPKM - reads per kilobase per milion). However Laurencon et al (2007) did not find evidence of any expression in testes/spermatozoa. To clarify

this discrepancy I have performed CG6129 KD adult testes in situ hybridisation a number of times. Unfortunately no staining was visible in neither the WT control or the knock down. Therefore I have carried out a reverse transcription followed by a PCR using cDNA obtained from testes as a template (see Fig. 2.4 D). As controls I have used a Hale-bopp gene which is known to be very highly expressed in *Drosophila* testes and a tbp gene as a basal level expression control. Judging from the PCR product gel band intensity the Hale-bopp was highly expressed (in line with the FlyBase high throughput expression RNA-seq score of 675 RPKM (Fig. 2.4 E)). However the CG6129 gel band was much less intensive (see Fig. 2.4, D). This suggests that the FlyBase high throughput expression RNA-seq score for Rootletin (610 RPKM (Fig. 2.4 F)) might be somewhat misleading.

9.3 CG6129 RNAi knock down

Due to the lack of availability of *CG6129* mutant or P-element lines, all experiments examining the function of *CG6129* carried out during the course of this work were performed using RNAi knock down technique. Two different RNAi lines were used: w[1118]; P{GD11829}v22694 hereafter called a GD line and P{KK102209}VIE-260B hereafter called a KK line. The GD line is a part of a VDRC P-element GD library in which the RNAi constructs were inserted into a random position in the genome. The KK line is a part of the VDRC phiC31 KK library having the RNAi constructs inserted into a given position in the *Drosophila* genome. The two lines used in the course of this project are based on RNAi constructs complement to different parts of the *CG6129* gene - some experiments were performed on both of the lines to compare the results and to exclude the possibility of the results being an off target or position effect. The RNAi constructs were expressed under the control of a UAS enhancer (Dietzl et al., 2007) and the expression was driven by crossing the RNAi lines to

various Gal4 drivers - mainly scabrous-Gal4 for a knock-down specific to developing nervous system and Bam-Gal4 for a knock-down specific to testes (scabrous-Gal4 - (Klaes et al., 1994) and Bam-Gal4). In the case of sca-Gal4 driver the line also carried a UAS-Dcr2 construct. Dcr2 is a component of the RNAi silencing pathway and is often used in *Drosophila* RNAi knock downs to enhance phenotypes (Dietzl et al., 2007).

I performed RNA *in situ* hybridisation in order to evaluate the RNAi knock-down efficiency and its effect on the *CG6129* transcript levels during embryonic development. An overnight embryo collection was used in order to visualise the transcript levels during all stages of development. Embryos from the GD x scabrous-Gal4 cross had very little visible staining indicating that the RNAi silencing was very efficient (see Fig. 2.5, A-D). Although some residual expression takes place, the level of transcript was sufficiently low to possibly cause a phenotype in further experiments.

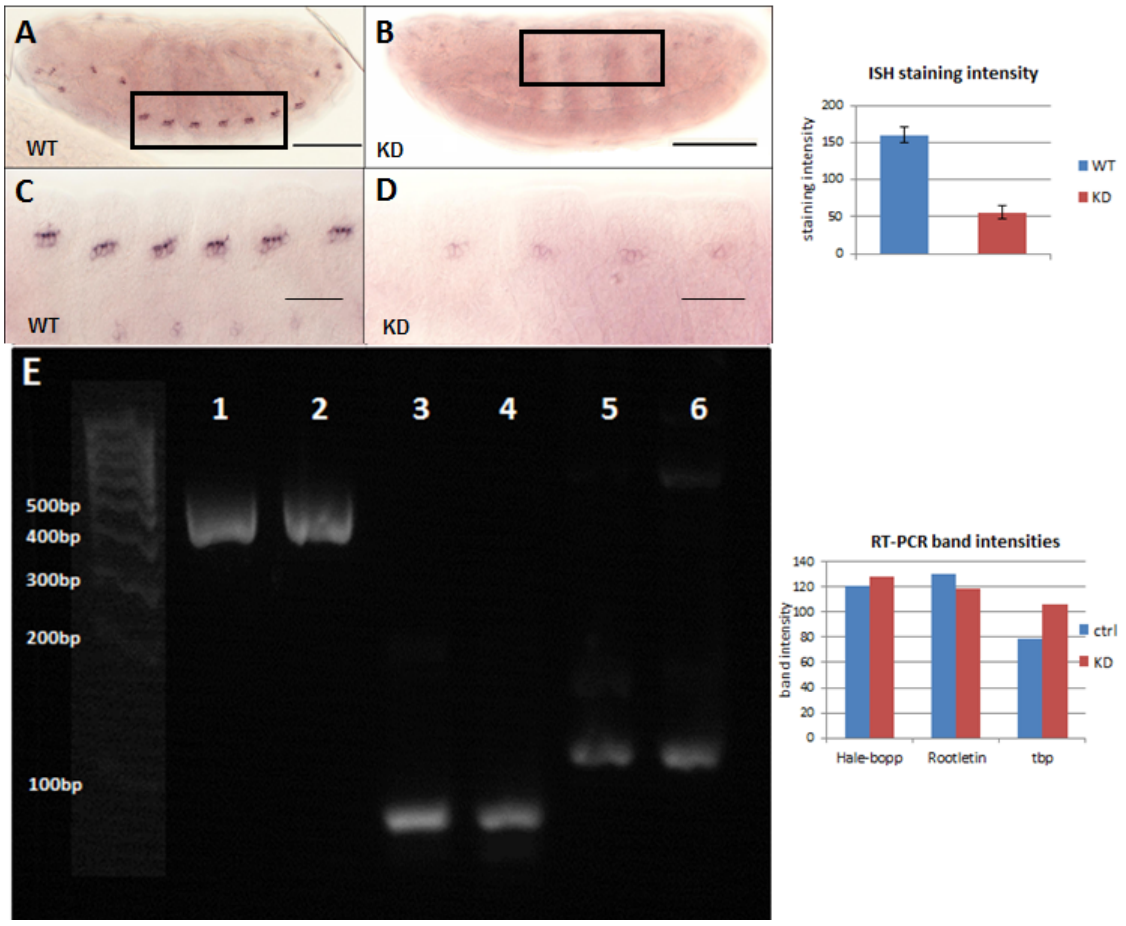

Figure 2.5. CG6129 RNA in situ hybridisation of WT and KD embryos and semi quantitative RT-PCR of CG6129 in WT and KD testes. A – stage 17 WT embryo, CG6129 transcript expression is strong and specific to the CHO, B – CG6129 KD embryo, CG6129 transcript expression is almost completely abolished, C – as in A but higher magnification, D – as in B but higher magnification, ISH stianing intensity chart, average from 6 embryos for area including the lch5 ch neurons. E – semi quantitative reverse transcription PCR of WT and CG6129 KD testes. lane 1 - Hale-bopp WT, lane 2 - Hale-bopp CG6129 KD, lane 3 - CG6129 WT, lane 4 - CG6129 CG6129 KD, lane 5 - tbp WT, lane 6 - tbp CG6129 KD. RT-PCR band intensity chart, average from 3 experiments. Scale bars 100um (A,B), 30um (C,D).

In order to test the CG6129 knock-down efficiency in testes I have carried out a PCR with cDNA obtained from testes as a template (see Fig 2.5 E). The CG6129 expression level in the knock-down seems to be very slightly lower than in the WT control (average from 3 experiments - 67 vs 82 band colour intensity as measured

with the ImageJ software). It was quite surprising seeing that this RNAi construct had cause an almost complete knock-out in the embryos. No severe knock down in testes might be caused by low efficiency of the Bam-Gal4 driver or the fact that this driver line does not carry the Dcr2 RNAi pathway component overexpression construct.

9.4 CG6129 silencing does not affect cell divisions in the chordotonal organ lineage

As shown in Bahe et al., 2005 human Rootletin functions in centrosome cohesion and lack of Rootletin causes centrosome splitting. Correct centrosome function is crucial for successful mitosis so it might be hypothesised that *Drosophila* CG6129 has a role in mitotic cell divisions. In fact mouse Rootletin overexpression causes chromosomal aberrations, multinucleation, micronucleation and various irregularities in the shape and size of the nucleus (Yang et al., 2006). However as said before *CG6129* does not appear to be expressed in non-ciliated cells in *Drosophila* which means it cannot have a role in mitosis in general. Nevertheless since CG6129 is expressed from early to late in the Ch organ lineage, it is possible that it has a role in the asymmetric cell divisions in the lineage. I therefore wanted to see whether CG6129 is crucial for mitotic cell divisions of chordotonal organ SOP. Chordotonal organs consist of 4 cell types (cap, scolopale, neuron, ligament) which are formed and differentiated from one precursor cell in the series of asymmetric cell divisions.

If *CG6129* knock-down causes cell division disruptions some CHO cells might be lacking or be duplicated. In order to visualise all cell types of the mature CHO I have performed a Couch Potato fluorescent antibody staining on *CG6129* knock-down larval pelts. Couch Potato is expressed in all sensory organ precursors (SOPs)

and the differentiated PNS cell types that derive from them - also all cells of the CHO (Bellen et al., 1992). The antibody staining showed all chordotonal organ cells in correct numbers and arrangement suggesting that *CG6129* knock-down does not cause any cell division defects in the chordotonal organ lineage (see Fig. 2.6).

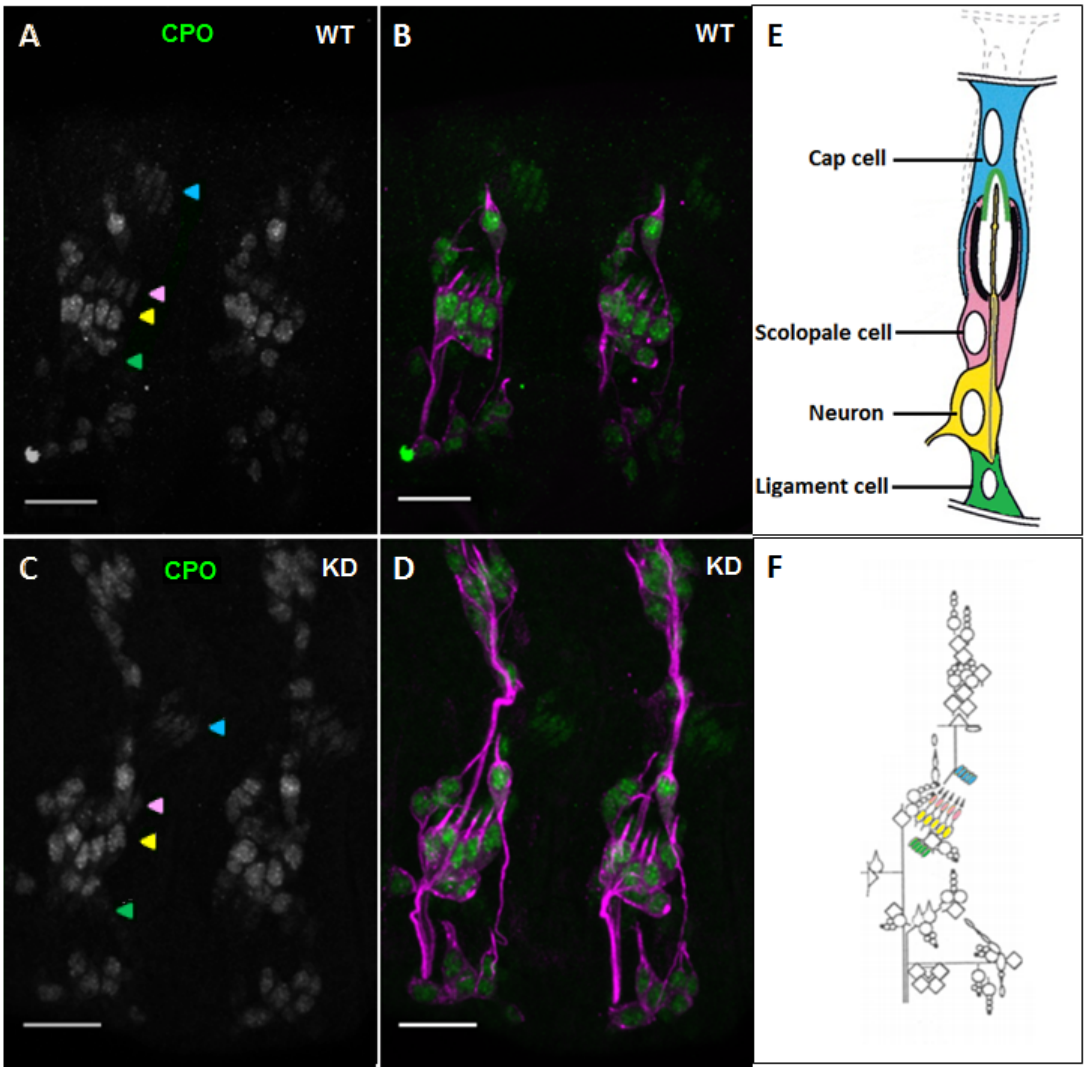

Figure 2.6. Chordotonal organ cell types. Couch Potato staining of embryonic chordotonal organs. A – WT embryonic chordotonal organs stained with Couch Potato (CPO) antibody, all four cell types visible, marked with arrowheads, blue – cap cell, pink – scolopale cell, yellow – neuron, green – ligament cell; B – the same as A, green- CPO,magenta- 22C10 counterstain; C – CG6129 KD embryonic chordotonal organs stained with Couch Potato antibody, all four cell types visible, marked with arrowheads, blue – cap cell, pink – scolopale cell, yellow – neuron, green – ligament cell; D – the same as C, green- CPO,magenta- 22C10 counterstain; E – schematic representation of the chordotonal organ showing four cell types (adapted from Studies of mechanosensation using the fly. A. Jarman, 2002); F – schematic representation of all neuronal cells in one embryonic segment, colours represent cell types within chordotonal organs (adapted from Bellen et al 1992). Scale bars represent 10um.

9.5 CG6129 silencing does not affect spermatogonia cell divisions

Drosophila spermatogonia undergo a specific set of mitotic and meiotic divisions that lead to formation of 64 spermatids from one gonialblast (see Fig 7 E). If the CG6129 knock-down in testes affects those cell divisions the number of sperm cells in a bundle might differ from 64. In order to assess this I have performed an immunostaining on young adult testes using a gamma-tubulin marker and a PI (propidium iodide) counterstain to visualise nuclei. Gamma-tubulin stains so called Gamma-TuRCs (gamma-tubulin ring complexes) at the base of cilia (Moritz et al., 2000).

The CG6129 testes look grossly normal (see Fig. 2.7 A and B). When zoomed in to the areas where gamma-tubulin staining is clearly visible the gamma-TuRCs in a particular bundle were counted (see Fig. 2.7 C and D). The numbers of sperm cells in a bundle did not differ between WT and CG6129 knock-down and in both cases amounted to 64 (± 2) (see Fig. 2.7 F). This result suggests that CG6129 does not have a role in the cell divisions during spermiogenesis. This is in line with my previous result showing that CG6129 KD does not affect asymmetric cell divisions in the sensory lineage. Any aberration from the predicted number of spermatids was probably caused by the fact that some spermatids might have been out of the image focus. It should also be taken into consideration that the CG6129 KD in the testes was so innefficient that could not be causative of any phenotype.

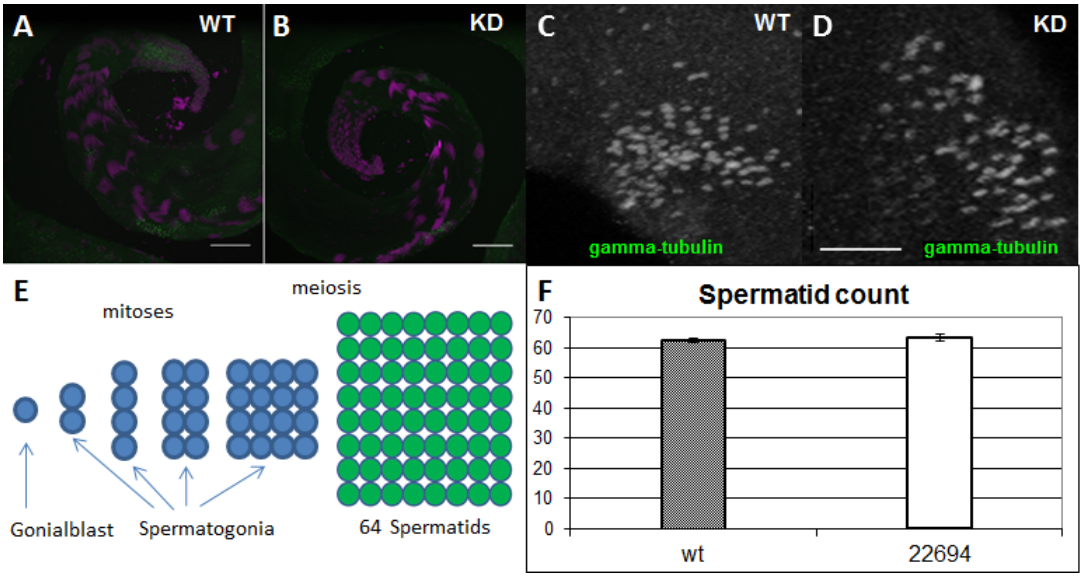

Figure 2.7 . CG6129 knock-down testes. **A** - WT whole testis view stained with gamma-tubulin (green) and PI (magenta), **B** - CG6129 whole testis view stained with gamma-tubulin (green) and PI (magenta), **C** - WT, closeup on a single sperm cells bundle stained with gamma-tubulin, **D** - CG6129 knock-down, closeup on a single sperm cells bundle stained with gamma-tubulin, **E** - diagram showing the mitotic and meiotic cell divisions leading to a formation of one spermatid bundle, **F** - graph showing numbers of gamma-TuRCs in one spermatid bundle, n(bundles in different testes)=6, p=0.58, error bars represent standard error. Scale bars represent 50um (A, B) and 10um (C, D).

9.6 CG6129 expression in non-ciliated tissues

Seeing that the CG6129 knock-down does not affect cell divisions in the chordotonal cell lineage and in spermatogonia it would be interesting to see whether CG6129 could be in any way connected to cell divisions in general. If CG6129 was linked to centrosomes in non-ciliated cells it would have to expressed in non-ciliated tissues. In order to establish whether *Drosophila* Rootletin is expressed in non-ciliated tissues CG6129 RT-PCR has been carried out. Tissues used for this experiment were whole heads (containing antennae) and ovaries (non-ciliated tissue). CG6129 primers used were spanning over an intron to ensure all PCR product was made on the cDNA template. Tbp - gene evenly expressed accross tissues (according to high-throughput

expression data presented on FlyBase), has been used as a loading control.

The cDNA obtained from whole heads has produced a strong CG6129 band (see Figure 2.8). Strikingly the amount of product from the PCR reaction carried out with cDNA obtained from ovaries was significantly lower (75% less than from heads cDNA) (see Fig. 2.8). This result suggests that *Drosophila* Rootletin is expressed at very low levels in the non-ciliated tissues.

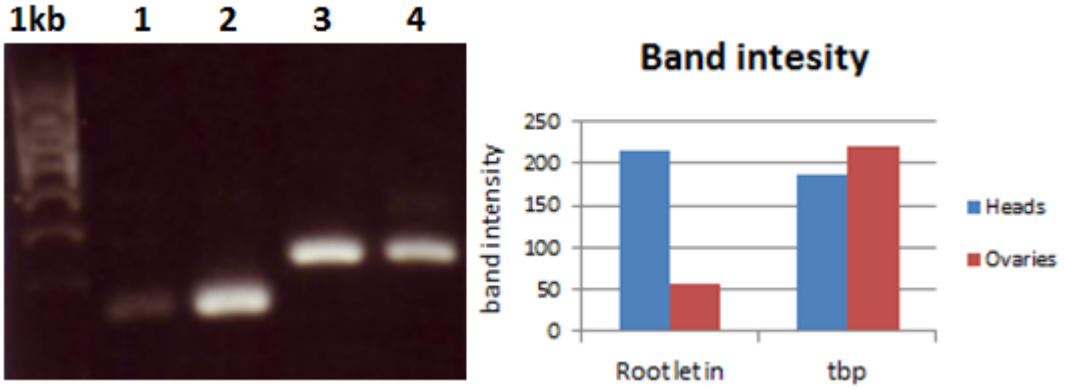

Figure 2.8. CG6129 expression in non-ciliated tissues. Reverse transcription followed by PCR reaction performed on RNA obtained from W1118 flies whole heads (15 heads) and ovaries (15 pairs). Lane 1 - CG6129 in ovaries, lane 2 - CG6129 in heads, lane 3 - loading control, tbp in ovaries, lane 4 - loading control, tbp in heads. Band intensity - average from 3 experiments.

9.7 CG6129 is a major protein component of the ciliary rootlets in *Drosophila*

The potential homology of CROCC/Rootletin and CG6129 was based on the gene and amino acid sequence similarity between the two (Yang et al., 2002). In order to see whether CG6129 RNA silencing would cause ciliary rootlet disruptions transmission electron microscopy was performed. Adult knock-down fly antennae were fixed and sent off for analysis. Wild type control (UAS-Dcr2;sca-Gal4 driver flies) Johnston's organ sections showed a robust striated structure spanning from the ciliary

basal body through the dendrite inner segment down to the cell body (see Fig. 2.9 A). Less electron dense striated linker was visible between the proximal and distal centriole (see Fig. 2.9 D, asterisk). In mice striated linker can be observed extending between the two centrioles, consistent with a role in tethering the two together (Yang et al 2002). The ciliary axonemes were showing 9-fold symmetry with clearly visible 9 microtubule doublets (see Fig. 2.9 B, asterisks). This is consistent with the widely described arrangement of microtubules within the axoneme. In general immotile cilia (the *Drosophila* Cho cilium is an example of such) exhibit a 9+0 microtubule arrangement meaning there are 9 microtubule doublets arranged in a 9-fold circular symmetry with no microtubules in the centre. The motile cilia exhibit a 9+2 arrangement - they have two microtubules in the centre of the microtubule doublets circle.

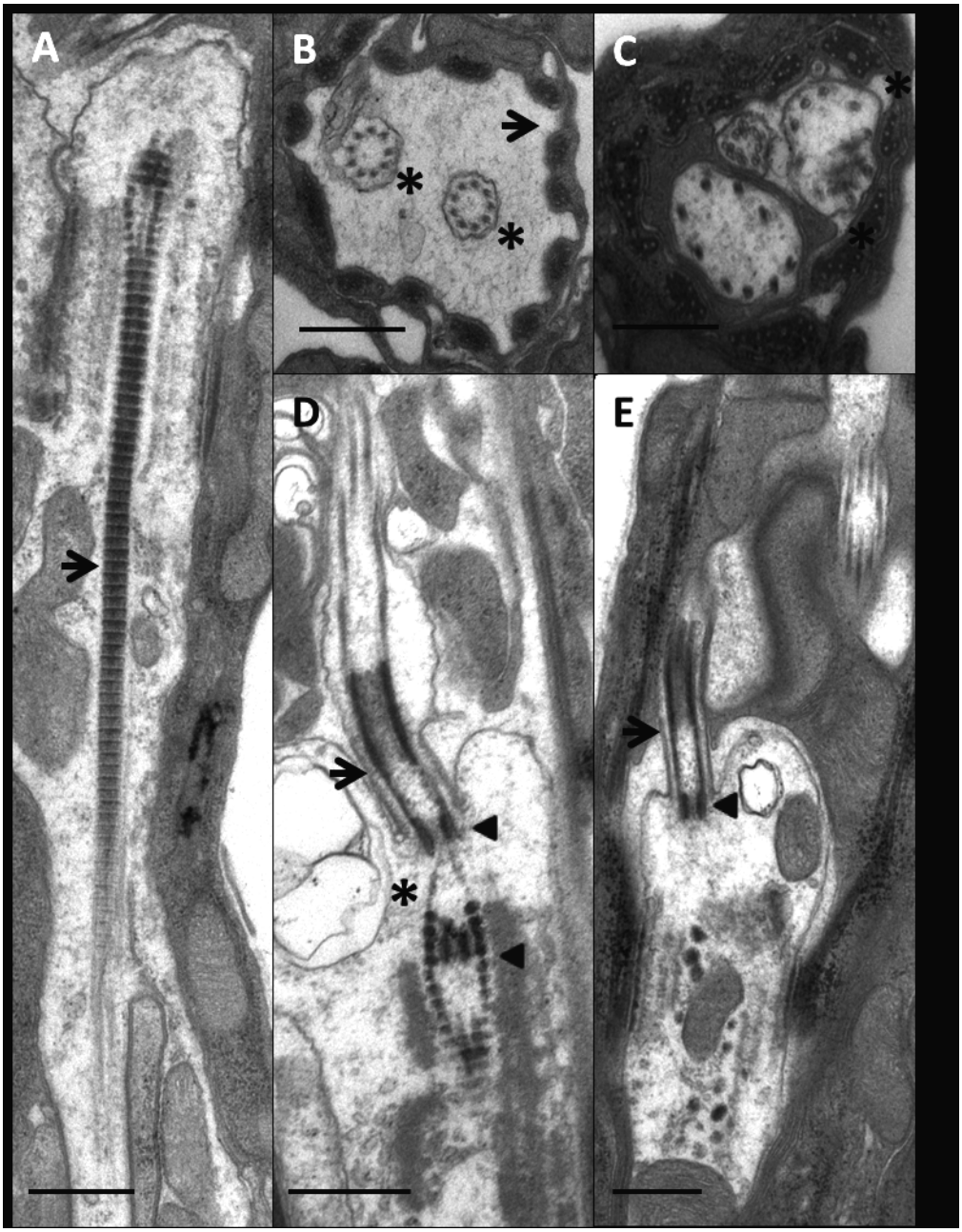

Figure 2.9. Transmission electron microscopy of CG6129 KD adult fly antennal Johnston's organ. Each panel shows a section of a single chordotonal organ. A – WT longitudinal section, black arrow shows a robust, striated rootlet, B – WT transverse section, two cilia (asterisks) enclosed in a scolopidium (arrow), C – CG6129 KD transverse section, three cilia within the scolopidium, microtubules arrangement slightly distorted and the cilia appear swollen (asterisks), D – WT longitudinal section, proximal end of the axoneme (arrow) together with distal and proximal ciliary centrioles (arrowheads), striated structure of the ciliary rootlet appears to be connecting the centrioles (asterisk), E – CG6129 KD longitudinal section, no rootlet visible, proximal end of the axoneme (Arrow)with the distal centriole present (arrowhead) but the proximal centriole missing. Scale bars – 500nm.

In the Johnston's organs from *CG6129* knock-down flies no ciliary rootlet structure was visible (see Fig. 2.9 E). This finding is entirely consistent with CG6129 being a major protein component of the ciliary rootlet and therefore supports the hypothesis that *CG6129* is indeed the *Rootletin* homologue. Due to this the CG6129 gene with hereby be called *DmRootletin* gene. Electron dense aggregates were visible proximally to the base of the cilium possibly representing low levels of DmRootletin protein not able to form the fibrous structure. Apart from the missing ciliary rootlet *DmRootletin* knock-down chordotonal organs show two other disruptions.

Firstly the proximal ciliary centriole was missing from all sections showing the base level of the cilium (see Fig. 2.9 E). The distal ciliary centriole was well formed and localised at the base of the axoneme which looked largely normal. It is impossible to tell whether the missing proximal centriole was not formed at all or whether it was detached and delocalised out of the image focus. Further experiments using fluorescent immunostaining with centriolar markers were done to answer this question (section 9.8 of this chapter).

Secondly a potential phenotype was visible in ciliary tips after *DmRootletin* knock-down. Some of the cross sections showed a mild swelling and the 9-fold symmetry was slightly disrupted (see Fig. 2.9 C, asterisks).

9.8 Effect of loss of rootlets on *Drosophila* proprioception

9.8.1 Larval hearing assay

During my PhD I have supervised an Honours student whose project was to test a collection of RNAi lines for putative ciliary genes for the ability to hear. One of the genes tested was DmRootletin. The project was based on use of a larval hearing assay. The larval hearing assay is based on an assumption that larvae receive sound

stimuli (pure tone of 1000Hz) with their chordotonal organs and respond with body retraction. During the assay five 3rd instar larvae were placed on a grape juice agar plate (positioned directly on the top of a speaker. A one second 1000Hz tone was played 3 times (1 second apart) and reaction of each larva was scored during each tome (0 - no retraction and 1 - retraction). A sum of scores (for example five times score 1 = 5) was taken from each played tone and an average of three sums was treated as result. The scores were also recorded before the tone was played in order to spot a baseline spontaneous retraction. The assay shows that wild type larvae very rarely retract spontaneously (this could be just normal movements scored as retraction) and respond with a consistent retraction during the tone (see Fig. 2.10). This result means that WT larvae can hear and respond to the sound stimulus. The DmRootletin knock-down larvae do not retract spontaneously before the tone and almost completely lack any response to the sound (see Fig. 2.10). This result possibly mean that DmRootletin knock-down larvae cannot hear the sound stimulus therefore their chordotonal organs are most probably functionally impaired.

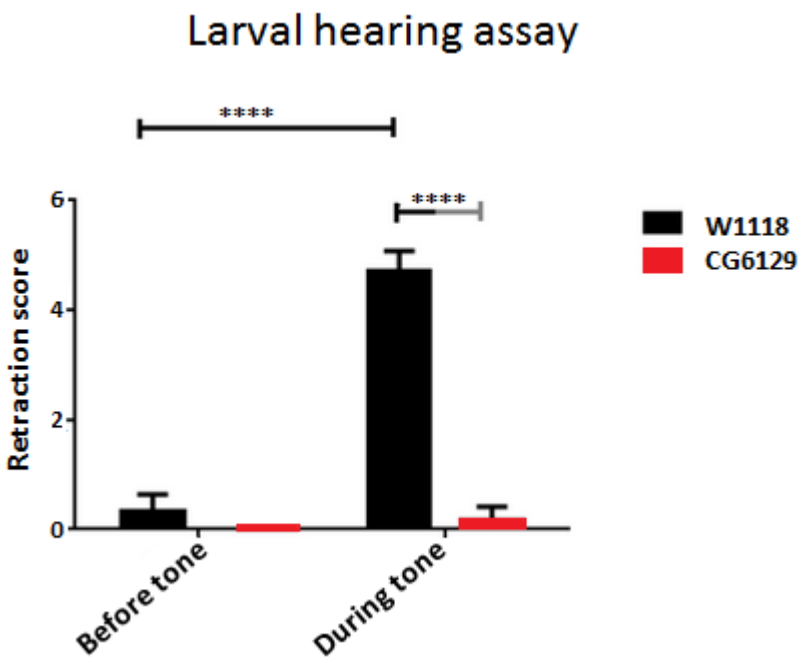

Figure 2.10. DmRootletin knock-down larval hearing assay. n=8, p<0.005 (Two-way Anova), error bars represent standard deviation.

9.8.2 Larval crawling assay

During my MSc project I analysed the *DmRootletin* knock-down larvae for proprioceptive defects using a larval crawl assay. This assay tests the coordination of the crawling motion - chordotonal organs are responsible for the feedback on the body position and therefore for the coordination of crawling. If the chordotonal organs are impaired the larvae crawl much slower (Cachero et al., 2011). The result of this assay is represented as a crawl path length (in cm) underwent within 2 minutes.

In line with the hearing assay results and other functional analysis of Cho the larval crawling assay shows a severe coordination impairment in DmRootletin knock-down larvae (see Fig. 2.11). This can be interpreted as a gross functional impairment of chordotonal organs. In fact the DmRootletin knock-down larval crawling result is comparable to the one of atonal mutant larvae which lack chordotonal organs

altogether (see Fig. 2.11).

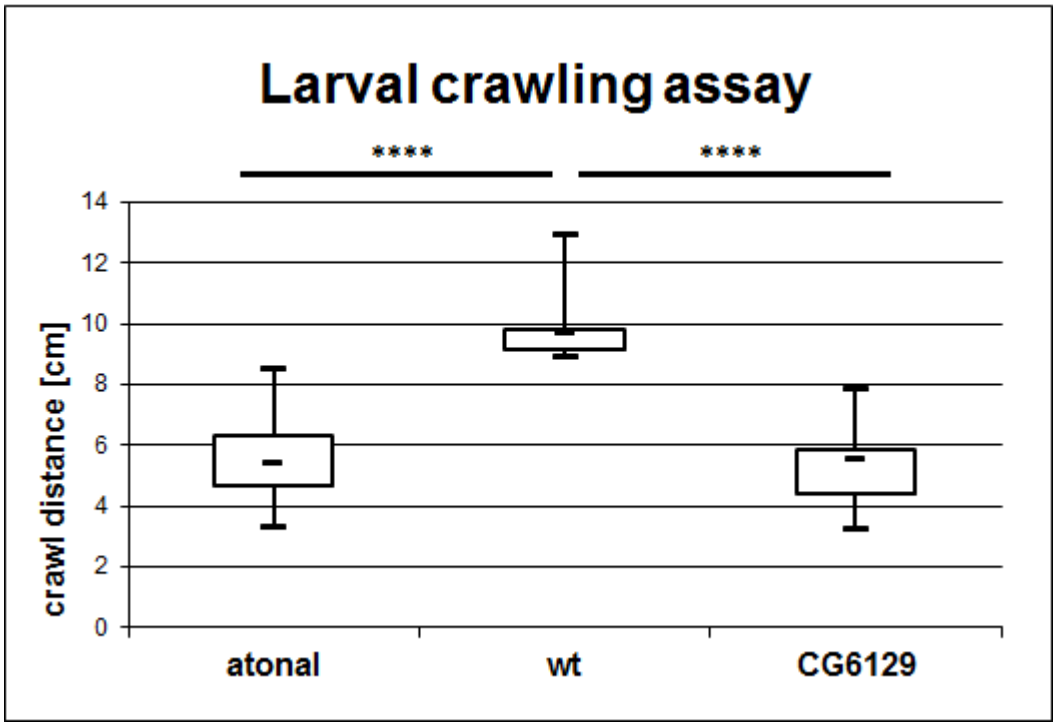

Figure 2.11. ***DmRootletin*** **knock-down larval crawling assay boxplot**. n=11, p<0.0005.

9.8.3 Adult climbing assay

In the course of the PhD project an adult climbing assay was also carried out to follow up the MSc results. The climbing assay tests the fly's ability to respond to gravity force - WT flies have a tendency to exhibit negative gravitaxis (Hirsch and Erlenmeyer-Kimling, 1961). This behaviour relies on the antennal Johnston's organs - antennal third segment can be deformed by gravity and this mechanic stimuli is registered by the Johnston's organs mechanosensory neurons (Kamikouchi et al., 2009). Adult *DmRootletin* knock-down flies have significantly lower performance in the climbing assay (see Fig. 2.12). They fall down from the walls of the measuring cylinder and walk up more slowly which results in lower average distance walked up during 10 seconds (see Fig 2.12). This phenotype is presumably caused by the

morphological defects within antennal Johnston's organ cilia. Defects in antennal Johnston's organ could be causing a weaker response to the gravity stimulus while defective femoral chordotonal organs might cause problems with the body posture and therefore the ability of flies to walk on the vertical surfaces. Therefore, Dm-Rootletin KD defects interfere with chordotonal organ function. This could be due to loss of rootlets, loss of proximal centriole or some other effect on ciliary function.

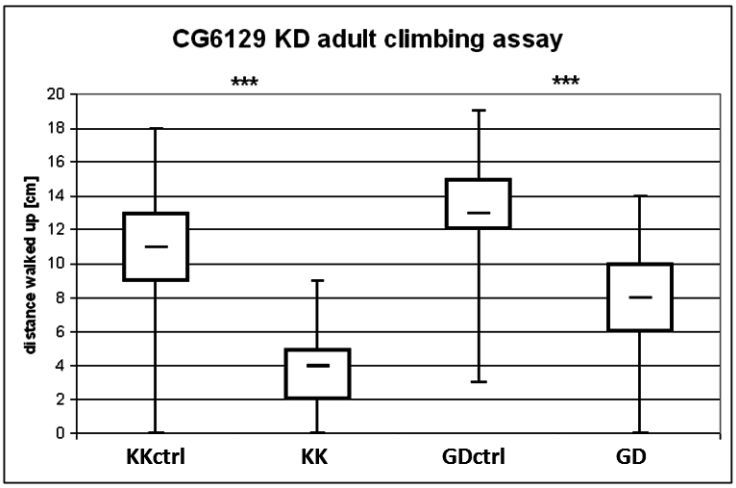

Figure 2.12. DmRootletin KD climbing assay. Box plot of the distance flies walked up in 10 seconds. Both KK and GD DmRootletin RNAi lines tested together with appropriate controls. N=53-71, Mann-Whitney test p>0.0001

9.9 Chordotonal organ morphology in *DmRootletin* KD

In order to determine any morphological defects in the chordotonal organs lacking the ciliary rootlet I have carried out a fluorescent immunostaining with a variety of markers at different stages in chordotonal neuron development and function.

9.9.1 Larval pelts

Immunostaining of the 3rd instar larvae chordotonal organs was performed to visualise the morphology of mature, functionally active organs. In order to see any general

gross morphology defects I have used 22C10 antibody (anti-Futsch, localizes to all cellular compartments of some CNS neurons and all PNS neurons (Hummel et al., 2000) and anti-HRP antibody (binds neuronal membranes in PNS, some components of CNS (Jan and Jan, 1982)). In the control larval chordotonal organs HRP staining shows two bands within the scolopale lumen - one at the the basal body level and another below the ciliary dilation (see Fig. 2.13 schematic representation, A and B). The 22C10 antibody staining also shows staining in the scolopale lumen at the level of the basal body. In the *DmRootletin* KD larval CHO the neurons look largely normal. However in many cases the 22C10 basal body level band was missing (see Fig. 2.13 C and D, red arrowhead). This indicates that apart from the centriolar tethering defect at the base of the cilia there might be some disruptions in proteins localisation in the region of the basal body.

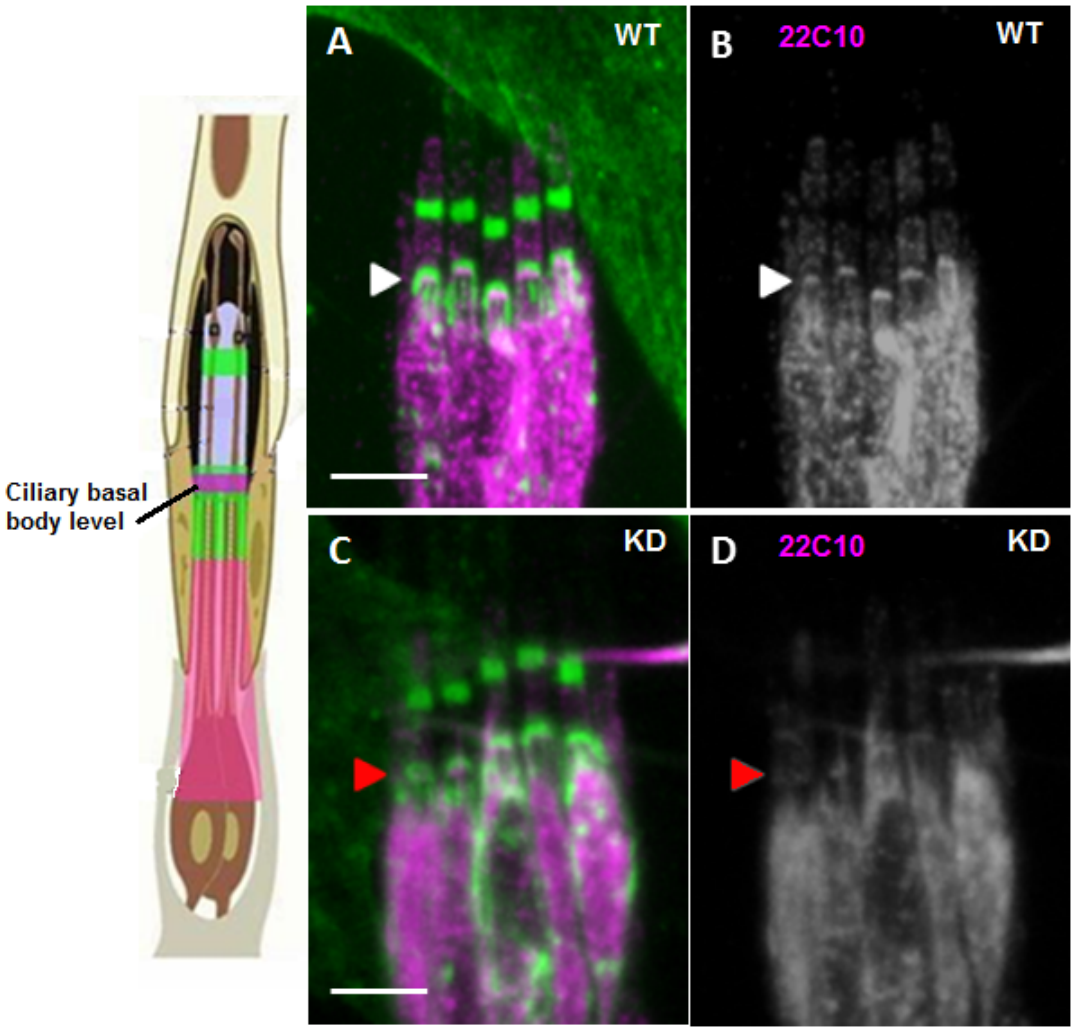

Figure 2.13. Immunostaining of larval (lch5) chordotonal organs. Schematic picture of chordotonal organ (Adapted from Bechstedt & Howard (2008) Hearing Mechanics: A Fly in Your Ear. Current Biology 18(18), R869-R870) showing the localisation of antibodies staining – HRP in green and 22C10 in magenta. A – WT larval CHO stained with 22C10 (magenta) and HRP (green) markers, white arrowhead shows the basal body level where both markers stain a band within the scolopale lumen; B – separated magenta channel for better visibility of the WT 22C10 staining; C – *DmRootletin* KD larval CHO 22C10 and HRP staining, the red arrowhead shows the same band as in A for the green HRP staining, the magenta 22C10 staining is missing in this location; D – separated magenta channel for better visibility of the 22C10 staining band missing. Scale bars – 5um.

In order to look closer at the ciliary centrioles cohesion defect I have performed immunostaining with centriole specific marker Sas4 (a centriolar protein providing a

scaffold for the pericentriolar molecules (Gopalakrishnan et al., 2011)) counterstained with monoclonal 21A6 (anti-eyes shut, localizes to the scolopale lumen on the level of the basal body and ciliary dilation (Husain et al., 2006)). In control the Sas4 staining shows two distinct puncta at the ciliary basal body level corresponding to two ciliary centrioles (see Fig. 2.14 schematic representation, A and B, white arrows). They are approximately 0.5μm apart from each other. In the *DmRootletin* KD in many chordotonal dendrites the Sas4 staining shows just one dot corresponding to the distal centriole; in other dendrites it shows two puncta but they are much further apart (i.e. ~1μm) (see Fig. 2.14 C and D). The Sas4 staining shows that the proximal centriole can be present but largely fails to localise at the basal body. The variety of the phenotype is shown in numbers in the Table 1. It is possible that the proximal centriole is absent from some immunostaining images because it was dislodged so far from its original place that it was no longer in focus of the image. The fact that there is some variation in the phenotype can be explained by possible residual levels of the DmRootletin expression across the tissue. The variety is also due to the use of either sca-Gal4 driver or sca-Gal4;UAS-Dcr2 driver which gives a stronger phenotype.

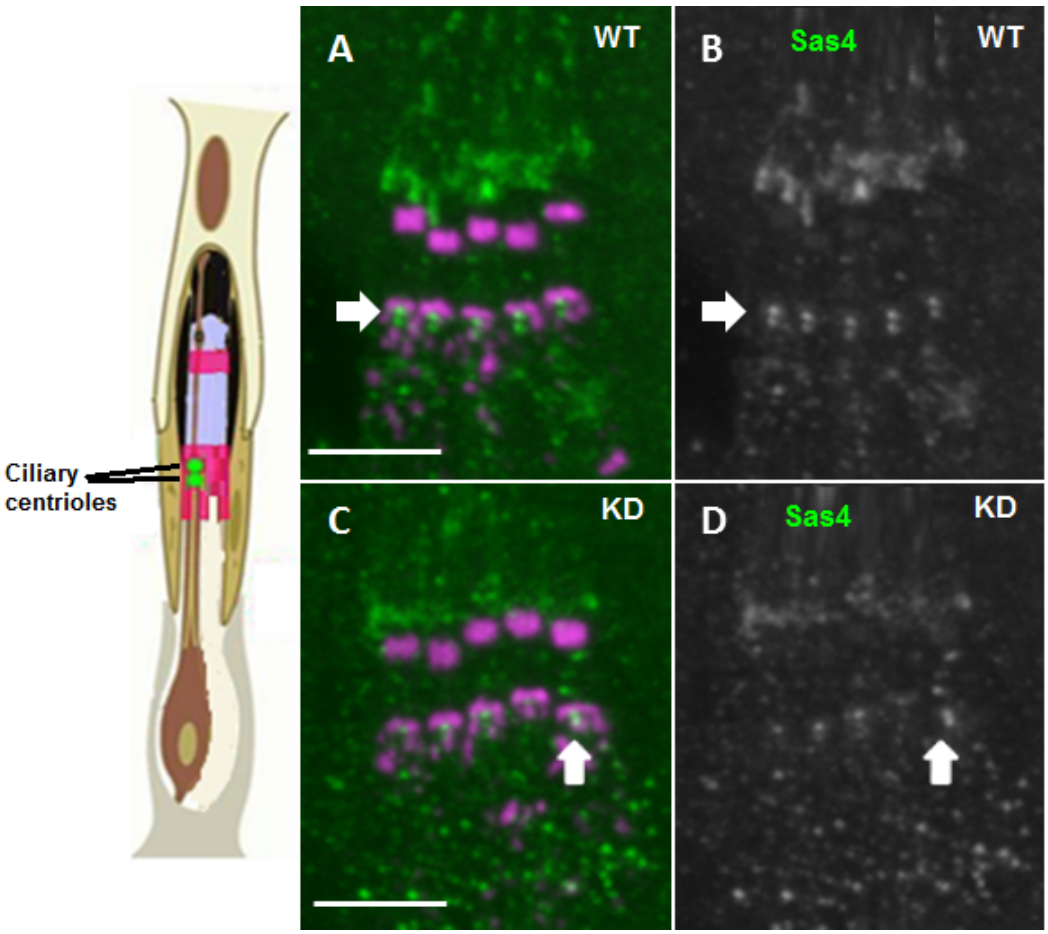

Figure 2.14. Immunostaining of larval (lch5) chordotonal organs. Schematic picture of chordotonal organ (Adapted from Bechstedt & Howard (2008) Hearing Mechanics: A Fly in Your Ear. Current Biology 18(18), R869-R870) showing the localisation of antibodies staining – Sas4 in green and 21A6 in magenta. A – WT larval CHO stained with 21A6 (magenta) and Sas4 (green) markers, the white arrow shows the Sas4 staining visible as two distinct puncta in each neuron, representing two ciliary centrioles for each of the five cilia, B – separated green channel for better visibility of the Sas4 staining; C – *DmRootletin* KD larval CHO stained with 21A6 and Sas4, the white arrow shows the only neuron with unaffected Sas4 staining, the remaining four neurons have one of the three possible distortions: 1 – both Sas4 puncta visible but further apart, 2 and 3 – only the distal Sas4 punctum visible, 4 – no Sas4 staining at all; D – separated green channel for better visibility of the abrupt Sas4 staining. Scale bars 5um.

	WT	GDxSca-Gal4	GDxUAS-Dcr;Sca-Gal4
two centrioles	25	8	0
one centriole	0	16	22
no basal body	0	1	3

Table 1: **Number of centrioles in the ciliary basal body of DmRootletin KD larval cho**. Sas4 staining quantification in WT and KD larval cho. Numeric representation of the number of centrioles in the basal body. Results show a stronger phenotype in the KD cross with the Dcr component.

9.9.2 Embryos

To test the same type of cells as above but at an earlier developmental stage I have performed the staining with the Sas4 centriolar marker and the 22C10 neuronal marker on embryos. Similar to what was seen in the larval stage the embryonic neurons look largely normal. However the Sas4 staining shows the same centriolar defect as in the larval chordotonal organs. In the WT embryos all chordotonal neurons have two centriolar puncta of the Sas4 staining (see Fig. 2.15 A and B). The *DmRootletin* knock-down neurons are often missing one Sas4 staining dot (see Fig. 2.15 C and D). Such phenotype was visible as early as the stage 16th of embryonic development. This suggests that the centriolar tethering defect occurs before stage 16 of embryonic development.

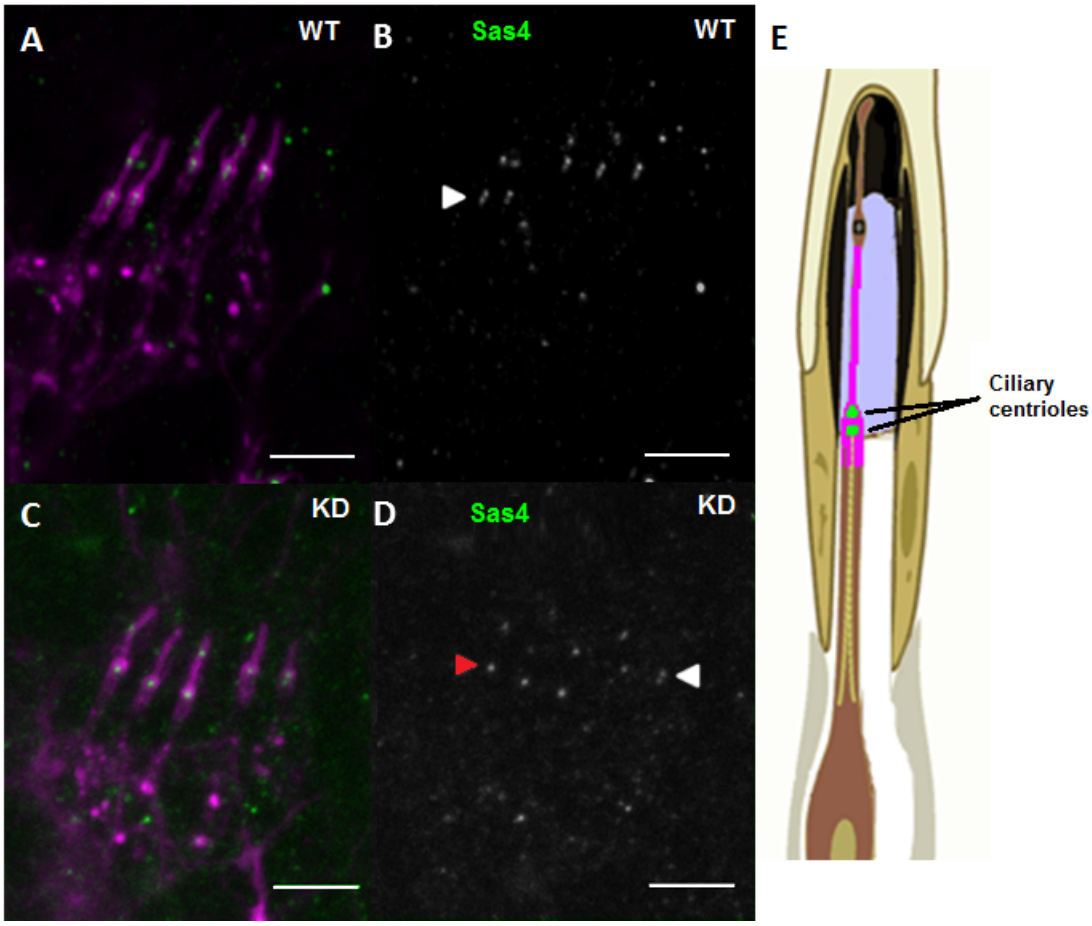

Figure 2.15. Ciliary centrioles embryonic chordotonal organs. Schematic picture of chordotonal organ (Adapted from Bechstedt & Howard (2008) Hearing Mechanics: A Fly in Your Ear. Current Biology 18(18), R869-R870) showing the localisation of antibodies staining – Sas4 in green and HRP in magenta. A – WT larval CHO stained with HRP (magenta) and Sas4 (green) markers, the white arrowhead shows the Sas4 staining visible as two distinct puncta in each neuron, representing two ciliary centrioles for each of the five cilia, B – Sas4 staining on its own, the white arrowhead shows the centriolar puncta; C – *DmRootletin* KD larval CHO stained with HRP and Sas4; D – separated green channel for better visibility of the abrupt Sas4 staining, the white arrowhead shows the only neuron with unaffected Sas4 staining, the remaining four neurons have only the distal Sas4 dot visible, red arrowhead indicates a single Sas4 dot. Scale bars 5um.

9.9.3 Pupal antennal chordotonal organs

To examine whether the ciliary basal body terthering defect is widespread in all *Drosophila* somatic ciliated cells I have performed Sas4/21A6 immunostaining on

pupal antennae. At about 24h after pupation the antennae are formed and the sensory neurons of Johnston's organ are differentiated. The antennal Johnston's organ chordotonal organ neurons tested here correspond to those in the TEM analysis.

In control antennal chordotonal organs the Sas4 antibody shows two pairs of dots (in the scolopale of each antennal chordotonal organ there are two neurons and hence two cilia) positioned closely to each other at the base of the cilium (judging from the 21A6 staining) (see Fig. 2.16 B). These puncta represent a pair of centrioles for each of the two mechanosensory neurons within one Ch organ. In the *DmRootletin* KD antennae the Sas4 staining shows a range of disruptions (see Fig. 2.16 D). Some proximal centrioles are missing while both proximal and distal centriolar dots are missing in other neurons. A very small proportion of neurons had a normally arranged pair of centrioles. This variety is shown in numbers in the Table 2. Again this variety might be caused by incomplete knock-down of the *DmRootletin* RNAi construct accross the tissue. Various levels of KD means that in some cells there is more *DmRootletin* protein than in others and this allows some cells to localise the tethered centrioles properly. The fact that the centrioles tethering defect is prominent in the pupal Johnston's organ suggests that lack of *DmRootletin* causes developmental disruptions within the morphology of the ciliated sensory neuron. It cannot be ruled out that the defect deepens during the function of the mechanosensory organs.

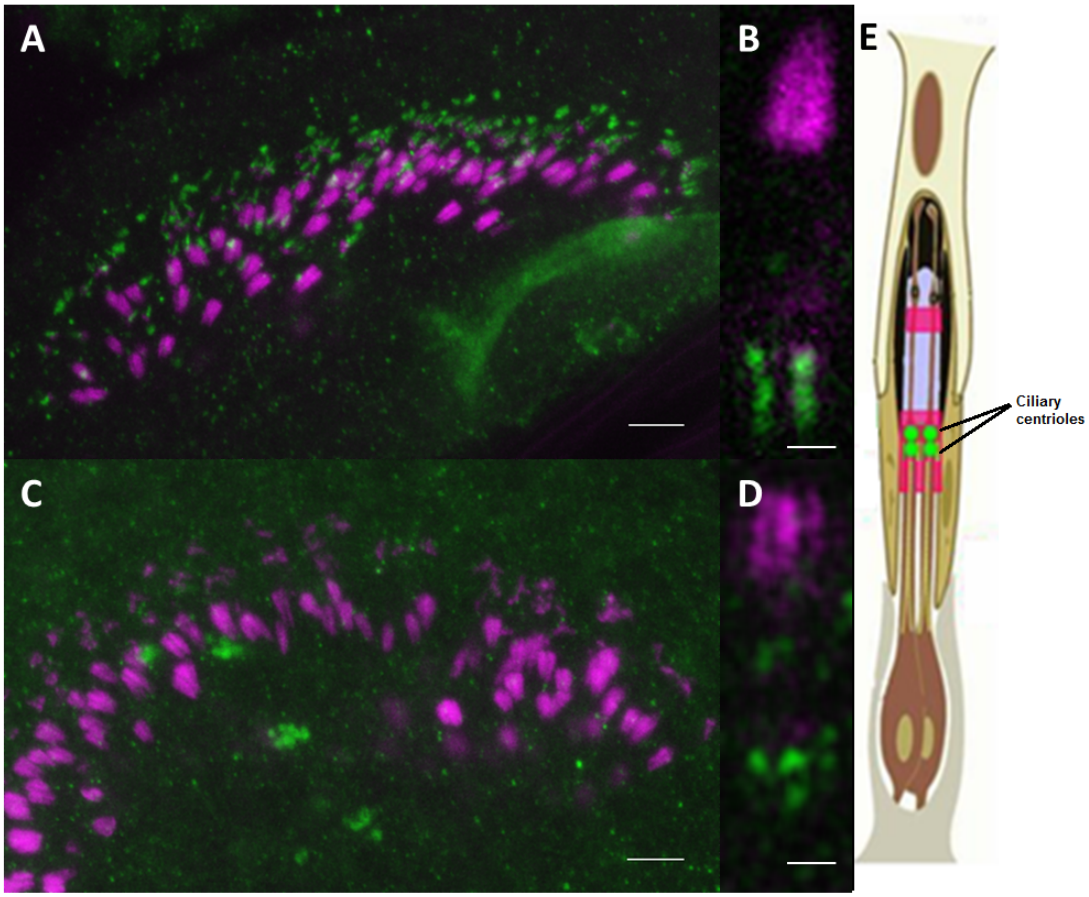

Figure 2.16. Immunostaining of antennal (Johnston's organ) chordotonal organs. A – WT antennal CHO stained with 21A6 (magenta) and Sas4 (green), whole Johnston's organ view; B – close-up on a single cho from A, two pairs of Sas4 dots represent a pair of ciliary centrioles for each of the two cilia; C – DmRootletin KD antennal CHO stained with 21A6 and Sas4, whole Johnston's organ view; D – close-up on a single cho from C, one pair of the Sas4 dots represent unaffected basal body of one of the cilia, the other cilium only has the distal Sas4 dot visible. Scale bars 5um in A and C, 1um in B and D. E – schematic representation of the markers localisation within the cho (adapted from Bechstedt & Howard (2008) Hearing Mechanics: A Fly in Your Ear. Current Biology 18(18), R869-R870) showing the localisation of antibodies staining – Sas4 in green and 21A6 in magenta.

Table 2:

	WT	GDxSca-Gal4	GDxUAS-Dcr;Sca-Gal4
two pairs	20		
one pair,one single		3	4
two singles		12	20
one pair		2	

Number of centrioles in the single DmRootletin KD antennal cho depending on the Gal4 driver used. Sas4 staining quantification in antennal Johnston's organ cho. Quantification done on 25x25um whole JO image area through 10 Z sections. Total numbers of cho per examined area: WT=20, GDxSca-Gal4=17, GDxUAS-Dcr;Sca-Gal4=24. Results show a stronger phenotype in the KD cross with the Dcr component.

9.10 DmRootletin might be involved in IFT

As shown on the TEM images earlier in this work the *DmRootletin* KD cilia seem to have swollen tips and distorted 9 microtubule doublets array. Such phenotype is usually indicative of an IFT-A defect. To test whether the DmRootletin is involved in IFT I have performed a NompC antibody staining on 3rd instar larval pelts. NompC is a mechanically-activated ion channel that localises at the tips of the mechanosensory cilia in *Drosophila* (Lee et al., 2010). If the intraflagellar transport was affected in any way it is possible that the NompC protein localization would be aberrant. I have also examined localisation of two different ciliary proteins - RempA, an orthologue of IFT140, an IFT-A component (Lee et al., 2008), and NompB, an orthologue of IFT-B component IFT88 (Han et al., 2003).

In the WT larval chordotonal organs NompC protein localizes to the ciliary dilation and to the tip of the cilium (see Fig. 2.17, A and A'). There is almost no antibody staining visible proximal to the ciliary dilation. In the *DmRootletin* KD chordotonal organs the NompC antibody stains the whole length of the cilium in many but not all cases (see Fig. 2.17 B and B'). In some cilia large fluorescent protein aggregates

are visible (see Fig. 2.17 C and C'). Also the ciliary dilation staining does not seem to be so defined and prominent in the KD cilia as in the WT.

In WT larval cho RempA-YFP fusion protein localises to the ciliary dilation (Lee et al., 2008). This localisation is not affected in the DmRootletin KD larvae (see Figure 2.17, D and E).

In the report by Han et al, (2008) the NompB-GFP fusion protein localises proximally to the ciliary dilation in the pupal antennal, embryonic lateral and adult femoral chordotonal organs. As seen the figure 2.17 F in WT larval chordotonal organs the IFT88 orthologue fusion protein NompB-GFP localises specifically to the ciliary dilation. In the DmRootletin KD the ciliary dilation localisation was not affected but some NompB-GFP seemed to be mislocalised to the scolopale lumen (see Figure 2.17 G). The 'leakage' of the NompB-GFP protein to the scolopale lumen was not consistent and was only visible in a half of the examined larvae (n=10).

While subtle changes in the NompC localisation suggest that DmRootletin might be indirectly involved in some aspects of IFT, no change in the localisation of IFT protein orthologues implies that any possible role of DmRootletin in IFT cannot be important. The fact that the NompB-GFP protein appears to have 'leaked' into the scolopale lumen is hard to explain (especially given the very high levels of the stained protein), but might suggest some impairment within the transition zone where some proteins are docked to the ciliary membrane (Garcia-Gonzalo et al., 2011).

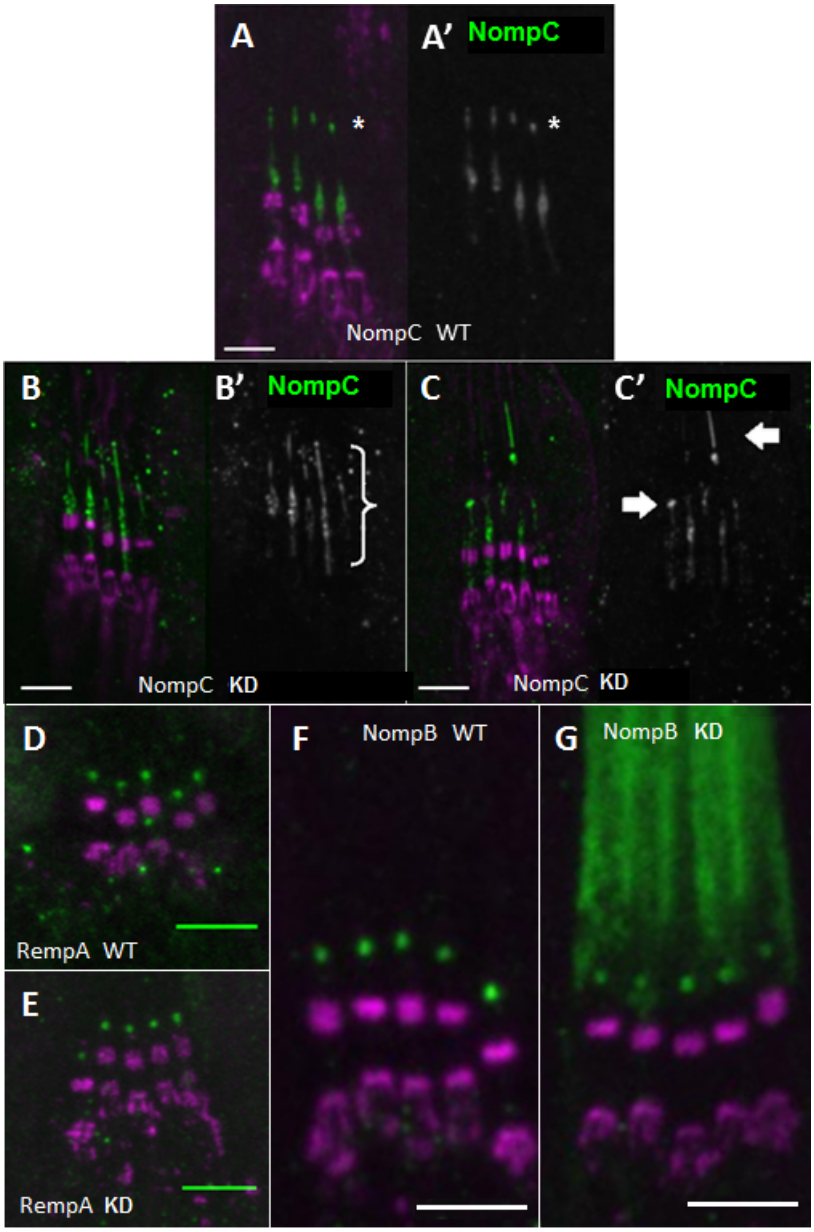

Figure 2.17. Possible DmRootletin involvement in IFT. A and A' – WT larval CHO, NompC marker visible in the ciliary dilation and the tips of the cilia, almost no staining visible in the proximal part of the cilia, B and B' – DmRootletin KD, NompC staining appears slightly distorted, white bracket indicates green staining visible along the whole length of the cilium, ciliary dilation staining not as prominent as in WT control, C and C' – another DmRootletin KD larval CHO, white arrows show abnormal aggregates of the NompC antibody, no ciliary tip staining visible in this lch5 cluster. D - WT larval cho, RempA-YFP in green and 21A6 in magenta. RempA-YFP localises to the ciliary dilation, E - DmRootletin KD, RempA-YFP localisation is not affected, F - WT larval cho, NompB-GFP localises to the ciliary dilation, G - DmRootletin KD larval cho, NompB-GFP still localises to the ciliary dilation with additional protein visible in the scolopale lumen. Scale bars 5um.

9.11 *DmRootletin* KD does not influence the length of the CHO cilia

As shown before DmRootletin KD causes proprioception defects and centriolar cohesion disruption. It would be interesting to know whether the lack of DmRootletin affects the integrity of the cilium. It could be hypothesised that some mechanic stress the chordotonal organ cilium is prone to and the lack of the anchoring structure might cause some cilia to degenerate or break off. In order to test this I visualised the cilia with mCD8-GFP fusion protein expression construct. The mCD8-GFP localizes to neuronal membranes - also the membrane along the cilium - and so is the only marker that could be used to visualise the whole cilium length. It would seem logical to test the hypothesis on the antennal Johnston's organ cilia but due to very poor visibility of the mCD8-GFP fusion protein in adult antennae those could not be used in this experiment. Instead I have measured the femoral chordotonal organs cilia length. The result of the climbing assay has already suggested that the function of those organs may be disrupted - *DmRootletin* KD flies fall down of vertical surfaces due to possible uncoordination of leg movements. To be able to show that any ciliary length changes are causative of the proprioception phenotype I have dissected the same flies that have been used in the climbing assay described in the paragraph 9.8.3.

In the WT control flies the femoral chordotonal cilium length was approximately 9-11μm (n=10) (see Fig. 2.18 A). The ciliary dilation was clearly visible in all measured cilia. There was no difference in the ciliary length of the *DmRootletin* KD flies in comparison to control (see Fig. 2.18 B). This result implies that the lack of the ciliary rootlet and defective centrosome cohesion does not influence the cilium integrity.

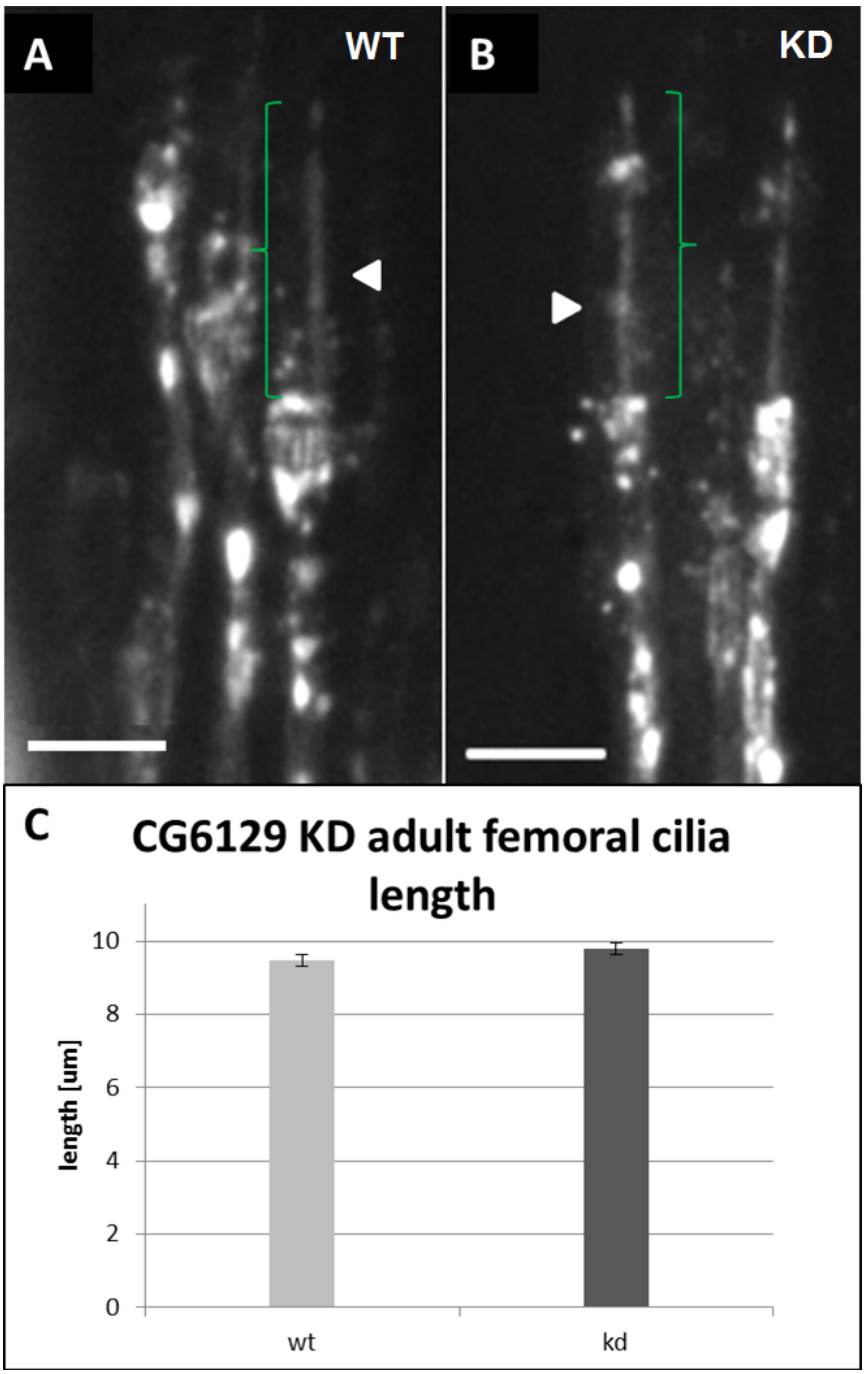

Figure 2.18. Adult femoral chordotonal organ cilia visualised by mCD8-GFP fluorescent fusion protein. A – WT fly CHO, white arrowhead indicates the cilium, green bracket indicates its length approximately 10um in length, B – *DmRootletin* KD fly CHO, white arrowhead shows the cilium, green bracket indicates its length, also approximately 10um in length. Scale bars 5um. C – cilia length measurements performed in ImageJ open source software, n=15 for both WT and KD, t-test p=0.48.

9.12 *DmRootletin* KD causes a progressive loss of the mechanoreceptor function

The Yang et al (2005) findings show that DmRootletin in mice is necessary to maintain a long term stability of cilia. In this study they see a clear negative correlation between the age of examined specimen and the integrity of cilia. Mouse photoreceptors degenerate/break off when the ciliary rootlets are missing. Taking this into consideration I tested whether the phenotype caused by *Drosophila* DmRootletin KD worsens when the flies age. I have performed a climbing assay on ageing flies. Each test was performed in the same way as the previous climbing assay (section 1.2.6). The only difference was that the flies were kept and re-examined every 3 days from day 7 after eclosion to day 25 after eclosion.

WT flies performance decreases slightly with ageing (14.6cm at day 7 down to 10cm at day 25) (see Fig. 2.19 A). This is to be expected and a decrease in ageing WT flies performance in the climbing assay has been shown previously (Rhodenizer et al., 2008). However the *DmRootletin* KD performance decreased with a much faster rate (from 6.5cm at day 7 to 0.5cm at day 25). At the start of the experiment the *DmRootletin* KD flies performance can be rated as 56% worse than that of WT. In the last test at the 25 day from eclosion the *DmRootletin* KD flies performance was 95% worse than the WT (see Fig. 2.19 B). This result can be interpreted as a significant mechanoreceptor degeneration that is progressive with age. It can be hypothesised that the degeneration is due to mechanical stress those cilia are prone to during their function.

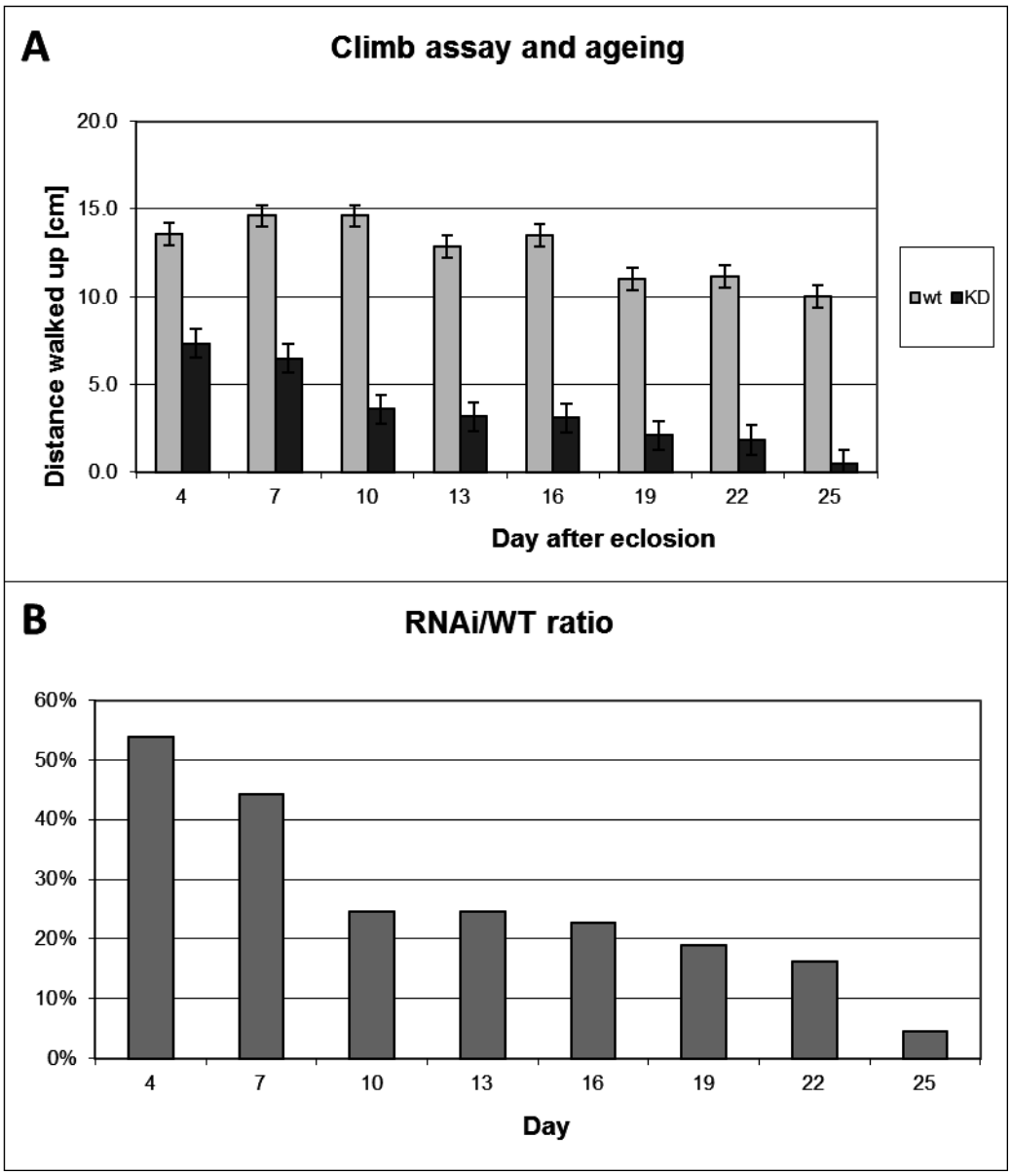

Figure 2.19. Climbing assay of ageing flies. A – assay results, KD is the *DmRootletin* GD RNAi line, results show an average of averages from 4 replicas each testing 15 flies, the same flies were used in each timepoint, error bars represent standard error, two-way Anova $p>0.003$, B – KD/WT ratio plotted to show a faster rate decrease in the *DmRootletin* KD flies.

In order to assess any progressive morphological disruptions in the mechanosensory cilia I have performed a mCD8-GFP femoral chordotonal cilia length measurements in ageing flies. As shown earlier again there was no difference between the WT and

the *DmRootletin* KD cilia length at every given time point. Also there was no change in the ciliary length in time.

9.13 Nek2 expression pattern

DmRootletin has been shown to interact with Nek2 kinase in U2OS cells (Bahe et al., 2005). In order to determine whether such interaction is probable in *Drosophila* I have looked for an overlap in DmRootletin and Nek2 expression patterns. I have performed a Nek2 RNAi in situ hybridisation on embryos and a Nek2 antibody staining in embryos, 3rd instar larvae and pupal antennae.

The Nek2 transcript is highly expressed from earliest stages of development and up to stage 6 resembles a pattern characteristic of a gap gene (see Fig 2.20 A and A'). In the later stages it is expressed in some components of CNS and possibly PNS (SOPs at stage 12 as shown in the figure 2.20 F). In order to examine whether Nek2 is indeed expressed in SOPs I have performed Atonal antibody costaining together with the Nek2 transcript visualisation (see Fig. 2.20 F). There does not seem to be any overlap between Atonal and Nek2 expression patterns suggesting that Nek2 is not expressed in *Drosophila* PNS. In line with this is the fact that the Nek2 gene was not on the list of genes enriched in ciliated cells (Cachero et al., 2011).

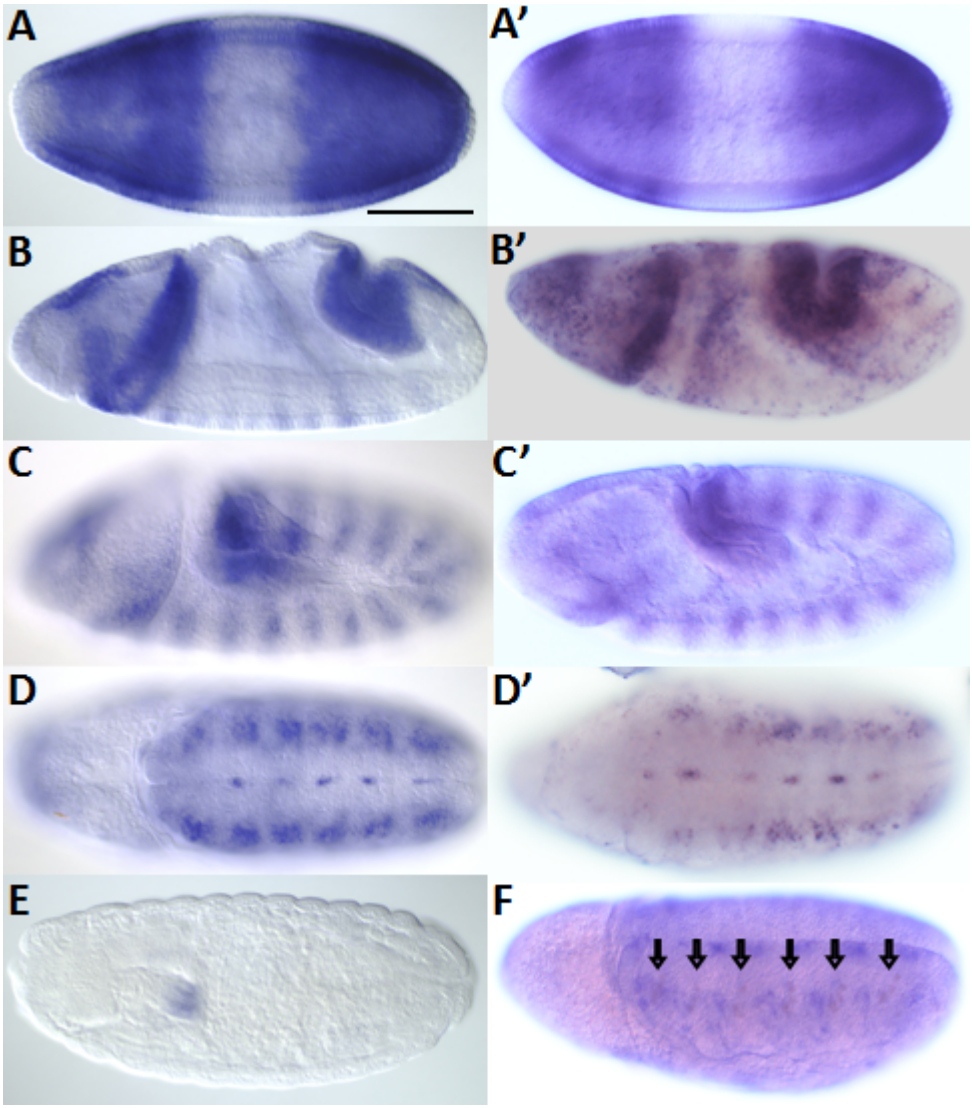

Figure 2.20. Nek2 expression pattern in embryos visualised by RNA in situ hybridisation. A - stage 2 of embryonic development, image obtained from http://insitu.fruitfly.org/cgi-bin/ex/insitu.pl; A' - corresponding developmental stage staining performed by me; B - stage 7, image obtained from http://insitu.fruitfly.org/cgi-bin/ex/insitu.pl; B' - corresponding stage staining obtained by me; C - stage 9 of embryonic development, image obtained from http://insitu.fruitfly.org/cgi-bin/ex/insitu.pl; C' - corresponding stage staining obtained by me; D - stage 11 of embryonic development, image obtained from http://insitu.fruitfly.org/cgi-bin/ex/insitu.pl; D' - corresponding stage staining obtained by me; E - stage 16 of embryonic development, image obtained from http://insitu.fruitfly.org/cgi-bin/ex/insitu.pl, no corresponding stage staining obtained by me; F - stage 10 of embryonic development, staining shows ISH of Nek2 together with anti-Atonal antibody staining in brown (indicated by black arrows). Scale bar represents 200um.

Surprisingly the Nek2 antibody staining shows a different picture. Indeed the Nek2 antibody staining in *Drosophila* embryos is only prominent in the chordotonal organs. In embryos the Nek2 staining only appears from the late stage 14 when the chordotonal organs mature onwards. It is localised to the base of the cilium proximally to both ciliary centrioles in the whole width of the dendrite and spanning approximately 1μm (Fig 2.21 A and A'). In 3rd instar larvae chordotonal organs are functional and the Nek2 staining looks somewhat different. It is still very specific to the chordotonal organs but is localised to the whole length of the dendrite - similarly to where the DmRootletin-GFP fusion protein localises (Fig. 2.21, B, B', B"). The Nek2 protein seems to be positioned around the ciliary rootlet with a gap where the rootlet is (Fig. 2.21, C, C', C"). Those findings show that DmRootletin and Nek2 are very closely localised in all stages of development, both in non-functional and functional chordotonal organs. It suggests that it is possible that those proteins interact in *Drosophila*. In the antennal Johnston's organ Nek2 protein is very clearly positioned between the ciliary centrioles connecting them as a slim stripe (Fig. 2.21, D, E, E').

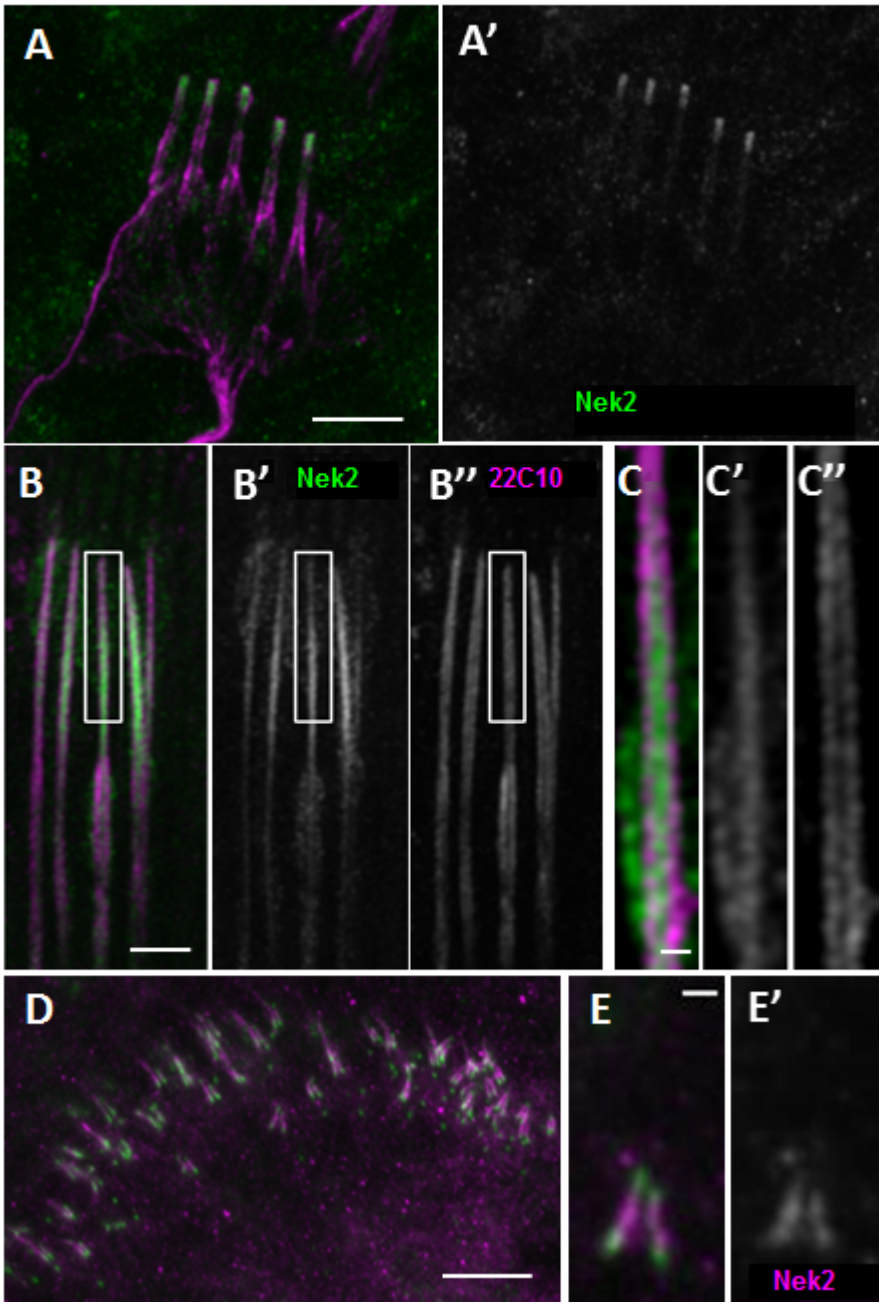

Figure 2.21. Nek2 protein localisation in various *Drosophila* tissues. A - Nek2 (green) and 22C10 (magenta) staining of embryos. A' - Nek2 green channel separated; B - Nek2 (magenta) and DmRootletin-GFP (green) in *Drosophila* 3rd instar larvae. The image shows the tip of the dendrite. The white rectangle shows the area shown in C, C' and C", B' - DmRootletin-GFP separated; B" - Nek2 separated. C - close-up tip of the dendrite; C' - DmRootletin-GFP separated; C" - Nek2 separated; D - antennal Johnston's organ stained with Sas4 (green) and Nek2 (magenta); E - close-up on a single antennal chordotonal organ with two neurons. Two pairs of Sas4 puncta visible represent a pair of ciliary centrioles for each neuron; E' - Nek2 separated. Scale bars represent 5um in A, B, and D, 1um in C and E.

It is unclear why is the Nek2 transcript localised differently than the protein itself. It is possible that low levels of transcript are present in the CHO but the fact that higher levels are visible in other tissues explains why the Nek2 is not enriched in ciliated cells. As for the antibody staining it is possible that the Nek2 protein is indeed present in other tissues than CHO as small centriolar puncta (as in S2 cells - Prigent et al.,2005) but for the lack of appropriate counterstaining (PI,DAPI to visualise nuclei) they cannot be distinguished. It is also possible that the anti-Nek2 antibody cross reacts with other proteins and is therefore not specific to Nek2.

9.14 Nek2 kinase localisation is affected in DmRootletin KD

In order to examine the possibility that DmRootletin and Nek2 kinase might interact I have carried out a Nek2 antibody staining on *DmRootletin* KD embryos and antennae. In both examined tissues the Nek2 antibody staining is much less prominent in the KD than in the controls (see Fig. 2.22). In some embryonic CHO the Nek2 staining almost disappears or is severely dispersed (see Fig. 2.22 B and B'). In the antennal CHOs the clear Nek2 staining visible as a pronounced narrow stripe connecting the centrioles (Sas4) is reduced to a faint amorphous cloud of magenta staining surrounding the centriolar pair (see Fig. 2.22 D and D').

These results show that the Nek2 localisation in the chordotonal organs might depend on the presence of a robust ciliary rootlet. Although very indirectly those findings support the hypothesis that DmRootletin interacts (directly or indirectly) with Nek2 kinase.

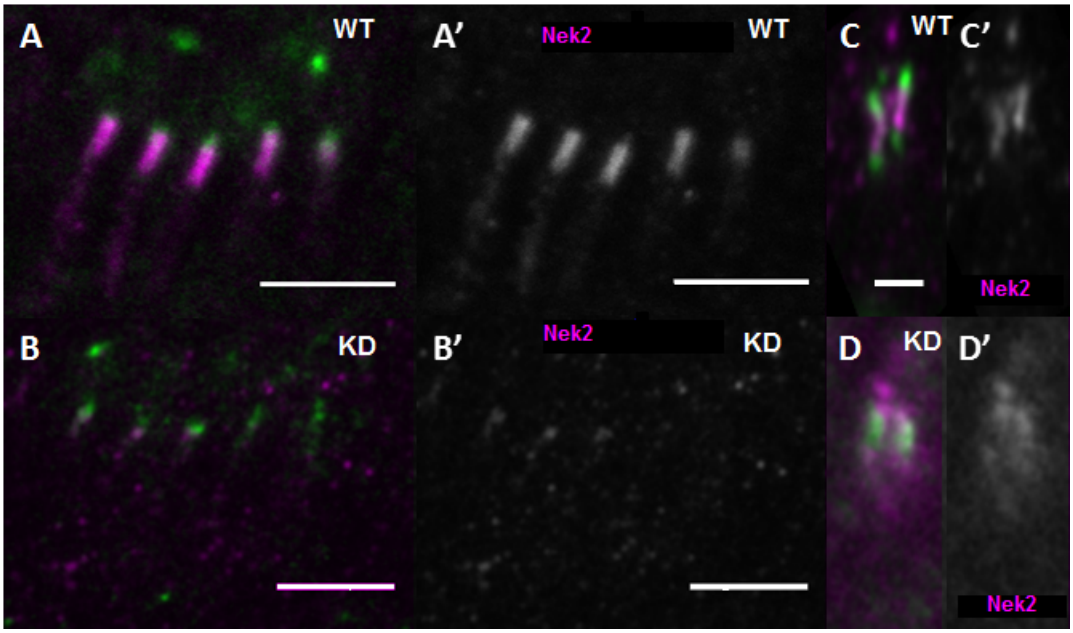

Figure 2.22. Nek2 antibody staining in DmRootletin KD. A - WT embryonic chordotonal organ stained with Sas4 (green) and Nek2 (magenta), **A'** - Nek2 staining separated; **B** - DmRootletin knock-down embryonic chordotonal organ, Sas4 (green), Nek2 (magenta), **B'** - Nek2 staining separated; **C** - WT antennal single chordotonal organ stained with Sas4 (green) and Nek2 (magenta), **C'** - Nek2 staining separated; **D** - DmRootletin knock-down antennal single chordotonal organ stained with Sas4 (green) and Nek2 (magenta), **D'** - Nek2 staining separated. Scale bars represent 5um (A, A', B B'), and 1um (C, C', D, D').

9.15 Nek2 antibody specificity

The discrepancy between the ISH Nek2 probe localisation and the Nek2 antibody staining suggests the antibody might not be entirely specific to the Nek2 protein. The fact that the Nek2 antibody staining localisation is affected in the DmRootletin knock-down allows to hypothesise the antibody cross reacts with the DmRootletin protein. In order to test this hypothesis I have performed a Western blot using whole heads of the DmRootletin-GFP flies to isolate proteins. I have used an anti-GFP antibody to identify the DmRootletin-GFP fusion and the Nek2 antibody to identify the endogenous Nek2. Two different controls have been used - non ciliated tissue

control (ovaries) to see whether Nek2 and putative DmRootletin bands are weaker there, and w[1118] flies for a control of GFP antibody specificity. A loading control has also been used (anti-Actin antibody).

As described by Regis Giet (personal communication) the Nek2 antibody gives several unspecific bands (see Fig 2.23 A, left side). However a strong band can be seen migrating at the ~100kDa speed which is likely to be the Nek2 protein (Fig. 23 A, arrowheads). It is visible in both heads and ovaries lysates but the levels of Nek2 protein seem to be lower in non-ciliated tissue (Fig. 2.23 B). Both GFP and Nek2 antibodies produce a band migrating at over 260kDa. Although DmRootletin molecular weight is 220kDa it could be possible this bigger band represents DmRootletin. Reason for that is some Western blotting kits' manufacturers suggest that in SDS-MOPS gels proteins migrate at different speeds than in SDS-PAGE gels and therefore the protein ladder might actually indicate a slightly different molecular weight. The fact that the GFP antibody produces the 260kDa bands in w[1118] flies suggests that the antibody is not specific and that it cross reacts with a protein different than GFP (Fig. 2.23 A, right side, lanes 3 and 4). This result renders the experiment of little use for this work as no clear conclusions can be drawn.

9.16 DmRootletin in other ciliated sensory neurons

Chordotonal organ neurons are not the only ciliated sensory neurons in *Drosophila*. The other ciliated PNS components are the external sensory neurons. They harbour a very small rudimentary cilia and therefore it is possible that they also have ciliary rootlets. The fact that the *DmRootletin* transcript is only transiently expressed in the ES cells suggests that the level of the protein in those cells might be very low. In line with this is that the DmRootletin-GFP fusion protein cannot be found in the ES cells. This however might be caused by the fact that the GFP construct expression

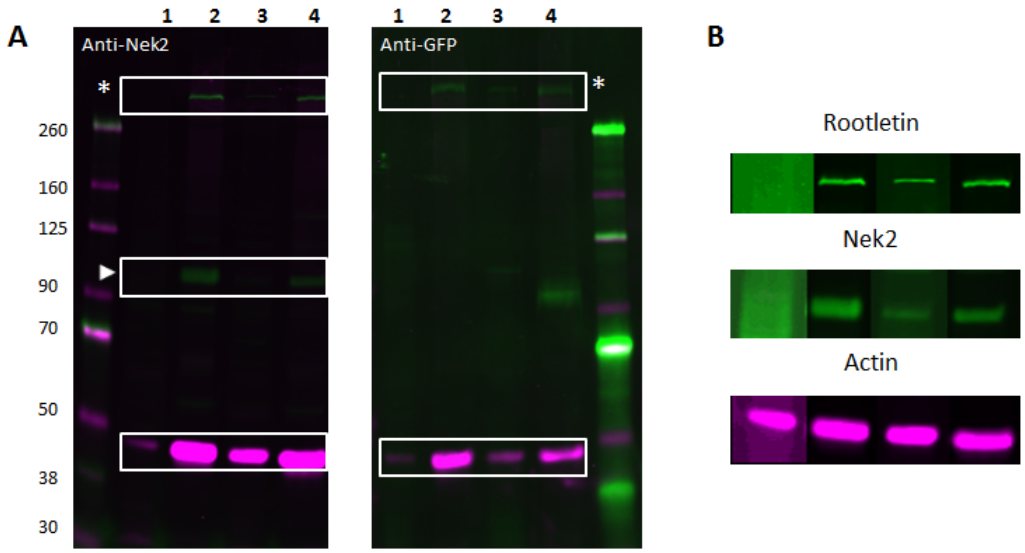

Figure 2.23. Nek2 and DmRootletin-GFP Western blot - Nek2 antibody specificity. A - Western blot membranes, lane 1 - DmRootletin-GFP ovaries lysate, lane 2 - DmRootletin-GFP heads lysate, lane 3 - W1118 ovaries lysate, lane 4 - W1118 heads lysate. Asterices - possible DmRootletin protein, arrowheads - Nek2 protein. **B -** protein bands intensity normalised for uneven loading. Lysate for each sample has been obtained from 15 female flies (i.e. either 15 heads or 15 pairs of ovaries).

is only controlled by a part of the endogenous DmRootletin enhancer.

In order to examine whether the *DmRootletin* has a role in ES organs function I have attempted to find any morphological changes in the external sensory organs by carrying out immunostaining with various markers (data not shown). This has proven to be challenging due to the small size of the cilium and difficulties in making out certain details of the ES organs. I have therefore chosen to test the hypothesis by performing a behavioural assay - the grooming assay. It is based on the fact that flies use their bristles (macrocheatae) to detect mechanosensory stimuli like touch (Jarman, 2002) (see Fig. 2.24 A and B). During the assay the bristles are stimulated by gentle touch which results in a robust cleaning reaction in the stimulated area. All WT flies respond to gentle touch with a cleaning reaction. The control used in this experiment was the sca-Gal4;UAS-Dcr2 driver line flies. It was conceivable that those flies having the Dcr2 RNAi pathway component overexpressed might have a

poorer performance than WT flies. Using those flies as a control helped to set the background response threshold appropriately to make sure the obtained result would be statistically significant. Indeed the driver line flies had significantly lower response rate than WT flies (see Fig. 2.24 C). Nevertheless the *DmRootletin* KD flies showed mildly but statistically significant decrease in the response rate in comparison to both controls.

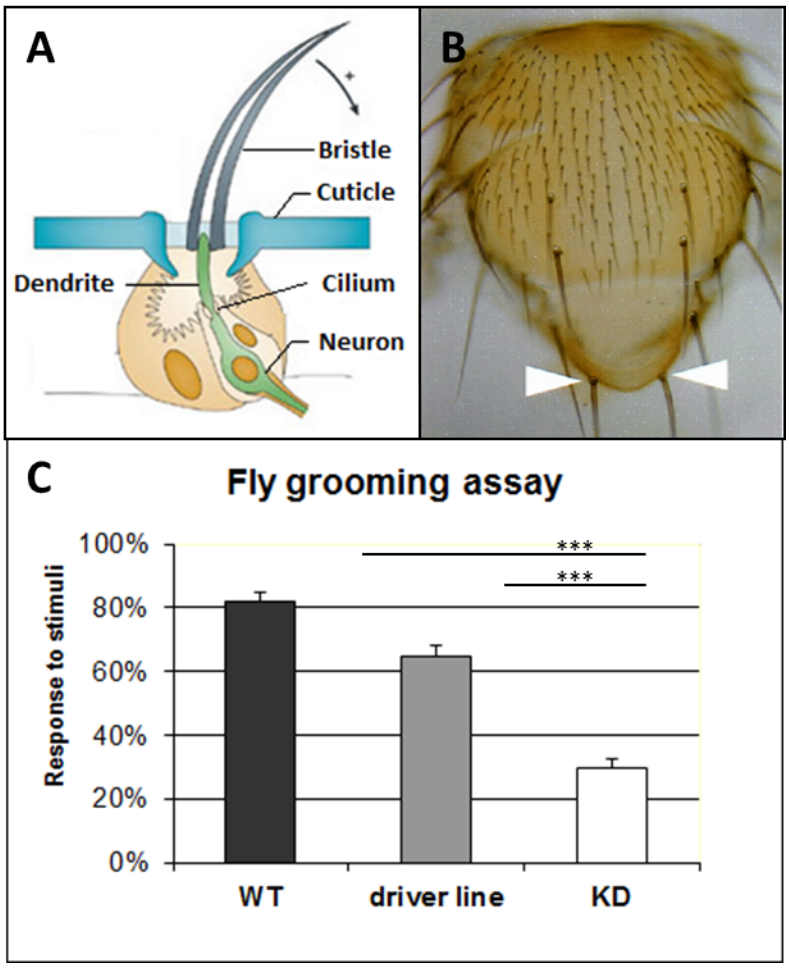

Figure 2.24. Examination of DmRootletin KD ES neurons functionality – the grooming assay. A – schematic representation of the external sensory organ, movement of the bristle stimulates the neuron, B – adult fly thorax view (Knoblich et al., 1997), white arrowheads show the two bristles on the scutellum that were stimulated during this assay, C – assay results, average of averages from 6 replicas each testing 5 flies, shown as percentage of flies responding to the stimuli, error bars represent standard error, t-test $p>0.0005$. Thorax picture in panel B from 'The N terminus of the *Drosophila* Numb protein directs membrane association and actin-dependent asymmetric localization'. Knoblich JA, Jan LY, Jan YN. Proc Natl Acad Sci U S A. 1997 Nov 25;94(24):13005-10.

Those results suggest that even though only expressed at very low levels DmRootletin has a role in the ES organs function.

9.17 DmRootletin influence on male fertility

As shown earlier in this chapter *DmRootletin* is expressed in testes. It would therefore be interesting to know whether knocking the DmRootletin gene down might cause any fertility defects.

Despite the fact that *DmRootletin* does not have a role in the cell divisions leading to sperm formation the lack of flagellar rootlets might cause fertility defects. I have performed a male fertility assay to measure the fertility of *DmRootletin* KD males in comparison to WT males (see Fig. 2.25). The average number of progeny from one WT male under the conditions described in the protocol was 85.7 (n=7). KD male progeny number was slightly lower - 68.7 (n=7) - but the difference was not statistically significant (p=0.09). This result suggests that the DmRootletin KD does not influence male fertility but a trend towards subfertility of the males lacking the ciliary rootlets may be possible.

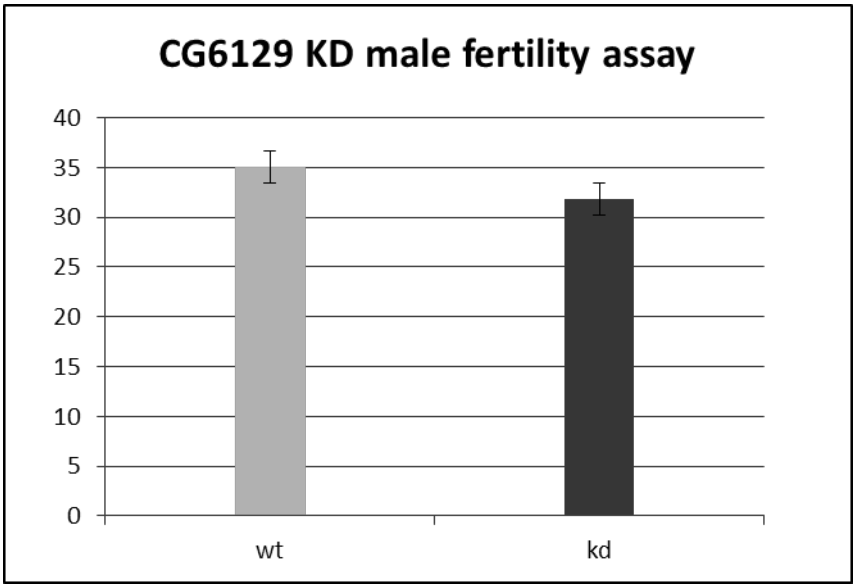

Figure 2.25. DmRootletin kd male fertility assay. Number of progeny per one male mated with two virgin females after 4 days laying. N=11 for both WT and KD, t-test p=0.28

10 Discussion

10.1 CG6129 is an orthologue of Rootletin and is important for the sensory neuron function in *Drosophila*

10.2 Expression in non-ciliated cells

In mice Rootletin is expressed abundantly in ciliated tissues but also at low levels in all non-ciliated cells (Yang et al., 2002). It has been shown that Rootletin localises to the centrosomes and plays an important role in centrosomal cohesion during the interphase of non-ciliated cells. In *Drosophila* however the centrosomal tether during the G1-S-G2 phases of the cell cycle is not widely occurring (Debec et al., 1999; Basto et al., 2006). It is interesting that *Drosophila* cells can cope with cell divisions without fully functional MTOCs (Megraw et al., 2001; Mohan et al., 2013). The only instance in which the mitosis progression appears disrupted when MTOCs are not functional are the neuroblasts asymmetric cell divisions. In general Mohan et al postulate that *Drosophila* can develop grossly normally without functional centrosomes. Seeing that DmRootletin is expressed at low levels in non-ciliated cells it would be interesting to know what is its role in those cells. It seems counterintuitive that protein responsible for interphase centrosomal cohesion (in vertebrates) is present in *Drosophila* non-ciliated cells where centrosomal cohesion during interphase is dispensable. It is possible that the DmRootletin expression in non-ciliated cells is caused by a leaky promoter or enhancer. On the other hand DmRootletin could associate with centrosomes in non-ciliated cells but its function there could be of little importance to the cell fate.

10.3 *Drosophila* centrosome cycle - could Nek2 be involved?

In the light of the fact that DmRootletin is expressed in non-ciliated cells it is worth noting that fruitflies posses an orthologue of Nek2 kinase which interacts with Rootletin in U2OS cells (Bahe et al., 2005). Nek2 function is to disrupt the centrosome G1-G2 tether to enable the entry into mitosis. Murine Rootletin is a substrate of Nek2 and once phosphorylated detaches from the centrioles - this step is necessary for the cell division to occur (Bahe et al., 2005). However, as mentioned before, the centrosome G1-G2 tether is not widely present in *Drosophila* dividing cells so it remains unclear what could be the function of Nek2 in fruitflies. It is interesting that *Drosophila* Nek2 and DmRootletin seem to localise very close to each other in the ciliated cells (as shown by antibody staining). This could possibly mean that those two proteins can interact but more experiments (yeast two hybrid, coimmunoprecipitation) should be carried out to confirm this hypothesis.

The expression pattern of Nek2 (shown by IHS) seems to be grossly limited to the CNS during embryonic development. It is remarkable for one reason. In *Drosophila* neuroblasts asymmetric cell division is a very important step in the CNS development (Wodarz and Huttner, 2003). One of the crucial factors contributing to a proper asymmetric spindle formation is presence of functional microtubule organising centre - centrosome. Flies lacking functional centrosomes do not cope very well with the asymmetric cell divisions (Mohan et al., 2013). If *Drosophila* Nek2 localises to the centrosomes in non-ciliated cells of CNS it is plausible that it could have a role in modulating neuroblasts asymmetric cell divisions.

10.4 Importance of cilia anchoring in *Drosophila* - is the cho cilium prone to mechanical stress?

As shown in Yang et al (2002) on a mouse model the connecting cilia of photoreceptors need robust anchoring in order to remain intact during the adult life. When photoreceptors are devoid of the ciliary rootlets the cilia degenerate and break off. It has been proposed that those short connecting cilia are prone to mechanical stress and that the ciliary rootlets provide a necessary structural support. It is interesting whether *Drosophila* ciliary rootlets function in a similar way and whether they are responsible for maintaining stability and integrity of mechanosensory cilia. This has been addressed in a climbing assay performed on ageing adult flies and in measurements of the length of femoral cilia in the same ageing flies. There is a clear progression in the mechanoreceptor function loss. This may suggest that the chordotonal cilium is prone to mechanical stress and that when devoid of rootlets gives in which in turn is visible as a progressive loss of function. It is possible that chordotonal cilia without rootlets would break or become truncated. However there was no change in ciliary length in the ageing flies. This shows that rootletless cilia do not break off or become truncated but it remains possible that some subtle structural disruptions that cannot be visualised by the marker (mCD8-GFP) occur within the cilium. Seeing that apart from anchoring the cilia DmRootletin can have a role in IFT it is conceivable that the functional mechanosensory neuron degeneration is caused by a cumulative IFT aberration. In order to show this a timescale set of experiments using IFT specific markers would have to be carried out.

10.5 Centriolar cohesion defect occurs during the development and deepens with age

The TEM analysis of the *DmRootletin* KD chordotonal organs has shown a ciliary centrioles defect. There are two possible stages when those defect can occur: during the development or in a mature and functional organs. Firstly the separation of centrioles can be caused by the mechanical stress the cilium is prone to during its function in the mechanosensory organ. Lack of both the ciliary rootlet and the linker between the ciliary centrioles can possibly lead to detachment and delocalisation of the proximal centriole. It would be an attractive model to propose that when chordotonal cilia are pulled during a mechanical stimuli the centrioles at the basal body are pulled apart when no ciliary rootlets connects them. In fact it is possible that mechanical stress could be a contributing factor to the mechanosensory function loss in chordotonal organs of ageing flies. However the fact that the centriole tethering phenotype (as shown by Sas4 marker staining) is prominent in late stage embryos (stage 17) and in pupal antennae (developing tissues, Cho not yet functional) would suggest that the centriole separation takes place during the development. Unfortunately imaging earlier stages of embryonic development did not elucidate the moment in which the separation happens as the Sas4 staining becomes quite obscure in early embryos (data not shown). Taking all of the above into consideration it is conceivable that the centriolar cohesion defect in DmRootletin knock-down flies occurs during the development and possibly deepens as the fly ages.

10.6 Possible involvement of DmRootletin in IFT

Involvement in intraflagellar transport has been proposed to be one of the functions of Rootletin. A recent paper by Svetha Mohan et al (2013) suggests that *C. elegans*

orthologue of Rootletin CHE-10 is involved in IFT regulation. One could hypothesize that DmRootletin being localised at the base of the cilium and spanning all the way to the nucleus can be crucial in engaging some of the IFT machinery components to the ciliary transition zone. The fact that the globular head domain of murine Rootletin interacts with Kinesin Light Chain 3 supports this hypothesis (Yang et al, 2002). As shown indirectly in the section 9.8.3 and figure 2.14 in DmRootletin knock-down larval Cho the IFT might be affected. The NompC marker staining localisation is slightly disrupted and shows some mislocalisation from ciliary tips to the more proximal parts of the cilium. Also the subtle ciliary tip swelling is visible in the TEM images - this is a phenotype characteristic of an IFT-A defect. This and the NompC marker mislocalisation provide an indirect evidence that movement of proteins along the cilium could be disrupted or misregulated. The fact that example of both IFT-A (RempA) and IFT-B (NompB) components are positioned in their normal localisations in the DmRootletin KD shows that if DmRootletin has a role in IFT it cannot be of great importance.

10.7 Role of DmRootletin in external sensory organs

As shown in the section 1.2.14 of the results DmRootletin knock-down affects the ES organs function. External sensory neurons bear a small rudimental cilium which is crucial for the organs function. It is possible that those short cilia need rootlets for anchoring however it has not been shown that DmRootletin protein is actually present in the ES cells. The fact that DmRootletin is transiently expressed in the developing ES organs suggests that some protein might be present in mature ES. Upon closer examination the ES neurons in DmRootletin knock-down seem grossly normal but no subcellular structure could be visualised due to technical difficulty of the dissection and staining.

It is worth noting that the functional defect in ES organs is not as prominent as in the chordotonal organs. One reason for this could be that the DmRootletin gene is only transiently expressed in the developing ES organs and that the DmRootletin protein level is significantly lower in ES than in Cho organs. It is possible that DmRootletin does not have such an important role in the ES as in the Cho organs where the cilia are much longer.

10.8 Role of DmRootletin in fertility

Expression of DmRootletin gene in *Drosophila* testes has been confirmed for the first time during this project. Using a semiquantitative method of reverse transcription followed by a PCR with cDNA as a template it has been shown that DmRootletin is expressed at low levels in adult testes. Using a Hale-bopp gene (known to be very highly expressed in testes) as a control I have established that, despite what is stated in the FlyBase high throughput expression database, DmRootletin is not highly expressed in testes. The expression is quite low and not visible in the RNA in situ hybridisation despite specificity and good quality of the RNA probe (very clear staining in embryos).

It is worth noting that the RNAi silencing of DmRootletin in testes does not significantly reduce the genes expression (as shown by RT-PCR). It is possible that the level of expression is so low that it cannot be significantly lowered by the RNAi construct. Another possibility would be a different, testes specific DmRootletin splice variant to which the RNAi construct is not specific. It is also possible that the lack of significant effect on DmRootletin expression level is caused by the fact that Bam-Gal4 testes driver does not carry the Dcr2. Without overexpression of this RNAi silencing pathway component the knock-down is not as prominent.

In line with a low efficiency of the DmRootletin expression reduction the fertility of the DmRootletin knock-down males does not seem to be affected. It could be caused by a low knock-down efficiency in testes. A more plausible explanation is, seeing the very low DmRootletin expression level in testes, that DmRootletin does not play an important role in the sperm cells formation and function.

10.9 General conclusions

The orthology between human Rootletin and *Drosophila* DmRootletin gene has been confirmed in this chapter. Firstly the TEM results show a clear and complete lack of ciliary rootlets in the *DmRootletin* knock-down Johnston's organ. Secondly the functional analysis of the DmRootletin knock-down shows that DmRootletin has similar functions as the human Rootletin.

It has been confirmed here that DmRootletin is a main protein component of ciliary rootlets in *Drosophila* and that the rootlet structure is responsible for centriolar cohesion at the base of the cilium. Other possible DmRootletin function might be modulation of IFT. DmRootletin gene is specifically expressed in ciliated cells (Cho, ES and sperm) but is only responsible for normal function of the Cho organs and ES organs. *DmRootletin* knock down causes severe disruptions in the Cho organs function and mild disruptions in the ES organs. DmRootletin does not seem to have an important role in sperm cells formation/function despite some expression in those cells (albeit at very low levels).

Chordotonal organ functional disruption progresses as the flies age. This leads to a conclusion that the structural disruptions in the DmRootletin knock-down chordotonal organs accumulate causing the worsening of the phenotype.

Drosophila Rootletin orthologue is a putative interactor of the Nek2 kinase. Al-

though the in situ hybridisation results for both genes do not show an obvious expression pattern overlap the DmRootletin-GFP fusion protein is localised closely to the Nek2 protein (as shown by antibody staining). Moreover the Nek2 antibody staining is disrupted in the DmRootletin knock-down. It remains unclear what could be the function of the interaction between Nek2 and DmRootletin in *Drosophila*.

Part III

Transcriptional regulation of DmRootletin

11 Introduction

11.1 Transcriptional regulation of ciliogenesis

Cilia biogenesis is a complex process that has to be tightly correlated with cell division and maturation. Cilia that bear specialised functions usually appear only when a cell is completely differentiated. However in some cases cilia are assembled and disassembled in coordination with the cell cycle. In both cases some regulation of the ciliogenesis process is clearly necessary. Such regulation on a gene transcription level was first documented in *Chlamydomonas* (Lefebvre, 1980) where mRNA levels of α-tubulin and β-tubulin have been shown to be elevated after induced deciliation followed by ciliogenesis. This has been shown on a wider scale by a transcriptome analysis of cilia regenerating *Chlamydomonas* (Stolc et al., 2005) and also by comparative genomics approach analysing genomes of organisms that contain or do not contain cilia (Avidor-Reiss et al., 2004). Those two approaches have proven very successful in identifying novel ciliary genes however they did not provide an insight into what transcription factors might be regulating ciliary genes expression. For long it has also remained unclear as to how the formation of different ciliated cell types is regulated. It is now known that two major types of transcription factors are involved in formation of cilia diversity and in the ciliogenesis per se: RFX family members

and the FOXJ1.

11.1.1 RFX factors

The RFX transcription factor family consists of several proteins whose common feature is a highly conserved winged-helix DNA binding domain (DBD). RFX proteins bind DNA by contacting the minor groove with the wing domain (Gajiwala et al., 2000). Members of the RFX family are capable of forming homo- or hetero-dimers and can bind DNA as a monomers or dimers (Iwama et al., 1999). The RFX factors target binding site (called an X-box) is a symmetrical motif that consists of two imperfect inverted repeats linked by a variable linker of 1-3 nucleotides. The RFX protein dimers make contact with DNA by binding the inverted repeats on the opposite sides of the DNA strand (Gajiwala et al., 2000).

Seven different RFX transcription factors have been identified in mammals (Emery et al., 1996; Aftab et al., 2008) based on the high conservation of the DNA binding domain with the eighth member of the RFX family annotated recently (Choksi et al., 2014). Strikingly all those RFX proteins are predicted to be present in all vertebrates with some exceptions only in fish where an additional RFX gene is present. A smaller number of *RFX* genes have been identified in invertebrates like *Drosophila* (Durand et al., 2000; Otsuki et al., 2004), *C. elegans* Swoboda et al., 2000 and also in yeast *S. pombe* (Wu and McLeod, 1995). Such a wide variety of organisms in which RFX proteins are present and the fact that some of them are involved in ciliary genes regulation suggests high evolutionary conservation of the function they have.

The first experimental evidence of RFX family member involvement in transcriptional regulation of cilia genes was published by Swoboda et al (2000). *C. elegans* has only one RFX gene - *Daf-19*, and it is expressed very specifically in all ciliated cells (60 ciliated sensory neurons). When the *Daf-19* is mutated the sensory neurons

are still formed but fail to ciliate. This result suggests that Daf-19 is necessary for cilia formation. The vertebrate members of the RFX family shown to regulate core ciliary genes are *RFX1*, *RFX2*, *RFX3* and *RFX4*. The *RFX1* was initially shown to be involved in regulation of genes that have no relation to cilia (Steimle et al., 1995; Iwama et al., 1999) but has recently been found to regulate expression of a ciliary basal body-protein ALMS1 (Purvis et al., 2010). *RFX2* has been shown to be crucial for formation of both motile and immotile cilia and mutations in *RFX2* lead to truncation of cilia, defects in motility and also defects in cilia-dependent signal transduction (Chung et al., 2012). *RFX3* in mice is expressed in various parts of brain and also in the pancreas. *RFX3* mutants exhibit defects in brain development leading to severe hydrocephalus. Some of the brain and also the pancreas defects could be linked to disregulation of the Hedgehog signaling pathway which is dependent on primary cilia (Ait-Lounis et al., 2007; Benadiba et al., 2012). *RFX4* mutant mice exhibit severe and perinatally lethal midline and brain defects. Those again are possibly linked to malformation of cilia which leads to misregulation of the HH pathway and subsequent CNS patterning defects.

In general RFX transcription factors are thought to regulate the expression of core cilia structural genes. However it has been shown that some of the RFX downstream targets are transcription factor genes themselves Efimenko et al., 2005. This suggests that RFX factors not only regulate cilia molecular architecture but can possibly also be involved in regulating cilium specific developmental cascades (Efimenko et al, 2005).

11.1.2 Foxj1

Foxj1 is a divergent member of the FOX (forkhead box) transcription factor family. The FOX transcription factors are involved in regulation of a wide array of biological

processes. The *FoxJ1* gene was first identified by Clevidence et al. (1993). The expression of this mammalian gene is restricted to tissues that possess motile cilia (Brody et al., 2000; Yu et al., 2008). Based on the spatial expression pattern it has been suggested by Murphy et al (1997) that the Foxj1 might be involved in transcriptional regulation of ciliary genes. Indeed the fact that the Foxj1 protein is localised in the nuclei and that the highest levels of expression occur directly prior to ciliogenesis in various tissues (Blatt et al., 1999) supports this hypothesis. The involvement of the Foxj1 transcription factor in the regulation of motile cilia formation has since been independently confirmed by two groups (Brody et al., 2000; Chen et al., 1998). The study by Brody et al (2000) reports that *FoxJ1* mutant mice exhibit almost complete loss of motile (9+2) cilia in the nasal epithelium. The loss of motile cilia in *FoxJ1* mutant mice has also been reported in proximal respiratory epithelium, oviduct, sperm cells, and choroid plexus (Chen et al, 1998). Another defect caused by *FoxJ1* mutation in mice is the impairment of ciliary basal body docking to the cell membrane (Brody et al, 2000). The study by Stubbs et al (2008) show that *Xenopus FoxJ1* homologue can transcriptionally regulate expression of many ciliary genes like dynein arms homologues (Dnah9, Dnah8, Dnai1, Tctex-1), potential dynein assembly factor, dynein associated protein (Roadblock), one protein component of the central pair complex (Spag6), various radial spoke proteins (Rshl2, Rshl3 and radial spoke protein 44), and four tektin isoforms. The direct transcriptional regulation of *dynein* and *WDR74* motile cilia specific genes by *FoxJ1* homologue has been shown by chromatin immunoprecipitation in zebrafish (Yu et al., 2008).

11.1.3 RFX and Foxj1 cooperation

As explained before RFX factors are responsible for regulation of both motile and immotile cilia genes while the Foxj1 is necessary for making the motile cilia specifically. Because both RFX and Foxj1 are involved in motile cilia formation it has been suggested that they might cooperate in regulation of expression of motile cilia genes. This has first been shown in *Drosophila* by Newton et al (2012), and was later confirmed in human cultured cells where Foxj1 is capable of inducing the expression of *RFX2* and *RFX3* during the formation of cilia (Didon et al., 2013). The potential reciprocal regulation possibly works vice versa because the RFX3 has been shown to bind to the *FoxJ1* promoter and partially modulate Foxj1 expression in mouse ependymal cells (El Zein et al., 2009). Apart from mutual transcriptional regulation another model of Foxj1 and RFX cooperation has been suggested. A working model has been proposed in *Drosophila* (Newton et al, 2012) and later in human cells (Didon et al, 2013) in which RFX acts as co-factor for Foxj1 (*Drosophila* fd3F) in motile cilia biogenesis regulation. This hypothesis is supported by the fact that RFX and Foxj1 seem to interact with each other at the protein level in cultured mammalian cells (Ravasi et al., 2010, Didon et al, 2013). A third model proposed for the functional cooperation between RFX factors and Foxj1 is a redundancy model. In mouse embryonic floor plate RFX3 and Foxj1 act in parallel to regulate the formation of motile cilia. Interestingly in a *Foxj1* null mutant mice those motile cilia are unaffected and the expression of *RFX3* is not changed. This suggests that RFX3 is able to compensate for the absence of FoxJ1 and seems to be sufficient for the biogenesis of this certain type of motile cilia (Cruz et al., 2010).

Although a lot is now known about the RFX and FoxJ1 roles in the transcriptional regulation of ciliary genes the modulation of ciliary diversity and ciliary specification remains largely unclear. It is likely that the ciliary diversity is achieved via differential

transctriptional regulation but the precise regulatory network behind this has yet to be clarified.

11.2 Transcriptional regulation of ciliogenesis in *Drosophila*

In *Drosophila* the specification of ciliated cells starts with expression of specific proneural factors. As explained in detail in the introductory chapter the main proneural factors responsible for specification and differentiation of ciliated PNS neurons are Atonal and members of the Achaete-scute complex (Bertrand et al., 2002). In a simplified schematic the Achaete-Scute complex modulates expression of transcription factors responsible for formation and function of the external sensory organs cilia (Jiménez and Campos-Ortega, 1990) while Atonal transcriptionally regulates the genes modulating the formation of chordotonal organs cilia (Jarman et al., 1993, 1995). Another proneural gene - *amos* - is also capable of driving the chordotonal organs specification but only in the missexpression context (Goulding et al., 2000). Some core ciliary genes (encoding basic components of the ciliary architecture) are regulated by both Atonal and Scute proneural factors. As shown in the figure 3.1 the key transcription factors (targets of the proneural gene *atonal* based on microarray data and conserved *atonal* binding motifs presence in the upstream regions (Cachero et al, 2011)) involved in regulation of cilia structural and functional genes are RFX and fd3F.

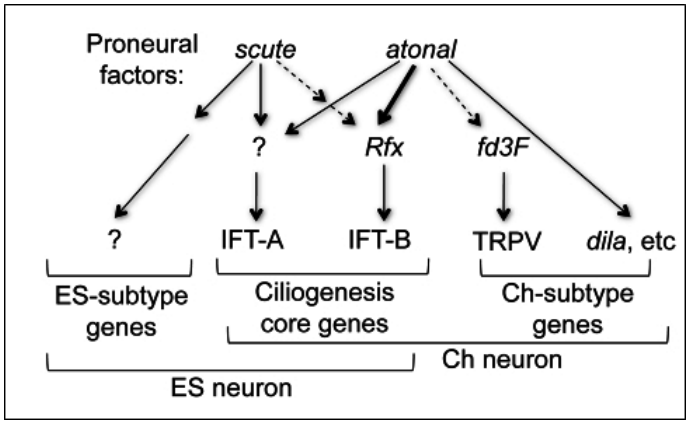

Figure 3.1. Diagram showing the transcriptional regulatory network of *Drosophila* cilia specification. Proneural factors scute and atonal act in specification of precursor cells of the ciliated neurons. Once the sensory precursor (SOP) is determined the downstream transcription factors are expressed in their appropriate specific tissues - fd3F in Ch neurons and RFX in both ES and Ch neurons. RFX regulated core ciliary genes while fd3F regulates genes necessary for ciliary motility characteristic in Ch neurons. Taken from Cachero et al (2011).

11.2.1 Role of RFX in *Drosophila* ciliogenesis

Two *RFX* genes have been identified in *Drosophila* (Durand et al, 2000). One of them was found using a human *RFX1* DBD low stringency probe to screen the *Drosophila* genome. It is a homologue of mammalian *RFX1* and is also very similar to *RFX2* and *RFX3*. This *Drosophila RFX* isoform has a very highly conserved DNA binding domain. The other *Drosophila RFX* is very divergent but seems to have motifs similar to the mammalian *RFX5* - the most degenerate member of the RFX family. The *RFX5 Drosophila* homologue has not been studied extensively, does not seem to involved with cilia and will not be mentioned more in this work. All the following mentions of *Drosophila* RFX will refer to the RFX1-3 homologue.

The *RFX* is expressed in adult brain, PNS and testes. During the embryonic development the expression pattern of *RFX* starts in stages 10-11 and is specific to the SOP cells P (posterior) and A (anterior) which give rise to type I sensory neurons

(Durand et al., 2000). In later stages (stage 14-17 of embryonic development) the *RFX* expression is restricted to the chordotonal organ neurons but weak transient expression is seen in the external sensory organs (Dubruille et al., 2002). Such expression pattern is called chordotonal enriched (Cachero et al, 2011). Interestingly a transient expression has been noted in the chordotonal organs support cells. As shown by Dubruille et al (2002) *Drosophila RFX* mutants are severely uncoordinated which is a phenotype characteristic of affected ciliated mechanosensory neurons. Another functional defect has been shown in the ES organs where the external sensory neurons do not respond to mechanical stimuli (Dubruille et al, 2002). The functional defects in the mechanosensory organs are reflected in the morphology. The chordotonal organs seem to have severely shortened to completely absent cilia. The axoneme organisation in the remaining truncated cilia is also severely disrupted. Interestingly, some defects have also been noted in the chordotonal organs' supporting cells which is consistent with the transient expression of RFX in those cells. In line with the generally described function of the RFX family members the *RFX* is therefore necessary for correct ciliogenesis and for proper function of cilia in *Drosophila*.

The first study to identify putative RFX target genes was done by Avidor-Reiss et al (2004). In this study an X-box search coupled with comparative genomic approach (ciliated vs non-ciliated organisms) screen has been used. Avidor-Reiss et al identified 41 RFX candidate targets 14 of which are known ciliary genes. Another genome wide computer screen approach using a conserved RFX DNA binding domain sequence coupled with expression screen in RFX mutants has identified 35 candidate RFX target genes (Laurençon et al., 2007). Among those are all known *Drosophila* homologues of genes defective in the Bardet-Biedl syndrome - a human ciliopathy. Other genes fall into the category of compartmentalised ciliogenesis genes (Avidor-Reiss et al, 2004). 18 of them are downregulated over 2 fold in the *RFX* mutant

background (Laurencon et al, 2007). Some genes found in this screen are not yet characterised but have a highly predicted function in ciliogenesis. Interestingly only some subgroups of ciliary genes seem to be regulated by RFX. As stated by Laurencon et al (2007) IFT-B components are regulated by RFX while none of the known IFT-A genes are. Also retrograde motors (*btv, CG3769*) seem to be significantly downregulated in RFX mutant while the anterograde motors like *CG10642/KIF3A, CG17461/Kif3C/osm-3,* and *CG7293/Klp68D* are invariably expressed in *RFX* mutant. The strict division between the IFT-A and IFT-B components in terms of *RFX* regulation has later been disproven (Newton et al, 2012). Apparently the rempA (IFT-A protein (Lee et al, 2008)) gene expression is strongly reduced in the *RFX* mutant. The possible reason for which this gene has not come up as an RFX target in earlier studies is that the X-box motif present upstream of the rempA gene does not conform completely to the consensus sequence. This is a characteristic feature of a novel regulatory model in which RFX cooperates with fd3F in regulation of some target genes (explained more in the section 11.2.3).

Another gene that has been identified as an RFX target gene is *DmRootletin* (Laurencon et al, 2007). The presence of a conserved X-box motif in the *DmRootletin* upstream region has been confirmed by Cachero et al (2011). It is an interesting example because its expression pattern follows the chordotonal-enriched characteristic. Such an expression pattern is followed by many other ciliary genes and it serves as a possible explanation of the differential specification of ciliated sensory neurons in *Drosophila* (Cho and ES cells). Seeing that expression pattern of *RFX* itself is chordotonal-enriched it is likely that the differences in the cilium structure between the Cho and ES organs are achieved by the different levels of the RFX factor in each cell type (Cachero et al, 2011).

11.2.2 Role of fd3F *Drosophila* ciliogenesis

Drosophila gene *CG12632* is a highly divergent homologue of the Forkhead transcription factors family (Cachero et al, 2011). Named *fd3F* (forkhead domain at position 3F), it seems to be the cell-type-specific (cho) transcription factor that RFX has been speculated to cooperate with in order to give rise to cilia diversity (Thomas et al., 2010). *Fd3F* has been recognised as the atonal downstream target gene encoding a transcription factor (Cachero et al, 2011). Upon closer examination it has been shown that *fd3F* mutant flies cilia motility aspect is severely affected (Cachero et al, 2011). Its expression is very strictly limited to developing and differentiating chordotonal neurons. *Fd3F* mutant flies are uncoordinated and although the chordotonal neurons are present and grossly normal their function is severely affected (Newton et al, 2012). It has been shown that fd3F regulates genes involved in specific aspects of cilia differentiation and maturation which are crucial for motility. As described in the introductory chapter chordotonal cilia exhibit some motility which is important for augmentation of the mechanical stimuli (Göpfert et al., 2005). In fact fd3F is involved in direct regulation of numerous axonemal dynein components (*Dhc16F, Dhc62B, CG8800, CG34192, CG6971, and CG13930*) and also the genes encoding the axonemal dynein assembly factors like *tilB* and *CG14905* (Newton et al, 2012). This is apparent in the TEM analysis of Johnston's organ from *fd3F* mutant in which a complete loss of the axonemal dynein arms is visible. Another phenotype suggesting that *fd3F* mutant cilia loose their motility is the loss of nonlinnear mechanical amplification in JO. The non-linear mechanical amplification results from ciliary motility and is a phenomenon in which the antennal segment oscillates in response to a weak sound stimulus in order to optimise the sound receiver sensitivity (Gopfert et al, 2005). Interestingly fd3F regulates another group of genes which are not directly involved in cilia motility. The examples of those are cytoplasmic dyneins

CG3769 and *btv* (Newton et al, 2012) which are retrograde motors involved in ciliogenesis. Other retrograde transport components regulated by fd3F are *Oseg6* and *rempA*. It has been rationalised that components of this fd3F target genes group are necessary for the formation and maintenance of the functional division of cilium into two distinct zones which is therefore another important aspect of cilium specialisation.

In general fd3F seems not to be involved in regulation of ciliogenesis core genes but instead controls genes necessary for cilia motility and correct compartmentalisation of cilia into motile and non-motile zones.

11.2.3 Differential regulation of ciliary diversity

Drosophila RFX regulates ciliogenesis in two different types of ciliated cells - chordotonal neurons and external sensory neurons. Those two types of cells generate functionally and morphologically different cilia. It remains largely unclear how this diversity is achieved given that both cell types initially differentiate from one SOP. One of the possible explanations of this is the fact that *RFX* is expressed differentially (in terms of both time and expression level) in the Cho and ES cells. This so called chordotonal-enriched expression pattern is also characteristic to other ciliary genes and provides a clue as to how can the cilia diversity occur. Another means of different cilia formation could be RFX and fd3F cooperation. It has also been speculated that in specific conditions RFX cooperates with fd3F to modulate expression of chordotonal specific fd3F target genes (Newton et al, 2012). This was shown on the example of some fd3F target genes - *nan* (nanchung) and *iav* (inactive) - which are both components of the TRPV channel present in the proximal (motile) part of the chordotonal cilium (Gong et al., 2004). Both *iav* and *nan* are fd3F direct target genes and fd3F seems to be sufficient and necessary for their ex-

pression. Strikingly however the expression of both *iav* and *nan* is strongly reduced in *RFX* mutants. The cis-regulatory regions of those two fd3F target genes contain X-box motifs localised in near vicinity of the functional forkhead binding sites. Furthermore, when those X-boxes are mutated the expression of the reporter gene (nan/iav-enhancer-reporter constructs) is grossly abolished. While the *iav* and *nan* are chordotonal specific genes the similar model of RFX-fd3F cooperation is also true for some chordotonal-enriched genes like *CG3769* and *btv.* Newton et al concluded that while RFX regulates genes required in all ciliated neurons, the expression of genes specific to Cho organs is additionally modulated by fd3F. In the model proposed in this study fd3F is an obligatory coregulator of chordotonal-specific genes while in chordotonal-enriched genes it only enhances the expression level of some proteins that are specifically required for Cho specialised function. Example of this could be the retrograde transport protein rempA. RFX drives its expression in all ciliated sensory neurons (ES and Cho) to a sufficient level to for basic ciliogenesis while fd3F boosts its expression to higher levels to support the need for cilia compartmentalisation in the chordotonal organs.

In general the RFX modulation by fd3F is a good example of a cell specific cofactor that enables specification of two structurally distinct ciliated neurons by modulating the ciliary motility and compartmentalisation. There are however genes that follow the chordotonal-enriched expression pattern and do not fall into either motility or compartmentalisation categories. One such gene is *DmRootletin.* It remains unclear whether the regulatory mechanisms controlling the *DmRootletin* expression are similar to the ones explained above. The fact that some unpublished data (Newton et al., 2012) suggest that *DmRootletin* expression is independent of fd3F suggest that *DmRootletin* differential expression might be regulated in a novel previously uncharacterised manner.

11.2.4 Role of Zmynd10 in *Drosophila* ciliogenesis

Zmynd10 is another gene potentially involved in ciliary gene regulation. Human *Zmynd10* gene is present in the Cildb database (Arnaiz et al., 2009) and has also been clearly linked to ciliary motility (Ross et al., 2007). In the work presented by Moore et al (2013) human *Zmynd10* is shown to be a primary ciliary dyskinesia (PCD) causative gene, the mutation in which lead to partial loss of dynein arms in the axoneme and therefore to complete loss of ciliary motility. In *Drosophila* *Zmynd10* expression is strictly limited to the cells bearing motile cilia - chordotonal neurons and the sperm cells (Moore et al, 2013). The fact that *Drosophila Zmynd10* expression is dependent on both fd3F and RFX (Newton et al, 2012 and Dubruille et al, 2002) is strongly suggestive of its involvement in ciliary motility. In fact as shown in human PCD patients, *Drosophila Zmynd10* mutant cilia lack inner and outer dynein arms. There are two possible ways how Zmynd10 can be involved in ciliary motility modulation.

Zmynd10 possesses a conserved MYND domain which is suggested in protein-protein interactions (Gross and McGinnis, 1996). Indeed the human Zmynd10 has been shown to interact with *Drosophila* orthologue of LRRC6 (tilB) - a known dynein assembly factor - via its MYND domain (Moore et al, 2013). This result together with the fact that Zmynd10 protein is localised in the cytoplasm strongly suggests its direct role in the dynein assembly machinery.

Apart from possibly regulating ciliary motility on the protein level Zmynd10 has potential to regulate transcription of some ciliary genes. This potential is suggested by the fact that another interesting sequence is present in the Zmynd10 protein - a LxxLL motif (Moore et al, 2013). LxxLL motifs are known to participate in protein-protein interaction between transcription factors and their cofactors (Plevin et al.,

2005). Through those interactions LxxLL motifs are able to induce activation or repression of target genes (Plevin et al, 2005). It is worth noting that one of the Zmynd10 mutations found in PCD patient was an aminoacid substitution of one of the leucins of the LxxLL motif (Moore et al, 2013). This suggests that Zmynd10 may interact with transcription factors to modulate the ciliary genes expression. In fact the data presented by Zariwala et al (2013) suggest that some dynein arm component encoding genes transcript levels are reduced in Zmynd10 knock-down HTEpCs cells. However this result is very indirect and no firm evidence has so far been found of Zmynd10 involvement in the transcriptional regulation of any genes.

11.3 Aims of this chapter

This chapter aims to add to the existing knowledge of how genes are regulated to give rise to cilia specialisation and diversity. Previous work shows that RFX regulates core ciliogenesis genes, fd3F regulates aspects of chordotonal organs specialisation (motility and compartmetalisation), and also that RFX and fd3F cooperate to regulate these aspects. Not much is known however about regulation of other aspects of ciliogenesis. Apart from motility and compartmentalisation, the presence of a ciliary rootlet is another difference between the ES and Cho organs in *Drosophila*. This makes the *DmRootletin* regulation an interesting topic to pursue. *DmRootletin* is expressed in the chordotonal-enriched pattern and it has been shown to be directly regulated by RFX. However according to previous studies *DmRootletin* expression is not regulated by fd3F. Therefore it seems plausible that *DmRootletin* differential regulation might follow a previously undescribed model. The aim of this chapter it to elucidate the regulatory pathway/network that stands behind the *DmRootletin* chordotonal-enriched expression pattern. Answering this question will hopefully provide more data on the differential regulation leading to formation of different cilia

types.

12 Results

12.1 *DmRootletin* gene structure

DmRootletin is a large protein coding gene localised on the third chromosome (position 3R:24,113,286). It is 14908 bases long including the 5' UTR and 3' UTR (13268 excluding UTRs).The number of annotated exons differ depending on the database. According to FlyBase it has ten exons (see Fig. 3.2A) and according to NCBI it has eleven exons (Fig 3.2B). The first and the second (Flybase) exon are separated by a very large intron (7979bp). Another small gene (*CG13607*) is nested within this large intron. The first exon was not initially annotated as part of the transcript but has recently been added to the *DmRootletin* gene region. The first large intron has therefore initially been regarded as the upstream region in this project and in the following section it has been searched for putative regulatory elements (transcription factors' binding motifs). The first and the second (appearing only on NCBI) exons are non coding (Fig 3.2B).

The *DmRootletin* gene has three different transcript variants - F, D and E. Those isoforms differ in mRNA length. Variant E spans through the whole 14908 bases, variant D is 14599 bases long and lacks the beginning of the first exon, and the variant F is 9654 bases long and starts with the second exon. Variants E and D do not contain the second exon which is only annotated as such by NCBI but not FlyBase. All three mRNA variants when translated produce an identical protein of 2048 aminoacids.

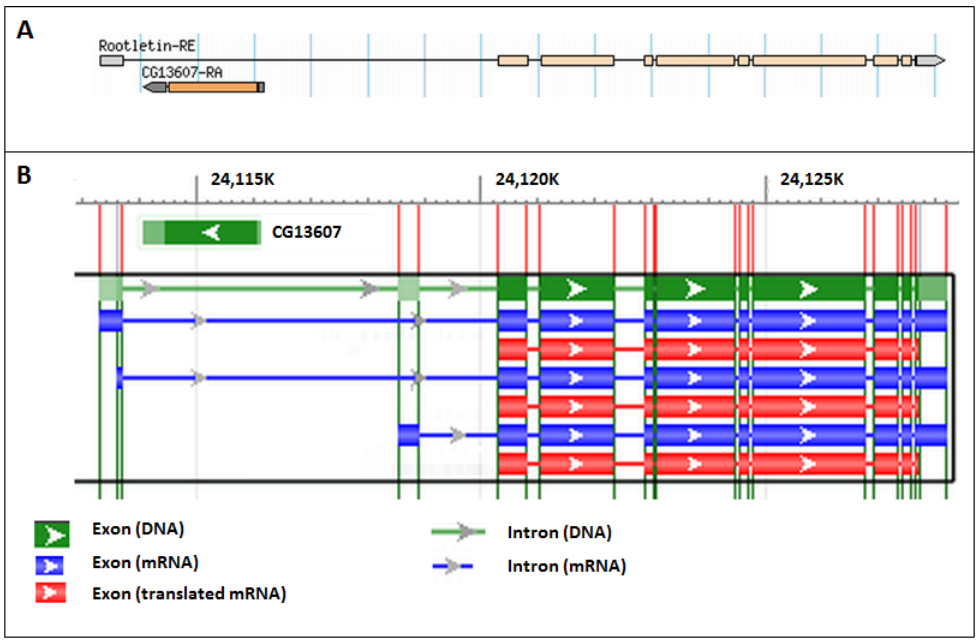

Figure 3.2. DmRootletin gene structure as annontated and presented in various databases. A - *DmRootletin* gene region as annotated by FlyBase. It has 10 exons and the first one is non-coding. B - *DmRootletin* gene region as annotated by NCBI. Here it has 11 exons and the first two are non-coding.

12.2 *DmRootletin* expression pattern

DmRootletin has an interesting expression pattern that follows the chordotonal-enriched characteristics. Its expression starts in stage 10 of embryonic development in a single SOP cell which underlies the formation of all sensory neurons. When the SOP divides (stage 11) the *DmRootletin* expression is only visible in the proneural clusters that divide to form both ES and Cho cells. Interestingly in the stage 14 a transient expression is visible in the external sensory cells. This expression entirely disappears in the stage 17 where *DmRootletin* mRNA is specifically expressed in chordotonal neurons.

DmRootletin is an example of a gene which expression pattern is called chordotonal enriched (Cachero et al, 2011). The *DmRootletin* is differentially expressed in two types of cells - ES cells and chordotonal cells. It is interesting that *DmRootletin* is

expressed in both Es cells and chordotonal cells from the very start of the lineage formation (single SOP) but its expression in the ES cells disappears in stage 16 while the Cho expression is on until the very end of embryonic development. This suggests that *DmRootletin* expression might be controlled differently in those two types of cells.

The exact sequence of events leading to differentiation of the two subtypes of type I sensory neurons and all the TFs involved are yet to be understood. One of the possible transcription factors that might be involved in *DmRootletin* regulation is RFX. *DmRootletin* mRNA expression pattern reflects that of RFX very closely (Durand et al, 2000, Vandaele et al., 2001). Another transcription factor known to regulate ciliary genes is fd3F. The evidence of RFX and fd3F involvement in *DmRootletin* regulation will be searched in the following sections.

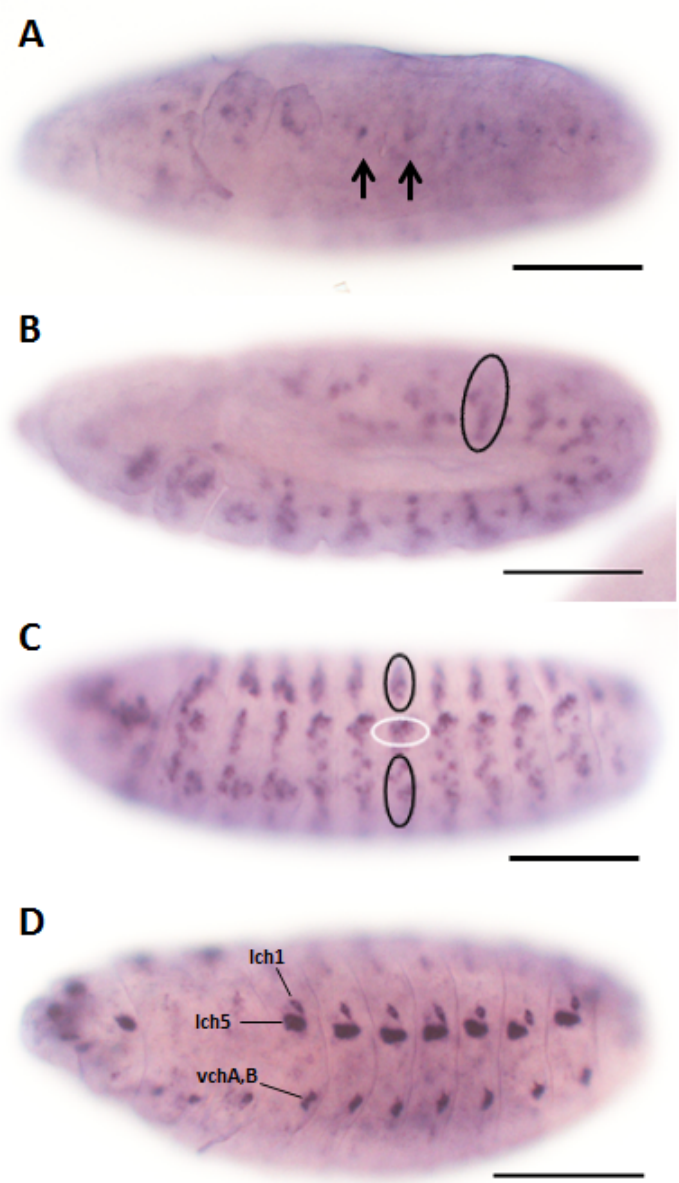

Figure 3.3. ***DmRootletin*** **expression pattern. A -** early stage 10, black arrows indicate single SOPs in two segments, the gene is expressed in all the segments, **B** - late stage 11, black elipse encircles a single proneural cluster, **C** - stage 14, the black elipses indicate the ES cells and the white elipse encircles the chordotonal cells, **D** - stage 17, black lines indicate the chordotonal neurons. Scale bars represent 100um.

12.3 dDmRootletin Cis-regulatory region and putative transcription factor binding site matches

The cis-regulatory sequences can be found either upstream, downstream or even inside a given gene. The enhancers are characterised by high conservation in related species. In case of the *DmRootletin* gene the upstream intergenic noncoding sequence is 2113 bases long. However as the first exon has not been initially annotated as part of *DmRootletin* gene the first intron has been examined as the putative regulatory region. The region between the nested intronic *CG13607* gene and the second *DmRootletin* exon (4225bp long) seems to be generally well conserved and has therefore been regarded as a possible cis-regulatory region for the *DmRootletin* gene. It has areas of great conservation across 12 *Drosophila* species which suggests possible localisation of enhancers in this area (Fig 3.4B). Considering the expression pattern of *DmRootletin* (from early stage 12 to late stage 17 of embryonic development) it is possible that the *DmRootletin* expression is regulated by the following transcription factors: atonal, RFX, and/or fd3F. The first intron has therefore been searched for putative atonal, RFX and fd3F binding site matches using the Gene Palette software (Rebeiz and Posakony, 2004). The atonal binding site is called an E-box and the consensus sequence is AWCAKGTGK (Powell et al, 2008). The RFX binding site is called an X-box and the consensus sequence is GYTRYYN(1-3)RRHRAC (Laurencon et al, 2007). The preferred binding site of the forkhead factors (and possibly fd3F) is called a forkhead binding site and the consensus sequence is RYMAAYA (Benayoun et al., 2011).

The GenePalette search revealed multiple hits for all three TF binding sites (Fig 3.4A). They did not seem to be grouped in a particular section of the examined region. On the contrary, the TF binding site matches were distributed evenly with

four cases of the X-box and the forkhead binding site positioned very closely to each other. The five atonal binding site matches found in the region are not well conserved. Out of 11 X-boxes, three localised on the 3' half of the region are highly conserved (see below). The 18 forkhead binding site matches are of varying conservation. In general some areas of the region exhibit no visible conservation and therefore they were not analysed in the next sections.

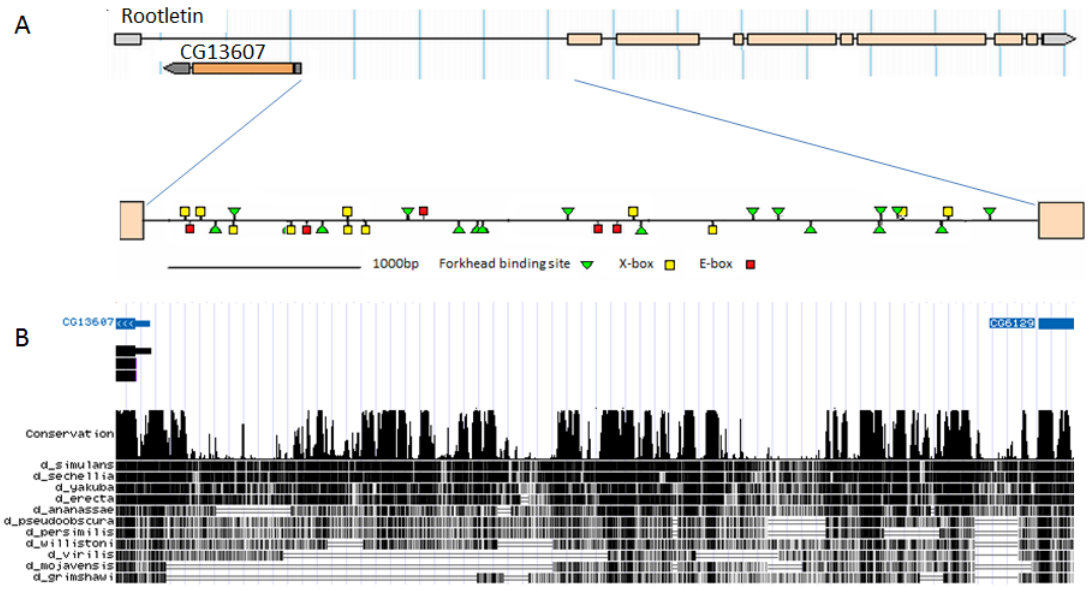

Figure 3.4. DmRootletin cis-regulatory region. A - atonal, RFX and fd3F binding site matches. Obtained from the GenePalette software. B - DmRootletin cis-regulatory region conservation across 12 *Drosophila* species. Obtained from UCSC Genome Browser at http://genome-euro.ucsc.edu/

12.4 Conservation of the putative TF binding sites across various *Drosophila* species

Conservation of the putative cis-regulatory region has been examined in order to reduce the number of putative TF binding sites to be investigated. I have used the Gene Palette software to line up the exact sequences of the TF binding sites with the conservation representation obtained from the UCSC genome browse database.

The majority of the TF binding site matches present in the *DmRootletin* regulatory region are not well conserved. Interestingly none of the E-boxes shows high conservation which suggest that *DmRootletin* might not be directly regulated by atonal. However, E-boxes tend to be poorly conserved anyway. It is worth noting that the highest conservation of X-boxes is seen in those that are positioned very closely to a forkhead binding site. This is also true for the forkhead binding motifs in the near vicinity of an X-box. In fact it has been shown before (Newton et al., 2012) that RFX and fd3F interact in a tandem fashion in transcriptional control of their target genes. *DmRootletin* could be an example of such RFX-fd3F target gene given the high conservation among forkhead binding sites - X-box tandems, although previously reported not to be an fd3F target gene. There are four such tandems in the *DmRootletin* putative cis-regulatory region and only the one that is localised at the far 5' end is not conserved. Conservation of the other three is shown in the figure 3.5.

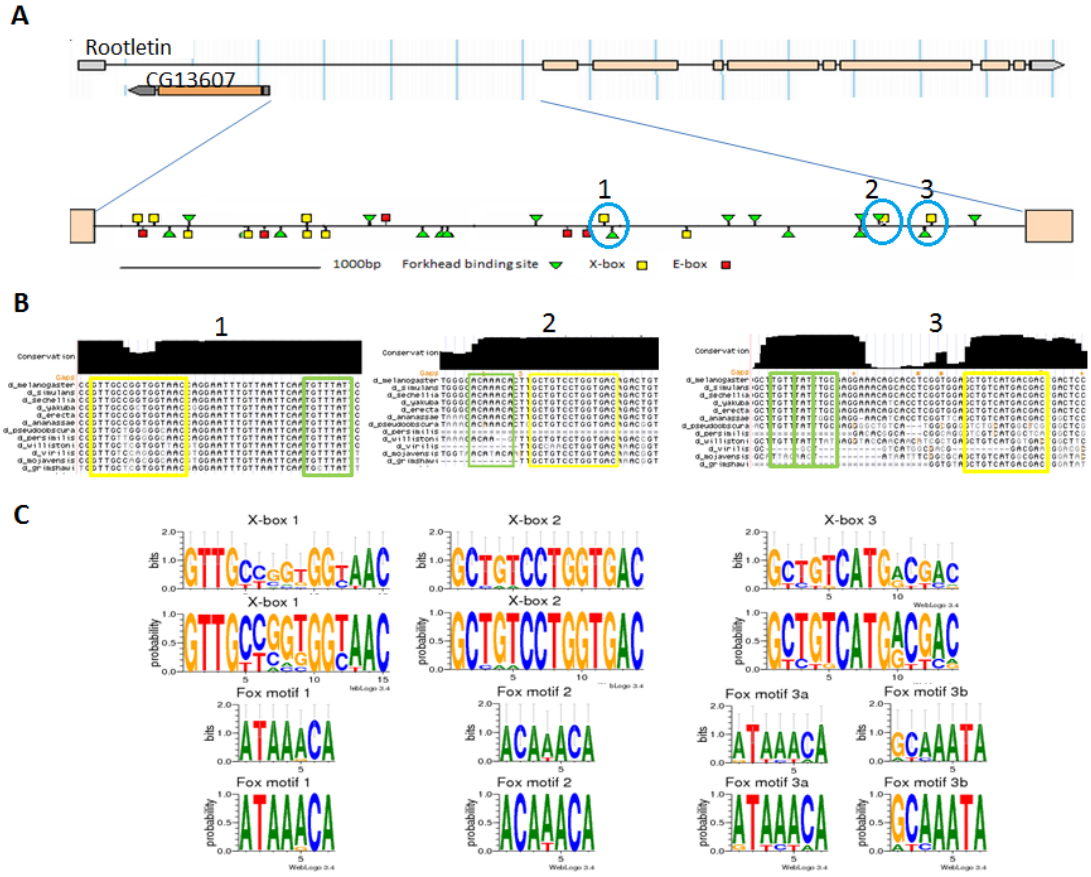

Figure 3.5. Conservation of the putative transcription factors binding sites. A - schematic representation of the *DmRootletin* putative cis-regulatory region and the Fox-motifs, X-boxes, and E-boxes present in this area, B - conservation of each X-box (in yellow) and Fox-motif (in green) tandem in 12 *Drosophila* species, obtained from UCSC genome browser (http://genome-euro.ucsc.edu), C - sequence logos summarising the alignment of the X-boxes (up) and Fox-motifs (down), present in the DmRootletin putative cis-regulatory region (obtained from http://weblogo.threeplusone.com online software).

12.5 Dependence of *DmRootletin* expression on sensory neuron transcription factors

In order to determine whether *DmRootletin* is controlled by RFX and/or fd3F, *DmRootletin* in situ hybridisation was carried out on *RFX* and *fd3F* mutant embryos. In the wild type control *DmRootletin* DIG-labeled probe gave clear and strong chor-

dotonal staining in stage 17 embryos (see Figure 3.6A). In the *RFX* mutants the *DmRootletin* mRNA was significantly lower with weak staining visible in some of the neurons in vch5 clusters (see Figure 3.6B). The *RFX* mutant line is heterozygous so the expected Mendelian ratio of homozygous null mutants to heterozygous embryos (unaffected) is 1:3. From the embryo collection tested 25 embryos in the stage 17 appeared normal while 8 embryos had significantly lower *DmRootletin* mRNA levels. The ratio of homozygotes to heterozygotes was 1:3.125 and therefore can be considered Mendelian. Interestingly, contrary to what has been previously reported (Newton et al, 2012), *DmRootletin* mRNA levels also appeared lower in the *fd3F* mutant background. The difference between the WT control and the *fd3F* mutant (see Fig. 3.6, G and H) was not as striking as in the *RFX* mutant case but nevertheless the *DmRootletin* expression is visibly reduced in *fd3F* mutants. Interestingly in the f*d3F;RFX* double mutant the *DmRootletin* expression was not completely abolished. The combined effect of the double mutant causes the *DmRootletin* mRNA to almost disappear but some residual staining is still visible. This suggests that *DmRootletin* might be controlled by another factor other that RFX or fd3F.

Interestingly the *DmRootletin* expression in the ES cells seems to be less dependent on the RFX (Fig 3.6D-F, black arrowhead). As far as can be distinguished from the weak ISH staining the area in which ES cells normally appear is not grossly affected by the lack of RFX (Fig 6E, black arrowhead). This is also true for the *fd3F;RFX* double mutant, but in this case the area in which the Cho cells should be, seems to be lacking the staining entirely (Fig 3.6F, black arrow), while the possible ES staining persists (Fig 3.6F, black arrowhead). Although the staining is too weak to extinguish the exact cells, it can be concluded that some ES-like expression of *DmRootletin* seems to be independent on RFX. Therefore this result could suggest the existence of another factor responsible for the DmRootletin chordotonal-enriched

expression.

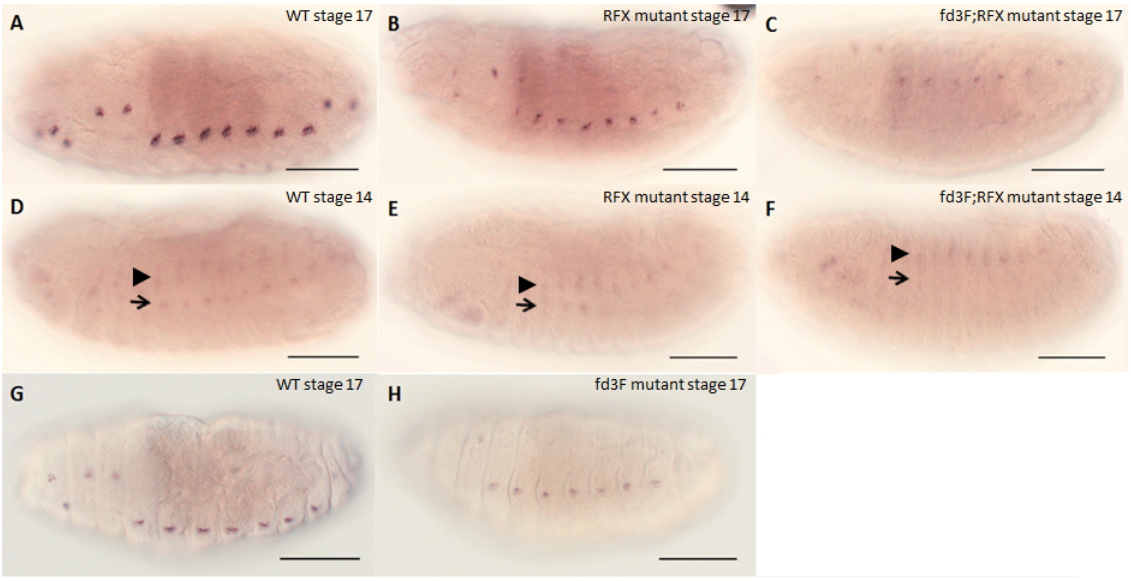

Figure 3.6. *DmRootletin* expression in *RFX* and *fd3F* mutant backgrounds shown by RNA *in situ* hybridisation. A - stage 17, *DmRootletin* expression in WT, **B** - stage 17, *DmRootletin* expression in RFX mutant, **C** - stage 17, *DmRootletin* expression in fd3F;RFX double mutant. **D -** stage 14, *DmRootletin* expression in WT, chordotonal cells indicated by the black arrow, ES cells indicated by the black arrowhead, **E -** stage 14, *DmRootletin* expression in RFX mutant, chordotonal cells indicated by the black arrow, ES cells indicated by the black arrowhead, **F -** stage 14, *DmRootletin* expression in fd3F;RFX double mutant, chordotonal cells indicated by the black arrow, ES cells indicated by the black arrowhead, **G** - stage 17, *DmRootletin* expression in WT, **H** - stage 17, *DmRootletin* expression in fd3F mutant. Scale bars represent 100um.

When the RFX and/or fd3F are overexpressed in the whole nervous system (UAS-RFX and/or UAS-fd3F constructs driven by sca-Gal4) the DmRootletin transcript is ectopically misexpressed. In embryos RFX overexpression alone causes ectopic *DmRootletin* transcript expression in the CNS but not in other PNS cells in both stage 14 and 17 (see Figure 3.7 C and D, CNS encircled with a black line). When fd3F is overexpressed *DmRootletin* transcript is ectopically expressed in other components of the PNS in the late stage 17 (see Fig 3.7 F, black arrowheads indicate the ES cells)- presumably the external sensory neurons in which the *DmRootletin* expression

disappears by the stage 16 (see Fig 3.7 B for DmRootletin expression in WT stage 17 embryo - no ES expression visible). fd3F overexpression alone does not cause any CNS *DmRootletin* expression. There does not seem to be any additive effect when both RFX and fd3F are overexpressed. In this case the *DmRootletin* is misexpressed in CNS (the RFX overexpression effect, see Fig 3.7 G, CNS encircled with a black line) and in the ES cells (fd3F effect, see Fig 3.7 H, black arrowheads indicate the ES cells).

The fact that RFX has a stronger effect in earlier stages of the development (that is in stage 14 the CNS ectopic expression of DmRootletin is more prominent than in the stage 17) might mean that this transcription factor is more active in earlier differentiation and ciliogenesis. fd3F on the other hand seems to have a stronger effect in the latest stages of development (DmRootletin ectopic expression in ES cells only visible in the stage 17).

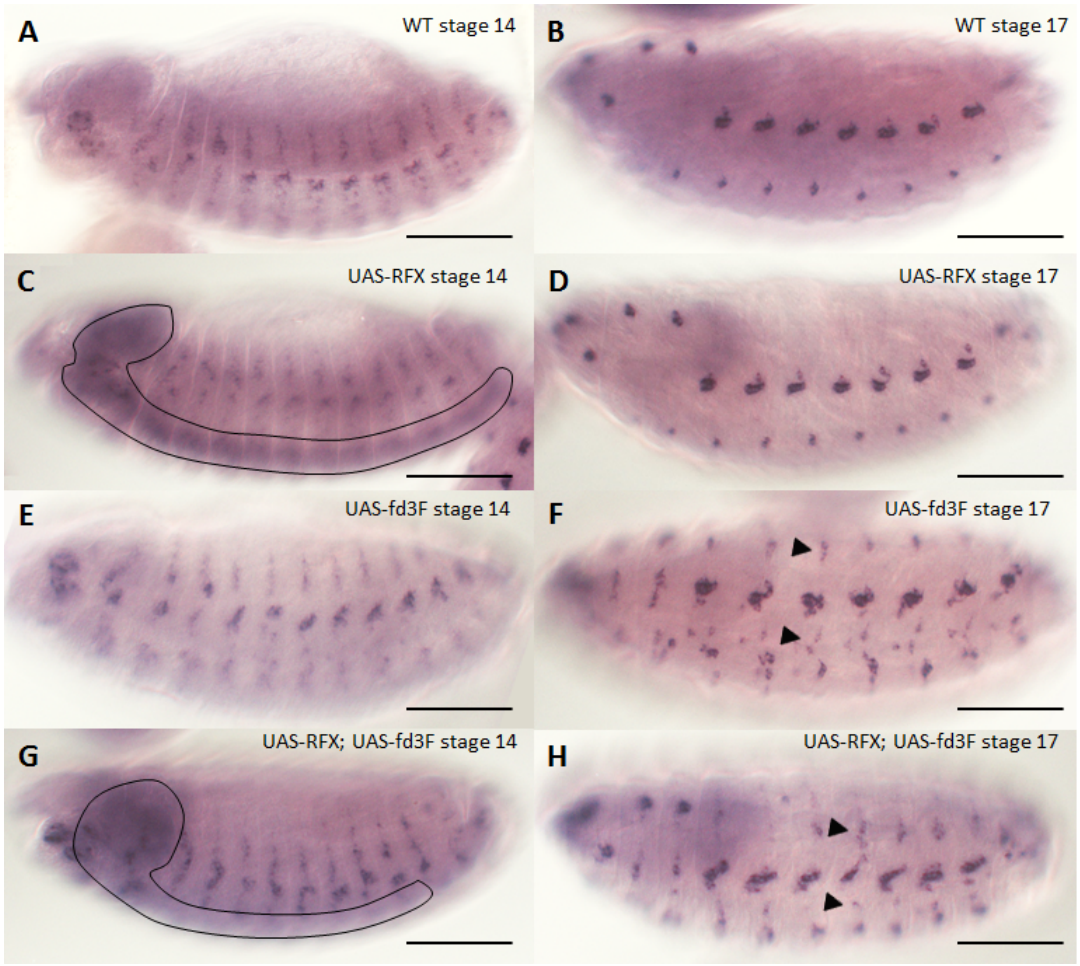

Figure 3.7. RFX and fd3F overexpression drives ectopic expression of DmRootletin. A - DmRootletin expression in stage 14 WT embryo, **B** - DmRootletin expression in stage 17 WT embryo, **C** - DmRootletin expression in stage 14 embryo overexpressing RFX (driven by the Sca-Gal driver), black line encircles ectopic expression in CNS, **D** - DmRootletin expression in stage 17 embryo overexpressing RFX, **E** - DmRootletin expression in stage 14 embryo overexpressing fd3F, **F** - DmRootletin expression in stage 17 embryo overexpressing fd3F, black arrowheads indicate ectopic expression in the ES cells,

12.6 Enhancer reporter gene constructs

In order to establish whether any of the transcription factor binding site matches found in the GenePalette search is capable of supporting the *DmRootletin* expression I have created the enhancer-reporter gene constructs. In short, the putative

regulatory regions have been cloned into a vector containing a reporter gene coding sequence (β-*gal*). The vector has then been injected into fly embryos that consecutively give rise to a line expressing the β-gal in the enhancer specific pattern.

Due to problems with cloning of the whole length (4225bp) of the chosen putative cis-regulatory region it has been subdivided in smaller parts. In order to choose what parts to clone the whole region has been examined in regards of the conservation of the putative transcription factor binding sites. As shown on the figure 5 three forkhead binding sites - X-box tandems are very highly conserved. I have therefore chosen to use three shorter sequences to make the enhancer-reporter gene constructs centered on these segments. Those *DmRootletin* upstream segments are shown in the figure 3.8 and will hereby be called sequence A, B and C.

The sequence A was chosen due to a large number of various putative transcription factor binding sites. The majority of them were not highly conserved but some exhibited moderate conservation. The forkhead binding site - X-box tandem has been included in this sequence in order to test whether it has any function in driving the *DmRootletin* gene. The sequence B includes an area of quite high general conservation and includes the very highly conserved forkhead binding site - X-box tandem number 1 as shown in the figure 3.3. It also includes two E-boxes and one forkhead binding motif but those are not well conserved. The sequence C only contains two very highly conserved forkhead binding site - X-box tandems shown in the figure 3.3 (2 and 3). The omitted sequences have not been included in the enhancer-reporter gene constructs due to poor conservation of the putative TF binding sites that are present.

The enhancer - reporter gene constructs were made by cloning the chosen putative enhancer sequence into the pLacZattB vector in which the β-galactosidase is a reporter gene. All the sequences have been cloned into the plasmid with EcoRI on the

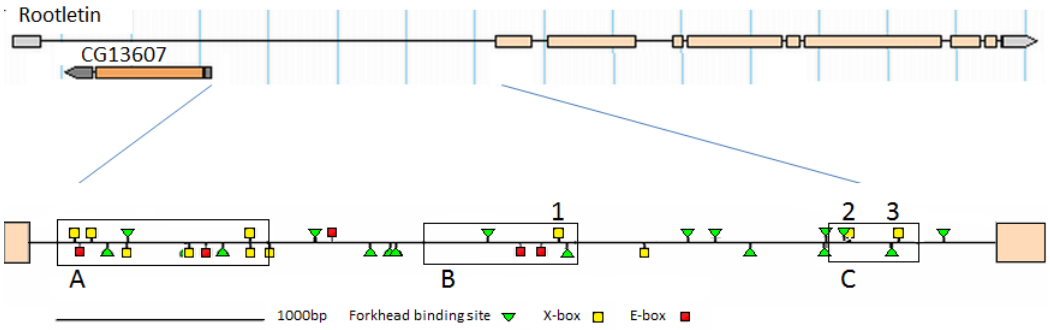

Figure 3.8. Sequences A, B, and C chosen for the enhancer - reporter gene constructs.

5' and XbaI on the 3'. All three constructs were subsequently injected into a fly line containing the attP site at 68E locus for a site specific recombination. When the recombination takes place (around 5-10% transformation efficiency) the enhancer - reporter construct is incorporated into the genome at a given insertion site that has been tested for a minimum/none position effects (Bischof et al., 2007).

12.7 Enhancer reporter gene expression patterns

The reporter gene expression represents the temporal and spatial pattern of the *DmRootletin* expression when driven by TFs binding to the given putative enhancer sequence (A, B or C). The three chosen short sequences gave different expression patterns.

The putative enhancer construct A did not give any specific expression pattern that would resemble the *DmRootletin* expression at any timepoint in the embryonic development. This suggests that the putative TF binding sites present within the sequence A are not responsible for driving the *DmRootletin* expression. This is in line with the conservation analysis shown in sections 12.3 and 12.4.

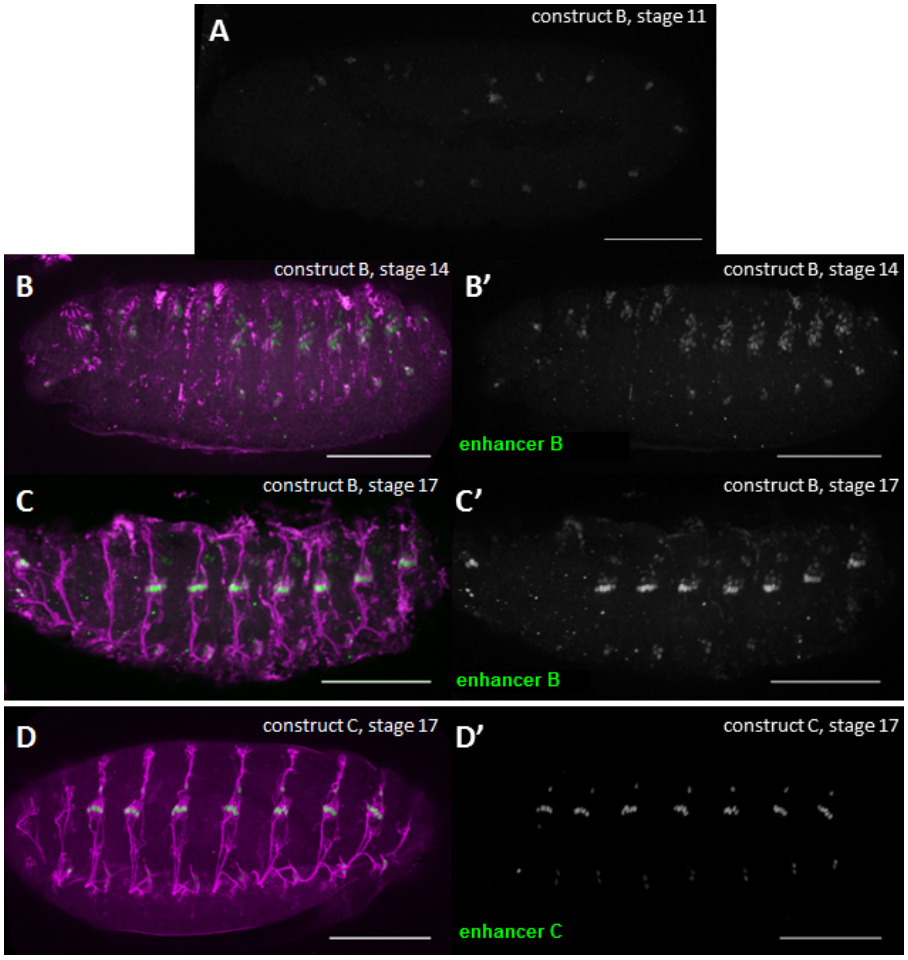

Figure 3.9. Enhancer - reporter gene expression patterns shown by a dual antibody staining - anti - β-gal in green and anti-Futsh (monoclonal 22C10 antibody) in magenta. A - construct B expression pattern in stage 11 embryo, B - construct B expression pattern in stage 14 embryo counterstained with the 22C10 antibody showing the PNS neurons, B' - the same as in B but a separated green channel, C - construct B expression pattern in stage 17 embryo counterstained with the 22C10 antibody showing the PNS neurons, C' - the same as in C but a separated green channel, D - construct C expression pattern in stage 14 embryo counterstained with the 22C10 antibody showing the PNS neurons, D' - the same as in C but a separated green channel. Scale bars represent 100um.

The fragment B gives a chordotonal specific expression pattern. The staining is visible from the stage 11 of embryonic development and is present in the SOPs which give rise to the cells of the chordotonal organ lineage (Fig 3.9 A). As the embryonic development progresses enhancer B drives the β-gal expression in all the

chordotonal organ lineage cells through stage 14 to the late stage 17 (Fig 3.9 B-C'). In the late stage 17 the β-gal expression is highest in the chordotonal organ neurons and lower expression is also visible in the support cells (Fig 3.9 C and C'). The reporter expression pattern suggests that the TFs putative binding sites present in the enhancer B are responsible for driving part of the *DmRootletin* expression in early to late stages of development. It is possible that the weak expression of the reporter gene in non-neuronal cells of chordotonal lineage is due to perdurance of the β-Gal protein from the SOP stage. The protein expressed early possibly perdures in all cells that arise from the SOP cell.

The fragment C gives a very specific chordotonal pattern of expression (Fig 3.9 D and D'). The β-gal is present at high levels only in chordotonal organ neurons in stage 17 embryos. No staining is visible in other Cho cells in the late development. Also no β-gal staining earlier than stage 16 is visible. This result suggests that the TFs putative binding sites present in the enhancer C are responsible for driving DmRootletin expression in very late stages of embryonic development and very specifically in the Cho neurons.

In summary the enhancer sequences B and C can be deemed responsible for driving *DmRootletin* expression in the chordotonal neuronal lineage throughout the embryonic development. However none of the examined enhancers is active in the external sensory neurons lineage. This means that some enhancer region must be present in the sequence regions that were not included in the enhancer-reporter gene constructs and that these enhancers are expected to drive expression in the external sensory neuronal lineage.

12.8 Expression of enhancer-reporter gene constructs on *fd3F* and *RFX* mutant background

The enhancer reporter lines B and C have been crossed into *RFX* and *fd3F* mutant background in order to test which transcription factor is necessary to drive the *DmRootletin* expression. Unfortunately it has not been possible to create a double mutant line containing the enhancer - reporter constructs as this would involve a balancer for 1st, 2nd and 3rd chromosome. Two separate crosses have been therefore carried out for each of the enhancer lines to put them on *RFX* and *fd3F* mutant background separately. The expression of the reporter gene has been then examined to test the influence of the lack of a given transcription factor on the *DmRootletin* expression.

The enhancer B - reporter gene expression was severely reduced in the *RFX* mutants (Fig 3.10 A-D). As shown in figure 9C there is some residual β-gal expression visible in the Cho neurons. No expression is visible in the other cells of the chordotonal lineage. This suggests that the RFX transcription factor is involved in *DmRootletin* transcriptional regulation via one of the conserved X-boxes present in the enhancer B.

The expression of the enhancer B - reporter gene in the *fd3F* mutant background was not affected (Fig 3.10 E-J). The β-gal antibody staining was clearly visible at the same levels in both the WT control and the *fd3F* mutant embryos at all developmental stages.

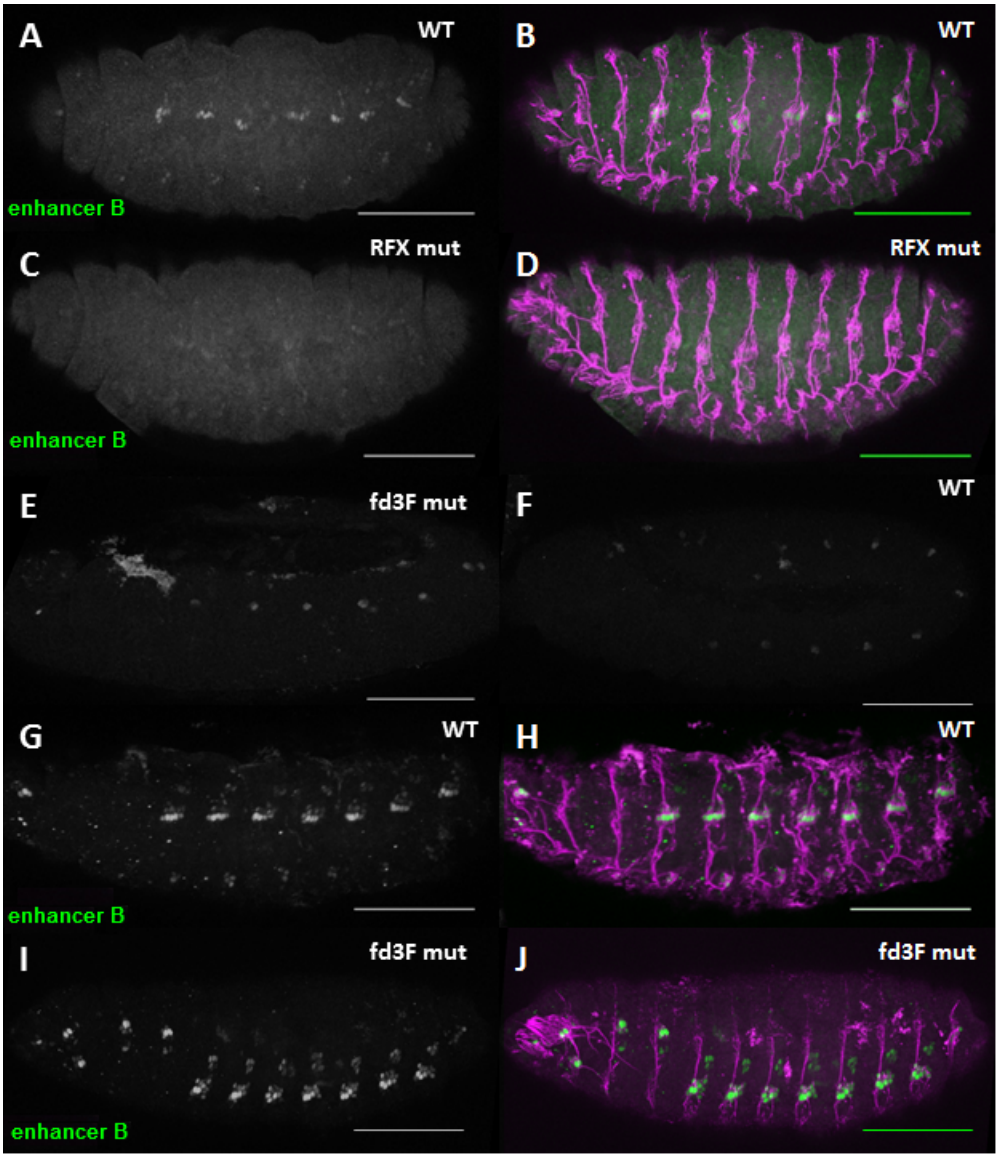

Figure 3.10. ***DmRootletin*** **enhancer B expression in the** ***RFX*** **and** ***fd3F*** **mutant backgrounds** (22C10 - magenta, β-gal - green). **A** - stage 17 WT enhancer B embryo stained with anti β-gal antibody, expression of the reporter gene visible in the Cho neurons, **B** - as in A but counterstained with 22C10 to visualise the PNS components, **C** - stage 17 RFX mutant enhancer B embryo stained with anti β-gal antibody, expression of the reporter gene is almost completely abolished, **D** - as in C but counterstained with 22C10 to visualise the PNS components, **E** - stage 11 WT enhancer B embryo stained with anti β-gal antibody, expression in Cho SOPs visible, **F** - stage 11 fd3F mutant enhancer B embryo stained with anti β-gal antibody, expression in Cho SOPs remains unchanged, **G** - stage 17 WT enhancer B embryo, green channel separated, expression in Cho visible, **H** - stage 17 WT enhancer B embryo, **I** - stage 17 fd3F mutant enhancer B embryo, green channel separated, expression in Cho not affected, **J** - stage 17 fd3F mutant enhancer B embryo. Scale bars represent 100um.

The expression of the enhancer C in the *fd3F* mutant background was severely affected (Fig 3.11 C and D). The β-gal staining was almost completely gone from the chordotonal neurons. This suggests that fd3F could contribute to the *DmRootletin* late expression via this enhancer. It can also be concluded that fd3F transcription factor binds to one of the well conserved forkhead binding sites present in the enhancer C sequence to drive the *DmRootletin* expression. The same goes for the DmRootletin expression in the RFX mutant background - the reporter gene expression was almost completely gone. This suggests that the late CG6120 expression is regulated by both RFX and fd3F transcription factors.

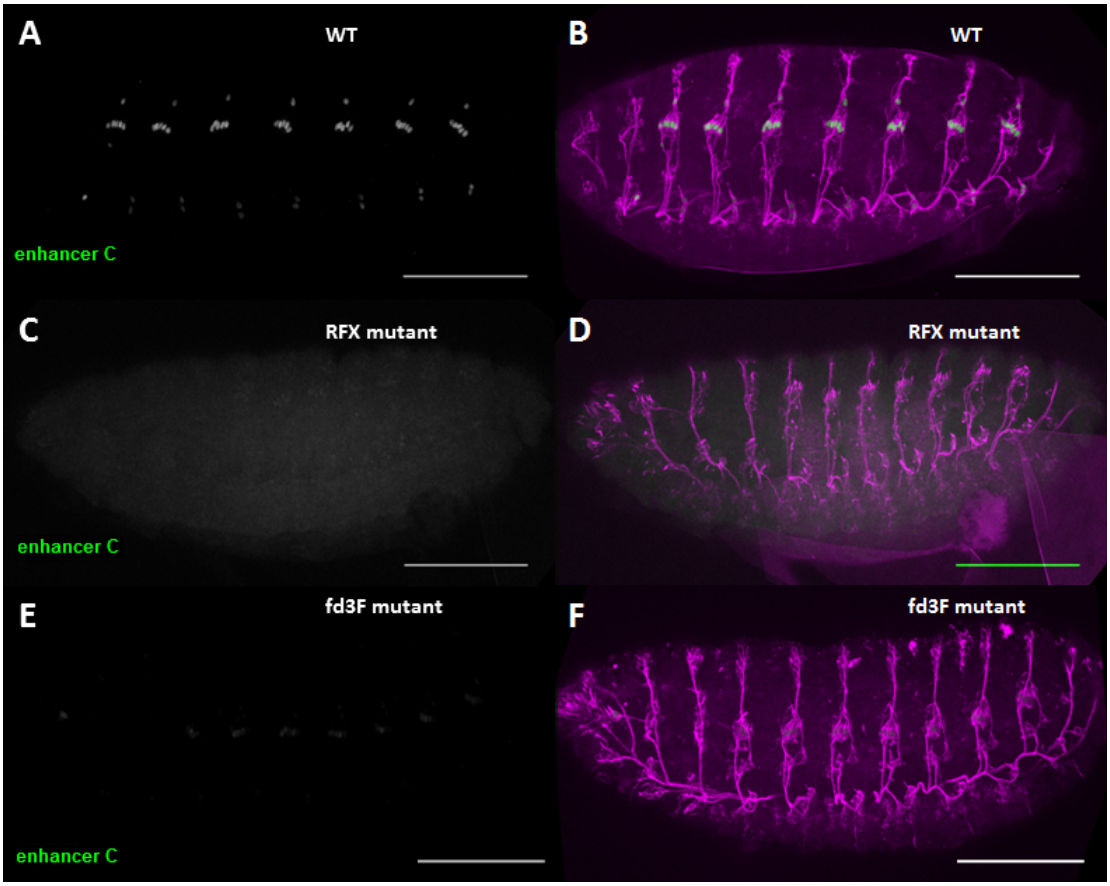

Figure 3.11. *DmRootletin* enhancer C expression in the *RFX* and *fd3F* mutant backgrounds (22C10 - magenta, β-gal - green. **A** - stage 17 WT enhancer C embryo stained with anti β-gal antibody, high expression of the reporter gene clearly visible in the Cho neurons, **B** - as in A, counterstained with 22C10, **C** - stage 17 RFX mutant enhancer C embryo stained with anti β-gal antibody, reporter gene expression in the Cho neurons in almost completely abolished, **D** - as in E, counterstained with 22C10. **E** - stage 17 fd3F mutant enhancer C embryo stained with anti β-gal antibody, reporter gene expression in the Cho neurons is almost completely abolished, **F** - as in E, counterstained with 22C10. Scale bars represent 100um.

The time frame in which the particular transcription factor has an effect on the enhancers reflects the RFX and fd3F overexpression data presented in the section 12.5 and Figure 3.7. In both cases RFX has an effect in the early to late stages of development while fd3F seems to only be actively regulating *DmRootletin* in the latest stages of development.

12.9 Zmynd10 - a potential coregulator of *DmRootletin*

Apart from atonal, RFX and fd3F transcription factors no other chordotonal specific transcriptional regulators are known. However, judging from the data presented above at least some *DmRootletin* expression is independent of RFX and fd3F. There is therefore a need to examine other genes that could possibly be involved in cilia genes regulation. One such gene is the *Drosophila Zmynd10* orthologue which has recently been described (see introduction). Through the LxxLL motifs present in its amino acid sequence it has a potential to transcriptionally regulate ciliary genes and therefore it is also possible that it might regulate the *DmRootletin* expression. In order to test this I have performed *DmRootletin* RNA in situ hybridisation on *Zmynd10* mutant embryos. The *Zmynd10* mutant line segregates a balancer (GFP containing) because homozygous males are infertile. The homozygous mutant embryos for the below experiments have therefore been hand-selected against the GFP expression under the bioluminescence microscope.

The expression of *DmRootletin* in *Zmynd10* mutant embryos does not entirely disappear. The *DmRootletin* expression level is the highest in the stage 17 embryonic Cho neurons. The embryos of this stage have therefore been examined in order to provide the best chance to evaluate any decrease in the *DmRootletin* expression. The DmRootletin staining in the wild type embryos show a strong and characteristic chordotonal pattern (see Fig. 3.12 A). Strikingly the *DmRootletin* expression in the *Zmynd10* mutant embryos seems quite strongly reduced. Some expression is still visible but in overall the levels of *DmRootletin* transcript are visibly lower (see Fig. 3.12 B) (n=15).

The above result has been confirmed with the PCR carried out on cDNA obtained from hand selected stage 17 *Zmynd10* mutant embryos. The WT cDNA produced a

strong 98bp band while the *Zmynd10* mutant cDNA band was very weak (see Fig. 3.12 C lanes 1 and 2). The amount of template for the PCR has been controlled by determining the RNA concentration used in the reverse transcription reaction step. In addition to that primers for a ubiquitously expressed and Zmynd10 independent gene *tbp* have been used, to show that the same amount of template was used for both WT and Zmynd10 PCR reactions (see Fig. 3.12 C, lanes 3 and 4).

The results suggest that *DmRootletin* expression is controlled by Zmynd10. It is however unclear whether this control is direct or indirect. The obtained result does not answer the question whether the Zmynd10 regulation of *DmRootletin* expression is transcriptional or post-transciptional.

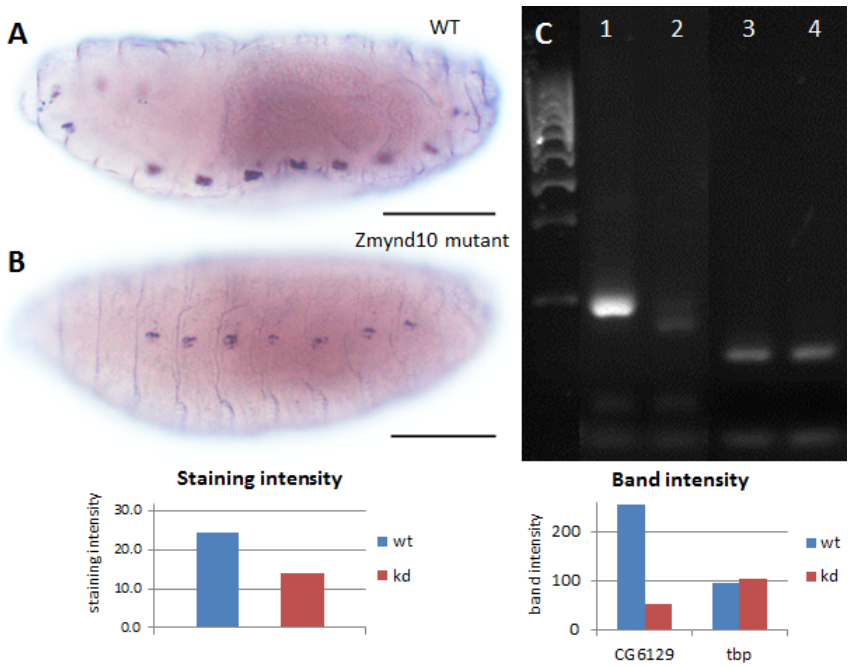

Figure 3.12. Expression of *DmRootletin* in *Zmynd10* mutant embryos. **A -** DmRootletin RNA in situ hybridisation on a WT stage 17 embryo, high levels of the DmRootletin transcript visible in the Cho neurons, **B** - DmRootletin RNA in situ hybridisation on a Zmynd10 homozygous mutant stage 17 embryo, clear reduction in the DmRootletin transcript level, staining intensity chart, n=7; **C** - RT-PCR performed on Zmynd10 mutant embryos, lane 1 - DmRootletin product (size) obtained from WT cDNA, lane 2 - DmRootletin product obtained from Zmynd10 mutant cDNA, lane 3 - tbp control, WT cDNA, lane 4 - tbp control, Zmynd10 mutant cDNA. Band intensity chart, n=3.

13 Discussion

The results presented in this chapter help elucidate the regulation of some aspects of *DmRootletin* expression. Namely the expression of *DmRootletin* in chordotonal lineage seems to depend on three regulators: RFX (previously shown by Laurencon et al, 2007), fd3F (contrary to what previously seen, Newton FG, unpublished), and Zmynd10 (not clear whether transcriptional or post-transcriptional control). The regulation of *DmRootletin* expression in the ES cells seems to be more complicated. Given the transcription factors' expression profiles and the previous reports (Laurencon et al, 2007) the RFX would be the factor that should drive the *DmRootletin* expression in ES cells. However the data presented in this chapter, suggest that at least part of the *DmRootletin* expression in ES cells is RFX independent. This would imply the existence of an unknown factor in the sensory cilia regulatory network in *Drosophila*. In general the chordotonal-enriched pattern of *DmRootletin* expression cannot be fully explained with the previously reported RFX-fd3F cooperation (Newton et al, 2012) due to remaining ES expression of unknown dependance.

Regulator	**Chordotonal cells**	**ES cells**
RFX	early to late expression via enhancers B and C	partially dependent on RFX but not entirely (Fig 6DEF)
fd3F	late expression via enhancer C	fd3F not expressed here
Zmynd10	transcriptional or post-transciptional regulation	Zmynd10 not expressed here
X?		unknown TF?

Table 1. *DmRootletin* expression dependance on various regulators.

13.1 Lack of enhancer - reporter expression in ES cells

As shown in the previous chapter *DmRootletin* is expressed in a so-called 'chordotonal-enriched' pattern. The highest levels of *DmRootletin* mRNA are seen in the chordotonal neurons right from the SOP stage to the very end of the embryonic development and lower levels are transiently observed in the ES neurons. These high levels of expression in the chordotonal cells are driven by two enhancers shown in this chapter. However none of the located enhancers is responsible for driving *DmRootletin* expression in the ES cells. Although the enhancer sequences have been chosen based on the high conservation across various *Drosophila* species it is possible that some of the omitted transcription factor binding sites can drive the ES cells expression. The most probable candidate would be one of the X-boxes given that RFX is a pan-sensory regulator and therefore the only known *DmRootletin* regulator which expression pattern covers the ES neurons. There is only one X-box that has not been included in any of the enahncer constructs. It only appears on the GenePalette graph when the software is allowed to show sites that have one mismatch within the given consensus sequence. Indeed the mismatched X-box has an adenine at the second position of the consensus sequence where either cytosine or thymine should be (see Figure 3.13 A, highlighted in orange). Moreover the 5' half of this X-box is highly degenerate but the 3' half is highly conserved and faithful to the consensus sequence. It has been reported that X-boxes presenting a similar pattern can actively interact with RFX in combination with fd3F (Newton et al, 2012) but all those X-boxes match the consensus sequence in full. It is therefore not likely that the mismatched X-box is responsible for the *DmRootletin* expression in ES cells.

It is also possible that the enhancer fragment B does not contain a full enhancer. The chosen sequence fragment incorporated in the enhancer-reporter gene construct B may have missed part of the actual enhancer that could be necessary for driving

DmRootletin expression in ES cells.

Another possibility is that there might be an unknown transcription factor that is expressed in ES neurons and that possibly drives *DmRootletin* expression in those cells. Indeed a fd3F like factor (CG32006) was recently annotated (Andrew Jarman, personal communication). It is enriched in *Drosophila* ciliated cells (Cachero et al, 2011) and its expression pattern includes the external sensory cells (Petra zur Lage, unpublished data). The CG32006 protein has the forkhead domain characteristic of the Fox family transcription factors but a detailed analysis has to be carried out to establish whether it is an active transcription factor.

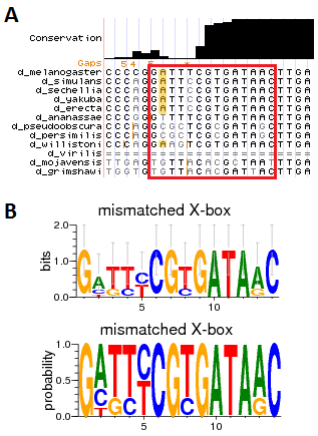

Figure 3.13. Mismatched X-box present in the omitted *DmRootletin* cis-regulatory sequence. **A -** multiple sequence alignment of the small part of DmRootletin upstream region in 12 *Drosophila* species, the mismatched X-box is shown in the red rectangle. The highlighted adenins are a mismatch from the X-box consensus sequence, **B** - sequence logos of the mismatched X-box showing that a degenerate 5' half and a stronger, more conserved 3' half (obtained from http://weblogo.threeplusone.com online software).

13.2 Does *DmRootletin* possess a shadow enhancer?

Apart from the primary enhancers a distinct category of regulatory elements has recently been named - the shadow enhancers. A shadow enhancer has two characteristics - it drives the same expression pattern as the primary enhancer, and it binds

the same transcription factors as the primary enhancer (Barolo, 2012). Shadow enhancers seem to be redundant with other regulatory sequences and some of them are not active in most conditions. Three possible functions of the existence of the shadow enhancers have so far been proposed. Shadow enhancers have been shown to confer a robust expression of a gene in a variety of conditions of environmental instability like higher temperature (Perry et al., 2010). Some shadow enahncers have an important role in the precise expression pattern of a gene (Perry et al., 2011). Another role of the existence of shadow enhancers could be creating evolutionary variety through slightly diverging the expression pattern of a gene (Barolo, 2012).

DmRootletin has at least two enhancers which are overlapping in terms of the spatial expression. Both of those enhancers contain an analogous pattern of putative transcription factor binding sites that are likely to be active due to their high conservation. It can be hypothesised that one of the examined enhancers is a shadow enhancer that supports the primary enhancer activity in certain environmental circumstances. Based on the conservation pattern of the transcription factor binding sites and the position in relation to the *DmRootletin* translation start site it could be possible that the enhancer C was evolutionarily first (X-box 2 is completely conserved in 11 *Drosophila* species). The *DmRootletin* could initially be driven by both RFX and fd3F via the enhancer C only. As a means of environmental adaptation in the course of evolution some additional *DmRootletin* expression might have been added by activation of another enhancer (enhancer B). In that terms the enhancer B could be a shadow enhancer that provides robustness of *DmRootletin* expression. Another possibility is that both enahncers (B and C) are necessary to drive a sufficient level of *DmRootletin* expression in the chordotonal cells to support the chordotonal cilium. In such case neither of the enhancers would be a shadow enhancer because the function of both of them would be indispensable.

13.3 Cooperation of RFX and fd3F

RFX and fd3F transcription factors have been shown to cooperate in regulation of some chordotonal specific and chordotonal enriched gene targets (Newton et al, 2012). *DmRootletin* seems to fall into that category although it is neither motility nor compartmentalisation gene. The two active enhancers of *DmRootletin* have highly conserved tandems of Fox-motifs and X-boxes and one of the enhancers does indeed seem to need both RFX and fd3F to activate the optimal expression of the target gene (enhancer C). A model of *DmRootletin* transcriptional regulation can be proposed in which RFX regulates the expression across all type I sensory neurons (chordotonal and external sensory neurons, although no such enhancer found during my project) and the RFX/fd3F transcription factors tandem cooperates to provide sufficient *DmRootletin* expression for chordotonal organs specifically. A similar model of RFX/fd3F cooperation has already been suggested by Newton et al (2012). Interestingly such model is valid for the target genes that are necessary for cilia motility. The fact that *DmRootletin* could be transcriptionally controlled in a similar manner as cilia motility genes suggests that *DmRootletin* function may have a role in ciliary motility as well. Otherwise it is also possible that fd3F does not only regulate ciliary motility genes. All in all in the light of the data shown in this chapter the previous reports on the cilia diversity regulation seem quite simplistic. The line dividing genes dependance on fd3F and RFX might be more blurred and there also might be more factors involved in cilia specification.

13.4 Zmynd10 as a potential transcriptional regulator

Zmynd10 has previously been shown to be necessary for motile cilia formation and function (Moore et al, 2013). It is likely that Zmynd10 is a component of dynein

assembly complex. But another function of Zmynd10 has also been proposed. Based on a presence of a highly conserved LxxLL protein motifs Zmynd10 has been suggested to have a role in transcriptional regulation (Zariwala et al, 2013). However, there is very little evidence supporting that possibility (Zariwala et al, 2013). The data presented in this work suggest that expression of a ciliary gene is reduced in *Zmynd10* mutant. *DmRootletin* mRNA levels are significantly lower in *Zmynd10* mutants than in the wild type control and this result was consistently prevalent in both RNA in situ hybridisation and reverse transcription followed by a PCR. These results can be interpreted in two ways. One possibility is that Zmynd10 is involved in transcriptional regulation of some ciliary genes. Another possibility that has to be taken into consideration is that Zmynd10 can influence the transcript stability of the target genes. The visibly lower levels of *DmRootletin* and *fd3F* in both RT-PCR and the in situ hybridisation could be caused by a stronger mRNA degradation in the lack of Zmynd10.

The results presented in this chapter do not allow to say definitely that Zmynd10 transcriptionally regulates *DmRootletin* but one interesting conclusion can be drawn. The fact that a ciliary motility specific gene - *Zmynd10* - is involved in *DmRootletin* regulation serves as another clue (next to possible RFX-fd3F cooperation in regulation) suggesting that DmRootletin might have a role in motility of cilia.

13.5 General conclusions

The results presented in this chapter show in the *DmRootletin* example that ciliary diversity in *Drosophila* is transcriptionally regulated by a network of transcription factors. Various ciliated tissue subtypes (chordotonal cells and external sensory cells) are controlled in a different manner. Based on the presence of conserved TF binding site tandems and changes of reporter gene expression in RFX and fd3F mutant

backgrounds it likely that optimal *DmRootletin* expression in chordotonal neurons is dependent on cooperation of both RFX and fd3F, although more experiments should be done in order to confirm direct involvement of those TFs. Either way it seems that RFX/fd3F cooperation is not limited to the ciliary motility/compartmentalisation genes as the *DmRootletin* does not typically conform to those categories.

Although the data presented in this chapter need to be confirmed, they suggest that some *DmRootletin* expression in ES cells is not RFX dependent. This implies that there might be another previously uncharacterised transcription factor that plays a role in ciliary transcription regulation network in *Drosophila*. A likely candidate is an uncharacterised fd3F-like factor (CG32006).

A novel role for the ciliary motility gene *Zmynd10* has been suggested here as has been suggested in other published data. *DmRootletin* is a first gene for which there is experimental evidence suggesting Zmynd10 dependent transcriptional regulation. It is unclear how does Zmynd10 could perform its role but is seems likely it acts as a coregulator for other transcription factors. Whether those factors would be RFX, fd3F or some other unknown TFs it remains to be elucidated.

In general *DmRootletin* serves as a good example of just how complicated the ciliary genes transcriptional regulation is in *Drosophila*. The fact that there are at least two putative novel factors (Zmynd10, CG32006) provides an insight into how much is still unknown about differential ciliary specialisation.

Part IV

Zmynd10 as a transcriptional regulator

14 Introduction

The data presented in the previous chapter suggest that Zmynd10 might have a role in regulation of a chordotonal-enriched gene *DmRootletin*. If confirmed, this would imply that Zmynd10 might act as yet another factor that mediates the differential cilia specialisation in *Drosophila*. It remains unclear whether the possible regulatory action takes place on the transcription level or later.

14.1 Zmynd10 in human and other species

Zmynd10 is a zinc-finger MYND domain containing protein. MYND-zinc finger type domain (myeloid, nervy, DEAF-1) (Gross and McGinnis, 1996) is a conserved domain present in a large group of proteins in many evolutionary divergent species. It consists of clusters of cysteine and histidine residues forming a potential zinc-binding motif. Although zinc-finger domains are known to bind DNA the MYND type is more known to be involved in protein-protein interactions. It has been shown to interact with other proteins and function as an indirect transcriptional co-repressor (Lutterbach et al., 1998; Melnick et al., 2000).

Zmynd10 (also known as *BLU*) was initially known as a tumor suppressor gene (Zhang et al., 2012; Park et al., 2013). It has been shown to inhibit carcinoma

cell growth via down regulating JNK and cyclin D1 activities through blocking the cyclin D1 promoter and blocking the c-Jun phosphorylation (Zhang et al, 1012). Interestingly based on Luciferase assay data it can be inferred that Zmynd10/BLU can interact with DNA. It has been proposed that this interaction could be mediated by the MYND domain (Zhang et al, 2012).

Zmynd10 has also been shown to be highly enriched in tissues exhibiting motile cilia. In mature human airway epithelial cells its expression is 14 times higher that in non differentiated/non-ciliated cells (Ross et al., 2007). Taking this into consideration, and the fact that *Zmynd10* appeared on a list of 208 putative PCD genes (Geremek et al., 2011) suggested that Zmynd10 is involved in cilia motility. It is also present in the Cildb ciliome database (Arnaiz et al., 2009).

The *Zmynd10* gene is conserved from human to *Drosophila melanogaster*. *Drosophila Zmynd10* (*CG11253*) has been identified as a ciliary specific gene by the transcriptome analysis performed on ciliated cells (Cachero et al, 2011). The expression of *Drosophila* ZMYND10 orthologue gene (*CG11253*) is specific and very high in ciliated chordotonal neurons (Cachero et al, 2011). This has also been confirmed by whole embryos RNA in situ hybridisation (Newton et al, 2012). In the study by Moore et al (2013) a CG11253-mVenus fusion protein line has been created to further investigate the localisation of the *Drosophila Zmynd10* protein. The Zmynd10-mVenus expression was consistently specific to all *Drosophila* cells bearing motile cilia - embryonic chordotonal neurons, pupal Johnston's organs neurons (Moore et al, 2013). As shown on the FlyBase the *Zmynd10* is also very highly expressed in adult testes (sperm cells have motile flagella). Another argument supporting the Zmynd10 involvement in cilia motility is its transcriptional regulation. *Zmynd10* expression is dependent on RFX ((Dubruille et al., 2002) and fd3F (Newton et al, 2011), and as shown in Newton et al (2011) the cooperation of these two transcrip-

tion factors seems to be a specific regulatory model that is true for genes involved in ciliary motility. Furthermore *Drosophila Zmynd10* mutant (P-element insertion) flies exhibit a phenotype that is characteristic to motile cilia disruption - uncoordination (Moore et al, 2013), deafness (Senthilan et al., 2012), and male infertility (Moore et al, 2013). When examined by TEM both chordotonal cilia and sperm flagella of the *Zmynd10* mutant show reduced numbers of inner and outer dynein arms (IDAs and ODAs). In addition to this the *Zmynd10* mutant sperm flagella also show axoneme splitting that suggests the central apparatus/radial spokes disruption (Moore et al, 2013).

To summarise, in all species *Zmynd10* has been examined, it seems to have a strong connection with ciliary motility.

14.2 PCD genes required for dynein arms/ciliary motility

Primary ciliary dyskinesia is a ciliopathy disease characterised by situs inversus, chronic sinusitis, otitis media, recurrent respiratory infections, bronchiectasis, and male and female infertility. Mutations in at least 19 genes have been linked to PCD (Horani et al, 2014). These genes include structural components of the ciliary outer dynein arms (*DNAH5, DNAI1, DNAL1, DNAI2, TXNDC3* and *DNAH11*), inner dynein arms (*CCDC39, CCDC40, CCDC164*), and central apparatus and radial spokes (*RSPH9, RSPH4A*, and *HYDIN*) (Horani et al, 2014). Interestingly an emerging separate category of non-ciliary genes is now also being linked to PCD. The examples of such genes are *LRRC6* (Kott et al., 2012) and *HEATR2* (Horani et al., 2012; Diggle et al., 2014).

The *LRRC6* (Leucin Rich Repeat Containing 6) has been shown to be expressed in flagella of *C. reinhardtii* (Li et al., 2004) as well as in human and mouse tissues bear-

ing motile cilia (McClintock et al., 2008). In the null allele of *Drosophila* orthologue - *tilB* (touch insensitive larva B) the flies exhibit all the characteristics of motile cilia impairment - uncoordination, deafness and male infertility (Kavlie et al., 2010). Human (Kott et al, 2012) as well as *Drosophila* (Kavlie et al., 2010) LRRC6 localises to the cytoplasm and axonemes. PCD patients in whom an *LRRC6* mutation has been identified exhibit the IDAs and ODAs loss from their nasal epithelium cilia and sperm flagella as well (Kott et al, 2012). Interestingly the LRRC6 possesses an α-crystallin-like protein domain that is characteristic for HSPB proteins that can act as chaperones (Vos et al., 2008). Based on the subcellular localisation , loss of IDAs and ODAs, and the presence of a domain associated with protein-folding assistance the LRRC6 has been suggested to act as a dynein arm assembly factor (Kott et al, 2012). Indeed the protein structure of LRRC6 bear many similarities to the known dynein assembly factor - DNAAF1.

The HEATR2 is a member of a family of HEAT repeat-containing protein. Interestingly none of the other members of this family have been linked to cilia (Horani et al., 2012). *HEATR2* is a highly conserved gene enriched in organisms with motile cilia (Horani et al, 2012). Interestingly mutation in the *HEATR2* has been found in PCD patients. The nasal epithelial cilia of those individuals are virtually immotile. In the cultured ciliated cells obtained from the PCD affected patients the DNAI1 (ODA component) do not assemble. This was not true for the IDA component - DNAH7. Based on above findings and on the fact that the HEATR2 protein localises to the cytoplasm but not the cilium, Horani et al suggest that HEATR2 might act as a dynein arm assembly factor (DNAAF) or have a role in transporting the ciliary proteins to the basal body. Another *HEATR2* mutation has more recently been found in PCD patients (Diggle et al., 2014). This study reveals a defect in both ODAs and IDAs in the *HEATR2* mutant *Drosophila* and in tissue obtained form the PCD

individuals. Based on the interaction between HEATR2 and DNAI2 shown in the co-immunoprecipitation analysis Diggle et al confirm that HEATR2 acts as a dynein arms assembly factor.

After initial indications from the expression profiles that *Zmynd10* might be a PCD causative gene (among many other genes, Geremek et al., 2011) two groups have reported *ZMYND10* mutations in PCD patients (Moore et al, 2013, and Zariwala et al, 2013). ZMYND10 biallelic mutation has been identified in three out of 11 (Moore et al, 2013) and 14 out of 300 (Zariwala et al, 2013) affected families. Some data shown in these two studies suggest that *Zmynd10* falls into the non-ciliary category of PCD causative genes and that it might be a dynein arm assembly factor.

14.3 Zmynd10 as a dynein arm assembly factor

The dynein arm assembly factors (DNAAFs) are members of a functional group of proteins that are involved in preassembly of axonemal dynein complexes in the cytoplasm before they are loaded to the cilium via IFT. One of the first DNAAFs to be identified was the Ktu/pf13 (Omran et al., 2008) (now also called DNAAF1). In all organisms examined (medaka fish, *C. reinhardtii,* mouse and human) a *Ktu* mutation causes IDA and ODA reduction/loss and loss of ciliary motility. Ktu protein localises to the cytoplasm and not the cilium and interestingly (apart from interaction with DNAI2) interacts with Hsp70 chaperone protein. This prompted Omran et al to suggest that Ktu is a dynein preassembly factor that may act as a co-chaperone to assist in proper dynein folding. Other confirmed DNAAFs are the ODA7 (also known as DNAAF2) (Duquesnoy et al., 2009; Loges et al., 2009) and DNAAF3 (Mitchison et al., 2012). All known DNAAFs fall in the beforementioned PCD causative genes non-ciliary category and are faithful to the following characteristics: they are localised cytoplasmically (low levels possible in the axoneme), the

null alleles lack either of or both IDAs and ODAs, the null alleles loose the ciliary motility.

Zmynd10 is another PCD causing gene that seems to follow the DNAAFs characteristics. Zmynd10-mVenus *Drosophila* fusion protein localises to the cytoplasm and (far less) the axoneme (Moore et al, 2013). Both PCD patients carrying a *ZMYND10* mutation and *Drosophila Zmynd10* mutants show lack or reduction of both IDAs and ODAs (Moore et al, 2013). The loss of ciliary motility is also prevalent in PCD individuals, *Drosophila* (Moore et al, 2013), and zebrafish (Zariwala et al, 2013). Interestingly both Moore et al. and Zariwala et al. show interaction between human ZMYND10 and a known dynein arm assembly factor LRRC6 on the protein level. According to Moore et al. this interaction is dependent on the zinc-finger MYND domain present in Zmynd10. The three DNAAFs characteristics and the interaction with a known DNAAF (LRRC6) strongly suggests that Zmynd10 might itself be involved in the dynein arms assembly.

14.4 Zmynd10 as a putative transcriptional regulator of the dynein arms proteins

Apart from regulating ciliary motility on the protein level Zmynd10 has a potential to regulate transcription of some ciliary genes. This potential is suggested by the fact that another interesting domain is present in Zmynd10 - an LxxLL motif. LxxLL is a signature motif for transcriptional co-activators. LxxLL motifs are very conserved and form a hydrophobic helix pocket in which each of the leucins is indispensable for the protein-protein interactions (Heery et al., 1997; McInerney et al., 1998). Several co-activators of nuclear steroid hormone receptors have been shown to possess more than one LxxLL motif through which they can bind to the nuclear receptors in a

ligand-dependent manner (Heery et al, 1997). Examples of such nuclear receptor and co-activator pairs include RIP140 and oestrogen receptor, SRC-1 and progesterone receptor, CBP/p300 and CREB transcription factor (Heery et al, 1997). The LxxLL dependent interaction can induce either activation or repression of the target gene transcription (Plevin et al, 2005). It is worth noting that one of the *Zmynd10* mutations found in PCD patients was an amino acid substitution of one of the leucines of the LxxLL motif (Moore et al, 2013). This indicates that the LxxLL motif present in Zmynd10 is functional. This in turn allows to hypothesise that Zmynd10 may act as a co-activator for some transcription factors to modulate the expression of ciliary genes. However no direct evidence has so far been found of Zmynd10 involvement in transcriptional regulation of any genes. There is however one piece of evidence suggesting that the human Zmynd10/BLU protein is able to bind DNA (Zhang et al, 2012). This is inferred from a luciferase assay in which BLU binds and blocks the AP1 reporter leading to c-Jun phosphorylation inhibition and modulation of the JNK signaling pathway.

The interaction between Zmynd10 and LRRC6 (Moore et al, 2013, Zariwala et al, 2013) supports the hypothetical Zmynd10 involvement in transcriptional regulation. Horani et al (2013) have shown that expression of two dynein arms components (*DNAI1* and *DNAH7*) is significantly reduced in nasal biopsies of PCD affected patients bearing an LRRC6 mutation. Although this data clearly needs confirmation and further, more direct evidence, it has been suggested that LRRC6 might be involved in transcriptional regulation of dynein arms genes (Horani et al, 2013).

Recently another LRRC6 interaction has been found with Reptin (Zhao et al., 2013). Reptin is an ATPase domain containing protein (Shen et al, 2000) which due to multiple diverse functions (chromatine remodelling (Shen et al., 2000), snoRNA assembly (King et al., 2001), telomere maintenance (Venteicher et al., 2008), and DNA dam-

age response (Jha et al., 2008)) has not been associated with cilia. However in the study by Zhao et al, (2013) *reptin* has been shown to be an essential gene for ciliary motility. Zebrafish *reptin* morphants exhibit cilia associated phenotypes which are caused by ciliary immotility and reduction in IDAs and ODAs. Zhao et al tested whether Reptin can regulate dynein arms genes on transcription level. Strikingly mRNA levels of some dynein arm components as well as all known DNAAFs and FoxJ1 were increased. This implies that loss of ODAs and IDAs is not caused by decreased expression of the relevant genes. Interestingly however the lack of Reptin did have an effect (however contrary to what would be expected) on expression of dynein arm genes.

Taking all of the above into consideration an attractive hypothesis can be put forward in which Zmynd10 is one of the components (together with LRRC6, Reptin and more?) of a protein complex which is involved in transcriptional regulation of dynein arm genes expression. The fact that the human BLU gene (Zmynd10 orthologue) has been shown have the ability to bind DNA (based on luciferase assay results, Zhang et al, 2012) could possibly add to this hypothesis.

14.5 Aims of this chapter

Preliminary data presented in the previous chapter suggest that a ciliary chordotonal enriched gene *DmRootletin* might be regulated by Zmynd10. In the light of the fact that *DmRootletin* is differentially expressed in two different ciliated cell types it would be interesting to know whether Zmynd10 dependent regulation can contribute to the specification of different cilia.

In this chapter the hypothesis of Zmynd10 involvement in transcriptional regulation of ciliary genes will be tested. The mRNA levels of some putative target genes (IDAs

and ODAs) will be tested via RT-PCR and RNA in situ hybridisation. The Zmynd10 influence on the putative target gene enhancer activity will also be tested using the enhancer-reporter gene constructs for selected target genes.

15 Results

15.1 Evaluation of the Zmynd10 RNAi line by climbing assay

Many of the following experiments testing Zmynd10 involvement in transcriptional regulation have been performed using a Zmynd10 RNAi knock-down line. It has been obtained from the KK library of the Bloomington Stock Centre and will hereafter be called a Zmynd10 KK line. Despite the availability of a null Zmynd10 mutant those flies could not be easily used for any experiments on embryos due to heterogenuos embryo population - the mutant males are infertile and the line segregates a balancer. I have therefore turned to a RNAi knock-down to obtain a homogenous embryo population. The efficiency of Zmynd10 knock-down had to be tested before embarking on any further experiments based on reduction/lack of Zmynd10 protein. In order to choose the conditions in which the Zmynd10 RNAi knock-down is the most efficient an evaluation experiment was carried out. The Zmynd10 KK RNAi line was crossed to the following driver lines: sca-Gal4 and UAS-Dcr;sca-Gal4. Three crosses with sca-Gal4 were set up and each of them was kept in different temperature (21^{o}C, 25^{o}C, and 29^{o}C) in order to establish a variety of the RNAi construct levels. The Dcr component of the second driver line used is involved in the RNA interference machinery and is widely used as an addition to enhance the expected knock-down phenotype. The efficiency of the Zmynd10 knock-down in each condition was evaluated by the adult climbing assay (see Fig 4.1) as the Zmynd10 null mutant shows a severe phenotype in this type of behavioural analysis (Moore et al, 2013).

The Zmynd x sca-Gal4 progeny kept in 21^{o}C performed slightly worse than the WT control but the difference was not statistically significant ($p>0.15$). The same goes for the flies form the cross kept in 25^{o}C ($p>0.07$). The Zmynd10 knock-down kept in 29^{o}C performed significantly poorer than that of the control ($p<1.66*10^{-12}$) but

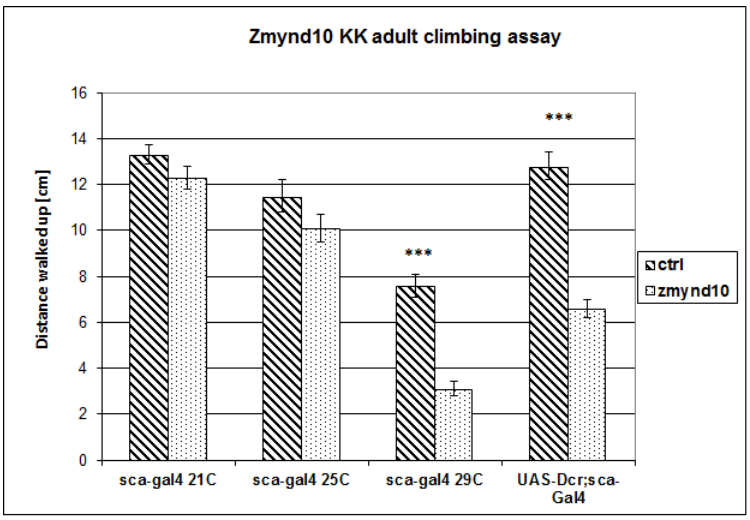

Figure 4.1. Evaluation of the Zmynd10 RNAi knock down efficiency in various conditions. n=45 flies, error bars represent standard error, $p<1.66*10^{-12}$, Student's t-test.

the control also performed poorly which is indicative of the overall poor conditions of flies kept in high temperatures. The best result were obtained when the RNAi construct was driven by the UAS-Dcr;sca-Gal4 driver. The progeny of that cross performed significantly worse ($p<1.19*10^{-13}$) than the control the performance of which was normally high.

In conclusion the Zmynd10 KK x UAS-Dcr2;sca-Gal4 cross has given the most significant result and can be predicted to give the strongest knock-down of the Zmynd10 gene expression. It has therefore been chosen to be used for the experiments presented in the following sections.

15.2 Initial attempts at in situs for IDA and ODA genes on Zmynd10 KK

In order to test whether Zmynd10 could be involved in transcriptional regulation of the inner (IDA) and outer (ODA) dynein arms components, the mRNA levels of examples of inner and outer dynein arms genes on the *Zmynd10* knock-down embryos

has been assessed by *in situ* hybridisation. *Drosophila* inner dynein arms homologues chosen for this experiment were *CG6971* and *Dhc62B*. The outer dynein arms homologues chosen were *CG9313* and *Dhc93AB*. *Dhc62B* and *CG9313* have been shown to be transcriptionally regulated by LRRC6 - a known Zmynd10 interactor (Horani et al, 2012), and *CG6971* has been suggested to be transcriptionally regulated by Zmynd10 in Zariwala et al (2013). Because Zmynd10 is thought to be involved in dynein arm assembly *Dhc93AB* has been chosen as another example of dynein arm component.

In the WT control (UAS-Dcr2;sca-Gal4 driver crossed to w[1118]) embryos all probes produced chordotonal specific pattern of expression (see Fig. 4.2). The levels of mRNA of all the four genes tested in the wild type control seem to be quite low. It is possible that such result reflects actual levels of mRNA needed for production of optimal protein levels for each gene. The other possibility is that the technique was not producing results of expected quality. The expression of the inner and outer dynein arms genes was not visibly reduced in the *Zmynd10* mutant embryos. Very low levels of IDAs and ODAs mRNAs in wild type embryos possibly contributes to the difficulty in seeing any subtle reduction of expression of those genes. The only gene for which some subtle difference between the mRNA levels could be seen was *Dhc93AB* (see Fig. 4.2 A and B).

15.3 RT-PCR of IDAs and ODAs in Zmynd10 knock down

A reverse transcription followed by PCR was performed as a more sensitive and semi quantitative method of testing the dynein gene transcript levels in Zmynd10 knock down. An overnight embryo collection was used to obtain the total RNA. The gene tested were the same set of ODAs and IDAs used in the previous experiment (*Dhc93AB*, *Dhc62B, CG6971, CG9313*). The *fd3F* has been used as an example of

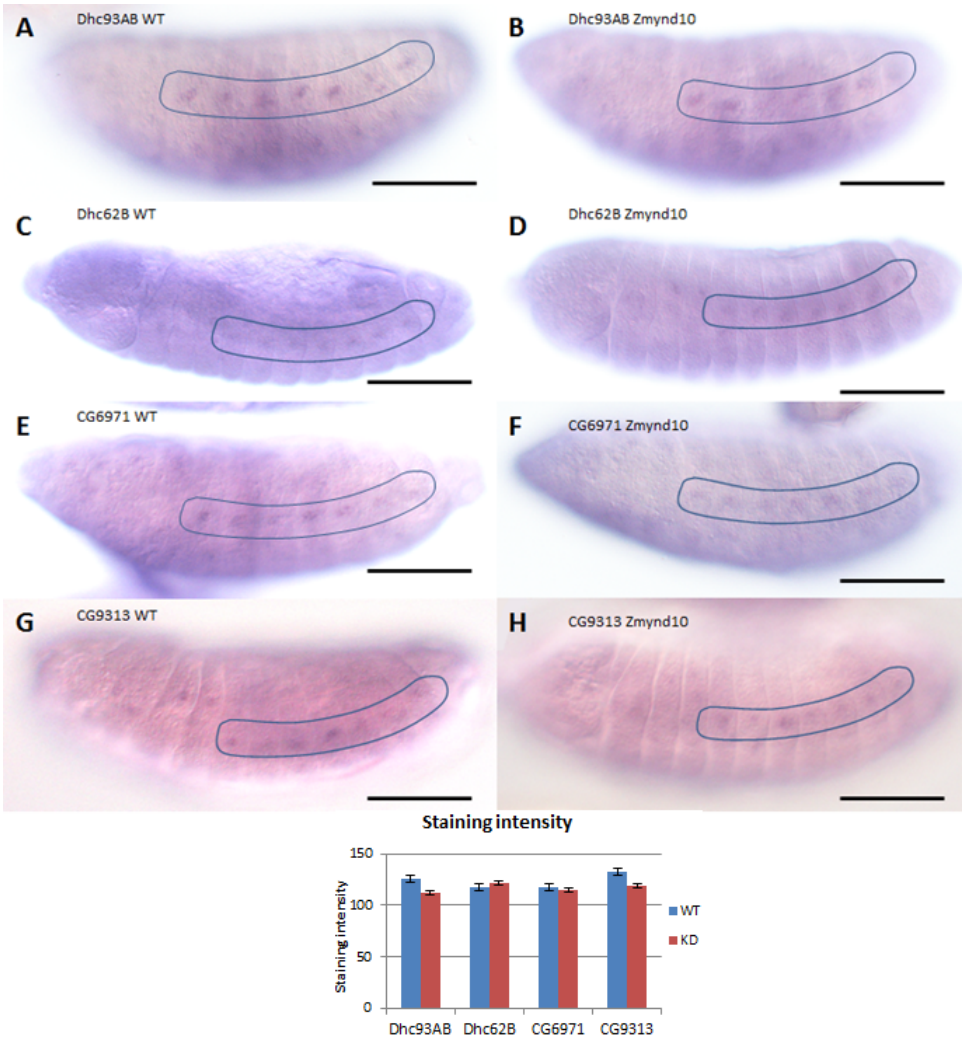

Figure 4.2. RNA *in situ* hybridisation of IDAs and ODAs performed on Zmynd10 knock-down embryos. **A -** *Dhc93AB* WT, **B** - *Dhc93AB Zmynd10* KD, **C** - *Dhc62B* WT, **D -** *Dhc62B Zmynd10* KD, **E -** *CG6971* WT, **F -** *CG6971 Zmynd10* KD, **G** - *CG9313* WT, **H** - *CG9313 Zmynd10* KD. Staining intensity chart, n=6 embryos. Scale bars represent 100um.

a gene whose expression levels are not expected to change in the *Zmynd10* knock down (an fd3F target gene - Newton et al, 2012).

Based on the PCR gel band intensity (measured with the ImageJ software) there was no significant difference in the transcript levels in most of the genes tested except for the *Dhc93AB* (see Fig. 4.3, lanes 1 and 2) and, strikingly, *fd3F* (see Fig. 4.3, lanes 9 and 10) . The *Dhc93AB* reduction appeared on two out of three repeats of the experiment (the other positive result gave a difference in the PCR bands intensity) and the *fd3F* reduction has been consistent in all three repeats.

The results imply that Zmynd10 influences the levels of *Dhc93AB* and *fd3F* transcripts. The fact that *Zmynd10* knock down causes a reduction of *fd3F* mRNA levels is very interesting and suggests the existence of some positive feedback loop in fd3F-Zmynd10 regulation.

15.4 *Dhc93AB* enhancer-reporter gene expression is affected in Zmynd10 KD

Another way to examine whether Zmynd10 could be involved in transcriptional regulation of some ciliary genes enhancer-reporter gene construct can be used. I have used a *Dhc93AB* enhancer-reporter gene construct made by one of the lab members (Fay Newton, unpublished data). The line contains the sca-Gal4 driver component and has been crossed with *Zmynd10* kk RNAi line. The resulting progeny contains the *Dhc93AB* enhancer and is a *Zmynd10* knock down. If Zmynd10 is involved in modulating *Dhc93AB* expression through this enhancer the reporter gene expression would be reduced in Zmynd10 KD.

In the WT *Dhc93AB* enhancer drives the reporter gene expression in chordotonal neurons in from stage 14 onwards. In order to ensure the best conditions for the

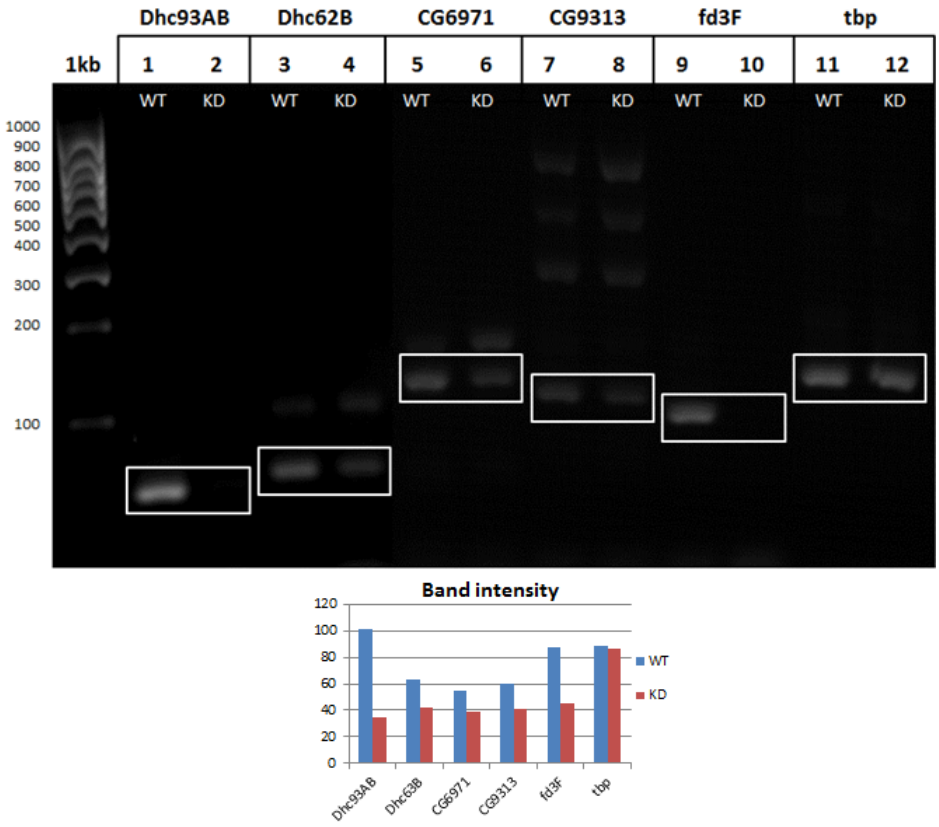

Figure 4.3. ODAs and IDAs RT-PCR performed on Zmynd10 knock down embryos. Lane 1 - *Dhc93AB* WT, **lane 2** - *Dhc93AB Zmynd10* KD, **lane 3** - *Dhc62B* WT, **lane 4** - *Dhc62B Zmynd10* KD, **lane 5** - *CG6971* WT, **lane 6** - *CG6971 Zmynd10* KD, **lane 7** - *CG9313* WT, **lane 8** - *CG9313 Zmynd10* KD, **lane 9** - *fd3F* WT, **lane 10** - *fd3F Zmynd10* KD, **lane 11** - *tbp*, loading control WT, **lane 12** - *tbp*, loading control *Zmynd10* KD. In each lane the bottom band represent the product from the cDNA. Any bigger bands are products from the genomic DNA. Band intensity chart represents average values from 3 experiments.

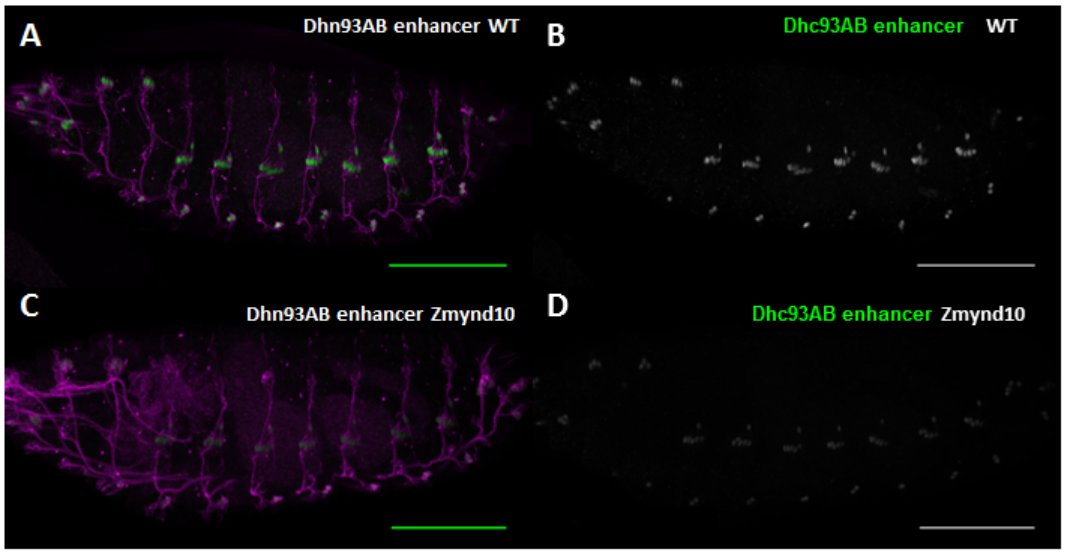

Figure 4.4. *Dhc93AB* enhancer activity in Zmynd10 knock-down. A - *Dhc93AB* enhancer - reporter gene construct expression in WT embryo stained with pan-neuronal 22C10 marker (magenta) and anti-βgal (green). Strong chordotonal specific expression of the reporter gene visible in green, **B** - separated green channel, **C** - *Dhc93AB* enhancer - reporter gene construct expression in Zmynd10 RNAi knock-down embryo stained with the same antibodies, **D** - separated green channel. Scale bars represent 100um.

reporter gene expression level comparison stage 17 has been imaged for both WT and Zmynd10 KK. It is the stage in which the WT *Dhc93AB* enhancer drives the highest levels of the reporter gene expression (see Fig. 4.4, A and B). The reporter gene expression was significantly reduced in the Zmynd10 knock down embryos (see Fig 4.4 C and D). Some expression was still visible but the difference between the wild type control and the Zmynd10 knock-down was quite clear.

This result provides a promising evidence that Zmynd10 could be involved in modulation of *Dhc93AB* expression via its enhancer.

15.5 *Zmynd10* RNAi knock down line is faulty

After the results presented in the previous sections have been obtained the Zmynd10 kk line appeared to have been faulty. Another lab member has not been able to

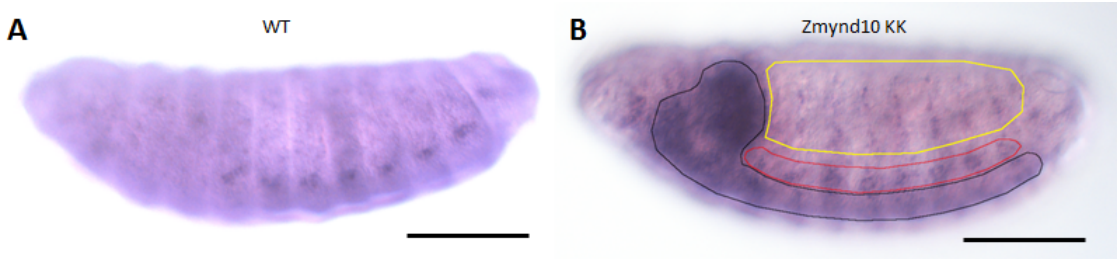

Figure 4.5. *Zmynd10* RNA in situ hybridisation on *Zmynd10* RNAi knock down. A - *Zmynd10* expression in wild type embryo, stage 17, expression specific to chordotonal neurons, **B** - *Zmynd10* expression in *Zmynd10* KK knock down, black line encircles the CNS expression, yellow line indicates the ES cells, and the red line shows the chordotonal neurons expression. Scale bars represent 100um.

reproduce the Zmynd10 KK line climbing assay and fertility assay results that have been done before with a positive result. It is possible that during the project the *Zmynd10* RNAi line has acquired a contamination/mutation. In order to establish whether the Zmynd10 RNAi construct knocks the *Zmynd10* expression down I have performed a RNA in situ hybridisation.

Strikingly the *Zmynd10* expression in Zmynd10 KK RNAi line appears not to be knocked down very efficiently. What is even more interesting the Zmynd10 probe produces staining in the ES cells (see Fig 4.5 B encircled in yellow) and also in the CNS (see Fig 4.5 B encircled in black line). The CNS and whole PNS staining is the expression pattern of the *scabrous* gene whose regulatory region was used in the driver line. What possibly happened is that the RNAi construct was not entirely auto complementary and instead of forming a hairpin was expressed as a single RNA strand. Such faulty RNAi construct could have bound the probe and produce *scabrous* pattern staining. It remains unclear as to when did the Zmynd10 KK line develop this fault. In the initial climbing assay experiment the line exhibited a clear and specific phenotype. Unfortunately due to inability to establish the exact time the Zmynd10 KK line developed the fault all the experiments performed with the use of the line have to be otherwise confirmed.

15.6 *Zmynd10* mutant, evaluation of the mRNA levels

Due to the fault of the *Zmynd10* KK line I have turned to the *Zmynd10* mutant line. In order to repeat some of the previous experiments on *Zmynd10* mutant the RNA in situ hybridisation has been carried out to ensure that the flies lack the *Zmynd10* expression. The *Zmynd10* mutant line ($\text{Zmynd10}^{\text{EY10866}}$) is a loss of function P element insertion. Although the P-element is inserted in the regulatory region of *Zmynd10* is effectively a null mutant (Moore et al, 2013). The disadvantage of this line for some experiments is that homozygous males are infertile. This means that the line produces a heterogenous population of embryos.

As previously shown *Zmynd10* is expressed from stage 11 to stage 17 of embryonic development. In stage 11 *Zmynd10* mRNA localises to the SOPs giving rise to the chordotonal lineage. The strongest *Zmynd10* expression is seen in the stage 14 in all chordotonal organs. This expression almost disappears through the later stages of embryonic development and only residual mRNA is seen in the chordotonal organ neurons in the stage 17. In the $\text{Zmynd10}^{\text{EY10866}}$allele the *Zmynd10* expression is completely lost in all developmental stages. This effectively confirms that $\text{Zmynd10}^{\text{EY10866}}$in a RNA null allele.

15.7 RT-PCR of IDAs and ODAs in $\textit{Zmynd10}^{\textit{EY10866}}$mutant

The $\textit{Zmynd}^{\textit{10EY10866}}$is viable but homozygous males are infertile so the line is kept over the TM3 balancer. This means that even when the homozygous females are selected and crossed to the fertile heterozygous males only half of the resulting progeny would be homozygous *Zmynd10* null. In order to obtain a homogeneous population of embryos for the RT-PCR experiment I have substituted the TM3 balancer with TM3, KrGFP balancer. The KrGFP is visible in embryos and the *Zmynd10* mutant

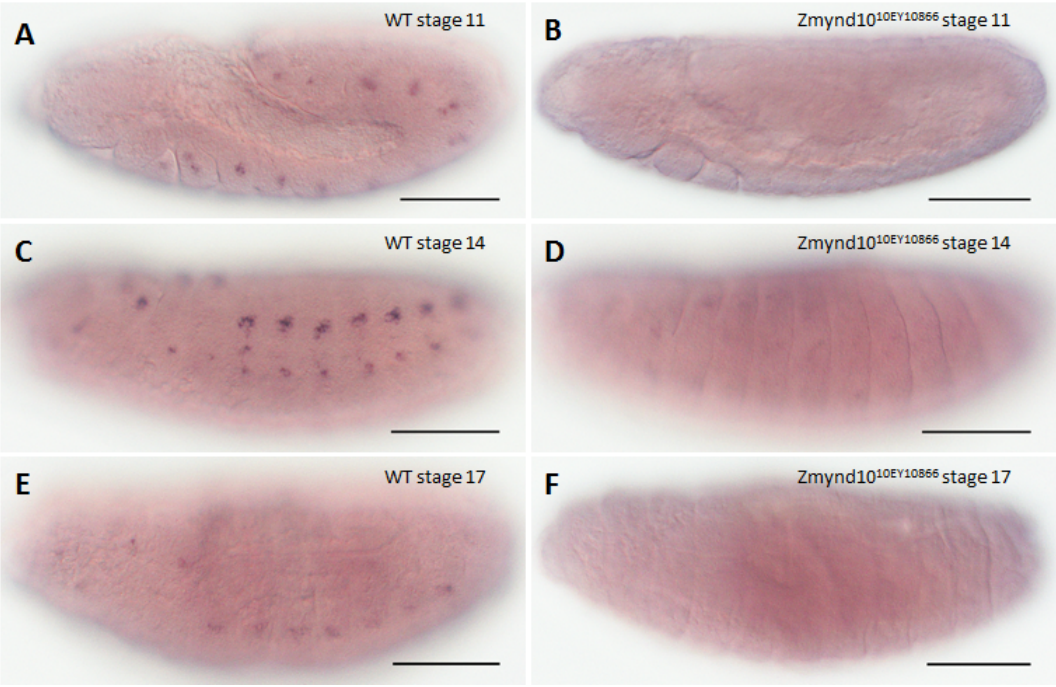

Figure 4.6. Evaluation of *Zmynd10* transcript levels in the *Zmynd10*^{EY10866} mutant allele by RNA in situ hybridisation. A - *Zmynd10* transcript localisation is a stage 11 WT embryo, **B** - stage 11 *Zmynd10*^{EY10866}embryo, **C** - stage 14 WT embryo, **D** - stage 14 *Zmynd10*^{EY10866}embryo, **E** - stage 17 WT embryo, **F** - stage 17 *Zmynd10*^{EY10866}embryo. Scale bars represent 100um.

embryos could be selected against GFP under a fluorescence stereomicroscope to obtain the homogeneous *Zmynd10* null embryo population. The embryos used for the RT-PCR experiment were 13-15 hours old and in the stages 14-17 of embryonic development. The w^{1118} strain has been used as a wild type control.

The same set of genes as in the previous RT-PCR experiment was used for this experiment. The preliminary data presented in the previous chapter suggested that *DmRootletin* might also be regulated by Zmynd10. In order to confirm this the *DmRootletin* gene has been tested along with the ODA and IDA genes. Interestingly $Zmynd^{10EY10866}$ seems to produce a strong reduction of *fd3F* (see Fig. 4.7, A, lanes 9 and 10, C, lanes 1 and 2) and *Dhc93AB* (see Fig. 4.7, B). This result confirms what has been shown in the Zmynd10 faulty RNA knock down. The *fd3F* was reduced by 2.08 fold (calculated from the PCR gel bands intensity obtained by ImageJ measure function, W^{1118} band intensity - 225, *Zmynd10* band intensity 108) and the *Dhc93AB* was reduced by 1.39 fold (W^{1118} band intensity - 86, *Zmynd10* band intensity - 62). Moreover the *DmRootletin* mRNA seems also to be reduced in the *Zmynd10* mutant embryos (see Fig. 4.7, C, lanes 3 and 4).The *DmRootletin* mRNA levels were reduced 8.84 fold (WT band intensity - 230, *Zmynd10* band intensity - 26). In order to control for the amount of template used in the PCR reaction and also for the gel loading a *tbp* gene fragment has been amplified and loaded on the gel. Other genes (*Dhc62B, CG6971, CG9313*) produced inconsistent results ranging from overexpression, no change, to reduction. The results for the affected genes (*Dhc93AB, fd3F* and *DmRootletin*) were either reproduced with a smaller difference in the mRNA levels or due to technical difficulties could not be reproduced but were confirmed by RNA in situ hybridisation (see next section).

The RT-PCR results suggest that Zmynd10 might be involved either in transcript stability of *fd3F*, *Dhc93AB* and *DmRootletin* or in transcriptional regulation of the

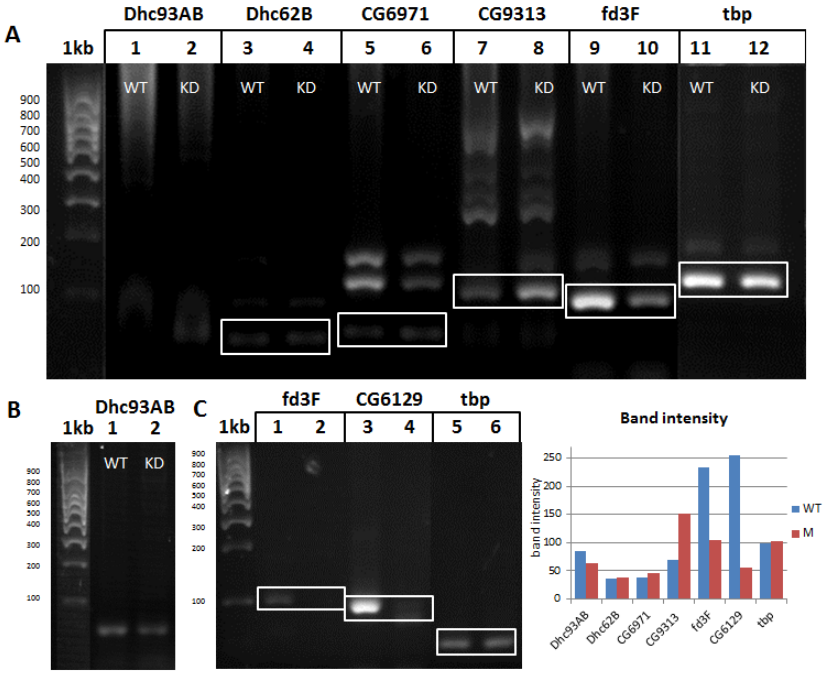

Figure 4.7. ODAs and IDAs RT-PCR performed on *Zmynd10* mutant embryos. A - lane 1 - *Dhc93AB* WT, **lane 2 -** *Dhc93AB Zmynd10*, **lane 3 -** *Dhc62B* WT, **lane 4 -** *Dhc62B Zmynd10*, **lane 5 -** *CG6971* WT, **lane 6 -** *CG6971 Zmynd10*, **lane 7 -** *CG9313* WT, **lane 8 -** *CG9313 Zmynd10*, **lane 9 -** *fd3F* WT, **lane 10 -** *fd3F Zmynd10*, **lane 11 -** *tbp*, loading control WT, **lane 12 -** *tbp*, loading control Zmynd10, **B - lane 1** - *Dhc93AB* WT, **lane 2** - *Dhc93AB Zmynd10*, **C - lane 1** - *fd3F* WT, **lane 2** - *fd3F Zmynd10*, **lane 3** - *DmRootletin* WT, **lane 4** - *DmRootletin Zmynd10*, **lane 11** - *tbp*, loading control WT, **lane 12** - *tbp*, loading control *Zmynd10*. Band intensity chart, n=3.

before mentioned genes.

15.8 RNA *in situ* hybridisation of selected genes on *Zmynd10*^{EY10866} mutant embryos

Due to the fact that the RT-PCR experiment has only given one positive result for *fd3F*, *DmRootletin* and *Dhc93AB* genes the possibility that Zmynd10 might regulate the expression of these genes had to be confirmed with another method. In order to do so RNA *in situ* hybridisation for each gene that seemed to be knocked down in

the *Zmynd10* mutant has been performed on selected *Zmynd10* homozygous mutant embryos. Although this method is less quantitative than RT-PCR it can provide useful and firm evidence for a hypothesis because of the relatively large number of biological replicates - each embryo pictured is a biological replicate.

Consistent with the RT-PCR results the *fd3F* RNA levels *in situ* seem significantly reduced in the *Zmynd10* embryos. This is apparent in both stage 14 (see Fig 4.8, A and B) and stage 17 (see Fig 4.8, C and D). The RT-PCR results for *DmRootletin* are also confirmed by the RNA in situ hybridisation. The *DmRootletin* transcript level is reduced in chordotonal neurons in stage 17 (see Fig 4.8 E and F). As shown in the section 15.2 of this chapter the *Dhc93AB* mRNA levels in the WT embryo were quite low (Fig 4.2A). This is indeed the case in this experiment but some weak chordotonal staining is Visible in the WT embryos. However the *Dhc93AB* transcript was virtually invisible in the *Zmynd10* mutant embryos.

These results support the RT-PCR outcome and further suggest that Zmynd10 is regulating the transcript levels of *DmRootletin*, *fd3F* and *Dhc93AB*.

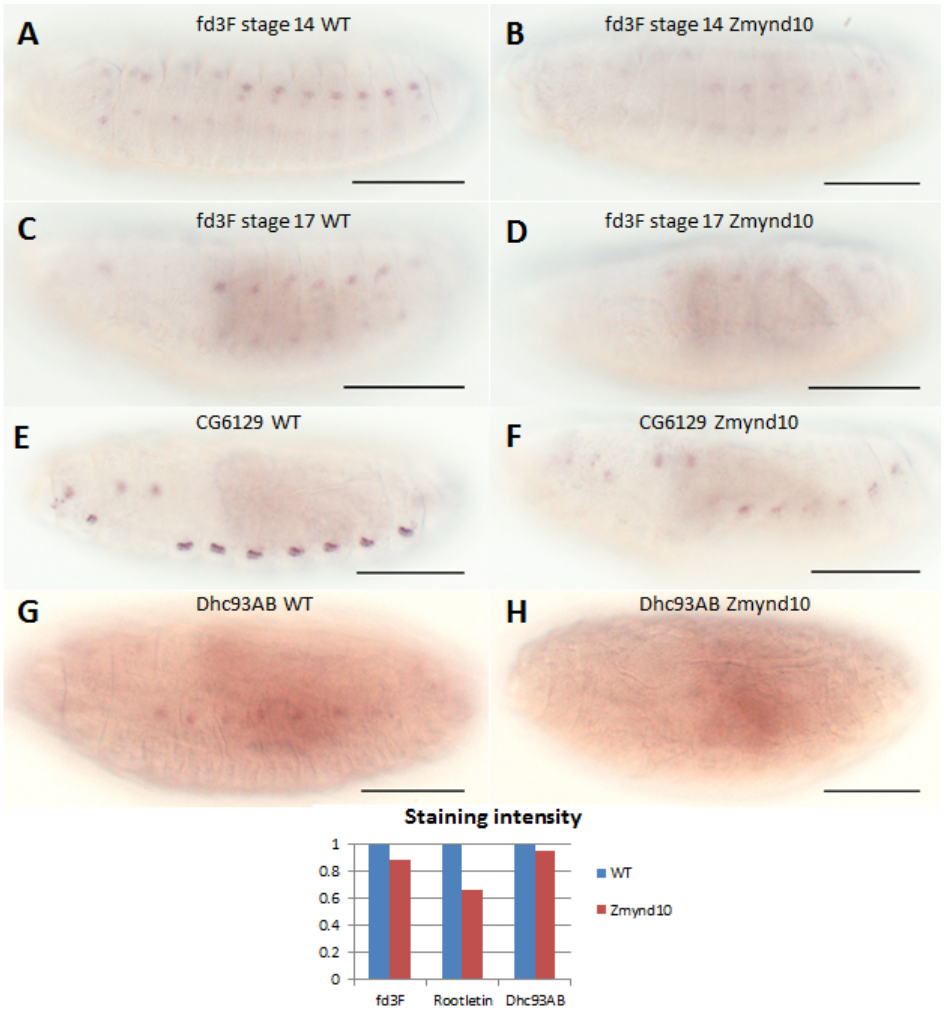

Figure 4.8. Zmynd10 putative target genes RNA in situ hybridisation performed on *Zmynd10* mutant embryos. A - stage 14, *fd3F* on WT embryo, **B** - stage 14, *fd3F* on Zmynd10 mutant embryo, **C** - stage 17, *fd3F* on WT embryo, **D** - stage 17, *fd3F* on Zmynd10 mutant embryo, **E** - stage 17, *DmRootletin* on WT embryo, **F** - stage 17, *DmRootletin* on Zmynd10 mutant embryo, **G** - stage 17, *Dhc93AB* on WT embryo**, H** - stage 17, *Dhc93AB* on *Zmynd10* mutant embryo. Scale bars represent 100um.

16 Discussion

16.1 Evidence that Zmynd10 regulates transcription

It has been proposed that Zmynd10 modulates the localisation of the ciliary dynein arms through possibly being a part of the dynein assembly complex (Moore et al, 2013). Indeed it has been shown to interact with LRRC6 which is also involved in dynein arms assembly (Kott et al, 2012). Apart from acting on the protein level Zmynd10 has been suggested to act on gene expression (Zhang et al, 2012). Indeed the results presented in this chapter imply that Zmynd10 influences the expression levels of some ciliary genes (*DmRootletin*, *Dhc93AB* and *fd3F*). This is inferred from semi quantitative RT-PCR performed on both *Zmynd10* knock-down and *Zmynd10* null mutant and confirmed by RNA *in situ* hybridisation on embryos. It is however uncertain as to how does this occur. Based on the presence of the LxxLL motifs in the Zmynd10 protein it is possible that it is involved in transcriptional regulation of the target genes. However the cellular localisation of Zmynd10 protein is mainly cytoplasmic (Moore et al, 2013). In order to assume the possibility of Zmynd10 being involved in transcriptional regulation its presence in nuclei would have to be tested. When this is confirmed another set of experiments would have to be carried out in order to assess whether Zmynd10 is involved in transcriptional regulation. One possible approach could be a nuclear run-on assay. It is an experiment that allows to evaluate the transcription rates of a given gene (Gariglio et al., 1981; Vazquez et al., 1993; García-Martínez et al., 2004). Another way to test the involvement of Zmynd10 in transcription regulation would be to establish if it is able to bind DNA (ChIP experiment). A different experiment assessing the human *Zmynd10* (*BLU*) ability to bind DNA has actually performed by Zhang et al (2012). The results of a luciferase assay carried out in this study show that *BLU* binds DNA and influences

the JNK signaling pathway through promoter blocking.

Despite the very attractive hypothesis that Zmynd10 might be a novel transcriptional regulator another possibility has to be take into consideration. The lower levels of *DmRootletin*, *Dhc93AB* and *fd3F* mRNA might be caused by transcript instability. It is conceivable that Zmynd10 could be involved in stabilising the target gene transcripts. In order to exclude (or confirm) this mode of operation the first step would be to redo the *in situ* hybridisation experiments together with the RT-PCR of putative target genes to obtain clearer and more robust results. Next a RIP-ChIP analysis could be carried-out. RIP-ChIP is an immunoprecipitation of RNA-binding proteins (Jain et al., 2011).

16.2 Mode of operation

If Zmynd10 is indeed a transcriptional regulator it would be interesting to know if it interacts with its target genes directly. A zinc-finger DNA binding domain is present in the Zmynd10 protein. It has however been shown to be involved in protein-protein interaction with another putative dynein assembly factor LRRC6 (Moore et al., 2013). Together with the cytoplasmic localisation of the Zmynd10 protein this suggests that Zmynd10 is not likely to bind DNA directly.

It is however plausible that Zmynd10 might act as a cofactor for some transcription factors to modulate their function in certain cells. The presence of conserved LxxLL motifs within the Zmynd10 protein strongly supports this hypothesis. It could be proposed that Zmynd10 regulates the transcription of ciliary motility target genes by binding the ciliary transcription factors (RFX, fd3F) and enhancing their activity in cells producing a motile cilium. If this is true it would add to the previously shown RFX-fd3F cooperation (Newton et al, 2012) which seems important in establishing

differential functions of the ciliated cells in *Drosophila*.

16.3 Does Zmynd10 regulate fd3F? positive feedback loop

The results shown in this chapter suggest that Zmynd10 might be involved in regulation of the *fd3F* transcript levels. This is a quite unexpected result as the *fd3F* has only been included in the RT-PCR experiments as a gene which is not expected to be influenced by the lack of Zmynd10. However the *fd3F* mRNA knock-down was consistent in both the RT-PCR and in the RNA in situ hybridisations. It is unclear whether this regulation exists on the transcription level but the results strongly imply that Zmynd10 might be a novel factor in the cilia regulatory network. *Zmynd10* itself is transcriptionally regulated by fd3F (Newton et al, 2012). Other genes tested in the RT-PCR experiments are also direct fd3F targets. It could be hypothesised that the genes that are affected by absence of Zmynd10 - *Dhc93AB*, *DmRootletin* - are actually directly knocked down by the lack of optimal levels of fd3F. It is suprising however that most of the ODA and IDA genes examined in this chapter do not seem to be affected in conditions of lower fd3F levels.

The fact that Zmynd10 could be involved in fd3F regulation suggests the existence of a positive feedback loop. In this model fd3F drives the expression of *Zmynd10* which in turn maintains optimal levels of fd3F. Such a loop could contribute to the differential expression of some genes in ES and chordotonal cells. Genes that fall into the 'chordotonal enriched' category could possibly be initially expressed in all type I neuronal lineage cells (driven by RFX) and then their expression could be additionally boosted by chordotonal specific factors (fd3F, Zmynd10). This model would explain the fact that the expression of some genes is quite low (or indeed transient) in ES cells, while in the chordotonal cells it is much higher. Examples of such genes are *DmRootletin, CG4525, CG8353, Oseg1, Oseg4, CG15161, CG3769,*

CG31291, and *CG11382* (Cachero et al, 2011).

16.4 Summary of DmRootletin regulation

As shown in the previous chapter *DmRootletin* is transcriptionally regulated by RFX and fd3F in a manner similar to what was explained in Newton et al (2012) for the chordotonal-enriched genes. In this regulation model RFX is responsible for expression of core ciliogenesis genes while fd3F drives the expression of chordotonal specific genes that are necessary for cilia motility and compartmentalisation. The only difference between *DmRootletin* and the genes previously proposed to be regulated according to this model is that *DmRootletin* is neither motility nor a compartmentalisation gene. Presented in this chapter is strong evidence that Zmynd10 takes part in the regulation of *DmRootletin* gene. Whether this regulation happens on the transcription level or post-transcriptionally it remains to be elucidated.

16.5 General conclusions

Zmynd10 could be a novel factor in the cilia differentiation regulatory network. It is unclear whether it is directly/indirectly involved in transcriptional regulation or whether it just modulates the target genes transcript stability. However, as a ciliary motility specific gene, it could be hypothesised that Zmynd10 can influence the expression of some genes that are involved in motile cilia function.

The role of Zmynd10 in cilia motility seem to be dual. On a protein level it has been suggested to be active as a dynein assembly factor. The cytoplasmic localisation and lack of inner and outer dynein arms in *Zmynd10* mutant, and interaction with LRRC6 (Moore et al, 2013) strongly supports this possibility. Zmynd10 can also act on the mRNA level. The results shown in this chapter imply that Zmynd10 can

influence some ciliary genes transcript levels. Moreover Zmynd10 seems to provide a positive feedback for its own transcriptional regulator - fd3F. An attractive model could be proposed in which Zmynd10 is one of the factors standing behind the regulation of differential gene expression in external sensory and chordotonal neurons. However additional experiments have to be performed in order to provide more firm evidence for the functionality of this model.

Part V

General Discussion

17 Is *DmRootletin* a motility gene?

The results shown in this work suggest that DmRootletin might have a role in the motility aspect of ciliary function.

Firstly *Drosophila* DmRootletin is regulated by fd3F transcription factor. *fd3F* is a divergent homologue of human *Foxj1* which encodes a transcription factor regulating ciliary motility genes. The FOX family transcription factor Foxj1 has been first shown to be necessary for motile cilia in mice (Brody et al., 2000). In later studies (Yu et al., 2008; Stubbs et al., 2008; Jacquet et al., 2009) Foxj1 has been shown to transcriptionally regulate genes that are directly or indirectly involved in cilia motility like axonemal dynein components (*Dnahc3*, *Dnahc5, Dnahc6, Dnahc9, Dnahc11, Dnahc12, Dnaic1, Dnali1*), *Tektin1, Tektin4*, axonemal kinesins (*Kif6/9/27*), WD-repeat containing proteins (*WDR40, WDR78*), and protein components of the axoneme radial spokes (*Rshl2, Rshl3*). Given that this long list of target genes includes only ciliary motility genes it is surprising that the expression of *Drosophila DmRootletin* is fd3F dependent. Although DmRootletin and ciliary rootlets have been studied extensively in the past (Klotz et al., 1986; Hagiwara et al., 2000; Yang et al., 2002; Bahe et al., 2005; Conroy et al., 2012; Mohan et al., 2013) it has never been specifically linked to ciliary motility.

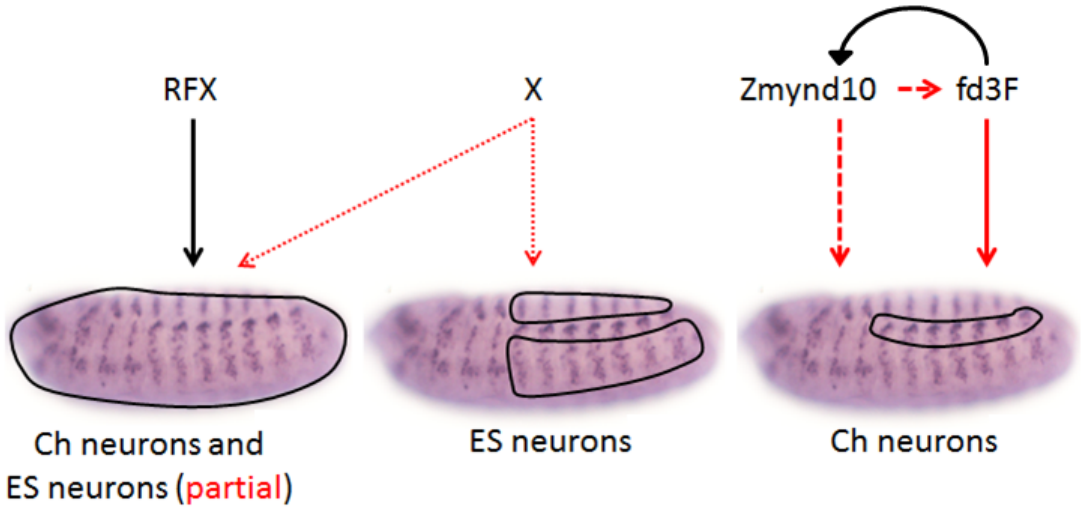

Figure 5.1. Expanded model of transcriptional effects on DmRootletin gene. Black line represents what has been known so far and the red colour represents the findings of this work. RFX regulates DmRootletin expression in both Ch and ES neurons. The dependence of DmRootletin on RFX in ES neuron is now known to be partial. The fine dashed red line represents a suggestion of existence of a previously unknown TF responsible for DmRootletins expression in ES neurons and possibly Cho neurons. The solid red line represents the transcriptional control by fd3F (contrary to what previously shown in Newton et al., 2011). The verticular dashed red line represents a regulation dependence on Zmynd10. Whether this dependence is transcriptional or posttrascriptional remains to be elucidated, the horizontal dashed red line represents a feedback loop between Zmynd10 and its transcriptional regulator fd3F.

Secondly DmRootletin is expressed in the chordotonal-enriched pattern. This means that very high levels of DmRootletin are expressed in the chordotonal cells (bearing motile cilia) and lower levels are transiently expressed in the ES cells (non-motile cilia). Such an expression pattern has been shown to be followed by many genes and has also been suggested to be created by a differential regulation of genes expression by RFX and fd3F (Newton et al, 2012). In this differential regulation model RFX (expressed in chordotonal-enriched pattern) regulates the expression of core ciliogenesis genes that are necessary for cilia formation in both chordotonal and external sensory cells. The higher level of RFX factor in chordotonal cells than in the ES

cell could correspond to and indeed underlie the difference in the cilia robustness between those two cell types. The other factor - fd3F - is chordotonal (motile cilia) specific and has been proposed to specifically regulate genes that are necessary for the development of chordotonal cilia characteristic features - motility and compartmentalisation. The RFX - fd3F cooperation regulatory model has been shown to be true for genes involved in ciliary motility (*CG3769* - human *DYN2LIC* orthologue, *btv* - *DYN2HC* orthologue, *rempA*, *Tektin*, and *Dhc93AB* orthologue) (Newton et al, 2012). In the same time this model was not confirmed for the genes that are/were not considered to be involved in motility (for example *dila*, *nompB*, *DmRootletin*) (Newton et al, 2012). The data presented in my work show (contrary to what stated in Newton et al, 2012) that *DmRootletin* expression not only depends on fd3F but also is regulated by RFX-fd3F cooperation possibly similar to what has been described by Newton et al (2012). This could be interpreted in two ways.

One interpretation would be that *DmRootletin* is a motility gene. Given the fact that DmRootletin forms ciliary rootlet structures in both motile and immotile cilia it could be easily hypothesised that if the link to motility indeed exists it will not be direct. It could be however that ciliary rootlets provide necessary structural support for motile cilia that are more prone to mechanical stress than their immotile counterparts. Another possibility could be that if DmRootletin modulates protein transport to the cilium some of the transported proteins could be involved in ciliary motility. An easy way to examine the involvement of DmRootletin in ciliary motility in *Drosophila* would be to test for the non-linearity in the sound stimulus amplification in JO (Gopfert et al, 2004) which arises for the cho cilia motility.

If however the indirect link between DmRootletin and ciliary motility does not exist it is possible that fd3F regulation (and RFX-fd3F cooperation model) is not specific to ciliary motility genes. A large scale experiment looking for the fd3F target genes

would elucidate whether they only belong to the motility category. This could be done by fd3F ChIP or fd3F expressing cells microarray or, ideally both methods combined.

18 Could fd3F regulate non-motility genes?

If DmRootletin is not in any way involved in motility, another possibility is that fd3F is not a ciliary motility specific transcription factor. Indeed it has been reported that apart from ciliary function Foxj1 plays a critical role in immune system (Lin et al., 2004). It has been shown to repress the Nuclear Factor $\varkappa$B (NF-$\varkappa$B) in mice (Lin et al, 2004). Due to the fact that Foxj1 homozygous mutant mice die perinatally because of severe cilia-specific phenotypes (hydrocephalus, heterotaxy) the Foxj1 mutation has been specifically induced in the lymphoid system. Such Foxj1 mutant chimeras displayed severe systemic autoimmune reaction. Although the cellular profile of the spleens and lymph nodes in WT and Foxj1 chimeras was comparable the Foxj1 deficient mice exhibited a high proportion of in vivo activated CD4+ lymphocytes (Lin et al, 2004). Lin et al have shown that Foxj1 binds to the NF-$\varkappa$B promoter and represses its activity. This leads to chronic overactivation of the CD4+ lymphocytes and thus a severe autoimmune reaction. Another interesting fact is that although Foxj1 has been strongly linked to cilia motility in vertebrates, no Foxj1 mutations are found in PCD patients (Maiti et al., 2000). It could be that any Foxj1 mutation that would be detrimental to its function, causes far more severe systemic disruptions than just the cilia connected PCD phenotype and is therefore lethal.

Although Foxj1 is involved in transcriptional regulation of genes that are not connected to cilia in any way, the dependance of non-motility ciliary genes on fd3F has not been studied. If DmRootletin does have any role in the ciliary motility it is pos-

sible that *Drosophila* DmRootletin is the first example of a non-motility ciliary gene that has been shown to be transcriptionally controlled by fd3F. This suggests that in the future search for fd3F target genes both non-ciliary and non-motility ciliary genes should be taken into consideration.

19 Regulation of cilia diversity

Maintaining normally differentiated cilia both during the development and adult life is important. This is mirrored by a number of highly varying symptoms caused by the failure of a given type of cilia. Many different cilia types have so far been characterised and studied extensively but the mechanisms of how this ciliary diversity is regulated are largely unknown.

On the protein level differential function of some IFT motors contributes to cilia variety. In *C. elegans* it has been shown that differentially functioning kinesins (Osm-2 and Kinesin II) are partially redundant in building the amphid channel cilia and completely redundant in building the AWC cilia (Evans et al., 2006). The cell specificity in terms of IFT kinesin motors function in *C. elegans* has also been suggested in Mukhopadhyay et al (2007). This implies that the structural differences between functionally diverse cilia can be achieved by various IFT mechanisms.

Another factor in the differential cilia function is the presence of specific sensory receptors like olfactory receptors in olfactory cilia or photoreceptors in rods and cones. The examples of such differentially expressed/localised receptors are G-protein coupled receptors (GPCRs) of *C. elegans* (Brear et al., 2014). The GPCRs are members of a large family of transmembrane sensory receptors that can evoke a response to various stimuli like photons, odourants, neurotransmitters and peptides (Brear et al, 2014). Other examples of differentially expressed sensory receptors are *Drosophila*

nan and iav. They are TRPV channel subunits (Gong et al, 2004) that are localised in the motile compartment of chordotonal cilia. Both iav and nan are specifically expressed in chordotonal cells and not other ciliated sensory cells (that is ES cells). The differential expression of various proteins in different ciliated cell types is due to differential transcriptional regulation.The best known and extensively studied regulators of ciliogenesis are members of the RFX family. RFX factors regulate the expression of core components of all types of cilia (Choksi et al, 2014) in *C. elegans* (Swoboda et al, 2000), *Drosophila* (Dubruille et al, 2002) and vertebrates (Chung et al, 2012). RFX dependent genes fall into two categories: core ciliary genes necessary for cilia formation and function regardless of the cilia type (IFT genes, transition zone genes, radial spokes components, BBsome genes), and cilia type specific genes.

20 Dynein arm assembly complex

PCD is a disease that affects ciliary motility. Understandably the first genes linked to PCD were the genes encoding the motility apparatus components like axonemal dyneins, radial spokes and central apparatus components. Recently genes encoding proteins involved in the assembly of axonemal dynein arms (DNAAF1, DNAAF2, DNAAF3, CCDC103, HEATR2, LRRC6 and Zmynd10) have also been linked to PCD (Omran et al, 2008, Loges et al., 2009; Duquesnoy et al., 2009, Horani et al, 2012, Kott et al, 2012, Mitchison et al, 2012, Moore et al, 2013, Diggle et al, 2014). Products of these genes are mainly (or only) localised in the cytoplasm with very low protein levels sometimes present in the cilium. Genes like Zmynd10 or HEATR2 have been shown to be involved in the axonemal dynein assembly. The hypothetical model is that a large multiprotein complex exists in the cytoplasm of cells bearing motile cilia. This complex contains the dynein assembly factors that together with

chaperone components help folding and pre-assembling the dynein arms.

A candidate for such complex is the R2TP complex. The R2TP complex is a Hsp90 associated complex that consists of Rvb1, Rvb2, Pih1 (protein interacting with Hsp90), and Tah1 (TPR containing protein associated with Hsp90) proteins (Kakihara and Houry, 2012, review). The R2TP complex is involved in numerous and very diverse pathways including chromatin remodelling, transcription, snoRNP biogenesis, telomerase complex assembly, mitotic spindle assembly, apoptosis and dynein arm assembly (Kakihara and Houry, 2012). Other components of the R2TP complex include the Prefoldin complex component - WDR92/Monad protein.

The *Chlamydomonas* and Medaka fish PIH1 family proteins PF13 and Ktu are involved in ciliary motility (Omran et al, 2008). Omran et al show that in both systems (*Chlamydomonas* and medaka fish) the Pih1 orthologue is involved in pre-assembly of the ODAs. Disrupted PF13/Ktu causes phenotypes such as cilia specific defect within the Kuppfer's vesicle (left-right symmetry organ in fish) in the Medaka fish and cilia immotility in *Chlamydomonas*. Interestingly mouse Ktu interacts with heat shock protein Hsp70 supporting the idea that Ktu/Pf13 is a component of the R2TP complex. Despite the very diverse functions of the R2TP complex human KTU protein has been shown to be involved in PCD (Omran et al, 2008). Another PIH1 family protein MOT48 has also been shown to be involved in the dynein arm assembly (namely IDAs) by Yamamoto et al (2010). Although MOT48 could be one of the R2TP complex components no interaction with Hsp90/70 proteins have been found (Yamamoto et al, 2010).

Despite the fact that the PIH1 family proteins have been shown to be involved in dynein assembly in various publications, there is no evidence that other components of the R2TP complex (Rvp1, Rvp2, and Hsp70/90, and Tah1) are involved in this pathway. However there are several premises suggesting that such involvement might

indeed be true. *Drosophila* orthologue of the Tah1 protein - Spag has been shown to interact with other R2TP complex component orthologues and Hsp70/90 (Benbahouche et al., 2014). In the model presented in this study the *Drosophila* R2TP complex includes the Monad protein orthologue (CG14353), Reptin (Rvb1), Pontin (Rvb2), Spag (Tah1), Pih1D1 and both Hsp90 and Hsp70. Although Benbahouche do not look at connection of any of these proteins in cilia the expression patterns of most of them (CG14353, my unpublished data, Reptin, Pontin, Hsp90 and Hsp70 - BDGP in situ database) are chordotonal specific in the late stages of embryonic development. This would imply a specific involvement of the *Drosophila* R2TP type complex in some cilia related pathway.

Interestingly Zmynd10 have also been suggested to be one of the R2TP complex components (Petra zur Lage, personal communication). In the preliminary unpublished data from murine tissue (Girish Mali, personal comunication) the Zmynd10 pulldown experiment revealed interaction with multiple Hsp proteins.

21 Conclusions

Drosophila gene *CG6129* is an orthologue of human Rootletin. This gene is specifically expressed in somatic ciliated cells with differential levels in Cho and ES cells. It is possible that these level/time point expression differences underlie the structural and thus functional differences between Cho and ES organs. Chordotonal organs bear long and specialised cilia and therefore also possess a robust ciliary rootlet structure. ES organs on the other hand have a short connecting cilium. Presumably this structure does not need that much anchoring and that might be why ES cells only have rudimental rootlets (Avidor-Reiss et al, 2004).

DmRootletin is differentially regulated in terms of both the time during the devel-

opment and the cell type. In a most probable model the RFX transcription factor regulates the *DmRootletin* expression at early to late stages of development (based on the activity of RFX dependent *DmRootletin* enhancers). As RFX is the only known transcription factor expressed in both ES and Cho cells it is likely it regulates *DmRootletin* expression in both. However data shown here suggest that some *DmRootletin* expression in ES cells is independent of RFX - this implies the existence of another transcription factor that would be active in ES cells. Apart from RFX I have shown that *DmRootletin* (contrary to what previously shown) is also regulated by fd3F. This Cho specific transcription factor regulates *DmRootletin* expression only at late stages of embryonic development. This fits with the model presented by Newton et al (2012) in which some *Drosophila* ciliary genes are regulated by RFX to a base level necessary for ciliogenesis in both ES and Cho cells, while fd3F provides an additional expression boost in Cho needed for the cells specialised function. However this model has been shown to be true for genes involved in ciliary motility only. The *DmRootletin* gene has not been linked to motility so far. It is possible that either DmRootletin has a role in ciliary motility or that the model presented by Newton et al (2012) is true for non-motility ciliary genes.

During the course of my project I have found that a PCD causing gene - *Zmynd10* - is also involved in regulation of some ciliary genes in *Drosophila*. It is not clear whether Zmynd10 regulates genes on the transcription or posttranscriptional level. The possibility of a positive feedback loop between fd3F and Zmynd10 suggests at least indirect involvement of Zmynd10 in gene transcription.

In conclusion my work provides an insight into the differential ciliogenesis and its regulation. Although RFX and fd3F are nominated the key ciliary transcription factors, a possibility emerges in which more regulators are involved in the intricate regulatory network governing the differences between various cilia types. One of those

regulators might be Zmynd10 but other potential ciliary transcription factors have been annotated in *Drosophila* based on the expression profiles and protein domain prediction. An example of such TF might be the product of the *CG32006* gene. It is important to take the possibility of a larger number of ciliary transcription factors into consideration when using the *Drosophila* model and possibly other species as well.

Part VI

Materials and Methods

22 Fly stocks

Fly stocks were raised on standard "Dundee Food" (1 litre: 25g cornflour, 50g sugar, 17.5g yeast, 10g agar, boiled, cooled to 40 $^{\circ}$ C and poured into bottles or vials to set) prepared by the media kitchen in the Swan Building (University of Edinburgh). Fly stocks were kept in 18 $^{\circ}$ C or 21 $^{\circ}$ C and most of the experiment crosses were reared in 25 $^{\circ}$ C. In some cases the UAS-Gal4 experiment crosses were kept in 29 $^{\circ}$ C.

23 Gene knock-down with use of RNA silencing

All the knock-downs presented in this work have been achieved through genetically induced RNA silencing. The expression of the shRNA construct has been driven in a tissue specific manner under the control of the Gal4-UAS system. The events leading to the RNA interference have been schematically shown in the figure 6.1.

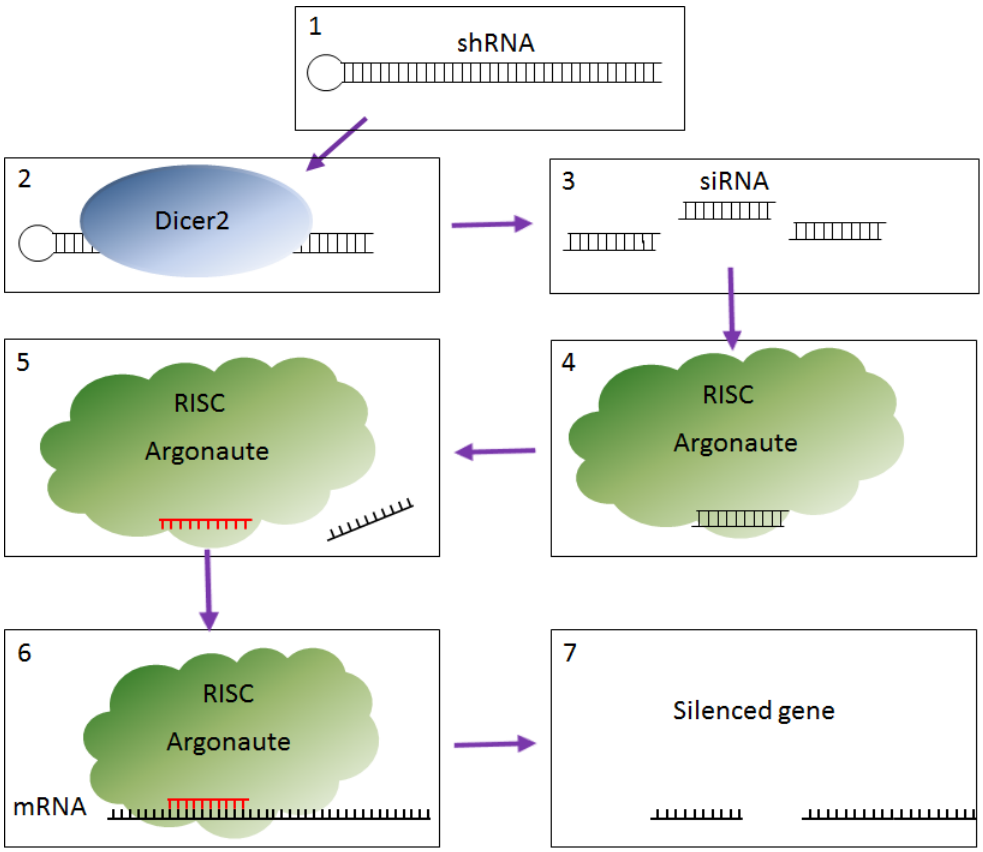

Figure 6.1. RNA silencing via the siRNA pathway. 1 - silencing is initiated by the shRNAs - short hairpin RNAs which are built of an inverted repeat complementary to the mRNA of the silenced gene, 2 - the Dicer2 protein recognises the double stranded RNA and 3 - cuts up the shRNA into short fragments (21 nucleotides) called the siRNAs. At this point siRNAs are in duplexes as they are still double stranded, 4 - the RISC complex (RNA induced silencing complex) which contains the Argonaute protein binds the duplex siRNAs, 5 - helicases the siRNA duplexes discarding the passenger siRNA (in black), 6 - the RISC complex assists in complementary binding of the guiding siRNA (in red) to the complementary fragment of the target gene and cuts it, 7 - this leads to fragmentation of the mRNA and stops the subsequent gene expression (Ghildiyal and Zamore, 2009).

24 Molecular Biology

24.1 Genomic DNA preparation from adult flies

25 adult flies were anesthetized and submerged in 250µl of Lysis Buffer (0.1M Tris HCl pH 9.0, 0.1M EDTA, 1% SDS) in a 1.5ml eppendorf tube. They were then homogenized using a plastic rotating pestle. The homogenate was incubated for 30 minutes in 70 ° C. After the incubation 35µl of 8M KAc was added to denature the proteins and the mixture was incubated on ice for 30 minutes. The lysate was spun down for 5 minutes at 13000rpm and the supernatant was transferred to a new tube. The DNA was extracted with Phenol-Chloroform until no protein precipitate was visible in the interphase. The DNA was precipitated with 150µl of isopropanol, centrifuged for 5 minutes at 10000rpm and the pellet was dried. The DNA was then resuspended in 100µl of TE.

24.2 Genomic DNA preparation from single flies

Individual flies were anesthetized and squashed using a yellow pipette tip in 50µl (10mM Tris-HCl pH8.2, 1mM EDTA, 25mM NaCl, 200µg/ml Proteinase K(Roche, cat. 01135836001))(Gloor et al., 1993). The samples were incubated in room temperature for 30 minutes. After the incubation the Proteinase K was heat inactivated in 95 ° C for 2 minutes. Such prepared single fly DNA was either used straight away or kept in 4 ° C. The sample was used directly as a PCR template (˜4µl) without need for further purification.

24.3 Plasmid DNA preparation

For cloning experiments the plasmid DNA was purified using the GeneJET Miniprep Kit (Thermo Scientific, cat. K0503) according to the manufacturers' instructions.

24.4 Plasmid DNA preparation for microinjection

50ml of inoculated medium was incubated overnight in 37 ° C in a shaking incubator. The culture was then transferred to a 50ml falcon tube and centrifuged for 15 minutes at 4500rpm. After thorough drying the pellets were resuspended in 2ml Solution I (50mM Glucose, 25mM Tris-HCl pH8, 10mM EDTA, 5mg/ml Lysosyme). After 10 minuets incubation in room temperature 4ml of Solution II (0.2M NaOH, 1% SDS) was added to lysate the bacteria. The lysates were incubated on ice for 10 minutes. After the incubation 3ml of Solution III (3M KOAc, 1.3M HCOOH) was added and the mixture was shaken vigorously and incubated on ice for 15 minutes. The solution was then centrifuged for 15 minutes at 4500rpm. The supernatant was transferred to a clean falcon tube and the DNA was precipitated using 0.6 volume of isopropanol and left on ice for 5 minutes. The solution was then centrifuged for 10 minutes at 4000rpm. The pellet was briefly rinsed in 2ml of 70% ethanol and dissolved in 1ml TE. The solution was split equally between two 1.5ml eppendorf tubes and incubated with an equal volume of ice cold 5M LiCl for 5 minutes on ice. The tubes were then centrifuged at 14000rpm at 4 ° C for 5 minutes and the supernatant was transferred to clean eppendorf tubes. An equal volume of isopropanol was added and the solution was incubated on ice for 10 minutes. Samples were then centrifuged at 14000rpm at 4 ° C for 5 minutes and the DNA pellet was air dried. After drying the DNA was resuspended in 300µl TE and incubated with 2µl DNase free RNase (10mg/ml stock) for 1 hour in 37 ° C. After the incubation an equal volume of PEG/NaCl

(15% 8000 PEG, 1.6M NaCl) was added and the solution was incubated on ice for 5 minutes. The DNA was collected by centrifugation at 14000rpm at 4 °C for 5 minutes and resuspended in 300µl TE. Phenol/chloroform extraction was performed until no protein precipitate was visible in the interphase. The purified DNA was precipitated using 1/20 volume of 3M NaOAc and 2 volumes of 100% ethanol. The tubes were incubated for a minimum of 2 hours in -20 °C. The DNA was spun down at 14000rpm for 15 minutes and the pellet was briefly washed in 1ml 70% ethanol, air dried and resuspended in 100µl of water.

DNA concentration was measured using the Nanodrop Spectrophotometer (Thermo Scientific) according to manufacturers' manuals.

24.5 RNA preparation

Overnight (1-22h) or two hours (20-22h) embryo collection was put into a sieve and washed for 4 minutes in 50% bleach to remove the chorion. The embryos were then rinsed with water, dried on a tissue and transferred to a clean and pre-weighted 1.5ml eppendorf tube. 20-30mg of embryos was homogenized with rotating pestle in 600µl of RLT buffer (RNeasy Mini Kit, Qiagen) until no intact embryos remained visible.

Ten pairs of testes per sample were dissected in PBS and put into 50ul of the RLT buffer. They were then homogenized for 20-30 seconds.

Ten adult brains (or whole heads) per sample were dissected in PBS and placed in 50ul of the RLT buffer. They were then homogenized for 20-30 seconds.

The RNA was extracted from the above tissues using the RNeasy Mini Kit (Qiagen, cat. 74106) according to manufacturer's protocol 'Total RNA from animal tissues'. Genomic DNA was removed using the additional step involving the DNase1 Kit

(Qiagen, cat. 79254) following the manufacturer's protocol.

24.6 Reverse transcription

Complete cDNA was synthesized using RNA as a template and primed with oligodT primers. 100ng-1µg of RNA was used in each 17µl reaction (ImProm-II reverse transcriptase kit, Promega, cat. A3802). Reactions were run according to manufacturer's manual.

24.7 Polymerase chain reaction (PCR)

All PCR reaction were carried out in either Biometra, Thermo Hybaid or Techne thermal cyclers with Roche Taq polymerase (cat. 11146173001), buffer and dNTP mix following manufacturers instructions. All primers used were made by Sigma Aldrich. 50µl reaction contained: 2µl of gDNA/cDNA, 5µl of each primer (10pmol/µl), 1µl of dNTP mix (2.5mM), 5µl 10X buffer, 0.5µl Taq polymerase, water up to 50µl. The cycling program as follows (unless otherwise stated in the results chapters):

94ºC	2 min	
94ºC	20 s	
55ºC	40 s	32 cycles
72ºC	1 min/kb	
72ºC	10 min	
4ºC	pause	

24.8 Gel electrophoresis

DNA was analysed using standard agarose electrophoresis. For most experiments 0.8% agarose gels were used (in 0.5X TBE with 0.7µl/ml GelRed (Biotium, cat. 41003). For RT-PCR products analyses 2% agarose gels were used. Molecular weight markers were used to estimate the size and concentration of the analysed DNA. Gels were run at 90V-130V.

24.9 DNA purification from PCR reactions and agarose gels

DNA fragments from PCR reactions or bands cut out of agarose gels were purified using the GeneJET Gel Extraction Kit (Thermo Scientific, cat. K0692) according to the manufacturer's instructions.

24.10 DNA restriction

For all cloning experiments the restriction enzymes used were provided by Roche, Promega or NEB. The digests were performed according to the manufacturers' protocols. All reactions were run for a minimum of 2h in 37 $^\circ$ C.

24.11 DNA dephosphorylation

The digested plasmids might spontaneously religate and re-circulate. To prevent this from happening the phosphate residue was removed from the 5' end of the linearised vectors using Antarctic Phophatase (NEB, cat. M0289S) following manufacturers' instructions. No additional purification was done after this step.

24.12 DNA ligation

All ligation reactions were carried out using the LigaFast Rapid DNA Ligation System (Promega, cat. M8221) according to manufacturer's manual. 5µl of the ligation reaction was used for the *E. coli* transformation.

24.13 DNA sequencing

DNA sequencing reactions were performed using the BigDye Terminator v3.1 Cycle sequencing kit (Applied Biosystems, cat. 4337454). Reaction mix contains 3µl of DNA, 2µl of sequencing buffer, 4µl of primer (1.6pmol/µl), 1µl BigDye reagent. The cycling conditions used were:

96ºC	1 min	
96ºC	10 s	
50ºC	5 s	25 cycles
60ºC	75 s	
4ºC	pause	

24.14 *E. coli* transformation

E. coli XL1-Blue competent cells were prepared using $CaCl_2$ procedure. After the preparation cells were aliquoted, snap frozen and kept in -80 ° C until use.

Directly before use the cells were thawed on ice. ~100ng of DNA was added to 30µl of cell suspension and incubated on ice for 20-30 minutes. After the incubation the cells were heat shocked in a water bath in 42 ° C for 45secs to allow for the DNA takeup. They were then allowed to recover on ice for 2 minutes. 50µl of preheated LB medium was added and the cell suspension was shaken in the 37 ° C incubator for 1h. After the initial growing period the entire volume of the transformation reaction was spread onto an agar plate with the appropriate antibiotic. The plates were incubated in 37 ° C overnight. For the white/blue selection 40µl of 2% X-gal and 100µl of IPTG was spread onto the plate before the cells were plated. In case of site-directed mutagenesis or T-A cloning the transformation was carried out following the manufacturer's protocol.

24.15 Site directed mutagenesis

The Site-Directed Mutagenesis Quick-Change IIXL Kit (Stratagene, cat. 200522-5) was used according to the manufacturers' instructions.

24.16 Bacterial culture growth

Liquid bacterial cultures were grown overnight by incubation in 37 ° C in an orbital shaker with moderate agitation (200rpm). The media was supplied with appropriate antibiotic (ampicilin - 100µl/ml). Single cell colony cultures were plated on 1.5% agar in LB supplemented with appropriate antibiotic.

25 Western blotting

Adequate tissue was dissected in PBS and transferred directly into the 2xSDS loading buffer (100mM Tris pH 6.8, 4% SDS, 0.2% gBPB, 20% glycerol) with 0.1M DTT. The tissue was then homogenized with rotating pestle for at least 20 seconds. The homogenate was heated up in 98^{o}C for 3 minutes and cooled down on ice. The homogenates were then spun down in 14000rpm for 3 minutes to get rid of the foam produced during homogenisation. 18ul of each such prepared sample was run on a SDS-PAGE gel (8%) at 170V for 1h.

Once the gel had run it was soaked in the blotting buffer (25mM Tris, 192mN Glycine, 20% methanol) for 15 minutes. In the meantime a PVDF membrane was cut, rinsed briefly in methanol and soaked in the blotting buffer for 10 minutes. The membrane was then placed on top of the gel with two blotting papers on either side (wet in blotting buffer). The proteins were then blotted to the membrane at 90V for 70 minutes with a magnetic stirrer. After the proteins have been transferred onto the membrane it has been blocked with the Odyssey Blocking Buffer (927-40100, Licor) with 0.1% Tween for 1h in room temperature with gentle shaking. Following the blocking the membrane has been incubated in the primary antibodies (in Blocking buffer, 0.2% Tween) as follows: RbAbGFP 1:2000, RbAbNek2 1:1000, and GtAbActin 1:400. The next day the primary antibodies were taken off and the membrane was rinsed once and washed 3 times for 15 minutes in 0.1% Tween in PBS. After the unbound primary antibodies have been washed off the secondary antibodies have been applied on the membrane (donkey anti rabbit, 926-32213, Licor and donkey anti goat, 926-68074, Licor) in 1:10000 dilution. After 1-2h incubation performed in the dark at room temperature (wrapped in tin foil) the membranes have been washed 4 times for 15 minutes in 0.1% Tween in PBS. After washes the membranes have been dried be-

tween two pieces of the blotting paper in the fridge for ~2h. They were then scanned using the Odyssey Classic imaging system. The obtained images were processed using the ImageJ software.

26 Immunohistochemistry

26.1 Sample fixation for antibody detection

26.1.0.1 Embryos Embryos were collected on red wine agar plate and transferred to a sieve. They were then incubated in 50% household bleach to remove the chorion and washed several times with water before transferring to a scintillation vial containing 3.75ml PBS, 1.25ml 37% formaldehyde and 5ml heptane. Embryos were fixed on an orbital shaker for 20-30 minutes in room temperature. After fixation the lower aqueous was removed and 10ml of 100% methanol was added. The vial was shaken vigorously to remove the vitelline membrane and embryos were allowed to sink. Embryos were collected, transferred to a clean eppendorf and washed 3 times with 100% methanol to remove the residual heptane. In case of immunohistochemistry embryos had to be rehydrated by washing in PBT (PBS with 0.3% Triton-X100) and then used immediately.

26.1.0.2 Larval pelts 3rd instar larvae were cleaned from the fly food and put on the Sylgard lined dish in a drop of PBS. The posterior and anterior end of the larva were pinned down and a longitudinal incision was made along the whole dorsum (inbetween the dorsal main trunks of the tracheal system). All the internal tissues were removed leaving cleared muscle fibers surface and the pelt was fully stretched opened and pinned down. Such prepared larval pelts were fixed in 3.7% formaldehyde in PBS for 20-30 minutes. After fixation the pins were removed along with the

head and tail sections and the pelts were washed in PBT three times to remove the formaldehyde. The pelts were then used immediately for the immunostaining.

26.1.0.3 Pupal antennae 24-48h old pupae were transferred to a Sylgard lined dish. The top of the pupal case was removed and a single lateral incision was made around the eye level to facilitate the fixative and antibodies entry. Such prepared pupae were then fixed in 3.7% formaldehyde in PBT for 20-30 minutes and washed 3 times in PBT to remove the fixative. The pupae were then transferred to the Sylgard lined dish and the antennae along with the covering membrane were dissected and transferred to 500µl of PBT in a clean reaction tube. The antennae were then immediately used for the immunostaining. All subsequent washes were carried out on the bench top allowing the antennae to sink for a minute each time before the wash solution was removed.

26.1.0.4 Testes The young adult testes were dissected in PBS and fixed either in 3.7% formaldehyde or 4% paraformaldehyde in PBT depending on the structure needing analysis. The fixation was carried out in 1.5ml reaction tube on the bench top in the room temperature. The fixative was removed by three PBT washes allowing the testes to sink for a minute each time the wash solution was changed.

26.1.0.5 Boiling fixation In cases the antibodies used do not work on formaldehyde fixed tissues (for example the anti-Nek2 antibody) the tissues were heat fixed for 3 minutes in 90 $^{\circ}$C in PBTx. Before going to the next steps the tissues were cooled down by removing the heated PBtX with room temperature PBTx. For embryos the permeabilisation/devitellinisation steps with heptane and methanol followed as with a normal embryo collection. For other tissues (pupal antennae and larval pelts) heating was followed directly by the addition of block.

26.2 Immunostaining

Fixed tissues were blocked for 2h in 2% bovine serum albumine (BSA, Roche) in PBT in room temperature on a rotating wheel. After blocking the primary antibody mix was prepared as follows: 2% BSA, 5% normal goat serum (NGS, Jackson Labs) and appropriate antibody dilutions (see Appendix C). The samples were incubated overnight in 4 $^{\circ}$C. After the incubation the primary antibody mix was removed and the samples were washed with PBT 3 times for 15 minutes. When residual primary antibody was removed the secondary antibody (Alexa Fluor conjugated, Molecular Probes) mix was prepared: 5% NGS in PBT and 1:500 of each antibody. Samples were incubated for at least 2h and the secondary antibody was removed by three 15 minutes washes in PBT. The samples were then mounted on microscope slides in the photo-bleaching protective Vectashield mounting medium (Vector Labs, cat. H-1000), covered with a coverslip and sealed with nail varnish. Slides were kept in 4 $^{\circ}$C in the dark.

26.3 Microscopy

Tissues stained with fluorescent antibodies were imaged using a Zeiss LSM Pascal system with the LSM Zeiss capture software. The same laser gain settings were used for both the sample and the control. In most cases the Z-stack was made using the ImageJ open source software (http://imagej.nih.gov/ij/).

27 *In situ* hybridisation

27.1 RNA *in situ* probe preparation

The template for the DIG-labelled antisense RNA probes were either a PCR products or a linearised plasmids. In cases where the template was a PCR product it was primed in a way that it had a T7 promoter at the 5' end. This was necessary to prime the reverse transcription reaction in turn. In cases where the linearised plasmid was used as a template the desired gene sequence was cloned into a polylinker site of the pSC-A vector (Stratagene, cat. 240205). The vector was linearised before the RNA synthesis reaction to facilitate the polymerase access. The synthesis reaction was carried out using the DIG RNA labeling kit (Roche, cat. 11175025910) following the manufacturers' instructions. The probe was cleaned up using the RNeasy Spin Columns (Qiagen, cat. 74134) following the manufacturer's manual. The probes were kept in -20 $^{\circ}$C until needed.

27.2 Sample fixation

Samples were fixed as described before with the difference being no rehydration was performed until the tissue was used for the in situ. The samples can be kept in methanol in -20 $^{\circ}$C until needed.

27.3 RNA *in situ* hybridisation

The embryos were rehydrated with three consecutive washes in 70%, 50% and 30% ethanol in PBT (0.1% Tween 20 in PBS) for 10 minutes each on a rotating wheel. After rehydration the embryos were rinsed a couple of times with PBT and post-fixed in 3.7% formladehyde in PBT for 20 minutes. The fixative was washed off by three

20 minute washes in PBT. After this the embryos were washed in 50% hybridisation buffer (50% deionised formamide, 5% SSC, 100µg/ml tRNA, 50µg/ml heparin, 0.1% Tween 20, pH 6.5, water) for 10 minutes and in 100% hybridisation buffer for another 10 minutes. The embryos were then incubated in the hybridisation buffer for at least 2h in 70 ° C to allow for prehybridisation. Before the probe was added to the embryos it was diluted (1:200 in the hybridisation buffer), heat shocked in 94 ° C and put straight on ice to prevent the secondary structure formation. The embryos were incubated with the probe for overnight on a 70 ° C dryblock. In the morning after the hybridisation the probe was taken off and the embryos were washed as follows: for 30 minutes in 100% hybridisation buffer, for 30 minutes in 50% hybridisation buffer in PBT, 4 times 30 minutes in PBT. All those washes were carried out in 70 ° C in dryblock. The embryos were then briefly washed in PBT in room temperature for 5 minutes on a rotating wheel. After this the embryos were incubated with the anti-DIG alkaline phosphate conjugate antibody (Roche, cat. 11093274910) 1:2000 in PBT for at least 2h in room temperature on a rotating wheel. After incubation the antibody was washed off 3 times for 30 minutes in PBT in room temperature on a rotating wheel. The samples were then transferred to a 24-well microtitre plate and washed with reaction solution (100mM Tris-HCl pH9.5, 100mM NaCl) three times to remove any residual PBT. The embryos were then stained using an NBT/BCIP solution (20µl/ml NBT/BCIP, Roche, cat. 11681451001 in ready solution). The intensity of the staining was checked occasionally using a stereomicroscope to prevent to dark staining. When the staining was satisfactory the reaction was stopped by adding 1ml PBT and the embryos were washed three times for 20 minutes in PBT on a rotating wheel to remove any residual reaction components. The embryos were mounted on microscope slides in 70% glycerol in PBT, covered with coverslips and sealed with nail varnish. Slides were kept in 4 ° C until needed.

27.3.1 Microscopy

The slides were analysed using an Olympus Provis system consisting of an Olympus AX70 microscope and a DP50 Olympus digital camera.

28 Transmission electron microscopy

Adult flies were rinsed in 0.5% Triton X in water to make the cuticle permeable to the phosphate buffer. Dissection was performed in 0.1M PB at pH7.4. Proboscis was removed to facilitate the fixative infiltration. After the fly heads were removed, they were fixed by immersion overnight in 4 $^{\circ}$C in a fixing solution (2.5% glutaraldehyde, 2% paraforlmaldehyde in 0.1M PB pH7.4. After fixing the heads were washed in PB and post-fixed with OsO_4 and dehydrated in an ethanol series. The samples were then embedded in Polybed 812 and ultra thin sections (75nm) were stained with aqueous uranyl acetate and lead citrate. Such prepared adult fly antennae were imaged using Philips CM100 Compustage (FEI) microscope with images taken with AMT CCD camera (Electron Microscopy Research Services, Newcastle University Medical School).

29 DNA injection to make transgenic fly lines

Constructs of interest were cloned into placZattB vector as described above and injected at a concentration of approximately 200ng/ml. This vector contains the attB sites which together with attP sites present in the injection cross flies (inserted in a specific and mapped locus) allow for site-specific recombination of the construct of interest in the presence of ΦC31integrase.

The flies expressing the site-specific recombination components were put is an embryo

collection cage a couple days in advance and fed regularly to encourage egg laying. On the day of injection the red wine agar plate with fresh yeast paste was changed every half an hour to remove any developed embryos and further encourage ample egg laying. The embryos for injection were collected every 30 minutes onto a filter. The embryos were dechorionated in 50% bleach for 4 minutes and washed extensively with water to remove residual bleach. They were then filter dried on a tissue and transferred onto a red wine agar plate for better visibility. Embryos were lined up with forceps to a rectangle of red wine agar with the micropyle (anterior) extending towards the edge of the agar block. The embryos were then transferred to a preglued coverslip with the posterior of each embryo positioned at the edge of the coverslip for injecting. The coverslip was put on a microscope slide and the embryos were dried for 7-9 minutes in a desiccator. After drying the embryos were covered in series 700 halocarbon heavy oil to prevent further dehydration and injected (into syncytial blastoderm) at 18 $^{\circ}$C using standard injecting microscope and injection device. Injected embryos were submerged in series 95 halocarbon oil on a weighing boat and left to develop for 2 days in 21 $^{\circ}$C. On a third day the hatched larvae were collected and transferred to a standard food vials and left until enclosure. The enclosed flies were crossed to each other and the progeny was screened for transformants on the basis of eye colour - visible marker was 'little' white gene variety so the eye colour of the transformant was pale orange. The transformants were crossed to Pin/Cyo second chromosome balancer flies and made homozygous by segregating the progeny against the balancer.

30 Behavioural analyses

30.1 Adult climbing assay

All climbing assays were performed in 25 $^{\circ}$C between 12.00 and 3.00pm. Young females were collected and transferred to a fresh food vial and left for at least 24h to recover from anesthetic. For the test 15 female flies was transferred to a 100ml measuring cylinder (without anesthesising) with marks at every cm up to 20cm. After approximately 1 minute recovery the cylinder was banged firmly on the table and the flies were allowed to walk up for 10secs at which point a picture was taken. The height to which each fly walked up during the 10 secs period was measured and treated as a single result. Separate replicas of experiments containing 15 flies were repeated 3-5 times giving the n=45 for each fly line tested and the statistical significance was measured using the Student t-test.

For the experiment performed on aging flies the climbing assay was performed as described above but the flies were then transferred to a fresh vial with fly food and re-tested every three days until they were 25 days old. The statistical significance of the aging flies climbing assay was calculated using the two-way Anova.

30.2 Male fertility assay

Individual 2-3 days old male flies were put into the fresh food vial together with 3 virgin wild type (Or-R) females and left to mate for 2 days. After the mating period the flies were transferred to a fresh food vial and left to lay eggs for 5 days. After 5 days the flies were tipped out and the progeny was counted after the enclosure. The number of progeny in each replica was treated as a separate result. The experiments was carried out in 6 replicas for each fly line tested and the statistical significance

was measured with Student t-test.

30.3 Grooming assay

Adult 2-3 days old flies were anesthetized, decapitated and left to recover for 2 hours in a humid container. After the recovery period flies able to maintain an upright posture were selected for the experiment. Touching a single scutellar macroachaeta with forceps for 10 secs results in vigorous cleaning reaction with forelegs. Each fly was scored 1 for a reaction and 0 for no reaction. N=35 was used for each fly line tested and the statistical significance was calculated using Student t-test.

Appendix A

Fly Stocks

General fly stocks

Genotype	Nature of allele	Source/reference
w^{1118}	used as WT	Bloomington
Sca-Gal4	Gal4 driver	Młodzik et al, 2002
P{w[+mC]=UAS-Dcr-2.D}1,w[1118];sca-Gal4	Gal4 driver	made by Lina Ma
yw;Pin/Cyo	Visible, dominant balancer	Bloomington
yw;Ly/TM3,Sb	Visible, dominant balancer	Bloomington
yw;Sp/Cyo,KrGFP;Sb/TM6B	Visible, dominant double balancer	from Dr G. Pennetta
Sc/FM6;P[hs-Gal4]/CyO	Visible, dominant double balancer	from Dr G. Pennetta

Part 2

Genotype	Nature of allele	Source/reference
w;Tft/Cyo;Bam-Gal4:VP16	Gal4 driver	Chen and McKearin, 2003
P{GD11829}v22694	DmRootletin GD RNAi line	VDRC
P{KK102209}VIE-260B	DmRootletin KK RNAi line	VDRC
P{KK100496}VIE-260B	Nek2 KK RNAi line	VDRC
y,w[1118];P{attP,y[+],w[3‘]	KK library control stock	VDRC
P{UAS-mCD8::GFP.L}LL6	mCD8-GFP fusion protein expressing line	Bloomington

Part 3

Genotype	Nature of allele	Source/reference
w, fd3F^{1}	deletion allele	Cachero et al, 2011
y,w; RFX^{49}/TM3,KrGFP,Sb	RFX mutant	Dubruille et al, 2002
fd3F;RFX^{49}/TM3,KrGFP,Sb	double mutant	made by Petra zur Lage

Part 4

Genotype	Nature of allele	Source/reference
P{KK100221}VIE-260B	Zmynd10 KK RNAi line	VDRC
y[1] w[67c23];P{w[+mC] y[+mDint2]=EPgy2} Zmynd10[EY10866]	Zmynd10 mutant	Bloomington
sca-Gal4;Dhc93AB enh-GFP	Dhc93AB enhancer reporter gene line	made by Fay G. Newton

Appendix B

Primers

Chapter 2

Name	Sequence	Application
DmRootletin 3' T7	GTAATACGACTCACTATAGGG TTGTAGGGCCATTTGTAGCC	RNA in situ hybridisation
DmRootletin 5'	GAAGGCTCAAGTGGAGTTCG	
*Hale-bopp 3' T7	GTAATACGACTCACTATAGGG CGCAATGAGGCTCTCTCTTCG	RT-PCR
*Hale-bopp 5'	AGTTCAATGGTGGCTTGGAC	
DmRootletin 3'	CGGGAAAAGTCGGAGCTACG	
DmRootletin 5'	CTCGCACTCCAACTGTTTGACT	
tbp 3'	CAGGGGCAAAGAGTGAGGAC	
tbp 5'	CTTGACATCGCAGGAGCCGA	
Nek2 3' T7	GTAATACGACTCATCATAGGG CGAGGATTCACTGCCGGTTTA	RNA in situ hybridisation
Nek2 5'	GCAGTCCTCGTGCTCTTACC	
Primers marked with * were obtained from Petra zur Lage		

Chapter 3

Name	Sequence	Application
DmRootletin 3' A	**TCTAGA**CAATAATGCATCGATCGTGC	enhancer-reporter constructs
DmRootletin 5' A	**GAATTC**CTGCTGGCAAAATCCGAACTG	
DmRootletin 3' B	**TCTAGA**TTGGCCGGGGTGCCTGGGAC	
DmRootletin 5' B	**GAATTC**GATCGGACTTTACGTGACTGC	
DmRootletin 3' C	**TCTAGA**CTCGCCTACGCTACAGACG	
DmRootletin 5' C	**GAATTC**ACGAGGACAAGGAAATTATTATGA	

Chapter 4

Name	Sequence	Application
*Dhc93AB 3' T7	GTAATACGACTCACTATAGGG CCGCTTCTCATTGGGCTTTAG	RNA in situ hybridisation
*Dhc93AB 5'	GGTGGCTGCTCTTCAGAATC	
*Dhc62B 3' T7	GTAATACGACTCACTATAGGG CGGTAGCATCGATCCGTCAGT	
*Dhc62B 5'	CAGCAGTGACAAGGAAACGA	
*CG6971 3' T7	GTAATACGACTCACTATAGGG CTACCTGTCTCACGAGCTTGG	
*CG6971 5'	CAAACCTGCTGAATTCCTGA	
*CG9313 3' T7	GTAATACGACTCACTATAGGG CTATTCTTCCACACCTTGACC	
*CG9313 5'	TATCCTCCCACACCTTGACC	
*fd3F 3' T7	GTAATACGACTCACTATAGGG CGGTTGAACTCGTCGCTGAAG	
*fd3F 5'	TAACCCACATTTTCGGAAGG	
Primers marked with * were obtained from Petra zur Lage		

Name	Sequence	Application
Dhc93AB 3’	AATGGCCAGAATCCAACTCCACACA	RT-PCR
Dhc93AB 5’	CTTGAGGCGATTGTTCCAAAATGT	
Dhc62B 3’	CGGGAGAAGTTCGACGTGTTCTT	
Dhc62B 5’	CGGAGGATCAGTGTCCCATAG	
CG6971 3’	CGCGAGCTGTACTCACAATGTTTTG	
CG6971 5’	GCAGTACAATGTTTCATAGGCCT	
CG9313 3’	CTCGACATCCTCGTCTTCTACGGC	
CG9313 5’	CTACACTGTGGTGGAGCAGCGCGA	
fd3F 3’	TGGAAGTACAGTCGGTCAACTCTAT	
fd3F 5’	GTAACAACCACGTCCTTGTGTATG	

Appendix C

Antibodies

Antibody	Dilution	Reference/Source
Mouse α 22C10	1:200	Developmental Biology
Mouse α 21A6	1:500	Hybridoma Bank, Iowa
Rabbit α HRP	1:500	Jackson Immuno Research labs
Rabit α GFP	1:200	Molecular probes, Invitrogen
Rabbit α Couch Potato	1:1000	Bellen et al., 1992
Mouse α NompC	1:100	Donated by Jonathan Howard
Rabbit α Sas4	1:200	Basto et al, 2006
Rabbit α β-gal	1:500	MP Biomedicals (former Cappel)
Rabbit α γ-tubulin	1:500	Sigma
Rabbit α Nek2	1:500 1:1000 for Western blot	Prigent et al, 2005
Goat α Actin	1:400	Santa Cruz Biotechnology

References

Acar, M., Jafar-Nejad, H., Giagtzoglou, N., Yallampalli, S., David, G., He, Y., Delidakis, C., Bellen, H. J., 2006. Senseless physically interacts with proneural proteins and functions as a transcriptional co-activator. Development (Cambridge, England) 133 (10), 1979–1989.

Aerts, S., Quan, X. J., Claeys, A., Sanchez, M. N., Tate, P., Yan, J., Hassan, B. A., 2010. Robust target gene discovery through transcriptome perturbations and genome-wide enhancer predictions in drosophila uncovers a regulatory basis for sensory specification. PLoS Biology 8 (7).

Aftab, S., Semenec, L., Chu, J. S.-C., Chen, N., 2008. Identification and characterization of novel human tissue-specific RFX transcription factors. BMC evolutionary biology 8, 226.

Ait-Lounis, A., Baas, D., Barras, E., Benadiba, C., Charollais, A., Nlend, R. N., Liègeois, D., Meda, P., Durand, B., Reith, W., 2007. Novel function of the ciliogenic transcription factor RFX3 in development of the endocrine pancreas. Diabetes 56 (4), 950–959.

Andersen, S. S., 1999. Molecular characteristics of the centrosome. International review of cytology 187, 51–109.

Archer, F. L., Wheatley, D. N., 1971. Cilia in cell-cultured fibroblasts. II. Incidence in mitotic and post-mitotic BHK 21-C13 fibroblasts. Journal of anatomy 109 (Pt 2), 277–292.

Arnaiz, O., Malinowska, A., Klotz, C., Sperling, L., Dadlez, M., Koll, F., Cohen, J., Jan. 2009. Cildb: a knowledgebase for centrosomes and cilia. Database : the

journal of biological databases and curation 2009, bap022.
URL http://www.pubmedcentral.nih.gov/articlerender.fcgi?artid=2860946&tool=pmce

Artavanis-Tsakonas, S., 1999. Notch Signaling: Cell Fate Control and Signal Integration in Development.

Aubusson-Fleury, A., Lemullois, M., de Loubresse, N. G., Laligne, C., Cohen, J., Rosnet, O., Jerka-Dziadosz, M., Beisson, J., Koll, F., 2012. FOR20, a conserved centrosomal protein, is required for assembly of the transition zone and basal body docking at the cell surface.

Avidor-Reiss, T., Maer, A. M., Koundakjian, E., Polyanovsky, A., Keil, T., Subramaniam, S., Zuker, C. S., 2004. Decoding Cilia Function.

Azimzadeh, J., Bornens, M., Jul. 2007. Structure and duplication of the centrosome. Journal of cell science 120 (Pt 13), 2139–42.
URL http://jcs.biologists.org/content/120/13/2139

Badano, J. L., Katsanis, N., 2006. Life without Centrioles: Cilia in the Spotlight.

Bahe, S., Stierhof, Y. D., Wilkinson, C. J., Leiss, F., Nigg, E. A., 2005. Rootletin forms centriole-associated filaments and functions in centrosome cohesion. Journal of Cell Biology 171 (1), 27–33.

Baker, J. D., Adhikarakunnathu, S., Kernan, M. J., 2004. Mechanosensory-defective, male-sterile unc mutants identify a novel basal body protein required for ciliogenesis in Drosophila. Development (Cambridge, England) 131 (14), 3411–3422.

Barolo, S., 2012. Shadow enhancers: Frequently asked questions about distributed cis-regulatory information and enhancer redundancy. BioEssays 34 (2), 135–141.

Basto, R., Brunk, K., Vinadogrova, T., Peel, N., Franz, A., Khodjakov, A., Raff, J. W., 2008. Centrosome Amplification Can Initiate Tumorigenesis in Flies. Cell 133 (6), 1032–1042.

Basto, R., Lau, J., Vinogradova, T., Gardiol, A., Woods, C. G., Khodjakov, A., Raff, J. W., 2006. Flies without Centrioles. Cell 125 (7), 1375–1386.

Bauer, M. C., O'Connell, D. J., Maj, M., Wagner, L., Cahill, D. J., Linse, S., 2011. Identification of a high-affinity network of secretagogin-binding proteins involved in vesicle secretion. Molecular bioSystems 7 (7), 2196–2204.

Bechstedt, S., Albert, J. T., Kreil, D. P., Müller-Reichert, T., Göpfert, M. C., Howard, J., 2010. A doublecortin containing microtubule-associated protein is implicated in mechanotransduction in Drosophila sensory cilia. Nature communications 1, 11.

Bejerano, G., Pheasant, M., Makunin, I., Stephen, S., Kent, W. J., Mattick, J. S., Haussler, D., 2004. Ultraconserved elements in the human genome. Science (New York, N.Y.) 304 (5675), 1321–1325.

Bellen, H. J., Kooyer, S., D'Evelyn, D., Pearlman, J., 1992. The Drosophila couch potato protein is expressed in nuclei of peripheral neuronal precursors and shows homology to RNA-binding proteins. Genes and Development 6 (11), 2125–2136.

Benadiba, C., Magnani, D., Niquille, M., Morlé, L., Valloton, D., Nawabi, H., Ait-Lounis, A., Otsmane, B., Reith, W., Theil, T., Hornung, J. P., Lebrand, C., Durand, B., 2012. The Ciliogenic Transcription Factor RFX3 regulates early midline distribution of guidepost neurons required for corpus callosum development. PLoS Genetics 8 (3).

Benayoun, B. A., Caburet, S., Veitia, R. A., 2011. Forkhead transcription factors: key players in health and disease. Trends in genetics : TIG 27 (6), 224–232.

Benbahouche, N. E. H., Iliopoulos, I., Török, I., Marhold, J., Henri, J., Kajava, A. V., Farkaš, R., Kempf, T., Schnölzer, M., Meyer, P., Kiss, I., Bertrand, E., Mechler, B. M., Pradet-Balade, B., Feb. 2014. Drosophila Spag is the homolog of RNA polymerase II-associated protein 3 (RPAP3) and recruits the heat shock proteins 70 and 90 (Hsp70 and Hsp90) during the assembly of cellular machineries. The Journal of biological chemistry 289 (9), 6236–47.
URL http://www.pubmedcentral.nih.gov/articlerender.fcgi?artid=3937688&tool=pmce

Bertrand, N., Castro, D. S., Guillemot, F., 2002. Proneural genes and the specification of neural cell types. Nature reviews. Neuroscience 3 (7), 517–530.

Betschinger, J., Knoblich, J. A., 2004. Dare to be different: Asymmetric cell division in Drosophila, C. elegans and vertebrates.

Bettencourt-Dias, M., Glover, D. M., 2007. Centrosome biogenesis and function: centrosomics brings new understanding. Nature reviews. Molecular cell biology 8 (6), 451–463.

Bettencourt-Dias, M., Rodrigues-Martins, A., Carpenter, L., Riparbelli, M., Lehmann, L., Gatt, M. K., Carmo, N., Balloux, F., Callaini, G., Glover, D. M., 2005. SAK/PLK4 is required for centriole duplication and flagella development. Current Biology 15 (24), 2199–2207.

Bhogaraju, S., Cajanek, L., Fort, C., Blisnick, T., Weber, K., Taschner, M., Mizuno, N., Lamla, S., Bastin, P., Nigg, E. a., Lorentzen, E., 2013. Molecular basis of tubulin transport within the cilium by IFT74 and IFT81. Science (New York,

N.Y.) 341 (6149), 1009–12.

URL http://www.ncbi.nlm.nih.gov/pubmed/23990561

Birnbaum, R. Y., Clowney, E. J., Agamy, O., Kim, M. J., Zhao, J., Yamanaka, T., Pappalardo, Z., Clarke, S. L., Wenger, A. M., Nguyen, L., Gurrieri, F., Everman, D. B., Schwartz, C. E., Birk, O. S., Bejerano, G., Lomvardas, S., Ahituv, N., 2012. Coding exons function as tissue-specific enhancers of nearby genes. Genome Research 22 (6), 1059–1068.

Bischof, J., Maeda, R. K., Hediger, M., Karch, F., Basler, K., 2007. An optimized transgenesis system for Drosophila using germ-line-specific phiC31 integrases. Proceedings of the National Academy of Sciences of the United States of America 104 (9), 3312–3317.

Blatt, E. N., Yan, X. H., Wuerffel, M. K., Hamilos, D. L., Brody, S. L., 1999. Forkhead transcription factor HFH-4 expression is temporally related to ciliogenesis. American Journal of Respiratory Cell and Molecular Biology 21 (2), 168–176.

Blochlinger, K., Bodmer, R., Jan, L. Y., Jan, Y. N., 1990. Patterns of expression of Cut, a protein required for external sensory organ development in wild-type and cut mutant Drosophila embryos. Genes and Development 4 (8), 1322–1331.

Blochlinger, K., Jan, L. Y., Jan, Y. N., 1991. Transformation of sensory organ identity by ectopic expression of Cut in Drosophila. Genes and Development 5 (7), 1124–1135.

Blouin, J. L., Meeks, M., Radhakrishna, U., Sainsbury, A., Gehring, C., Saïl, G. D., Bartoloni, L., Dombi, V., O'Rawe, A., Walne, A., Chung, E., Afzelius, B. A., Armengot, M., Jorissen, M., Schidlow, D. V., van Maldergem, L., Walt, H., Gardiner, R. M., Probst, D., Guerne, P. A., Delozier-Blanchet, C. D., Antonarakis, S. E.,

2000. Primary ciliary dyskinesia: a genome-wide linkage analysis reveals extensive locus heterogeneity. European journal of human genetics : EJHG 8 (2), 109–118.

Blow, M. J., McCulley, D. J., Li, Z., Zhang, T., Akiyama, J. A., Holt, A., Plajzer-Frick, I., Shoukry, M., Wright, C., Chen, F., Afzal, V., Bristow, J., Ren, B., Black, B. L., Rubin, E. M., Visel, A., Pennacchio, L. A., 2010. ChIP-Seq identification of weakly conserved heart enhancers. Nature genetics 42 (9), 806–810.

Bodmer, R., Barbel, S., Sheperd, S., Jack, J. W., Jan, L. Y., Jan, Y. N., 1987. Transformation of sensory organs by mutations of the cut locus of D. melanogaster. Cell 51 (2), 293–307.

Bodmer, R., Jan, Y. N., 1987. Morphological differentiation of the embryonic peripheral neurons in Drosophila. Rouxs Archives Of Developmental Biology 196 (2), 69–77.
URL http://www.springerlink.com/content/h88725m6371v3106/

Bonaccorsi, S., Giansanti, M. G., Gatti, M., Jan. 2000. Spindle assembly in Drosophila neuroblasts and ganglion mother cells. Nature cell biology 2 (1), 54–6.
URL http://www.ncbi.nlm.nih.gov/pubmed/10620808

Brear, A. G., Yoon, J., Wojtyniak, M., Sengupta, P., 2014. Diverse cell type-specific mechanisms localize G protein-coupled receptors to Caenorhabditis elegans sensory cilia. Genetics 197 (2), 667–684.

Brewster, R., Bodmer, R., 1995. Origin and specification of type II sensory neurons in Drosophila. Development (Cambridge, England) 121 (9), 2923–2936.

Brody, S. L., Yan, X. H., Wuerffel, M. K., Song, S. K., Shapiro, S. D., 2000. Ciliogenesis and left-right axis defects in forkhead factor HFH-4-null mice. American Journal of Respiratory Cell and Molecular Biology 23 (1), 45–51.

Buchman, J. J., Tsai, L.-H., 2007. Spindle regulation in neural precursors of flies and mammals. Nature reviews. Neuroscience 8 (2), 89–100.

Cachero, S., Simpson, T. I., zur Lage, P. I., Ma, L., Newton, F. G., Holohan, E. E., Armstrong, J. D., Jarman, A. P., 2011. The gene regulatory cascade linking proneural specification with differentiation in Drosophila sensory neurons. PLoS Biology 9 (1).

Caldwell, J. C., Eberl, D. F., Nov. 2002. Towards a molecular understanding of Drosophila hearing. Journal of neurobiology 53 (2), 172–89.
URL http://www.pubmedcentral.nih.gov/articlerender.fcgi?artid=1805767&tool=pmce

Caldwell, J. C., Miller, M. M., Wing, S., Soll, D. R., Eberl, D. F., 2003. Dynamic analysis of larval locomotion in Drosophila chordotonal organ mutants. Proceedings of the National Academy of Sciences of the United States of America 100 (26), 16053–16058.

Callaini, G., Riparbelli, M. G., 1990. Centriole and centrosome cycle in the early Drosophila embryo. Journal of cell science 97 (Pt 3), 539–543.

Carvalho-Santos, Z., Azimzadeh, J., Pereira-Leal, J. B., Bettencourt-Dias, M., 2011. Tracing the origins of centrioles, cilia, and flagella.

Chen, D., McKearin, D. M., 2003. A discrete transcriptional silencer in the bam gene determines asymmetric division of the Drosophila germline stem cell. Development (Cambridge, England) 130 (6), 1159–1170.

Chen, J., Knowles, H. J., Hebert, J. L., Hackett, B. P., 1998. Mutation of the mouse hepatocyte nuclear factor/forkhead homologue 4 gene results in an absence of cilia and random left-right asymmetry. Journal of Clinical Investigation 102 (6), 1077–1082.

Choksi, S. P., Lauter, G., Swoboda, P., Roy, S., 2014. Switching on cilia: transcriptional networks regulating ciliogenesis. Development (Cambridge, England) 141 (7), 1427–41.
URL http://www.ncbi.nlm.nih.gov/pubmed/24644260

Chung, M. I., Peyrot, S. M., LeBoeuf, S., Park, T. J., McGary, K. L., Marcotte, E. M., Wallingford, J. B., 2012. RFX2 is broadly required for ciliogenesis during vertebrate development. Developmental Biology 363 (1), 155–165.

Clevidence, D. E., Overdier, D. G., Tao, W., Qian, X., Pani, L., Lai, E., Costa, R. H., 1993. Identification of nine tissue-specific transcription factors of the hepatocyte nuclear factor 3/forkhead DNA-binding-domain family. Proceedings of the National Academy of Sciences of the United States of America 90 (9), 3948–3952.

Cole, E. S., Palka, J., 1982. The pattern of campaniform sensilla on the wing and haltere of Drosophila melanogaster and several of its homeotic mutants. Journal of embryology and experimental morphology 71, 41–61.

Conroy, P. C., Saladino, C., Dantas, T. J., Lalor, P., Dockery, P., Morrison, C. G., 2012. C-NAP1 and rootletin restrain DNA damage-induced centriole splitting and facilitate ciliogenesis. Cell Cycle 11 (20), 3769–3778.

Cottam, D. M., Tucker, J. B., Rogers-Bald, M. M., Mackie, J. B., Macintyre, J., Scarborough, J. A., Ohkura, H., Milner, M. J., 2006. Non-centrosomal microtubule-organising centres in cold-treated cultured Drosophila cells. Cell Motility and the Cytoskeleton 63 (2), 88–100.

Cruz, C., Ribes, V., Kutejova, E., Cayuso, J., Lawson, V., Norris, D., Stevens, J., Davey, M., Blight, K., Bangs, F., Mynett, A., Hirst, E., Chung, R., Balaskas, N.,

Brody, S. L., Marti, E., Briscoe, J., 2010. Foxj1 regulates floor plate cilia architecture and modifies the response of cells to sonic hedgehog signalling. Development (Cambridge, England) 137 (24), 4271–4282.

Culí, J., Modolell, J., 1998. Proneural gene self-stimulation in neural precursors: An essential mechanism for sense organ development that is regulated by Notch signaling. Genes and Development 12 (13), 2036–2047.

Deane, J. A., Cole, D. G., Seeley, E. S., Diener, D. R., Rosenbaum, J. L., 2001. Localization of intraflagellar transport protein IFT52 identifies basal body transitional fibers as the docking site for IFT particles. Current Biology 11 (20), 1586–1590.

Debec, a., Marcaillou, C., Bobinnec, Y., Borot, C., Jan. 1999. The centrosome cycle in syncytial Drosophila embryos analyzed by energy filtering transmission electron microscopy. Biology of the cell / under the auspices of the European Cell Biology Organization 91 (4-5), 379–391.
URL http://www.ncbi.nlm.nih.gov/pubmed/10519001

Didon, L., Zwick, R. K., Chao, I. W., Walters, M. S., Wang, R., Hackett, N. R., Crystal, R. G., 2013. RFX3 modulation of FOXJ1 regulation of cilia genes in the human airway epithelium. Respiratory research 14 (1), 70.
URL http://www.pubmedcentral.nih.gov/articlerender.fcgi?artid=3710277&tool=pmce

Dietzl, G., Chen, D., Schnorrer, F., Su, K.-C., Barinova, Y., Fellner, M., Gasser, B., Kinsey, K., Oppel, S., Scheiblauer, S., Couto, A., Marra, V., Keleman, K., Dickson, B. J., 2007. A genome-wide transgenic RNAi library for conditional gene inactivation in Drosophila. Nature 448 (7150), 151–156.

Diggle, C. P., Moore, D. J., Mali, G., zur Lage, P., Ait-Lounis, A., Schmidts, M., Shoemark, A., Garcia Munoz, A., Halachev, M. R., Gautier, P., Yeyati, P. L.,

Bonthron, D. T., Carr, I. M., Hayward, B., Markham, A. F., Hope, J. E., von Kriegsheim, A., Mitchison, H. M., Jackson, I. J., Durand, B., Reith, W., Sheridan, E., Jarman, A. P., Mill, P., Sep. 2014. HEATR2 plays a conserved role in assembly of the ciliary motile apparatus. PLoS genetics 10 (9), e1004577.
URL http://www.pubmedcentral.nih.gov/articlerender.fcgi?artid=4168999&tool=pmce

Dubruille, R., Laurençon, A., Vandaele, C., Shishido, E., Coulon-Bublex, M., Swoboda, P., Couble, P., Kernan, M., Durand, B., 2002. Drosophila regulatory factor X is necessary for ciliated sensory neuron differentiation. Development (Cambridge, England) 129 (23), 5487–5498.

Duquesnoy, P., Escudier, E., Vincensini, L., Freshour, J., Bridoux, A. M., Coste, A., Deschildre, A., de Blic, J., Legendre, M., Montantin, G., Tenreiro, H., Vojtek, A. M., Loussert, C., Clément, A., Escalier, D., Bastin, P., Mitchell, D. R., Amselem, S., 2009. Loss-of-Function Mutations in the Human Ortholog of Chlamydomonas reinhardtii ODA7 Disrupt Dynein Arm Assembly and Cause Primary Ciliary Dyskinesia. American Journal of Human Genetics 85 (6), 890–896.

Durand, B., Vandaele, C., Spencer, D., Pantalacci, S., Couble, P., 2000. Cloning and characterization of dRFX, the Drosophila member of the RFX family of transcription factors. Gene 246 (1-2), 285–293.

Eberl, D. F., 1999. Feeling the vibes: Chordotonal mechanisms in insect hearing.

Eberl, D. F., Hardy, R. W., Kernan, M. J., 2000. Genetically similar transduction mechanisms for touch and hearing in Drosophila. The Journal of neuroscience : the official journal of the Society for Neuroscience 20 (16), 5981–5988.

Efimenko, E., Bubb, K., Mak, H. Y., Holzman, T., Leroux, M. R., Ruvkun, G.,

Thomas, J. H., Swoboda, P., 2005. Analysis of xbx genes in C. elegans. Development (Cambridge, England) 132 (8), 1923–1934.

El Zein, L., Ait-Lounis, A., Morlé, L., Thomas, J., Chhin, B., Spassky, N., Reith, W., Durand, B., 2009. RFX3 governs growth and beating efficiency of motile cilia in mouse and controls the expression of genes involved in human ciliopathies. Journal of cell science 122 (Pt 17), 3180–3189.

Elliott, S. L., Cullen, C. F., Wrobel, N., Kernan, M. J., Ohkura, H., 2005. EB1 is essential during Drosophila development and plays a crucial role in the integrity of chordotonal mechanosensory organs. Molecular biology of the cell 16 (2), 891–901.

Emery, P., Durand, B., Mach, B., Reith, W., 1996. RFX proteins, a novel family of DNA binding proteins conserved in the eukaryotic kingdom.

Engel, B. D., Ishikawa, H., Wemmer, K. A., Geimer, S., Wakabayashi, K. I., Hirono, M., Craige, B., Pazour, G. J., Witman, G. B., Kamiya, R., Marshall, W. F., 2012. The role of retrograde intraflagellar transport in flagellar assembly, maintenance, and function. Journal of Cell Biology 199 (1), 151–167.

Engelmann, T. W., Dec. 1880. Zur Anatomie und Physiologie der Flimmerzellen. Pflüger, Archiv für die Gesammte Physiologie des Menschen und der Thiere 23 (1), 505–535.
URL http://link.springer.com/10.1007/BF01637532

Evans, J. E., Snow, J. J., Gunnarson, A. L., Ou, G., Stahlberg, H., McDonald, K. L., Scholey, J. M., 2006. Functional modulation of IFT kinesins extends the sensory repertoire of ciliated neurons in Caenorhabditis elegans. Journal of Cell Biology 172 (5), 663–669.

Everson, G. T., Taylor, M. R. G., Doctor, R. B., 2004. Polycystic disease of the liver.

Faragher, A. J., Fry, A. M., 2003. Nek2A kinase stimulates centrosome disjunction and is required for formation of bipolar mitotic spindles. Molecular biology of the cell 14 (7), 2876–2889.

Fawcett, D. W., Porter, K. R., Mar. 1954. A study of the fine structure of ciliated epithelia. Journal of Morphology 94 (2), 221–281.
URL http://doi.wiley.com/10.1002/jmor.1050940202

Field, L. H., Matheson, T., 1998. Chordotonal Organs of Insects. Advances in Insect Physiology 27 (C).

Follit, J. A., Tuft, R. A., Fogarty, K. E., Pazour, G. J., 2006. The intraflagellar transport protein IFT20 is associated with the Golgi complex and is required for cilia assembly. Molecular biology of the cell 17 (9), 3781–3792.

Follit, J. A., Xu, F., Keady, B. T., Pazour, G. J., 2009. Characterization of mouse IFT complex B. Cell Motility and the Cytoskeleton 66 (8), 457–468.

Fowkes, M. E., Mitchell, D. R., 1998. The role of preassembled cytoplasmic complexes in assembly of flagellar dynein subunits. Molecular biology of the cell 9 (9), 2337–2347.

Freshour, J., Yokoyama, R., Mitchell, D. R., 2007. Chlamydomonas flagellar outer row dynein assembly protein Oda7 interacts with both outer row and I1 inner row dyneins. Journal of Biological Chemistry 282 (8), 5404–5412.

Fry, A. M., 2002. The Nek2 protein kinase: a novel regulator of centrosome structure. Oncogene 21 (40), 6184–6194.

Fry, A. M., Mayor, T., Meraldi, P., Stierhof, Y. D., Tanaka, K., Nigg, E. A., 1998a.

C-Nap1, a novel centrosomal coiled-coil protein and candidate substrate of the cell cycle-regulated protein kinase Nek2. Journal of Cell Biology 141 (7), 1563–1574.

Fry, A. M., Meraldi, P., Nigg, E. A., 1998b. A centrosomal function for the human Nek2 protein kinase, a member of the NIMA family of cell cycle regulators. EMBO Journal 17 (2), 470–481.

Fry, A. M., Nigg, E. A., 1995. Cell cycle. The NIMA kinase joins forces with Cdc2. Current biology : CB 5 (10), 1122–1125.

Gajiwala, K. S., Chen, H., Cornille, F., Roques, B. P., Reith, W., Mach, B., Burley, S. K., 2000. Structure of the winged-helix protein hRFX1 reveals a new mode of DNA binding. Nature 403 (6772), 916–921.

Garcia-Gonzalo, F. R., Corbit, K. C., Sirerol-Piquer, M. S., Ramaswami, G., Otto, E. A., Noriega, T. R., Seol, A. D., Robinson, J. F., Bennett, C. L., Josifova, D. J., García-Verdugo, J. M., Katsanis, N., Hildebrandt, F., Reiter, J. F., 2011. A transition zone complex regulates mammalian ciliogenesis and ciliary membrane composition. Nature genetics 43 (8), 776–784.

Garcia-Gonzalo, F. R., Reiter, J. F., 2012. Scoring a backstage pass: Mechanisms of ciliogenesis and ciliary access. Journal of Cell Biology 197 (6), 697–709.

García-Martínez, J., Aranda, A., Pérez-Ortín, J. E., 2004. Genomic run-on evaluates transcription rates for all yeast genes and identifies gene regulatory mechanisms. Molecular Cell 15 (2), 303–313.

Gariglio, P., Bellard, M., Chambon, P., 1981. Clustering of RNA polymerase B molecules in the 5' moiety of the adult beta-globin gene of hen erythrocytes. Nucleic acids research 9 (11), 2589–2598.

Geremek, M., Bruinenberg, M., Zietkiewicz, E., Pogorzelski, A., Witt, M., Wijmenga, C., 2011. Gene expression studies in cells from primary ciliary dyskinesia patients identify 208 potential ciliary genes. Human Genetics 129 (3), 283–293.

Ghildiyal, M., Zamore, P. D., Feb. 2009. Small silencing RNAs: an expanding universe. Nature reviews. Genetics 10 (2), 94–108.
URL http://www.pubmedcentral.nih.gov/articlerender.fcgi?artid=2724769&tool=pmce

Ghysen, A., Dambly-Chaudière, C., Aceves, E., Jan, L. Y., Jan, Y. N., 1986. Sensory neurons and peripheral pathways in Drosophila embryos. Roux's Archives of Developmental Biology 195 (5), 281–289.

Ghysen, A., Dambly-Chaudière, C., Jan, L. Y., Jan, Y. N., May 1993. Cell interactions and gene interactions in peripheral neurogenesis. Genes & development 7 (5), 723–33.
URL http://www.ncbi.nlm.nih.gov/pubmed/8491375

Gilula, N. B., Satir, P., 1972. The ciliary necklace. A ciliary membrane specialization. Journal of Cell Biology 53 (2), 494–509.

Gönczy, P., 2002. Mechanisms of spindle positioning: Focus on flies and worms.

Gong, Z., Son, W., Chung, Y. D., Kim, J., Shin, D. W., McClung, C. A., Lee, Y., Lee, H. W., Chang, D.-J., Kaang, B.-K., Cho, H., Oh, U., Hirsh, J., Kernan, M. J., Kim, C., 2004. Two interdependent TRPV channel subunits, inactive and Nanchung, mediate hearing in Drosophila. The Journal of neuroscience : the official journal of the Society for Neuroscience 24 (41), 9059–9066.

Gopalakrishnan, J., Mennella, V., Blachon, S., Zhai, B., Smith, A. H., Megraw, T. L., Nicastro, D., Gygi, S. P., Agard, D. A., Avidor-Reiss, T., 2011. Sas-4 provides

a scaffold for cytoplasmic complexes and tethers them in a centrosome. Nature communications 2, 359.

Göpfert, M. C., Albert, J. T., Nadrowski, B., Kamikouchi, A., 2006. Specification of auditory sensitivity by Drosophila TRP channels. Nature neuroscience 9 (8), 999–1000.

Göpfert, M. C., Humphris, A. D. L., Albert, J. T., Robert, D., Hendrich, O., 2005. Power gain exhibited by motile mechanosensory neurons in Drosophila ears. Proceedings of the National Academy of Sciences of the United States of America 102 (2), 325–330.

Göpfert, M. C., Robert, D., Apr. 2003. Motion generation by Drosophila mechanosensory neurons. Proceedings of the National Academy of Sciences of the United States of America 100 (9), 5514–9.
URL http://www.pnas.org/content/100/9/5514.full

Goulding, S. E., zur Lage, P., Jarman, A. P., 2000. amos, a proneural gene for Drosophila olfactory sense organs that is regulated by lozenge. Neuron 25 (1), 69–78.

Graser, S., Stierhof, Y. D., Lavoie, S. B., Gassner, O. S., Lamla, S., Le Clech, M., Nigg, E. A., 2007. Cep164, a novel centriole appendage protein required for primary cilium formation. Journal of Cell Biology 179 (2), 321–330.

Gross, C. T., McGinnis, W., 1996. DEAF-1, a novel protein that binds an essential region in a Deformed response element. The EMBO journal 15 (8), 1961–1970.

Guichard, P., Desfosses, A., Maheshwari, A., Hachet, V., Dietrich, C., Brune, A., Ishikawa, T., Sachse, C., Gonczy, P., 2012. Cartwheel Architecture of Trichonympha Basal Body.

Hagiwara, H., Aoki, T., Ohwada, N., Fujimoto, T., 2000. Identification of a 195 kDa protein in the striated rootlet: Its expression in ciliated and ciliogenic cells. Cell Motility and the Cytoskeleton 45 (3), 200–210.

Haimo, L. T., Rosenbaum, J. L., Dec. 1981. Cilia, flagella, and microtubules. The Journal of cell biology 91 (3 Pt 2), 125s–130s.
URL http://www.pubmedcentral.nih.gov/articlerender.fcgi?artid=2112827&tool=pmce

Han, Y. G., Kwok, B. H., Kernan, M. J., 2003. Intraflagellar Transport Is Required in Drosophila to Differentiate Sensory Cilia but Not Sperm. Current Biology 13 (19), 1679–1686.

Hartenstein, V., 1988. Development of Drosophila larval sensory organs: spatiotemporal pattern of sensory neurones, peripheral axonal pathways and sensilla differentiation. Development 102 (4), 869–886.
URL http://dev.biologists.org/content/102/4/869.abstract

Hartenstein, V., Posakony, J. W., 1989. Development of adult sensilla on the wing and notum of Drosophila melanogaster. Development (Cambridge, England) 107 (2), 389–405.

Hartong, D. T., Berson, E. L., Dryja, T. P., 2006. Retinitis pigmentosa.

Heery, D. M., Kalkhoven, E., Hoare, S., Parker, M. G., 1997. A signature motif in transcriptional co-activators mediates binding to nuclear receptors. Nature 387 (6634), 733–736.

Heintzman, N. D., Ren, B., 2009. Finding distal regulatory elements in the human genome. Current opinion in genetics & development 19 (6), 541–549.

Helps, N. R., Luo, X., Barker, H. M., Cohen, P. T., 2000. NIMA-related kinase 2 (Nek2), a cell-cycle-regulated protein kinase localized to centrosomes, is complexed to protein phosphatase 1. The Biochemical journal 349 (Pt 2), 509–518.

Hirokawa, N., Noda, Y., Tanaka, Y., Niwa, S., 2009. Kinesin superfamily motor proteins and intracellular transport. Nature reviews. Molecular cell biology 10 (10), 682–696.

Hirsch, J., Erlenmeyer-Kimling, L., 1961. Sign of taxis as a property of the genotype. Science (New York, N.Y.) 134, 835–836.

Horani, A., Brody, S. L., Ferkol, T. W., 2013. Picking up speed: advances in the genetics of primary ciliary dyskinesia. Pediatric research 75 (1), 158–164.
URL http://www.ncbi.nlm.nih.gov/pubmed/24192704

Horani, A., Druley, T. E., Zariwala, M. A., Patel, A. C., Levinson, B. T., Van Arendonk, L. G., Thornton, K. C., Giacalone, J. C., Albee, A. J., Wilson, K. S., Turner, E. H., Nickerson, D. A., Shendure, J., Bayly, P. V., Leigh, M. W., Knowles, M. R., Brody, S. L., Dutcher, S. K., Ferkol, T. W., 2012. Whole-exome capture and sequencing identifies HEATR2 mutation as a cause of primary ciliary dyskinesia. American Journal of Human Genetics 91 (4), 685–693.

Hou, Y., Qin, H., Follit, J. A., Pazour, G. J., Rosenbaum, J. L., Witman, G. B., 2007. Functional analysis of an individual IFT protein: IFT46 is required for transport of outer dynein arms into flagella. Journal of Cell Biology 176 (5), 653–665.

Hummel, T., Krukkert, K., Roos, J., Davis, G., Klämbt, C., 2000. Drosophila Futsch/22C10 is a MAP1B-like protein required for dendritic and axonal development. Neuron 26 (2), 357–370.

Hurd, T. W., Hildebrandt, F., 2010. Mechanisms of nephronophthisis and related ciliopathies.

Husain, N., Pellikka, M., Hong, H., Klimentova, T., Choe, K. M., Clandinin, T. R., Tepass, U., 2006. The Agrin/Perlecan-Related Protein Eyes Shut Is Essential for Epithelial Lumen Formation in the Drosophila Retina. Developmental Cell 11 (4), 483–493.

Inbal, A., Volk, T., Salzberg, A., 2004. Recruitment of ectodermal attachment cells via an EGFR-dependent mechanism during the organogenesis of Drosophila proprioceptors. Developmental Cell 7 (2), 241–250.

Ishikawa, H., Kubo, A., Tsukita, S., Tsukita, S., 2005. Odf2-deficient mother centrioles lack distal/subdistal appendages and the ability to generate primary cilia. Nature cell biology 7 (5), 517–524.

Iwama, A., Pan, J., Zhang, P., Reith, W., Mach, B., Tenen, D. G., Sun, Z., 1999. Dimeric RFX proteins contribute to the activity and lineage specificity of the interleukin-5 receptor alpha promoter through activation and repression domains. Molecular and cellular biology 19 (6), 3940–3950.

Jacquet, B. V., Salinas-Mondragon, R., Liang, H., Therit, B., Buie, J. D., Dykstra, M., Campbell, K., Ostrowski, L. E., Brody, S. L., Ghashghaei, H. T., 2009. FoxJ1-dependent gene expression is required for differentiation of radial glia into ependymal cells and a subset of astrocytes in the postnatal brain. Development (Cambridge, England) 136 (23), 4021–4031.

Jafar-Nejad, H., Acar, M., Nolo, R., Lacin, H., Pan, H., Parkhurst, S. M., Bellen, H. J., 2003. Senseless acts as a binary switch during sensory organ precursor selection. Genes and Development 17 (23), 2966–2978.

Jain, R., Devine, T., George, A. D., Chittur, S. V., Baroni, T. E., Penalva, L. O., Tenenbaum, S. A., 2011. RIP-Chip analysis: RNA-Binding Protein Immunoprecipitation-Microarray (Chip) Profiling. Methods in molecular biology (Clifton, N.J.) 703, 247–263.

Jan, L. Y., Jan, Y. N., 1982. Antibodies to horseradish peroxidase as specific neuronal markers in Drosophila and in grasshopper embryos. Proceedings of the National Academy of Sciences of the United States of America 79 (8), 2700–2704.

Jarman, A. P., May 2002. Studies of mechanosensation using the fly. Human molecular genetics 11 (10), 1215–8.
URL http://www.ncbi.nlm.nih.gov/pubmed/12015281

Jarman, A. P., Ahmed, I., 1998. The specificity of proneural genes in determining Drosophila sense organ identity. Mechanisms of Development 76 (1-2), 117–125.

Jarman, A. P., Grau, Y., Jan, L. Y., Yuh Nung Jan, 1993. atonal Is a proneural gene that directs chordotonal organ formation in the Drosophila peripheral nervous system. Cell 73 (7), 1307–1321.

Jarman, A. P., Sun, Y., Jan, L. Y., Jan, Y. N., 1995. Role of the proneural gene, atonal, in formation of Drosophila chordotonal organs and photoreceptors. Development (Cambridge, England) 121 (7), 2019–2030.

Jean, C., Tollon, Y., Raynaud-Messina, B., Wright, M., Aug. 1999. The mammalian interphase centrosome: two independent units maintained together by the dynamics of the microtubule cytoskeleton. European journal of cell biology 78 (8), 549–60.
URL http://www.ncbi.nlm.nih.gov/pubmed/10494861

Jessberger, R., Oct. 2002. The many functions of SMC proteins in chromosome

dynamics. Nature reviews. Molecular cell biology 3 (10), 767–78.
URL http://www.ncbi.nlm.nih.gov/pubmed/12360193

Jha, S., Shibata, E., Dutta, A., 2008. Human Rvb1/Tip49 is required for the histone acetyltransferase activity of Tip60/NuA4 and for the downregulation of phosphorylation on H2AX after DNA damage. Molecular and cellular biology 28 (8), 2690–2700.

Jiménez, F., Campos-Ortega, J. A., 1990. Defective neuroblast commitment in mutants of the achaete-scute complex and adjacent genes of D. melanogaster. Neuron 5 (1), 81–89.

Kakihara, Y., Houry, W. A., Jan. 2012. The R2TP complex: discovery and functions. Biochimica et biophysica acta 1823 (1), 101–7.
URL http://www.ncbi.nlm.nih.gov/pubmed/21925213

Kamikouchi, A., Inagaki, H. K., Effertz, T., Hendrich, O., Fiala, A., Göpfert, M. C., Ito, K., 2009. The neural basis of Drosophila gravity-sensing and hearing. Nature 458 (7235), 165–171.

Kamikouchi, A., Shimada, T., Ito, K., 2006. Comprehensive classification of the auditory sensory projections in the brain of the fruit fly Drosophila melanogaster. Journal of Comparative Neurology 499 (3), 317–356.

Kamiya, R., 1995. Exploring the function of inner and outer dynein arms with Chlamydomonas mutants. In: Cell Motility and the Cytoskeleton. Vol. 32. pp. 98–102.

Kavlie, R. G., Kernan, M. J., Eberl, D. F., 2010. Hearing in drosophila requires TilB, a conserved protein associated with ciliary motility. Genetics 185 (1), 177–188.

Kernan, M., Cowan, D., Zuker, C., 1994. Genetic dissection of mechanosensory transduction: mechanoreception-defective mutations of Drosophila. Neuron 12 (6), 1195–1206.

Kernan, M. J., 2007. Mechanotransduction and auditory transduction in Drosophila.

Kim, J., Chung, Y. D., Park, D.-Y., Choi, S., Shin, D. W., Soh, H., Lee, H. W., Son, W., Yim, J., Park, C.-S., Kernan, M. J., Kim, C., 2003. A TRPV family ion channel required for hearing in Drosophila. Nature 424 (6944), 81–84.

King, T. H., Decatur, W. A., Bertrand, E., Maxwell, E. S., Fournier, M. J., 2001. A well-connected and conserved nucleoplasmic helicase is required for production of box C/D and H/ACA snoRNAs and localization of snoRNP proteins. Molecular and cellular biology 21 (22), 7731–7746.

Kinzel, D., Boldt, K., Davis, E. E., Burtscher, I., Trümbach, D., Diplas, B., Attié-Bitach, T., Wurst, W., Katsanis, N., Ueffing, M., Lickert, H., 2010. Pitchfork Regulates Primary Cilia Disassembly and Left-Right Asymmetry. Developmental Cell 19 (1), 66–77.

Klaes, A., Menne, T., Stollewerk, A., Scholz, H., Klambt, C., 1994. The Ets transcription factors encoded by the Drosophila gene pointed direct glial cell differentiation in the embryonic CNS. Cell 78 (1), 149–160.

Klotz, C., Bordes, N., Laine, M. C., Sandoz, D., Bornens, M., 1986. A protein of 175,000 daltons associated with striated rootlets in ciliated epithelia, as revealed by a monoclonal antibody. Cell motility and the cytoskeleton 6 (1), 56–67.

Kobayashi, T., Dynlacht, B. D., 2011. Regulating the transition from centriole to basal body.

Koch, F., Fenouil, R., Gut, M., Cauchy, P., Albert, T. K., Zacarias-Cabeza, J., Spicuglia, S., de la Chapelle, A. L., Heidemann, M., Hintermair, C., Eick, D., Gut, I., Ferrier, P., Andrau, J.-C., 2011. Transcription initiation platforms and GTF recruitment at tissue-specific enhancers and promoters. Nature structural & molecular biology 18 (8), 956–963.

Kott, E., Duquesnoy, P., Copin, B., Legendre, M., Dastot-Le Moal, F., Montantin, G., Jeanson, L., Tamalet, A., Papon, J. F., Siffroi, J. P., Rives, N., Mitchell, V., De Blic, J., Coste, A., Clement, A., Escalier, D., Touré, A., Escudier, E., Amselem, S., 2012. Loss-of-function mutations in LRRC6, a gene essential for proper axonemal assembly of inner and outer dynein arms, cause primary ciliary dyskinesia. American Journal of Human Genetics 91 (5), 958–964.

Kozminski, K. G., Beech, P. L., Rosenbaum, J. L., 1995. The Chlamydomonas kinesin-like protein FLA10 is involved in motility associated with the flagellar membrane. Journal of Cell Biology 131 (6 I), 1517–1527.

Kozminski, K. G., Johnson, K. A., Forscher, P., Rosenbaum, J. L., 1993. A motility in the eukaryotic flagellum unrelated to flagellar beating. Proceedings of the National Academy of Sciences of the United States of America 90 (12), 5519–5523.

Lanzetti, L., 2007. Actin in membrane trafficking.

Laurençon, A., Dubruille, R., Efimenko, E., Grenier, G., Bissett, R., Cortier, E., Rolland, V., Swoboda, P., Durand, B., 2007. Identification of novel regulatory factor X (RFX) target genes by comparative genomics in Drosophila species. Genome biology 8 (9), R195.

Lee, E., Sivan-Loukianova, E., Eberl, D. F., Kernan, M. J., 2008. An IFT-A Pro-

tein Is Required to Delimit Functionally Distinct Zones in Mechanosensory Cilia. Current Biology 18 (24), 1899–1906.

Lee, J., Gollahon, L., 2013. Mitotic perturbations induced by Nek2 overexpression require interaction with TRF1 in breast cancer cells. Cell Cycle 12 (23), 3599–3614.

Lee, J., Moon, S., Cha, Y., Chung, Y. D., 2010. Drosophila TRPN(=NOMPC) channel localizes to the distal end of mechanosensory cilia. PLoS ONE 5 (6).

Lefebvre, P., Jun. 1980. Increased levels of mRNAs for tubulin and other flagellar proteins after amputation or shortening of Chlamydomonas Flagella. Cell 20 (2), 469–477.
URL http://www.cell.com/article/0092867480906339/fulltext

Lemullois, M., Gounon, P., Sandoz, D., 1987. Relationships between cytokeratin filaments and centriolar derivatives during ciliogenesis in the quail oviduct. Biology of the cell / under the auspices of the European Cell Biology Organization 61 (1-2), 39–49.

Li, C.-S., Zhang, Q., Lim, M.-K., Sheen, D.-H., Shim, S.-C., Kim, J.-Y., Lee, S.-S., Yun, K.-J., Moon, H.-B., Chung, H.-T., Chae, S.-C., 2007. Association of FOXJ1 polymorphisms with systemic lupus erythematosus and rheumatoid arthritis in Korean population. Experimental & molecular medicine 39 (6), 805–811.

Li, J. B., Gerdes, J. M., Haycraft, C. J., Fan, Y., Teslovich, T. M., May-Simera, H., Li, H., Blacque, O. E., Li, L., Leitch, C. C., Lewis, R. A., Green, J. S., Parfrey, P. S., Leroux, M. R., Davidson, W. S., Beales, P. L., Guay-Woodford, L. M., Yoder, B. K., Stormo, G. D., Katsanis, N., Dutcher, S. K., 2004. Comparative genomics identifies a flagellar and basal body proteome that includes the BBS5 human disease gene. Cell 117 (4), 541–552.

Lin, L., Spoor, M. S., Gerth, A. J., Brody, S. L., Peng, S. L., 2004. Modulation of Th1 activation and inflammation by the NF-kappaB repressor Foxj1. Science (New York, N.Y.) 303 (5660), 1017–1020.

Loges, N. T., Olbrich, H., Becker-Heck, A., Häffner, K., Heer, A., Reinhard, C., Schmidts, M., Kispert, A., Zariwala, M. A., Leigh, M. W., Knowles, M. R., Zentgraf, H., Seithe, H., Nürnberg, G., Nürnberg, P., Reinhardt, R., Omran, H., 2009. Deletions and Point Mutations of LRRC50 Cause Primary Ciliary Dyskinesia Due to Dynein Arm Defects. American Journal of Human Genetics 85 (6), 883–889.

Lomvardas, S., Barnea, G., Pisapia, D. J., Mendelsohn, M., Kirkland, J., Axel, R., 2006. Interchromosomal Interactions and Olfactory Receptor Choice. Cell 126 (2), 403–413.

Lutterbach, B., Sun, D., Schuetz, J., Hiebert, S. W., 1998. The MYND motif is required for repression of basal transcription from the multidrug resistance 1 promoter by the t(8;21) fusion protein. Molecular and cellular biology 18 (6), 3604–3611.

Maiti, A. K., Bartoloni, L., Mitchison, H. M., Meeks, M., Chung, E., Spiden, S., Gehrig, C., Rossier, C., DeLozier-Blanchet, C. D., Blouin, J., Gardiner, R. M., Antonarakis, S. E., 2000. No deleterious mutations in the FOXJ1 (alias HFH-4) gene in patients with primary ciliary dyskinesia (PCD). Cytogenetics and cell genetics 90 (1-2), 119–122.

Mall, M. A., 2008. Role of cilia, mucus, and airway surface liquid in mucociliary dysfunction: lessons from mouse models. Journal of aerosol medicine and pulmonary drug delivery 21 (1), 13–24.

Martinez-Campos, M., Basto, R., Baker, J., Kernan, M., Raff, J. W., 2004. The

Drosophila pericentrin-like protein is essential for cilia/flagella function, but appears to be dispensable for mitosis. Journal of Cell Biology 165 (5), 673–683.

May, S. R., Ashique, A. M., Karlen, M., Wang, B., Shen, Y., Zarbalis, K., Reiter, J., Ericson, J., Peterson, A. S., 2005. Loss of the retrograde motor for IFT disrupts localization of Smo to cilia and prevents the expression of both activator and repressor functions of Gli. Developmental Biology 287 (2), 378–389.

Mayor, T., Stierhof, Y. D., Tanaka, K., Fry, A. M., Nigg, E. A., 2000. The centrosomal protein C-Nap1 is required for cell cycle-regulated centrosome cohesion. Journal of Cell Biology 151 (4), 837–846.

McClintock, T. S., Glasser, C. E., Bose, S. C., Bergman, D. A., 2008. Tissue expression patterns identify mouse cilia genes. Physiological genomics 32 (2), 198–206.

McInerney, E. M., Rose, D. W., Flynn, S. E., Westin, S., Mullen, T. M., Krones, A., Inostroza, J., Torchia, J., Nolte, R. T., Assa-Munt, N., Milburn, M. V., Glass, C. K., Rosenfeld, M. G., 1998. Determinants of coactivator LXXLL motif specificity in nuclear receptor transcriptional activation. Genes and Development 12 (21), 3357–3368.

Megraw, T. L., Kao, L. R., Kaufman, T. C., 2001. Zygotic development without functional mitotic centrosomes. Current Biology 11 (2), 116–120.

Melnick, A. M., Westendorf, J. J., Polinger, A., Carlile, G. W., Arai, S., Ball, H. J., Lutterbach, B., Hiebert, S. W., Licht, J. D., 2000. The ETO protein disrupted in t(8;21)-associated acute myeloid leukemia is a corepressor for the promyelocytic leukemia zinc finger protein. Molecular and cellular biology 20 (6), 2075–2086.

Menco, B. P., 1984. Ciliated and microvillous structures of rat olfactory and nasal

respiratory epithelia. A study using ultra-rapid cryo-fixation followed by freeze-substitution or freeze-etching. Cell and tissue research 235 (2), 225–241.

Meraldi, P., Nigg, E. A., 2001. Centrosome cohesion is regulated by a balance of kinase and phosphatase activities. Journal of cell science 114 (Pt 20), 3749–3757.

Merrill, A. E., Merriman, B., Farrington-Rock, C., Camacho, N., Sebald, E. T., Funari, V. A., Schibler, M. J., Firestein, M. H., Cohn, Z. A., Priore, M. A., Thompson, A. K., Rimoin, D. L., Nelson, S. F., Cohn, D. H., Krakow, D., 2009. Ciliary Abnormalities Due to Defects in the Retrograde Transport Protein DYNC2H1 in Short-Rib Polydactyly Syndrome. American Journal of Human Genetics 84 (4), 542–549.

Mitchison, H. M., Schmidts, M., Loges, N. T., Freshour, J., Dritsoula, A., Hirst, R. A., O'Callaghan, C., Blau, H., Al Dabbagh, M., Olbrich, H., Beales, P. L., Yagi, T., Mussaffi, H., Chung, E. M. K., Omran, H., Mitchell, D. R., Apr. 2012. Mutations in axonemal dynein assembly factor DNAAF3 cause primary ciliary dyskinesia. Nature genetics 44 (4), 381–9, S1–2.
URL http://www.pubmedcentral.nih.gov/articlerender.fcgi?artid=3315610&tool=pmce

Mohan, S., Timbers, T. A., Kennedy, J., Blacque, O. E., Leroux, M. R., 2013. Striated rootlet and nonfilamentous forms of rootletin maintain ciliary function. Current Biology 23 (20), 2016–2022.

Moore, D. J., Onoufriadis, A., Shoemark, A., Simpson, M. A., Zur Lage, P. I., De Castro, S. C., Bartoloni, L., Gallone, G., Petridi, S., Woollard, W. J., Antony, D., Schmidts, M., Didonna, T., Makrythanasis, P., Bevillard, J., Mongan, N. P., Djakow, J., Pals, G., Lucas, J. S., Marthin, J. K., Nielsen, K. G., Santoni, F., Guipponi, M., Hogg, C., Antonarakis, S. E., Emes, R. D., Chung, E. M. K.,

Greene, N. D. E., Blouin, J. L., Jarman, A. P., Mitchison, H. M., 2013. Mutations in ZMYND10, a gene essential for proper axonemal assembly of inner and outer dynein arms in humans and flies, cause primary ciliary dyskinesia. American Journal of Human Genetics 93 (2), 346–356.

Moritz, M., Braunfeld, M. B., Guénebaut, V., Heuser, J., Agard, D. A., 2000. Structure of the gamma-tubulin ring complex: a template for microtubule nucleation. Nature cell biology 2 (6), 365–370.

Mottier-Pavie, V., Megraw, T. L., 2009. Drosophila bld10 is a centriolar protein that regulates centriole, basal body, and motile cilium assembly. Molecular biology of the cell 20 (10), 2605–2614.

Mukhopadhyay, S., Lu, Y., Qin, H., Lanjuin, A., Shaham, S., Sengupta, P., 2007. Distinct IFT mechanisms contribute to the generation of ciliary structural diversity in C. elegans. The EMBO journal 26 (12), 2966–2980.

Munro, S., Nichols, B. J., 1999. The grip domain - A novel golgi-targeting domain found in several coiled-coil proteins. Current Biology 9 (7), 377–380.

Murphy, D. B., Seemann, S., Wiese, S., Kirschner, R., Grzeschik, K. H., Thies, U., Mar. 1997. The Human Hepatocyte Nuclear Factor 3/Fork Head Gene FKHL13: Genomic Structure and Pattern of Expression. Genomics 40 (3), 462–469.
URL http://www.ncbi.nlm.nih.gov/pubmed/9073514

Neal, C. P., Fry, A. M., Moreman, C., McGregor, A., Garcea, G., Berry, D. P., Manson, M. M., 2014. Overexpression of the Nek2 kinase in colorectal cancer correlates with beta-catenin relocalization and shortened cancer-specific survival. Journal of surgical oncology (May).
URL http://www.ncbi.nlm.nih.gov/pubmed/25043295

Newton, F. G., zur Lage, P. I., Karak, S., Moore, D. J., Göpfert, M. C., Jarman, A. P., 2012. Forkhead Transcription Factor Fd3F Cooperates with Rfx to Regulate a Gene Expression Program for Mechanosensory Cilia Specialization. Developmental Cell 22 (6), 1221–1233.

Nigg, E. A., 2006. Origins and consequences of centrosome aberrations in human cancers.

Nigg, E. A., 2007. Centrosome duplication: of rules and licenses.

Nigg, E. A., Stearns, T., 2011. The centrosome cycle: Centriole biogenesis, duplication and inherent asymmetries.

Nonaka, S., Tanaka, Y., Okada, Y., Takeda, S., Harada, A., Kanai, Y., Kido, M., Hirokawa, N., 1998. Randomization of left-right asymmetry due to loss of nodal cilia generating leftward flow of extraembryonic fluid in mice lacking KIF3B motor protein. Cell 95 (6), 829–837.

Omran, H., Kobayashi, D., Olbrich, H., Tsukahara, T., Loges, N. T., Hagiwara, H., Zhang, Q., Leblond, G., O'Toole, E., Hara, C., Mizuno, H., Kawano, H., Fliegauf, M., Yagi, T., Koshida, S., Miyawaki, A., Zentgraf, H., Seithe, H., Reinhardt, R., Watanabe, Y., Kamiya, R., Mitchell, D. R., Takeda, H., 2008. Ktu/PF13 is required for cytoplasmic pre-assembly of axonemal dyneins. Nature 456 (7222), 611–616.

Orgogozo, V., Grueber, W. B., 2005. FlyPNS, a database of the Drosophila embryonic and larval peripheral nervous system. BMC developmental biology 5, 4.

Otsuki, K., Hayashi, Y., Kato, M., Yoshida, H., Yamaguchi, M., 2004. Characterization of dRFX2, a novel RFX family protein in Drosophila. Nucleic Acids Research 32 (18), 5636–5648.

Ott, C. J., Blackledge, N. P., Kerschner, J. L., Leir, S.-H., Crawford, G. E., Cotton, C. U., Harris, A., 2009. Intronic enhancers coordinate epithelial-specific looping of the active CFTR locus. Proceedings of the National Academy of Sciences of the United States of America 106 (47), 19934–19939.

Palazzo, R. E., Vogel, J. M., Schnackenberg, B. J., Hull, D. R., Wu, X., 2000. Centrosome maturation. Current topics in developmental biology 49, 449–470.

Pan, J., You, Y., Huang, T., Brody, S. L., 2007. RhoA-mediated apical actin enrichment is required for ciliogenesis and promoted by Foxj1. Journal of cell science 120 (Pt 11), 1868–1876.

Panizzi, J. R., Becker-Heck, A., Castleman, V. H., Al-Mutairi, D. A., Liu, Y., Loges, N. T., Pathak, N., Austin-Tse, C., Sheridan, E., Schmidts, M., Olbrich, H., Werner, C., Häffner, K., Hellman, N., Chodhari, R., Gupta, A., Kramer-Zucker, A., Olale, F., Burdine, R. D., Schier, A. F., O'Callaghan, C., Chung, E. M. K., Reinhardt, R., Mitchison, H. M., King, S. M., Omran, H., Drummond, I. A., 2012. CCDC103 mutations cause primary ciliary dyskinesia by disrupting assembly of ciliary dynein arms.

Park, S. T., Byun, H. J., Kim, B. R., Dong, S. M., Park, S. H., Jang, P. R., Rho, S. B., 2013. Tumor suppressor BLU promotes paclitaxel antitumor activity by inducing apoptosis through the down-regulation of Bcl-2 expression in tumorigenesis. Biochemical and Biophysical Research Communications 435 (1), 153–159.

Parker, J. D. K., Hilton, L. K., Diener, D. R., Rasi, M. Q., Mahjoub, M. R., Rosenbaum, J. L., Quarmby, L. M., 2010. Centrioles are freed from cilia by severing prior to mitosis. Cytoskeleton 67 (7), 425–430.

Pazour, G. J., Agrin, N., Walker, B. L., Witman, G. B., 2006. Identification of

predicted human outer dynein arm genes: candidates for primary ciliary dyskinesia genes.

Pazour, G. J., Wilkerson, C. G., Witman, G. B., 1998. A dynein light chain is essential for the retrograde particle movement of intraflagellar transport (IFT). Journal of Cell Biology 141 (4), 979–992.

Perry, M. W., Boettiger, A. N., Bothma, J. P., Levine, M., 2010. Shadow enhancers foster robustness of drosophila gastrulation. Current Biology 20 (17), 1562–1567.

Perry, M. W., Boettiger, A. N., Levine, M., 2011. Multiple enhancers ensure precision of gap gene-expression patterns in the Drosophila embryo. Proceedings of the National Academy of Sciences of the United States of America 108 (33), 13570–13575.

Petrascheck, M., Escher, D., Mahmoudi, T., Verrijzer, C. P., Schaffner, W., Barberis, A., 2005. DNA looping induced by a transcriptional enhancer in vivo. Nucleic Acids Research 33 (12), 3743–3750.

Piel, M., Meyer, P., Khodjakov, A., Rieder, C. L., Bornens, M., 2000. The respective contributions of the mother and daughter centrioles to centrosome activity and behavior in vertebrate cells. Journal of Cell Biology 149 (2), 317–329.

Plevin, M. J., Mills, M. M., Ikura, M., 2005. The LxxLL motif: A multifunctional binding sequence in transcriptional regulation.

Powell, L. M., Deaton, A. M., Wear, M. A., Jarman, A. P., 2008. Specificity of Atonal and Scute bHLH factors: Analysis of cognate E box binding sites and the influence of Senseless. Genes to Cells 13 (9), 915–929.

Praetorius, H. A., Spring, K. R., 2005. A physiological view of the primary cilium. Annual review of physiology 67, 515–529.

Prigent, C., Glover, D. M., Giet, R., 2005. Drosophila Nek2 protein kinase knock-down leads to centrosome maturation defects while overexpression causes centrosome fragmentation and cytokinesis failure. Experimental Cell Research 303 (1), 1–13.

Purvis, T. L., Hearn, T., Spalluto, C., Knorz, V. J., Hanley, K. P., Sanchez-Elsner, T., Hanley, N. A., Wilson, D. I., 2010. Transcriptional regulation of the Alström syndrome gene ALMS1 by members of the RFX family and Sp1. Gene 460 (1-2), 20–29.

Raff, E. C., 1997. Microtubule Architecture Specified by a beta -Tubulin Isoform.

Ravasi, T., Suzuki, H., Cannistraci, C. V., Katayama, S., Bajic, V. B., Tan, K., Akalin, A., Schmeier, S., Kanamori-Katayama, M., Bertin, N., Carninci, P., Daub, C. O., Forrest, A. R. R., Gough, J., Grimmond, S., Han, J. H., Hashimoto, T., Hide, W., Hofmann, O., Kawaji, H., Kubosaki, A., Lassmann, T., van Nimwegen, E., Ogawa, C., Teasdale, R. D., Tegnér, J., Lenhard, B., Teichmann, S. A., Arakawa, T., Ninomiya, N., Murakami, K., Tagami, M., Fukuda, S., Imamura, K., Kai, C., Ishihara, R., Kitazume, Y., Kawai, J., Hume, D. A., Ideker, T., Hayashizaki, Y., 2010. An Atlas of Combinatorial Transcriptional Regulation in Mouse and Man. Cell 140 (5), 744–752.

Rebeiz, M., Posakony, J. W., 2004. GenePalette: A universal software tool for genome sequence visualization and analysis. Developmental Biology 271 (2), 431–438.

Reeves, N., Posakony, J. W., 2005. Genetic programs activated by proneural proteins in the developing Drosophila PNS. Developmental Cell 8 (3), 413–425.

Rhodenizer, D., Martin, I., Bhandari, P., Pletcher, S. D., Grotewiel, M., 2008. Genetic and environmental factors impact age-related impairment of negative geotaxis in Drosophila by altering age-dependent climbing speed. Experimental Gerontology 43 (8), 739–748.

Rieder, C. L., Faruki, S., Khodjakov, A., 2001. The centrosome in vertebrates: More than a microtubule-organizing center.

Riparbelli, M. G., Callaini, G., Megraw, T. L., 2012. Assembly and Persistence of Primary Cilia in Dividing Drosophila Spermatocytes. Developmental Cell 23 (2), 425–432.

Rosenbaum, J. L., Witman, G. B., 2002. Intraflagellar transport. Nature reviews. Molecular cell biology 3 (11), 813–825.

Ross, A. J., Dailey, L. A., Brighton, L. E., Devlin, R. B., 2007. Transcriptional profiling of mucociliary differentiation in human airway epithelial cells. American Journal of Respiratory Cell and Molecular Biology 37 (2), 169–185.

Rusan, N. M., Peifer, M., 2007. A role for a novel centrosome cycle in asymmetric cell division. Journal of Cell Biology 177 (1), 13–20.

Salisbury, J. L., Baron, A., Surek, B., Melkonian, M., 1984. Striated flagellar roots: Isolation and partial characterization of a calcium-modulated contractile organelle. Journal of Cell Biology 99 (3), 962–970.

Salisbury, J. L., Floyd, G. L., 1978. Calcium-induced contraction of the rhizoplast of a quadriflagellate green alga. Science (New York, N.Y.) 202 (4371), 975–977.

Sanyal, A., Lajoie, B. R., Jain, G., Dekker, J., 2012. The long-range interaction landscape of gene promoters.

Sarpal, R., Todi, S. V., Sivan-Loukianova, E., Shirolikar, S., Subramanian, N., Raff, E. C., Erickson, J. W., Ray, K., Eberl, D. F., 2003. Drosophila KAP Interacts with the Kinesin II Motor Subunit KLP64D to Assemble Chordotonal Sensory Cilia, but Not Sperm Tails. Current Biology 13 (19), 1687–1696.

Schmidt, K. N., Kuhns, S., Neuner, A., Hub, B., Zentgraf, H., Pereira, G., 2012. Cep164 mediates vesicular docking to the mother centriole during early steps of ciliogenesis. Journal of Cell Biology 199 (7), 1083–1101.

Schnackenberg, B. J., Palazzo, R. E., 1999. Identification and function of the centrosome centromatrix.

Schöckel, L., Möckel, M., Mayer, B., Boos, D., Stemmann, O., 2011. Cleavage of cohesin rings coordinates the separation of centrioles and chromatids. Nature cell biology 13 (8), 966–972.

Schultz, S. J., Fry, A. M., Sütterlin, C., Ried, T., Nigg, E. A., 1994. Cell cycle-dependent expression of Nek2, a novel human protein kinase related to the NIMA mitotic regulator of Aspergillus nidulans. Cell growth & differentiation : the molecular biology journal of the American Association for Cancer Research 5 (6), 625–635.

Seeley, E. S., Nachury, M. V., Feb. 2010. The perennial organelle: assembly and disassembly of the primary cilium. Journal of cell science 123 (Pt 4), 511–8.
URL http://www.pubmedcentral.nih.gov/articlerender.fcgi?artid=2818191&tool=pmce

Senthilan, P. R., Piepenbrock, D., Ovezmyradov, G., Nadrowski, B., Bechstedt, S.,

Pauls, S., Winkler, M., Möbius, W., Howard, J., Göpfert, M. C., 2012. Drosophila auditory organ genes and genetic hearing defects. Cell 150 (5), 1042–1054.

Shanbhag, S. R., Singh, K., Naresh Singh, R., 1992. Ultrastructure of the femoral chordotonal organs and their novel synaptic organization in the legs of Drosophila melanogaster Meigen (Diptera : Drosophilidae).

Shen, X., Mizuguchi, G., Hamiche, A., Wu, C., 2000. A chromatin remodelling complex involved in transcription and DNA processing. Nature 406 (6795), 541–544.

Signor, D., Wedatman, K. P., Orozco, J. T., Dwyer, N. D., Bargmann, C. I., Rose, L. S., Scholey, J. M., 1999. Role of a class DHC1b dynein in retrograde transport of IFT motors and IFT raft particles along cilia, but not dendrites, in chemosensory neurons of living Caenorhabditis elegans. Journal of Cell Biology 147 (3), 519–530.

Sjöblom, B., Salmazo, A., Djinović-Carugo, K., 2008. Alpha-actinin structure and regulation. Cellular and molecular life sciences : CMLS 65 (17), 2688–2701.

Sjostrand, F. S., Aug. 1953. The ultrastructure of the inner segments of the retinal rods of the guinea pig eye as revealed by electron microscopy. Journal of Cellular and Comparative Physiology 42 (1), 45–70.
URL http://doi.wiley.com/10.1002/jcp.1030420104

Skeath, J. B., Carroll, S. B., 1994. The achaete-scute complex: generation of cellular pattern and fate within the Drosophila nervous system. The FASEB journal : official publication of the Federation of American Societies for Experimental Biology 8 (10), 714–721.

Sleigh, M. A., Silvester, N. R., 1983. Anchorage functions of basal apparatus of cilia. Journal of Submicroscopic Cytology 15, 101–104.

Smith, E. F., Yang, P., Jan. 2004. The radial spokes and central apparatus: mechano-chemical transducers that regulate flagellar motility. Cell motility and the cytoskeleton 57 (1), 8–17.
URL http://www.pubmedcentral.nih.gov/articlerender.fcgi?artid=1950942&tool=pmce

Sorokin, S., 1962. Centrioles and the formation of rudimentary cilia by fibroblasts and smooth muscle cells. The Journal of cell biology 15, 363–377.

Sorokin, S. P., Jun. 1968. Reconstructions of Centriole Formation and Ciliogenesis in Mammalian Lungs. J. Cell Sci. 3 (2), 207–230.
URL http://jcs.biologists.org/content/3/2/207

Spira, A. W., Milman, G. E., Jul. 1979. The structure and distribution of the cross-striated fibril and associated membranes in guinea pig photoreceptors. The American journal of anatomy 155 (3), 319–37.
URL http://www.ncbi.nlm.nih.gov/pubmed/573060

Steimle, V., Durand, B., Barras, E., Zufferey, M., Hadam, M. R., Mach, B., Reith, W., 1995. A novel DNA-binding regulatory factor is mutated in primary MHC class II deficiency (bare lymphocyte syndrome). Genes and Development 9 (9), 1021–1032.

Stolc, V., Samanta, M. P., Tongprasit, W., Marshall, W. F., 2005. Genome-wide transcriptional analysis of flagellar regeneration in Chlamydomonas reinhardtii identifies orthologs of ciliary disease genes. Proceedings of the National Academy of Sciences of the United States of America 102 (10), 3703–3707.

Stubbs, J. L., Oishi, I., Izpisúa Belmonte, J. C., Kintner, C., 2008. The forkhead protein Foxj1 specifies node-like cilia in Xenopus and zebrafish embryos. Nature genetics 40 (12), 1454–1460.

Swoboda, P., Adler, H. T., Thomas, J. H., 2000. The RFX-type transcription factor DAF-19 regulates sensory neuron cilium formation in C. elegans. Molecular cell 5 (3), 411–421.

Szymanska, K., Johnson, C. A., 2012. The transition zone: an essential functional compartment of cilia.

Thomas, J., Morlé, L., Soulavie, F., Laurençon, A., Sagnol, S., Durand, B., 2010. Transcriptional control of genes involved in ciliogenesis: a first step in making cilia. Biology of the cell / under the auspices of the European Cell Biology Organization 102 (9), 499–513.

Tsou, M. F. B., Wang, W. J., George, K. A., Uryu, K., Stearns, T., Jallepalli, P. V., 2009. Polo Kinase and Separase Regulate the Mitotic Licensing of Centriole Duplication in Human Cells. Developmental Cell 17 (3), 344–354.

Tucker, R. W., Pardee, A. B., Fujiwara, K., 1979. Centriole ciliation is related to quiescence and DNA synthesis in 3T3 cells. Cell 17 (3), 527–535.

Uetake, Y., Lončarek, J., Nordberg, J. J., English, C. N., La Terra, S., Khodjakov, A., Sluder, G., 2007. Cell cycle progression and de novo centriole assembly after centrosomal removal in untransformed human cells. Journal of Cell Biology 176 (2), 173–182.

UGA, S., KUWABARA, M., Jan. 1965. On the Fine Structure of the Chordotonal Sensillum in Antenna of Drosophila melanogaster. Microscopy (Tokyo) 14 (3), 173–181.
URL http://jmicro.oxfordjournals.org/content/14/3/173.abstract

Vandaele, C., Coulon-Bublex, M., Couble, P., Durand, B., 2001. Drosophila regulatory factor X is an embryonic type I sensory neuron marker also expressed in

spermatids and in the brain of Drosophila. Mechanisms of Development 103 (1-2), 159–162.

Vazquez, J., Pauli, D., Tissières, A., 1993. Transcriptional regulation in Drosophila during heat shock: A nuclear run-on analysis. Chromosoma 102 (4), 233–248.

Venteicher, A. S., Meng, Z., Mason, P. J., Veenstra, T. D., Artandi, S. E., 2008. Identification of ATPases Pontin and Reptin as Telomerase Components Essential for Holoenzyme Assembly. Cell 132 (6), 945–957.

Vermeulen, K., Van Bockstaele, D. R., Berneman, Z. N., 2003. The cell cycle: A review of regulation, deregulation and therapeutic targets in cancer.

Visel, A., Prabhakar, S., Akiyama, J. A., Shoukry, M., Lewis, K. D., Holt, A., Plajzer-Frick, I., Afzal, V., Rubin, E. M., Pennacchio, L. A., 2008. Ultraconservation identifies a small subset of extremely constrained developmental enhancers. Nature genetics 40 (2), 158–160.

Visel, A., Rubin, E. M., Pennacchio, L. A., 2009. Genomic views of distant-acting enhancers. Nature 461 (7261), 199–205.

Vos, M. J., Hageman, J., Carra, S., Kampinga, H. H., 2008. Structural and functional diversities between members of the human HSPB, HSPH, HSPA, and DNAJ chaperone families.

Williams, C. L., Li, C., Kida, K., Inglis, P. N., Mohan, S., Semenec, L., Bialas, N. J., Stupay, R. M., Chen, N., Blacque, O. E., Yoder, B. K., Leroux, M. R., 2011. MKS and NPHP modules cooperate to establish basal body/transition zone membrane associations and ciliary gate function during ciliogenesis. Journal of Cell Biology 192 (6), 1023–1041.

Wilson, P. D., 2004. Polycystic kidney disease. The New England journal of medicine 350 (2), 151–164.

Wodarz, A., Huttner, W. B., 2003. Asymmetric cell division during neurogenesis in Drosophila and vertebrates.

Wolfrum, U., 1992. Cytoskeletal elements in arthropod sensilla and mammalian photoreceptors. Biology of the cell / under the auspices of the European Cell Biology Organization 76 (3), 373–381.

Wolfrum, U., Jan. 1995. Centrin in the photoreceptor cells of mammalian retinae. Cell motility and the cytoskeleton 32 (1), 55–64.
URL http://www.ncbi.nlm.nih.gov/pubmed/8674134

Wolfrum, U., Salisbury, J. L., 1998. Expression of centrin isoforms in the mammalian retina. Experimental cell research 242 (1), 10–17.

Worley, L. G., Fischbein, E., Shapiro, J. E., May 1953. The structure of ciliated epithelial cells as revealed by the electron microscope and in phase-contrast. Journal of Morphology 92 (3), 545–577.
URL http://doi.wiley.com/10.1002/jmor.1050920307

Worthington, W. C., Cathcart, R. S., Jan. 1963. Ependymal cilia: distribution and activity in the adult human brain. Science (New York, N.Y.) 139 (3551), 221–2.
URL http://www.ncbi.nlm.nih.gov/pubmed/14001896

Wu, S. Y., McLeod, M., 1995. The sak1+ gene of Schizosaccharomyces pombe encodes an RFX family DNA-binding protein that positively regulates cyclic AMP-dependent protein kinase-mediated exit from the mitotic cell cycle. Molecular and cellular biology 15 (3), 1479–1488.

Yamamoto, R., Hirono, M., Kamiya, R., 2010. Discrete PIH proteins function in the cytoplasmic preassembly of different subsets of axonemal dyneins. Journal of Cell Biology 190 (1), 65–71.

Yang, J., Adamian, M., Li, T., 2006. Rootletin interacts with C-Nap1 and may function as a physical linker between the pair of centrioles/basal bodies in cells. Molecular biology of the cell 17 (2), 1033–1040.

Yang, J., Li, T., 2005. The ciliary rootlet interacts with kinesin light chains and may provide a scaffold for kinesin-1 vesicular cargos. Experimental Cell Research 309 (2), 379–389.

Yang, J., Liu, X., Yue, G., Adamian, M., Bulgakov, O., Li, T., 2002. Rootletin, a novel coiled-coil protein, is a structural component of the ciliary rootlet. Journal of Cell Biology 159 (3), 431–440.

Yin, Y., Bangs, F., Paton, I. R., Prescott, A., James, J., Davey, M. G., Whitley, P., Genikhovich, G., Technau, U., Burt, D. W., Tickle, C., 2009. The Talpid3 gene (KIAA0586) encodes a centrosomal protein that is essential for primary cilia formation. Development (Cambridge, England) 136 (4), 655–664.

Yoder, B. K., Yoder, B. K., 2007. Role of primary cilia in the pathogenesis of polycystic kidney disease. Journal of the American Society of Nephrology : JASN 18 (5), 1381–8.
URL http://www.ncbi.nlm.nih.gov/pubmed/17429051

Yu, X., Ng, C. P., Habacher, H., Roy, S., 2008. Foxj1 transcription factors are master regulators of the motile ciliogenic program. Nature genetics 40 (12), 1445–1453.

Zariwala, M. A., Gee, H. Y., Kurkowiak, M., Al-Mutairi, D. A., Leigh, M. W., Hurd, T. W., Hjeij, R., Dell, S. D., Chaki, M., Dougherty, G. W., Adan, M.,

Spear, P. C., Esteve-Rudd, J., Loges, N. T., Rosenfeld, M., Diaz, K. A., Olbrich, H., Wolf, W. E., Sheridan, E., Batten, T. F. C., Halbritter, J., Porath, J. D., Kohl, S., Lovric, S., Hwang, D. Y., Pittman, J. E., Burns, K. A., Ferkol, T. W., Sagel, S. D., Olivier, K. N., Morgan, L. C., Werner, C., Raidt, J., Pennekamp, P., Sun, Z., Zhou, W., Airik, R., Natarajan, S., Allen, S. J., Amirav, I., Wieczorek, D., Landwehr, K., Nielsen, K., Schwerk, N., Sertic, J., Köhler, G., Washburn, J., Levy, S., Fan, S., Koerner-Rettberg, C., Amselem, S., Williams, D. S., Mitchell, B. J., Drummond, I. A., Otto, E. A., Omran, H., Knowles, M. R., Hildebrandt, F., 2013. ZMYND10 is mutated in primary ciliary dyskinesia and interacts with LRRC6. American Journal of Human Genetics 93 (2), 336–345.

Zhang, W., Yan, Z., Jan, L. Y., Jan, Y. N., 2013. Sound response mediated by the TRP channels NOMPC, NANCHUNG, and INACTIVE in chordotonal organs of Drosophila larvae. Proceedings of the National Academy of Sciences of the United States of America 110 (33), 13612–7.
URL http://www.pubmedcentral.nih.gov/articlerender.fcgi?artid=3746866&tool=pmce

Zhang, X., Liu, H., Li, B., Huang, P., Shao, J., He, Z., Jan. 2012. Tumor suppressor BLU inhibits proliferation of nasopharyngeal carcinoma cells by regulation of cell cycle, c-Jun N-terminal kinase and the cyclin D1 promoter. BMC cancer 12 (1), 267.
URL http://www.biomedcentral.com/1471-2407/12/267

Zhao, L., Yuan, S., Cao, Y., Kallakuri, S., Li, Y., Kishimoto, N., DiBella, L., Sun, Z., 2013. Reptin/Ruvbl2 is a Lrrc6/Seahorse interactor essential for cilia motility. Proceedings of the National Academy of Sciences of the United States of America 110 (31), 12697–702.
URL http://www.pubmedcentral.nih.gov/articlerender.fcgi?artid=3732945&tool=pmce

zur Lage, P. I., Prentice, D. R. A., Holohan, E. E., Jarman, A. P., 2003. The Drosophila proneural gene amos promotes olfactory sensillum formation and suppresses bristle formation. Development (Cambridge, England) 130 (19), 4683–4693.